INTER-INDIVIDUAL VARIABILITY IN METABOLISM AND TOXICITY OF TRICHLOROETHYLENE AND TETRACHLOROETHYLENE

A Dissertation

by

YU-SYUAN LUO

Submitted to the Office of Graduate and Professional Studies of
Texas A&M University
in partial fulfillment of the requirements for the degree of

DOCTOR OF PHILOSOPHY

Chair of Committee,	Ivan Rusyn
Committee Members,	Weihsueh A. Chiu
	Thomas J. McDonald
	Terry L. Wade
	David W. Threadgill
Head of Department,	Jane Welsh

August 2018

Major Subject: Toxicology

ABSTRACT

From the standpoint of public health, the purpose of chemical health risk assessment is to protect the susceptible individuals and to set up an action threshold against chemical hazards. Chemical toxicity is usually associated with toxicokinetics (absorption, distribution, metabolism, and excretion). One of the critical challenges in human health risk assessment is to address the inter-individual variability in metabolism and toxicity of chemicals. The inter-individual differences may be due to sex, genetics, dietary habits, and disease states. We hypothesized that the *inter-individual variability in genetics and disease states could affect the xenobiotic metabolism, which in turn has pronounced impacts on individual susceptibility toward chemical exposures*. Herein, we use two structurally similar chlorinated chemicals, trichloroethylene (TCE) and tetrachloroethylene (PCE), as model compounds. Organ-specific toxicities of TCE and PCE have been linked to their respective oxidative and glutathione (GSH) conjugation metabolism; however, little is known regarding GSH conjugation metabolism at target organs (i.e., liver and kidney) due to the lack of sensitive analytical assays. In this dissertation, we successfully developed two LC-MS/MS methods for simultaneous detection of GSH conjugation metabolites in multiple mouse tissues for TCE and. With these validated methods, we advanced our knowledge in metabolism and toxicity of TCE and PCE from several aspects. First, our data show that the default uncertainty factor of 3.16 for the toxicokinetic variability of TCE GSH conjugation metabolites is inadequate to protect 99% of the population for organ-specific toxicity mediated by DCVG, DCVC,

and NAcDCVC. Second, we found that nonalcoholic fatty liver disease states can also influence the kidney metabolism and toxicity of PCE. Third, our results demonstrate that the oxidative enzyme, cytochrome P450 2E1, can alter not only the oxidative but also the GSH conjugative metabolism, which in turn have pronounced impacts on the organ-specific toxicity of TCE and PCE. Finally, we observed that the one-atom replacement of chlorine can substantially affect the oxidative and GSH conjugative metabolism of TCE and PCE. Collectively, this doctoral dissertation advances our understanding of metabolism and toxicity of TCE and PCE, and provides data for more refined health risk assessment of TCE and PCE.

ACKNOWLEDGEMENTS

I would like to thank my doctoral mentor, Dr. Ivan Rusyn, for his guidance and general support throughout the course of my doctoral research. During the period of 3-year research, I've learned how to become a scientist: rationalize your study, organize your work, collaborate with other people, communicate with others, and most importantly, focus on details. I also wish to show my deepest gratitude to my dissertation committee, Drs. Weihsueh A. Chiu, Thomas J. McDonald, Terry Wade, and David W. Threadgill for the guidance and fruitful discussion on my doctoral dissertation.

My doctoral dissertation would not even be possible without a number of individuals. I'd like to show my deepest appreciation to Dr. Shinji Furuya, for his guidance on carrying out western blotting and immunohistochemistry staining; Dr. Cichocki A. Joseph, for the fruitful scientific discussion on tetrachloroethylene and trichloroethylene, and the guidance on my scientific writings; Mr. Steven T. Sweet, for his technical support on GC-MS analyses; Dr. Abhishek Venkatranam, for his guidance on carrying out TCA and TCOH analysis; Dr. Hisataka Fukushima and Ms. Lauren Lewis, for their assistance on animal study; Dr. Yasuhiro Iwata, for his help on H&E histopathological readings; Drs. Hong Sik Yoo, Valerie Y. Soldatov, and Oksana Kosyk, for their previous work on the animal studies. I also want to thank Mr. Oleksii Seniutkin for being lab buddy to take classes, to apply tax refund, and to enjoy the graduate life together.

I'd also like to acknowledge Taiwan government to provide the financial support for my doctoral research. Additionally, I appreciate receiving several awards from the

Society of Toxicology and the College of Veterinary Medicine, Texas A&M University, based on my doctoral research.

Pursuing a Ph.D. degree in the other country is challenging; fortunately, I have my parents, sister, brother, and the whole family support me to explore knowledge in Toxicology. I also acknowledge my girlfriend Ms. En-Hsuan Lu who always gives me spiritual supports and suggestions on selecting Japanese drama when I encounter difficulties in experiments. Thank you.

CONTRIBUTORS AND FUNDING SOURCES

This work was evaluated by a dissertation committee consisting of Professors Ivan Rusyn, Weihsueh A. Chiu of the Department of Veterinary Integrative Biosciences, Professor Thomas J. McDonald of the Department of Environmental and Occupational Health, Professor Terry Wade of the Department of Oceanography, and Professor David W. Threadgill of the Department of Veterinary Pathobiology.

The data analyzed for Chapter IV was provided by Dr. Cichocki A. Joseph. The animal studies used in Chapter V were conducted in part by a former graduate student from Rusyn's lab, Dr. Hong Sik Yoo. The animal study depicted in Chapter VI were carried out in 2012 by a former lab member Ms. Valerie Y. Soldatow.

All other work conducted for the dissertation was completed by the student independently.

Graduate study was supported by grants from National Institute of Health (P42 ES 005948) and the United States Environmental Protection Agency (STAR RD83561202), and a Government Scholarship to Study Abroad from Ministry of Education, Taiwan.

NOMENCLATURE

ACGIH	American Conference of Government Industrial Hygienists
ALT	Alanine aminotransferase
AST	Aspartate aminotransferase
ATSDR	Agency for Toxic Substances and Disease Registry
AUC	Area under curve
BrdU	5-bromo-2'-deoxyuridine
BUN	Blood urea nitrogen
CC	Collaborative cross mice
CCBL	Cysteine S-conjugate beta lyase
CCS	Collision cross section
CH	Chloral hydrate
CTAC	Chlorothionoacetyl chloride
CTK	Chlorothioketene
CYP2E1	Cytochrome P450 2E1
Cyp2e1(-/-)	Cyp2e1-null mice
CYPs	Cytochrome P450s
DCA	Dichloroacetate
DCVC	S-(1, 2-dichlorovinyl)-L-cysteine
DCVCSO	DCVC sulfoxide
DCVG	S-(1, 2-dichlorovinyl)-glutathione

DCVT	1, 2-dichlorovinylthiol
DP	Dipeptidase
EWAS	Environment-wide association study
FDR	False discovery rate
FMO	Flavin-containing monooxygenase
GC-MS	Gas chromatography-mass spectrometry
GGT	Gamma-glutamyl transferase
GSD	Geometric standard deviation
GSH	Glutathione
GSTs	Glutathione-S-transferases
H&E	Hematoxylin and eosin
hCYP2E1	humanized CYP2E1 mice
HFD	High-fat diet
IARC	International Agency for Research on Cancer
IDLH	Immediately Dangerous to Life or Health
IMS	Ion mobility spectroscopy
Ke	Elimination rate constant
KIM-1	kidney injury molecule 1
Km	Formation rate constant
LC-MS/MS	Liquid chromatography-triple quadrupole tandem mass spectrometry
LFD	Low-fat diet
LOD	Limit of detection

LOQ	Limit of quantification
MCD	Methionine/choline/folate-deficient diet
MOA	Mode of action
MRLs	Minimal Risk Levels
MTBE	Methyl tert-butyl ether
NAcDCVC	N-acetyl-(1, 2-dichlorovinyl)-L-cysteine
NAcDCVCSO	NAcDCVC sulfoxide
NAcTCVC	N-acetyl-(1, 2, 2-trichlorovinyl)-L-cysteine
NIOSH	National Institute for Occupational Safety and Health
NAFL	Nonalcoholic fatty liver
NAFLD	Nonalcoholic fatty liver disease
NASH	Nonalcoholic steatohepatitis
NAT	N-acetyl transferase
NHAES	National Health and Nutrition Examination Survey
NTP	National Toxicology Program
PBPK	Physiologically based pharmacokinetic
PCE	Tetrachloroethylene
PPAR	Peroxisome proliferator-activated receptor
qRT-PCR	Quantitative reverse transcriptase real-time polymerase chain reaction
RfC	Reference concentration
RfD	Reference dose
SPE	Solid-phase extraction

TCE	Trichloroethylene
TCOG	Trichloro-glucuronide conjugate
TCVC	S-(1, 2, 2-trichlorovinyl)-L-cysteine
TCVCSO	TCVC sulfoxide
TCVG	S-(1, 2, 2-trichlorovinyl)-glutathione
TD	Toxicodynamic
TK	Toxicokinetic
TLV-TWA	Threshold Limit Values for Time-Weighted Average
UF	Uncertainty factor
UGTs	UDP-glucuronosyltransferases
USEPA	United States Environmental Protection Agency

TABLE OF CONTENTS

Page

LIST OF FIGURES

Page

LIST OF TABLES

Page

CHAPTER I

INTRODUCTION

1.1 Trichloroethylene (TCE) and tetrachloroethylene (PCE): Highlighted chemicals to be re-evaluated for their risks to environment and human health

1.1.1 General use, sources of human and animal exposure

Trichloroethylene (TCE) and tetrachloroethylene (PCE) are structurally-similar, chlorinated olefins that have been widely used in industrial applications, such as metal degreasing, dry cleaning, and chemical production (ATSDR, 2014; ATSDR, 1997). The initial production of TCE for commercial uses in the USA can be traced back to 1925, with the increasing needs in vapor degreasing and dry cleaning industry. From the mid-1950s, the use of TCE in dry cleaning has been replaced by PCE (IARC, 2014), although the current use of PCE in dry cleaning is also being phased out by the California EPA (EPA, 2017). Even though the use of TCE and PCE has been reduced over decades, the environmental releases of these chlorinated olefins were approximately 2.22 million pounds for TCE and 0.8 million pounds for PCE in the USA in 2016, according to the EPA Toxic Release Inventory program (USEPA, 2018). Due to their high production volume and widespread use, both TCE and PCE are commonly found in ambient air, ground and drinking water (IARC, 2014), and frequently detected at the National Priority List sites in the United States (ATSDR, 2014; ATSDR, 1997; Fay and Mumtaz, 1996).

The exposure to TCE and PCE for the general population mainly occurs via inhalation or ingestion of drinking water (ATSDR, 2014; ATSDR, 1997). Assuming an ambient TCE concentration range of 100-500 ppt and an adult breathing rate of 20 m^3/day, the average daily intake of TCE through inhalation was estimated as 11-33 μg/day for the general population. The average daily intake of TCE through ingestion was 2-20 μg/day, assuming a concentration range of 2-7 ppb and total water consumption of 2 liters/day (ATSDR, 1997). On the other hand, the total daily intake of PCE was estimated in the range of 1.22 to 2.67 μg/body weight (bw) for the general population in Canada, where drinking water ingestion only account for a minor amount of the total exposure, estimated to be 0.002 to 0.06 μg/kg bw per day (CEPA, 1993). As indicated in 1999-2000 National Health and Nutrition Examination Survey (NHANES), the mean blood levels of these chlorinated olefins were 0.013 ng/mL in 290 subjects, with a detection rate of 11.6% for TCE, and 0.138 ng/mL in 276 subjects, with a detection rate of 77.3% for PCE (Jia *et al.*, 2012). In the most recent 2013-2014 NHANES, the mean blood levels of these chlorinated solvents were 0.010 ng/mL in 3103 subjects, with a detection rate of 0.6% for TCE, and 0.05 ng/mL in 2970 subjects, with a detection rate of 7.4% for PCE (CDC, 2017). Besides, the detection rate of the urinary biomarker of TCE exposure, n-acetyl-s-(1, 2-dichlorovinyl)-L-cysteine (NAcDCVC), was also extremely low (0.08%) with 2475 subjects (CDC, 2017). The declines in the detection rates of TCE and PCE among the U.S. population demonstrate that the exposure of TCE and PCE to the general population had been substantially decreased, in line with the regulatory interventions. However, TCE and PCE remain to be environmental contaminants of high concerns at hazardous waste sites,

because that they show multi-organ toxicities in animals and humans, and that they are among the top 10 chemicals that EPA will evaluate for risks to human health under the new Frank R. Lautenberg Chemical Safety for the 21st Century Act (U.S. EPA, 2017).

1.1.2 Potential health hazards of TCE and PCE to animals and humans

TCE and PCE can pose both cancer and non-cancer hazards at multiple organs to humans and animals, as concluded by U.S. EPA (U.S. EPA, 2011b; U.S. EPA, 2011c), IARC (IARC, 2014), and NTP (NTP, 2015). For cancer hazards, TCE was classified as a human carcinogen, based on the substantial evidence on kidney cancer and the limited evidence on non-Hodgkin lymphoma and liver cancer (Table 1.1). On the other hand, even though the carcinogenic evidence is sufficient in animals, there is no consistent epidemiologic data for the association between PCE and cancers. Therefore, PCE has been classified as a probable human carcinogen (Group 2A) by IARC.

Table 1.1 Weight of evidence for the carcinogenicity of TCE and PCE at multiple organs

	TCE		PCE	
Target organ	Animal	Human	Animal	Human
Liver	S	L	S	N
Kidney	S	S	L	L
Bladder	N	N	N	L
Lung	S	N	N	L
Immune system	L	L	S	L
Brain	N	N	L	N
Testis	N	N	S	N

*S, Strong evidence; L, suggestive/limited evidence; N, no evidence

For non-cancer hazards, TCE exposure causes toxicities at multiple sites, such as liver, kidney, central nervous system, immune system, and male reproductive system(U.S. EPA, 2011c). PCE exposure also induces toxicity at similar target sites, including liver, kidney, central nervous system, and developing fetus (U.S. EPA, 2011b). Despite both TCE and PCE can induce qualitatively-similar toxicities, the severity of these toxicities could be different. The toxicity and regulatory values for TCE and PCE are summarized in Table 1.2, where TCE is considered more toxic than PCE in general.

Table 1.2 Toxicity and regulatory values for TCE and PCE

Institute, toxicity value	TCE	PCE
EPA, oral slope factor	5×10^{-2} per mg/kg-day	2×10^{-3} per mg/kg-day
EPA, inhalation unit risk	2×10^{-2} per ppm	2×10^{-3} per ppm
EPA, RfD	5×10^{-4} mg/kg-day	6×10^{-3} mg/kg-day
EPA, RfC	4×10^{-4} ppm	5.8×10^{-3} ppm
ACGIH, TLV-TWA	10 ppm	25 ppm
ATSDR, chronic inhalation MRLs	0.0004 ppm	0.04 ppm
NIOSH-IDLH	1000 ppm	150m

1.1.3 Target-organ metabolism and toxicity of TCE and PCE

Upon absorption, both TCE and PCE can be metabolized through both oxidative and GSH conjugative pathways (Figure 1.1). For oxidative metabolism, both TCE and PCE are mainly oxidized by CYPs to form their respective epoxide intermediate and chloral hydrate (CH). These upstream metabolites can be further converted to several oxidative metabolites, where trichloroacetate (TCA) is thought to be the major oxidative metabolite of TCE and PCE. TCA is a known activator for peroxisome proliferator-activated receptor

α (PPARα), which may contribute to the liver carcinogenesis of TCE and PCE in mice (Corton, 2008). The other crucial oxidative metabolite, trichloroethanol (TCOH), is a TCE-specific metabolite that is formed through oxidation of TCE-epoxide to CH. TCOH can further conjugate with glucuronide via UDP-glucuronosyltransferases (UGTs) to generate TCOH-glucuronide conjugate (TCOG). These TCE-specific metabolites can be subject to enterohepatic recirculation and would be a significant source of TCA (Stenner *et al.*, 1997). On the other hand, the subsequent oxidation of PCE-epoxide mainly occurs through trichloroacetyl chloride (TCAC), which further converts to the major metabolite TCA and minor metabolite DCA (Chiu *et al.*, 2007).

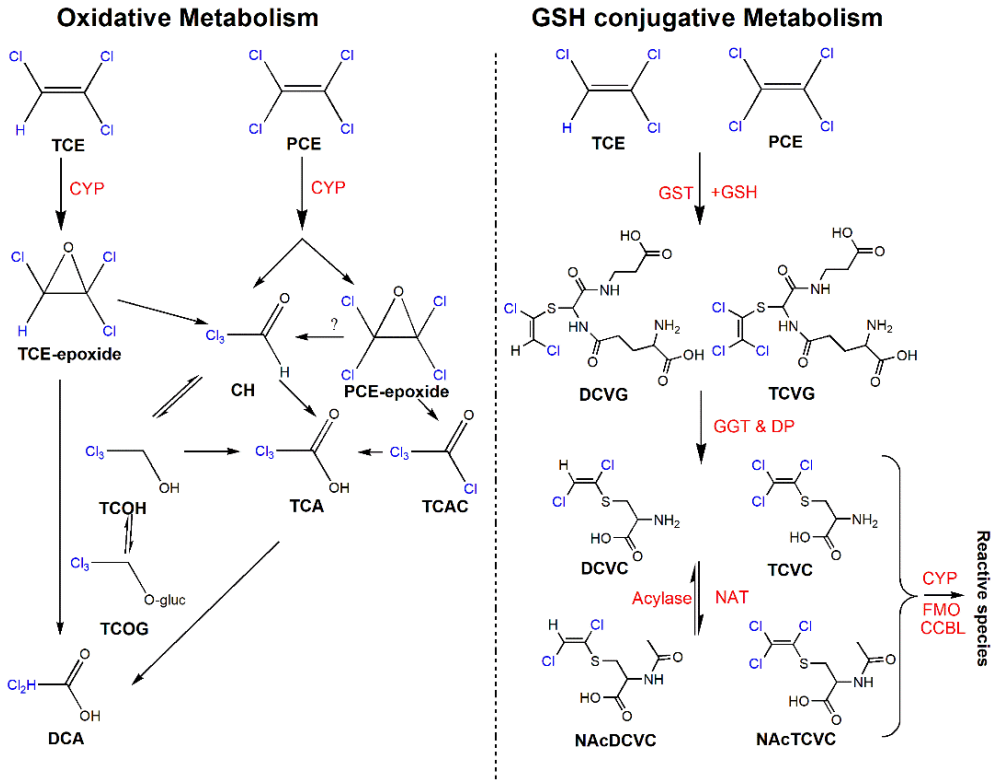

Figure 1.1 Overview of the metabolic pathways of TCE and PCE (This figure is reprinted with permission from Oxford University Press, Luo et al., 2018 (https://doi.org/10.1093/toxsci/kfy099))**.** Upon absorption, TCE and PCE can either be oxidized via cytochrome P450s (CYPs) or conjugated with glutathione (GSH) via glutathione s-transferases (GSTs). Abbreviations: trichloroethylene, TCE; tetrachloroethylene, PCE; chloral hydrate, CH; trichloroethanol, TCOH; trichloroacetate, TCA; trichloroacetyl chloride, TCAC; trichloro-glucuronide conjugate, TCOG; dichloroacetate, DCA; S-(1,2-dichlorovinyl)-glutathione, DCVG; S-(1,2-dichlorovinyl)-cysteine, DCVC; N-acetyl-S-(1,2-dichlorovinyl)-cysteine, NAcDCVC; S-(1,2,2-trichlorovinyl)-glutathione, TCVG; S-(1,2,2-trichlorovinyl)-cysteine, TCVC; N-acetyl-S-(1,2,2-trichlorovinyl)-cysteine, NAcTCVC; gamma-glutamyl transferase, GGT; dipeptidase, DP; n-acetyl transferase, NAT; flavin monooxygenase, FMO; cysteine conjugate beta-lyase, CCBL.

In addition to the oxidative metabolism, both TCE and PCE can conjugate with glutathione (GSH) by glutathione-s-transferases (GSTs) to generate their respective dichloro- and trichloro- GSH conjugates (DCVG and TCVG), which can be further

metabolized by renal and hepatic gamma-glutamyl transferases (GGTs) and dipeptidases (DPs) to their corresponding cysteine conjugates (DCVC and TCVC). These cysteine conjugates are then either detoxified through n-acetylation by n-acetyltransferases (NATs) to NAcDCVC and NAcTCVC, or further bio-activated via cysteine conjugate β lyase (CCBL), Flavin-monooxygenase (FMO), or CYPs to form reactive species such as thioketenes and sulfoxides. These and other reactive species generated from GSH conjugation are thought to be significant contributors to the nephrotoxicity of TCE and PCE (Lash and Parker, 2001; Lash *et al.*, 2007; Lash *et al.*, 2003).

Target-organ toxicity of TCE and PCE (i.e., liver and kidney toxicity) is thought to be determined by their target-organ metabolism in humans and animals. For instance, both TCE and PCE can induce liver tumors in mice. The hepatocarcinogenesis of TCE and PCE has been attributed to their oxidative metabolites, TCA and DCA, as they are known PPARα activators that may induce cell proliferation in mouse liver (Maloney and Waxman, 1999). Aside from TCA and DCA, T/PCE-epoxide, CH, and TCAC are proposed metabolites that contribute to liver toxicity and carcinogenicity of TCE and PCE (U.S. EPA, 2011b; U.S. EPA, 2011c). CH is a known genotoxicant that can induce aneuploidy (Sbrana *et al.*, 1993). Interestingly, TCOH--- the downstream metabolite comes from CH, is consistently detected in TCE-exposed but not in PCE-exposed humans and animals (Chiu, *et al.*, 2007; U.S. EPA, 2011b). On the other hand, reactive species generated from GSH conjugation pathway may contribute to kidney toxicity and carcinogenicity of TCE and PCE. Cell-based assays have demonstrated the genotoxicity (Dekant *et al.*, 1986; Vamvakas *et al.*, 1989a; Vamvakas *et al.*, 1988; Vamvakas *et al.*,

1989b) and nephrotoxicity (Lash *et al.*, 2001b) for DCVG/DCVG and TCVG/TCVC. With metabolic-activation by using kidney subcellular fractions, DCVG and DCVC further manifested enhanced genotoxic responses (Vamvakas, *et al.*, 1988). The reactive sulfoxides derived from cysteine conjugates of TCE and PCE, DCVCSO and TCVCSO, showed a stronger mutagenic activity compared to DCVC and TCVC in the Ames Salmonella typhimurium TA100 strain (Irving and Elfarra, 2013). As the high expressions of GGTs and DPs (Fagerberg *et al.*, 2014) in kidney, kidney toxicity of TCE and PCE has been attributed to cysteine conjugates of TCE and PCE, and their bio-activated species. However, most of the studies on cysteine conjugates of TCE and PCE were conducted *in vitro*. Further *in vivo* evidence would advance our knowledge on the development of TCE and PCE-induced kidney toxicity in humans and animals.

The other hypothesis for TCE-induced kidney toxicity is through the formation of CH metabolite, TCOH, which has been shown to induce formic acid excretion, cell replication, protein accumulation and increased tubular regeneration in the cortex of rat kidney (Green *et al.*, 2003). TCE also induces formic aciduria in F344 rats (Yaqoob *et al.*, 2013) and C57BL/6OlaHsd mice (Lock *et al.*, 2017). However, opposite result on TCOH and kidney toxicity was also reported (Yaqoob *et al.*, 2014). Although TCOH alone does not sufficiently account for TCE-induced renal effects (U.S. EPA, 2011c), this TCE-specific metabolite may explain, at least in part, the stronger weight of evidence of kidney cancer for TCE compared to PCE. Further studies are required to clarify the role of TCOH in developing the kidney toxicity of TCE.

1.2 Inter-individual variability in metabolism and toxicity of environmental toxicants: TCE and PCE as model compounds

The purpose of chemical health risk assessment is to set up an action threshold against environmental and occupational exposures of chemicals. By setting up the action thresholds, we anticipate that most of the general population can be protected from the adverse responses of chemical exposures. Therefore, determining the susceptible individuals among the general population is critical to the health risk assessment of chemicals.

The inter-individual differences in responses to pharmaceuticals (Cattaneo *et al.*, 2016; Harrill *et al.*, 2009; Tracy *et al.*, 2016) mainly arise from the differences in pharmacokinetics (i.e. absorption (AboulFotouh *et al.*, 2018), distribution, metabolism (Shirasaka *et al.*, 2016; Tracy, *et al.*, 2016), and excretion (Wijma *et al.*, 2018)). Several factors, including genetics, sex, age, diet, tobacco smoking, chemical co-exposures, and pre-existing disease states (Thummel and Lin, 2014; Zeise *et al.*, 2013), may influence the pharmacokinetics of drugs and toxicokinetics (TKs) of environmental toxicants, which in turn further elicit differences in therapeutic responses and/or toxicities. In this dissertation, we will probe the inter-individual variability in genetics, enzyme expression, and disease state on TKs and TDs of environmental chemicals.

The activity of enzymes from CYP family, the most important drug-metabolizing enzymes, showed a high degree of inter-individual variability (8-158 fold) in human liver from 27 individuals (Thummel and Lin, 2014). CYPs may reduce or enhance the toxicity of xenobiotic chemicals, depends on the mode of action for chemical toxicity. If the

chemical has direct toxicity (e.g., terfenadine (Kivisto *et al.*, 1994)) and the P450-generated product is less toxic, then CYP-mediated metabolism may reduce toxicity. On the other hand, if the chemical toxicity is exhibited through bio-activation to generate reactive species that can either (i) form covalent binding to macromolecules or (ii) interacts with molecular targets to cause toxicity, then CYP-mediated metabolism may enhance toxicity (Guengerich, 2001). Typical examples include hexane (Stclair *et al.*, 1988), butadiene (Goggin *et al.*, 2009), and TCE and PCE (Cichocki *et al.*, 2016). Considering the dual functions of CYPs in developing chemical toxicity, the inter-individual variability in expression of CYPs is critical to identifying the susceptible individuals towards the exposures of xenobiotic chemicals.

Different disease states may also alter the TKs of the xenobiotic chemicals, which in turn translate into the inter-individual variability in responses. Nonalcoholic fatty liver disease (NAFLD) represents a disease spectrum for a prevalent disease in developed countries. NAFLD initially presents as nonalcoholic fatty liver (NAFL) and can progress to nonalcoholic steatohepatitis (NASH), as characterized by hepatic inflammation, hepatic injury, and concomitant NAFL (Chalasani *et al.*, 2012). NAFLD has been shown to alter the expression of transporter and metabolism genes in the liver (Cichocki *et al.*, 2017a; Cichocki *et al.*, 2017b; Hardwick *et al.*, 2014; Uno *et al.*, 2018), which can affect the delivered dose of xenobiotics to this organ and others. The different delivered doses may further alter target-organ toxicities of xenobiotics.

As discussed above, TCE and PCE can induce multi-organ toxicities, which are associated with their respective oxidative and GSH conjugative metabolism. The multi-

organ toxicity and the well-characterized metabolism make TCE and PCE the ideal compounds for studying inter-individual variability in metabolism and toxicity of environmental toxicants. In this dissertation, by using TCE and PCE as model compounds, we will address the effects of genetics, critical metabolic enzyme, and disease states on TKs and TDs of environmental toxicants.

1.3 Current challenges in studying inter-individual variability in metabolism and toxicity of TCE and PCE

Several challenges exist for the studies on inter-individual variability in metabolism and toxicity of TCE and PCE. First, little is known regarding PCE GSH conjugative metabolism *in vivo* due to lack of sensitive analytical assays. Second, even though analytical methods for simultaneous detection of DCVG and DCVC in mouse tissues do exist (Kim *et al.*, 2009a; Yoo *et al.*, 2015a; Yoo *et al.*, 2015b), the inconsistency of extraction protocols has confounded cross-tissue comparison. In addition, the limited sensitivity of current analytical assay has hindered the characterization of inter-tissue and inter-strain variability in GSH conjugative metabolism of TCE. Third, despite the effects of NAFLD on liver metabolism and toxicity of PCE have been reported (Cichocki, *et al.*, 2017a; Cichocki, *et al.*, 2017b), little is known regarding the effects of NAFLD on kidney metabolism and toxicity of PCE. Forth, *in vivo* contribution and inter-species differences of CYP2E1 in TKs and TDs of TCE and PCE remains unclear. Even though previous studies have shown that both hepatotoxicity and production of oxidative metabolites were ameliorated in male CYP2E1 knockout (*Cyp2e1*(-/-)) mice (Kim and Ghanayem, 2006;

Ramdhan *et al.*, 2008), the exact role of CYP2E1 in TCE TKs is not well understood. Besides, to the best of our knowledge, no study has examined the metabolism and toxicity of PCE in Cyp2e1(-/-) or humanized CYP2E1 (hCYP2E1) mice. At last but not least, though deemed to be similar based on chemical structures, the TKs of TCE and PCE, and their respective metabolites, have not been directly compared.

1.4 Specific aims

To expand our understanding regarding T/PCE GSH conjugative metabolism *in vivo*, we aim to develop LC-MS/MS methods for simultaneous detection of D/TCVG, D/TCVC, and NAcD/TCVC in multiple mouse tissues (**Specific Aim 1&2**). By these methods, our first goal is to fully characterize the inter-tissue and inter-strain variability in TCE GSH conjugative pathway and to derive the chemical-specific uncertainty factors for TK variability in mouse tissues (**Specific Aim 2**). Next, we would examine how extrinsic (diet-induced disease states, **Specific Aim 3**) and intrinsic factors (endogenous expression and activity of CYP2E1, **Specific Aim 4**) affect the metabolism and toxicity of xenobiotics, using TCE and PCE as model compounds. To fill in the data gap that lies in the similarities and differences between TCE and PCE, we further aim to compare their TKs with an identical study design (**Specific Aim 5**).

CHAPTER II

SIMULTANEOUS DETECTION OF THE TETRACHLOROETHYLENE METABOLITES S-(1,2,2-TRICHLOROVINYL)GLUTATHIONE, S-(1,2,2-TRICHLOROVINYL)-L-CYSTEINE, AND N-ACETYL-S-(1,2,2-TRICHLOROVINYL)-L CYSTEINE[1]

2.1 Overview

Tetrachloroethylene (perchloroethylene; PCE) is a high-production volume chemical and a ubiquitous environmental contaminant that is hazardous to human health. Toxicity of PCE is mediated through oxidative and glutathione conjugation metabolites. The conjugation of PCE by glutathione-s-transferase to generate S-(1,2,2-trichlorovinyl) glutathione (TCVG), which is subsequently metabolized to form S-(1,2,2-trichlorovinyl)-L-cysteine (TCVC) is of special importance to human health. Specifically, TCVC can be metabolized to N-acetyl-S-(1,2,2-trichlorovinyl)-L-cysteine (NAcTCVC) which is excreted through urine, or to electrophilic metabolites that are nephrotoxic and mutagenic. Little is known about toxicokinetics of TCVG, TCVC, and NAcTCVC as analytical methods for simultaneous determination of these metabolites in tissues have not yet been

[1] The text of this chapter is an Author's Original Manuscript of an article published by Taylor & Francis Group in the Journal of Toxicology and Environmental Health, Part A on 11 July 2017, available online: https://doi.org/10.1080/15287394.2017.1330585

reported. Hence, we aimed to develop an ultra-high performance liquid chromatography electrospray ionization tandem mass spectrometry-based method for analysis of TCVG, TCVC, and NAcTCVC in liver, kidney, serum, and urine. We show that the method is rapid, sensitive, robust, and selective for detection all three analytes in every tissue examined, with limits of detection ranging from 1.8-68.2 femtomoles on column, depending on the analyte and tissue matrix. We also demonstrated that this method can be applied to quantify levels of TCVG, TCVC, and NAcTCVC in tissues from mice treated with PCE (10 to 1000 mg/kg, orally) with limits of quantitation of 1-2.5 pmol/g in liver, 1-10 pmol/g in kidney, 1-2.5 pmol/mL in serum, and 2.5-5 pmol/mL in urine. This method is useful for further characterization of the glutathione conjugative pathway of PCE in vivo and improved understanding of PCE toxicity.

2.2 Introduction

Tetrachloroethylene (perchloroethylene; PCE) is a high-production volume chlorinated olefin solvent with wide-ranging industrial applications, which include dry cleaning, metal degreasing, and chemical synthesis; however, the use of PCE in dry cleaning has been curtailing in the United States since 2006. Exposure to PCE is common in humans because PCE is difficult to remediate from contaminated sites and it is a ubiquitous contaminant of soil, ground and drinking water, and air (IARC, 2014). PCE is also one of the most commonly found contaminants at hazardous waste sites(National Research Council, 2010). Federal and international regulatory agencies are concerned about understanding PCE toxicity (IARC, 2014; U.S. EPA, 2011b) and PCE is among the

first 10 chemicals that EPA will evaluate for risks to human health under the new Frank R. Lautenberg Chemical Safety for the 21st Century Act (U.S. EPA, 2017).

In both rodents and humans, the liver and kidney are main target organs for cancer and non-cancer effects of PCE; however, few studies have examined PCE toxicity (Cichocki, *et al.*, 2016; Lash *et al.*, 2002). The liver and kidney bioactivate PCE to reactive metabolites *in situ* through both oxidative and conjugative metabolic pathways (Guyton *et al.*, 2014; Lash and Parker, 2001). Oxidation of PCE yields trichloroacetate (TCA) as the primary metabolite and is thought to occur mostly via hepatic cytochrome P450s (Cichocki, *et al.*, 2016). PCE is also conjugated with glutathione (GSH) via hepatic or renal glutathione-S-transferases (GSTs) to form S-(1,2,2-trichlorvinyl) glutathione (TCVG)(Dekant, 1993; Lash and Parker, 2001). TCVG can be further metabolized in the kidney by gamma-glutamyl transferase (GGT) and dipeptidase to form S-(1,2,2-trichlorovinyl)-L-cysteine (TCVC). TCVC can either be detoxified via N-acetyltransferases to N-acetyl-S-(1,2,2-trichlorovinyl)-L-cysteine (NAcTCVC), bioactivated to 1,2,2-trichlorovinylthiol via cysteine conjugate β-lyase, or to TCVC sulfoxide via flavin-containing monoxygenase 3 and cytochrome P450s (Ripp *et al.*, 1997). Both 1,2,2-trichlorovinylthiol and TCVC sulfoxide can spontaneously form a reactive thioketene which can adduct to DNA and proteins(IARC, 2014). PCE metabolites from the GSH conjugation pathway are cytotoxic *in vitro* (Birner *et al.*, 1997; Irving and Elfarra, 2013; Lash, *et al.*, 2002)and nephrotoxic *in vivo* (Birner, *et al.*, 1997; Elfarra and Krause, 2007). They are also mutagenic (Irving and Elfarra, 2013; Vamvakas, *et al.*, 1989a; Vamvakas, *et al.*, 1989b). Therefore, determining tissue-specific levels of these

metabolites is critical to establishing concentration-response relationships for PCE exposure and effects (Cichocki, *et al.*, 2016).

The quantification of TCVG in in vitro experiments using isolated rodent hepatocytes, renal cortical cells, and/or subcellular fractions has been described (Lash *et al.*, 1998). The development of a method that can simultaneously detect TCVG, TCVC, and NAcTCVC in multiple tissues from animals and humans is hindered by their very low abundance as compared to oxidative metabolites of PCE (Chiu and Ginsberg, 2011). Still, characterization of the flux of PCE to nephrotoxic (TCVG, TCVC, or their distal metabolites) or n-acetylated (NAcTCVC) metabolites is needed to fill a critical data gap and improve public health assessments of PCE.

To this end, a method for extraction and quantification of TCVG, TCVC, and NAcTCVC in multiple tissues was developed. Efficient extraction of these analytes was achieved by solid-phase extraction (SPE). By coupling reverse-phase ultra-high performance liquid chromatography (UPLC) to electrospray ionization tandem mass spectroscopy (MS/MS), levels of all three PCE conjugates were simultaneously quantified from a relatively small amount of biological material (50 mg or µL of tissue). This method proved to be sensitive, robust, and precise, and was utilized to quantify levels of TCVG, TCVC, and NAcTCVC in a series of studies in mice. This method will be useful for future animal and human studies.

2.3 Methods

2.3.1 Chemicals

2-amino-5-[(1-{[(¹³C)carboxy(¹³C)methyl](¹⁵N)amino}-1-oxo-3-[(trichloroethenyl)sulfanyl]propan-2-yl)amino]-5-oxopentanoic acid (TCVG*, purity: 90.4%), 2-(¹⁵N)amino-3-[(trichloroethenyl)sulfanyl](¹³C_3)propanoic acid (TCVC*, purity: 97.5%), and 2-[acetyl(¹⁵N)amino]-3-[(trichloroethenyl)sulfanyl](¹³C_3)propanoic acid (NAcTCVC*, purity: 99.0%) were used as internal standards (I.S.) for TCVG, TCVC, and NAcTCVC, respectively. TCVG (purity: 98.9%), TCVC (purity: 98.4%), and all stable isotopically-labeled I.S. were synthesized and provided by Dr. Avram Gold at the University of North Carolina, Chapel Hill, NC. Purity of the synthetized standards was determined using HPLC-UV/Vis (Thermo Fisher Scientific, Waltham, MA) detection in a full scan mode for the wavelength range from 190 to 600 nm followed by a detection at the wavelength set at 254 nm (Figure A-1). NAcTCVC (CAS:111348-61-9, reported purity: 99.7%) was obtained from Toronto Research Chemicals (Toronto, Canada).

2.3.2 Animals and treatments

Two studies were conducted to collect tissues for these experiments. Both used male C57BL/6J mice (6-8 weeks of age) from the Jackson Laboratory (Bar Harbor, ME). Animals were acclimated for 1 week before treatments. All animal treatments and procedures were approved by the Institutional Animal Care and Use Committee at Texas A&M University.

In the first study, mice were intragastrically dosed with 0, 100, 300, or 1000 mg/kg PCE (5 mL/kg in 5% alkamuls-EL620 in saline) via gavage (n=3/group). These doses were selected based on previous studies in mice that showed saturation of PCE oxidative metabolism at similar doses (Buben and O'Flaherty, 1985; Philip *et al.*, 2007); thus, we aimed to determine whether GSH conjugation metabolism of PCE might be also saturated at these doses. In addition, this dose range was used in a chronic cancer bioassay via oral exposure to PCE in mice (National Toxicology Program, 1977). Mice were euthanized two hours after gavage and blood and organs were snap-frozen for determination of metabolites. As no other study has examined PCE metabolism through the GSH pathway *in vivo*, we selected the two hour time point based on studies of toxicokinetics of the conjugative metabolites of trichloroethylene (Bradford *et al.*, 2011; Kim *et al.*, 2009b; Yoo *et al.*, 2015c), a chemical which is structurally similar to PCE.

In the second study, to characterize the urinary excretion of the GSH conjugation metabolites of PCE, mice were intragastrically dosed with 10, 100, or 1000 mg/kg PCE in a vehicle detailed above and then housed in metabolic cages (Hatteras Instruments, Cary, North Carolina) for collection of urine into a chilled container over a 24 hr period (n=3 per group).

2.3.3 Tissue Processing

Serum (50 µL) was thawed on ice, spiked with 10 pmoles of each internal standard, and then mixed with 100 µL of methanol to precipitate protein. The sample was then vortexed and centrifuged (14,000 g, 5 min, 4 ºC). The supernatant was diluted with 850

μL of distilled deionized water prior to SPE. Liver or kidney (50 mg) was spiked with 10 pmoles of each internal standard, and then homogenized in 200 μL of methanol and 200 μL of chloroform using stainless steel beads in a Bead Ruptor 24 (Omni Inc, Kennesaw, GA) for 30 seconds at 4 m/s. Homogenates were centrifuged (10,000 g, 5 min, room temperature), the supernatant was vortexed with 1000 μL of water and centrifuged again (10,000 g, 5 min, room temperature). The supernatant was used for SPE (see below). Urine (50 μL) was spiked with 10 pmoles of each internal standard, and then mixed with 100 μL of methanol for protein precipitation. The sample was then vortexed and centrifuged (10,000 g, 5 min, room temperature). The supernatant was diluted with 350 μL of ammonium formate buffer (15 mM, pH=7) for direct LC-MS/MS analysis without the use of SPE.

2.3.4 Solid Phase Extraction (SPE)

Strata-X-AW (cat no. 8E-SO38-TGB, sorbent lot no. S308-0066; Phenomenex, Torrance, CA) 96-well SPE cartridges were used to trap the anionic analytes. Cartridges were conditioned with 600 μL acidified methanol (0.1% acetic acid, v:v) and equilibrated with UPLC-grade water (600 μL), no vacuum was applied to the SPE manifold and reagents were allowed to flow through via gravity. Samples were then loaded onto cartridges and washed with 300 μL water. Analytes were eluted with 300 μL basified methanol (pH 10.8 via NH_4OH) under gravity; at the end of the procedure, gentle vacuum (650 mBa) was applied to capture as much sample as possible. The entire eluent was transferred to a 1.5 mL microcentrifuge tube and was taken to dryness in vacuo; typically,

an overnight drying was necessary in the vacuum concentrator at room temperature. The residue was reconstituted in 50 µL of water: methanol (80:20, v:v) containing 0.1% acetic acid and transferred to an autosampler vial. Samples were stored at or below -20^{o}C prior to analysis.

2.3.5 UPLC parameters

Samples were maintained at 4^{o}C in the auto-sample manager of a Waters Acquity H-class UPLC (Waters, Milford, MA) during analyses. Samples (10 µL) were automatically injected into the UPLC and were chromatographed on a ZORBAX SSHD Eclipse Plus C18 column (3.0x50 mm, 1.8 µm, cat no. 959757-302; Agilent, Santa Clara, CA) with a guard column (2.1x5 mm, 1.8 µm, cat no.821725-901; Agilent, Santa Clara, CA). For each sample analysis, initial chromatographic conditions were 80% solvent A (water with 0.1% formic acid) and 20% solvent B (methanol with 0.1% formic acid). Conditions were maintained from 0-1 min, then increased to 90% of solvent B by 3 mins, then to 98% of solvent B by 4 mins, then to 20% of solvent B by 4.2 mins. Then, 20% of solvent B was maintained until 7 mins to allow sufficient equilibration time prior to the next injection. Flow rate was maintained at 0.4 mL/min. Column temperature was controlled at 25^{o}C.

2.3.6 MS/MS parameters

An Agilent 6470 triple-quadrupole mass-spectrometer was used for all analyses. To optimize the MS/MS parameters for each analyte, pure material was dissolved in

mobile phase and directly injected (column off-line) into the MS at the flow rate of 0.5 mL/min (methanol:water, 50:50, v: v, containing 0.1% formic acid). The Optimizer Tool (MassHunter, ver. B.08.00) on the Agilent software was used to achieve optimization of the fragmentor, collision energy, cell accelerator voltage, and mass transition for each analyte (Table B-**1**). Capillary voltage, sheath gas pressure, sheath gas temperature, and capillary temperature were optimized manually along with real chromatographic condition (column in-line, Table B-**2-5**).

2.3.7 Method Validation

Matrix-matched calibration curves were prepared with serum, urine, liver, and kidney obtained from untreated mice. Blank serum (50 µl), urine (50 µl), liver (50 mg), or kidney (50 mg) was spiked with standards for TCVG, TCVC (both at 0, 0.25, 0.5, 1.25, 2.5, 6.25, 18.75, and 31.25 pmoles), and NAcTCVC (0, 0.5, 1.25, 2.5, 6.25, 18.75, and 31.25 pmoles). All standard solutions were also spiked with 10 pmoles of each internal standard. Quantitative analysis was achieved by using the peak area ratios of standards and internal standards.

Selectivity of the method was determined by using tissues obtained from six different animals. Sensitivity was defined as a limit of detection (LOD, the concentration with signal to noise ratio of 3), and a lower limit of quantification (LLOQ, the lowest concentration to be quantifiable at 20% of precision and accuracy). Sample to sample carry-over effect, as well as inter-channel cross talk were tested by using the highest concentration in the calibration curve.

Intra-day precision and accuracy (six injections per matrix and concentration) were evaluated by using serum, urine, liver, and kidney obtained from untreated mice spiked with TCVG, TCVC (both at 0.25, 2.5, and 25 pmoles), and NAcTCVC (2.5 and 25 pmoles). Inter-day precision and accuracy were further assessed in six consecutive days. Recovery (RE%), matrix effect (ME%), and process efficiency (PE%) were calculated as detailed elsewhere (Matuszewski *et al.*, 2003).

Freeze and thaw stability, short-term stability, long-term stability, and on-tray stability of TCVG, TCVC, and NAcTCVC were evaluated by comparing peak areas of extracted samples before and after each test condition. Three freeze-thaw cycles at -20^{o}C were applied to test the freeze and thaw stability. Samples were placed at room temperature for 4 h to evaluate short-term stability. For long-term stability, samples were stored at -20^{o}C for 30 days. On-tray stability was evaluated at 4^{o}C for 6 h. Stability of stock solutions was evaluated after they were placed at room temperature for 6 h.

2.3.8 Statistical analyses

GraphPad Prism (ver. 5, GraphPad Software, La Jolla, CA) was used to conduct one-way ANOVA and post-hoc tests. A p-value of less than 0.05 was considered significant in all analyses.

2.4 Results and Discussion

2.4.1 Product ion transitions and MS/MS parameters

Product ion spectra of all standards were obtained in positive ion mode via direct injection without a column (Figure 2.1). The precursor ion $(M+H)^+$ of TCVG is *m/z* 436, which is consistent with the chemical structure of TCVG and with previous report. Fragment ions of TCVG include *m/z* 307 by loss of trichloroethenyl moiety, *m/z* 290 by loss of γ-glutamyl moiety, and *m/z* 361 by loss of glycine moiety. The precursor ions for TCVC and NAcTCVC were determined experimentally. For TCVC, the precursor ion is *m/z* 250. Fragment ions of TCVC include *m/z* 233 by loss of an ammonium group, *m/z* 203.8 by loss of a carboxyl group, and *m/z* 160.8 by loss of a trichloroethenylthiol group. The precursor ion of NAcTCVC is *m/z* 292. Fragment ions include *m/z* 232.9 by loss of an acetylamine group, *m/z* 250 by loss of an acetyl group, and *m/z* 203.9 by loss of an acetyl and a carboxyl group. The quantifier and qualifier ion transitions of each analyte are summarized in Table 2.1.

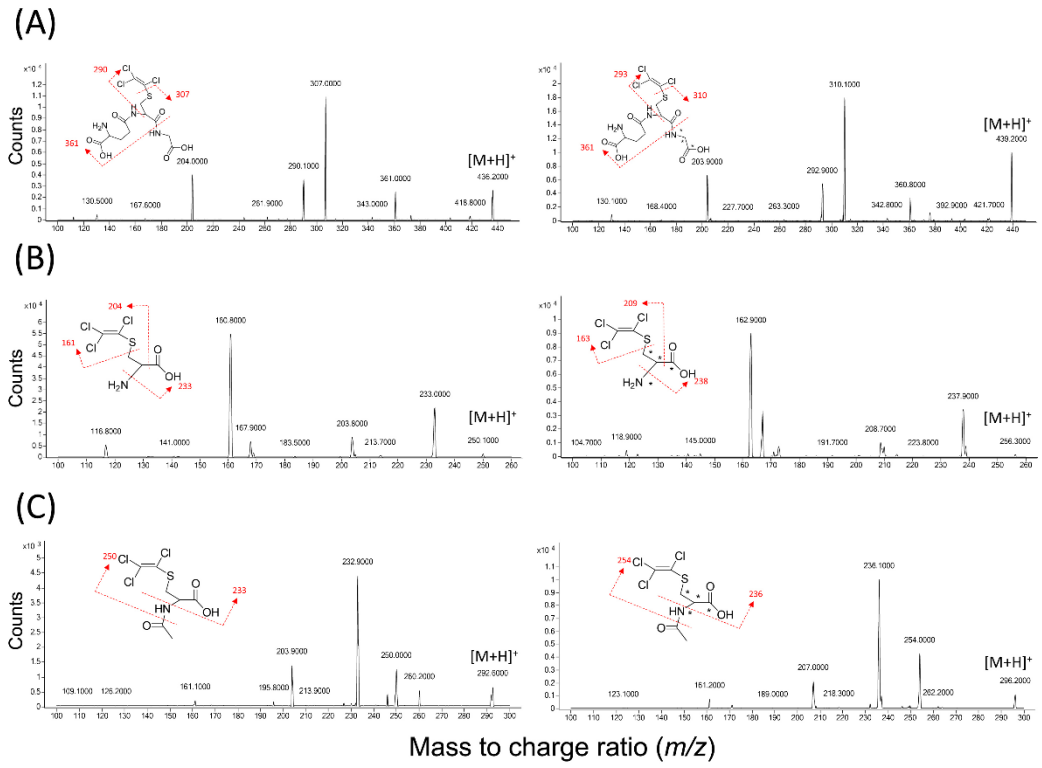

Figure 2.1 Product ion spectra of (A) TCVG (left) and TCVG* (right), (B) TCVC (left) and TCVC* (right), and (C) NAcTCVC (left) and NAcTCVC* (right). The precursor ion (M+H+) of TCVG is m/z 436. Fragment ions of TCVG include m/z 307 (-C2Cl3), m/z 290 (-C5H9N2O3), and m/z 361(-C2H4NO2). (B) The precursor ion (M+H+) of TCVC is m/z 249.9. Fragment ions of TCVC include m/z 233 (-NH3), m/z 203.8 (-COOH), and m/z 160.8 (-C2Cl3S). (C) The precursor ion of NAcTCVC is m/z 291.9. Fragment ions include m/z 232.9 (-C2H4NO), m/z 250 (-C2H3O), and m/z 203.9 (-C2H3O and –COOH). TCVG*, TCVC*, and NAcTCVC* share the identical fragmentation with their corresponding unlabeled standard.

Considering the natural abundance of chlorine isotopes (^{35}Cl, ^{37}Cl), and the pattern of stable-isotope labelling of the all three internal standards, alternative ion transitions were selected to avoid cross-talk among channels. The ion transition of *m/z* 443→313.8, not *m/z* 439→310.1, was used as the quantifier of TCVG*. Likewise, *m/z* 295.9→235.8 ion transition was selected as the quantifier of NAcTCVC* because of its unique

fragmentation (due to position of the stable-isotope labels) which can distinguish NAcTCVC* from NAcTCVC (*m/z* 295.9→236.8). There was no ion channel cross-talk effect observed for TCVC and TCVC*.

To avoid the interference from matrices, matrix-specific mass transitions were used for quantification of each analyte (Table 2.1). In general, the most abundant mass transition of each compound was used as a quantifier. However, we observed interferences in quantifier channels of TCVC* (255.9→237.8) in serum. Therefore, we used *m/z* 255.9→162.9 as the quantifier of TCVC* specifically in serum. The quantifiers listed in Table 1 show good selectivity of the method in liver, kidney, and urine.

Table 2.1 Quantifiers and qualifiers for analysis of TCVG, TCVG, and NAcTCVC in multiple tissue.

Analytes	Ion transition (*m/z*)	Collision energy (V)	Fragmentor (V)
TCVG	436.0→306.8	13	118
	436.0→203.9	25	118
	438.0→308.8†	13	118
TCVG*	443.0→313.8†	17	118
	439.0→309.8	13	118
TCVC	251.9→234.8†	9	90
	249.9→160.8	21	90
	249.9→232.8	9	90
TCVC*	255.9→237.8†	9	90
	255.9→162.9‡	21	90
NAcTCVC	291.9→249.8†	9	90
	291.9→232.8	17	90
	293.9→251.8	9	90
NAcTCVC*	295.9→235.8†	9	90
	295.9→253.8	17	90

† Selected quantifier for analysis. ‡ Alternative quantifier of TCVC* in serum. Dwell time and cell accelerator voltage were set at 25 ms and 2 V.

2.4.2 Ionization parameters

Ionization parameters including capillary voltage, sheath gas temperature, drying gas temperature, and nebulizer gas pressure were optimized along with the chromatographic conditions. Given that efficient separation for TCVG, TCVC, and NAcTCVC was achieved, analytes were optimized individually. In the positive ion mode, the abundance of all three analytes was optimal with a capillary voltage of 3600V. Signal

variation increased when sheath gas temperature was above 350^{o}C. Drying gas temperature was optimal at 300^{o}C. The increased variation and signal depression likely resulted from thermolysis of precursor ions. Optimization of nebulizer gas pressure showed that TCVC and TCVG need higher gas pressure for ionization.

2.4.3 Method validation

Figure 2.2 shows representative chromatograms of the analytes. Peaks of TCVC and TCVC*, TCVG and TCVG*, and NAcTCVC and NAcTCVC* co-eluted at 3.28, 3.58, and 4.04 min, respectively for each pair. Matrix-matched calibration curves were constructed for serum, urine, liver, and kidney (Figure 2.3). Slopes of calibration curves were similar across different matrices (CV<5%), demonstrating no inter-tissue matrix effects when stable isotope-labeled internal standards are employed. No sample-to-sample carryover effect was observed for TCVC analysis across tissues (data not shown). TCVG and NAcTCVC showed minimal sample-to-sample carryover (TCVG <0.22 % and NAcTCVC <1% at 6.25 pmoles of each metabolite on column).

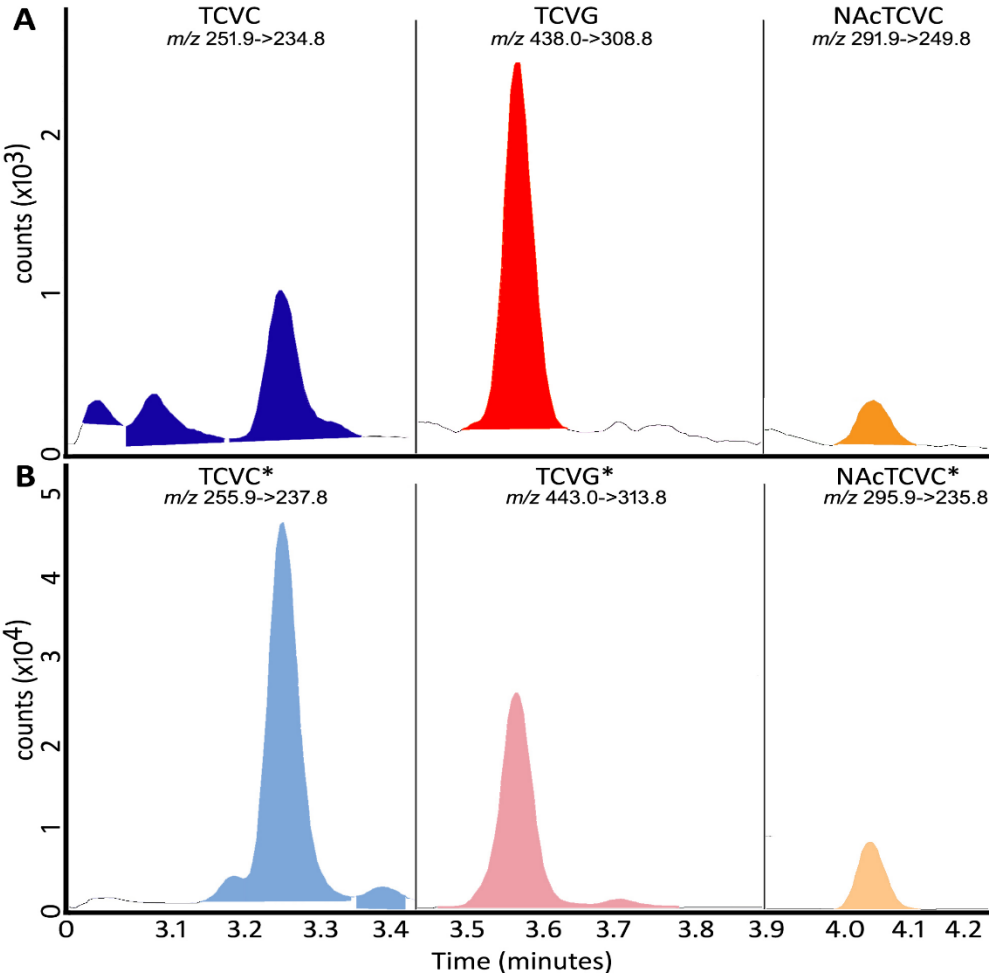

Figure 2.2 Representative LC-MS/MS chromatogram for (A) standards and (B) internal standards of TCVG, TCVC, and NAcTCVC in liver. The spiked amount on-column was 0.025 pmoles for TCVG and TCVC, 0.05 pmoles for NAcTCVC, and 2 pmoles for TCVG*, TCVC*, and NAcTCVC*.

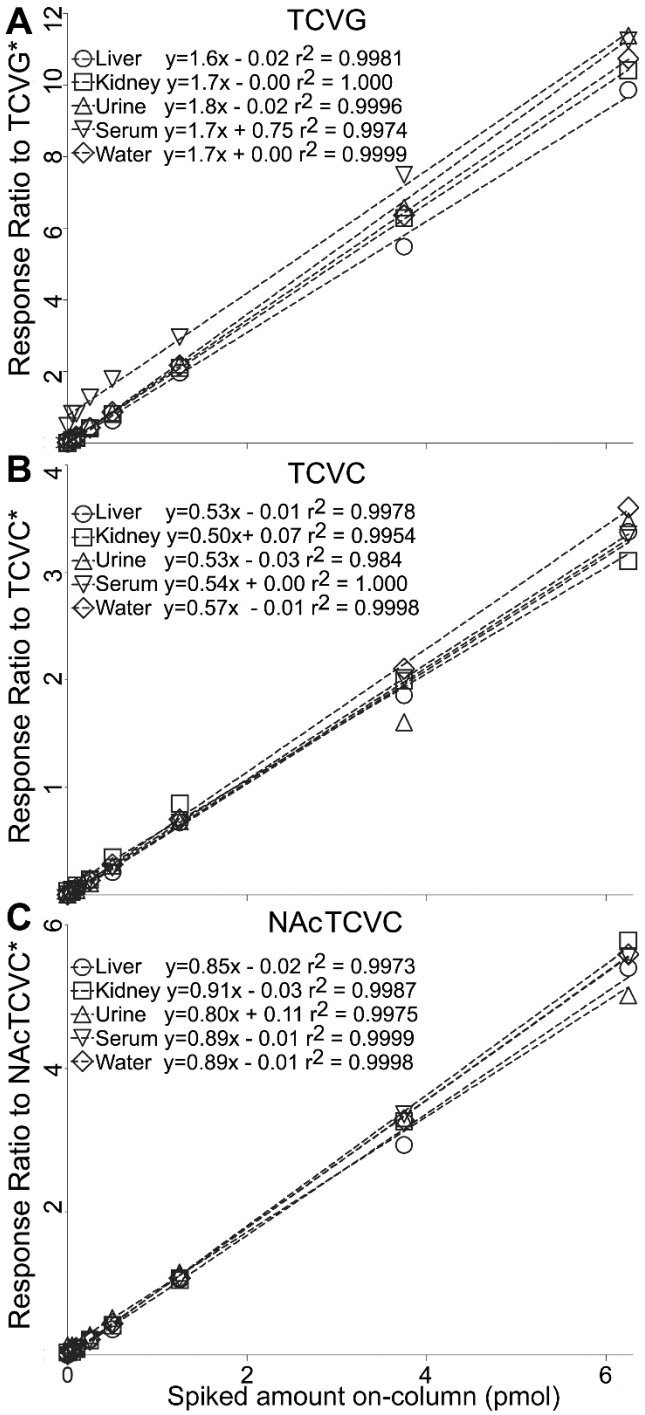

Figure 2.3 Matrix matched calibration curves for (A) TCVG, (B) TCVC, and (C) NAcTCVC. *X* axis, expected amount of spiked standards on column; *y* axis, peak area ratio of standard to internal standard.

The method described herein was highly sensitive for the analysis of TCVC, TCVG, and NAcTCVC across tissues and represents the first study to report on the method for TCVC in tissues (Table 2.2). As compared to previously published method for TCVG (Lash, *et al.*, 1998), we show about 10^4 lower LOD. Even though the sensitivity of NAcTCVC detection was reduced by applying positive, versus negative, electrospray ionization to achieve higher sensitivity of TCVG and TCVC, the sensitivity for urinary analysis of NAcTCVC is still superior to previously published methods (Bartels, 1994; Birner *et al.*, 1996; Volkel *et al.*, 1999). Interestingly, the LOD of NAcTCVC in serum is 3-6 fold lower than that in other matrices, which probably results from the ion enhancement effect of NAcTCVC in serum (See below)

Table 2.2 Comparative analysis of LODs for TCVG, TCVC, and NAcTCVC between tissues and studies.

Reference	Matrix	Extraction method*	Detect Method	TCVG† (fmole)	TCVC (fmole)	NAcTCVC (fmole)
This study	Liver	LL-SPE	LC-MS/MS	4.5	22.7	31.3
	Kidney			4.2	68.2	17.8
	Serum	PP-SPE		3.4	9.4	5.4
	Urine	PP-Direct dilution		13.5	22	26.3
	Instrumental LOD‡			2.1	1.8	14
Bartels et al., 1994	Urine	LL and derivatization with methanolic HCl	NICI-GC-MS/MS	N/R	N/R	4
Birner et al., 1996	Urine	Derivatization with diethylether/diazomethane	GC-MS	N/R	N/R	60,000
Lash et al., 1998	Hepatocyte	Derivatization with 1-fluoro-2,4-dinitrobenzene	HPLC-UV	50,000	N/R	N/R
Volkel et al., 1999	Urine	LL and derivatization with methanolic BF_3	NICI-GC-MS	N/R	N/R	20

† Limit of detection (LOD) is defined as the tested concentration with the signal-to-noise ratio equals to 3, and expressed with the on-column amount of analyte. N/R: Not reported. ‡ Instrumental LOD was tested in de-ionized water. *LL-SPE: liquid-liquid extraction coupled with SPE; PP-SPE: protein precipitation coupled with SP

2.4.4 Extraction recovery and matrix effect

Methanol:chloroform was selected as the homogenizing solution to standardize the extraction procedure in liver and kidney samples and because analyte recovery was significantly improved (Figure A-2). Serum was extracted by protein precipitation rather than liquid-liquid extraction to avoid sample loss. Urine was diluted with ammonium formate buffer to balance pH.

Recoveries and matrix effects of TCVG, TCVC, and NAcTCVC varied at different tested concentrations and among tissues (Table B-**6-9**). The recovery of analytes was generally highest in urine and serum, and lowest in liver and kidney. Variability in recovery was observed, which may have been a consequence of experimental error in the liquid-liquid or solid-phase extraction steps, or may be a result of differential composition among matrices. Overall, there was negligible matrix effect, except in urine where we observed appreciable concentration-dependent ion suppression or enhancement (Table 2.3). Despite these matrix effects, the use of stable isotope-labeled internal standards permitted accurate and precise quantitation (see below).

		Liver			Kidney			Serum			Urine		
		TCVG	TCVC	NAcTCVC	TCVG	TCVC	NAcTCVC	TCVG	TCVC	NAcTCVC	TCVG	TCVC	NAcTCVC
	RE(%)[†]	50	32	58	53	43	60	56	43	68	81	91	102
	ME(%)	115	100	91	107	102	85	90	94	110	126	91	105
	PE(%)	57	32	53	57	44	51	51	40	74	102	83	107
Intra-day[₸]	Accuracy(%)	-2.5	-0.1	+1.0	+11.5	+3.2	+6.5	+0.8	+1.3	+8.6	+1.2	+5.9	+4.9
	Precision(%)	5.5	3.4	11.6	9.8	6.9	10.0	6.1	2.9	10.8	5.4	10.9	19.9
Inter-day	Accuracy(%)	-3.2	-2.7	+0.5	-1.5	+2.3	-8.1	+4.9	-0.8	+2.2	+6.0	+5.0	+17.7
	Precision(%)	10.3	1.7	9.0	2	3.3	8.3	6.9	5.4	6.7	4.7	18.0	7.6
On-tray stability (%)[*]		102 ± 12	99 ± 6	104 ± 9	106 ± 1	105 ± 1	103 ± 1	102 ± 1	105 ± 1	104 ± 3	103 ± 3	101 ± 6	97 ± 11
Short-term stability (%)		106 ± 7	106 ± 5	108 ± 6	102 ± 1	101 ± 1	102 ± 2	101 ± 1	102 ± 1	98 ± 2	99 ± 3	101 ± 3	99 ± 6
Long-term stability (%)		98 ± 2	102 ± 3	114 ± 4	102 ± 2	101 ± 6	99 ± 2	100 ± 6	98 ± 2	99 ± 3	107 ± 6	53 ± 8	102 ± 85
Freeze-thaw stability (%)		102 ± 2	98 ± 3	88 ± 3	98 ± 2	99 ± 6	101 ± 2	100 ± 6	102 ± 2	101 ± 3	94 ± 5	193 ±31	301 ± 396

Table 2.3 Comparative analysis of method performance of TCVG, TCVC, and NAcTCVC in multiple tissues. [†]Method validation for analysis of TCVG, TCVC, and NAcTCVC was compared at level of 50 pmole/g tissue or mL serum across different tissues. Recovery (RE), matrix effect (ME), and process efficiency (PE) were determined from n=5. [₸] Inter-day (n=6) and intra-day (n=6) accuracy (%) are expressed as bias deviated from the nominal concentration. Precision (%) is expressed as relative standard deviation. * Results of stabilities are expressed in average ± standard deviation (n=3).

2.4.5 Inter- and intra-day accuracy and precision

Inter-day accuracy and precision were further evaluated across six different days; intra-day accuracy and precision were assessed by using six biological replicates in the same day. Our results show that this method is accurate (bias <15%) and reliable (precision <15%) for analysis of TCVG, TCVC, and NAcTCVC in liver, kidney, and serum (Table 2.3). Urinary analysis of NAcTCVC exhibited slightly higher variability; however, it still passed the criteria for determining the LLOQ (accuracy and precision <20%). The inferior performance of NAcTCVC is not surprising because this method is operated in positive ion mode, which is optimized for TCVG and TCVC, but not for NAcTCVC. Also, some blank urine samples had background levels of NAcTCVC, which may also introduce the variability into urinary analysis of NAcTCVC.

2.4.6 Analyte stability

Stock solutions and extracted samples were evaluated with respect to the stability of TCVG, TCVC, and NAcTCVC under various storage conditions. Stock solutions were stable at room temperature for up to 6 hours (data not shown). Analytes were stable in liver, kidney, and serum when evaluated for the on-tray, short-term, long-term, and freeze-thaw conditions (Table 2.3). Results in urine show that TCVC and NAcTCVC are unstable for long-term storage at -20^{o}C or three freeze and thaw cycles. However, analytes in extracted urine samples are considered stable on-tray or for short-term storage. Thereby, long-term storage and repeated freeze and thaw cycles should be avoided for analysis of these analytes in urine samples.

2.4.7 Application to toxicokinetic profiling of PCE in vivo

Next, we applied this method to quantitate TCVG, TCVC, and NAcTCVC in multiple tissues of PCE-exposed mice. First we conducted a study where mice were treated with a single dose of PCE (100, 300, or 1000 mg/kg) and euthanized 2 hrs after oral gavage. Tissue levels of analytes demonstrated a dose-dependent increase with ascending dose of PCE (Figure 2.4). Levels of all three metabolites varied across tissues in a metabolite-specific manner. For instance, in mice treated with 1000 mg/kg PCE, we found that TCVG level was 16.7-fold higher in liver as compared to that in kidney or serum. TCVC level in kidney was higher than that in liver (18.3-fold) or serum (2.1-fold). Likewise, NAcTCVC level in urine was higher than that in liver (1.7-fold), kidney (13.7-fold), and serum (4.6-fold) (Figure 2.5A).

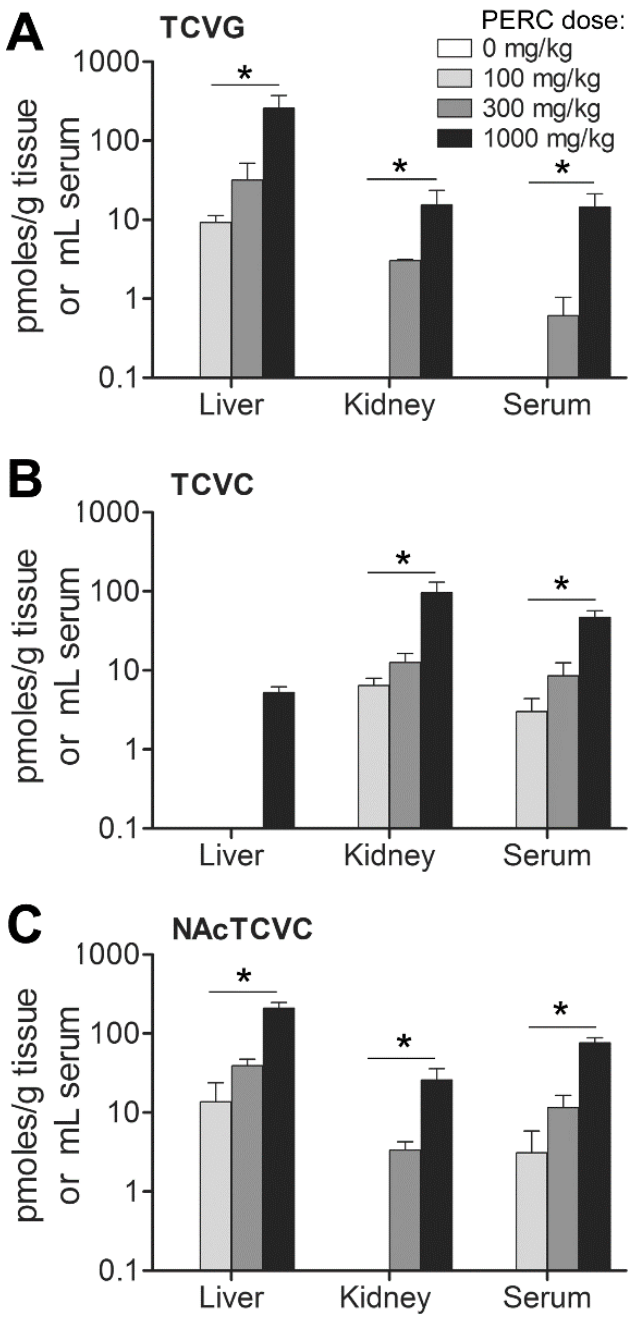

Figure 2.4 Dose-response relationships of (A) TCVG, (B) TCVC, and (C) NAcTCVC in liver, kidney, and serum of mice treated with PCE (n=3 for each dose as indicated in the inset). Data shown are group means with standard deviations. The significance of dose-response relationships in each tissue was tested by one-way ANOVA and post-hoc test for a linear trend (*$p < 0.05$).

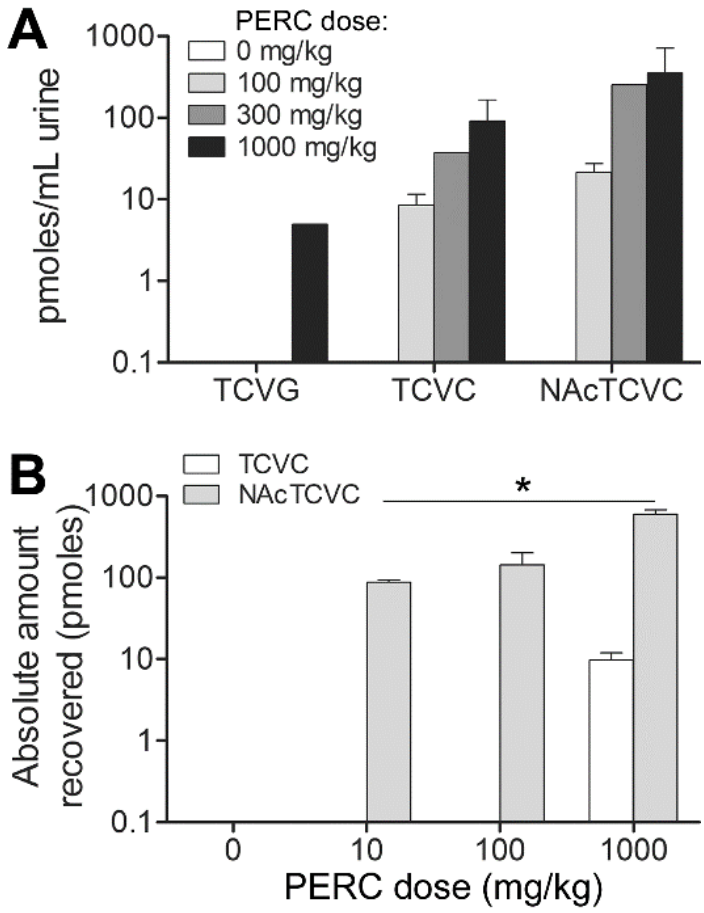

Figure 2.5 Analysis of TCVG, TCVC, and NAcTCVC in urine of PCE-treated mice at (A) 2 hrs or (B) 24 hrs after dosing. Data shown are group means with standard deviations. The significance of the dose-response relationship was tested by one-way ANOVA and post-hoc test for a linear trend (*$p < 0.05$).

The observed differences in metabolite levels across different tissues are consistent with PCE metabolism pathways. GSH conjugation of PCE and other chemicals predominantly occurs in liver because of the high activity of GSH S-transferases (Moron *et al.*, 1979). Renal GGT and dipeptidase activity is responsible for high levels of TCVC in kidney (Griffith and Meister, 1979). Also, the reabsorption of cysteine S-conjugates, as demonstrated in rat kidney (Heuner *et al.*, 1991) and LLC-PK1 cells (Schaeffer and

Stevens, 1987), and the deacetylation of NAcTCVC that is catalyzed by renal aminoacylase (Uttamsingh *et al.*, 1998) can also contribute to the high levels of TCVC in kidney. Interestingly, we found large quantities of NAcTCVC in liver even though the activity of gamma-glutamyl transpeptidase is approximately one-fifth of that in kidney (Whitfield, 2001). Intrahepatic conversion of GSH conjugates to mercapturic acids by N-acetyltransferase activity has been reported in rat and guinea pig livers (Hinchman *et al.*, 1991), which could account for the generation of NAcTCVC in liver. Further mechanistic investigation on the fate of PCE conjugative metabolites *in vivo* is possible using this method.

Next, we quantified urinary levels of NAcTCVC in mice treated with PCE (10, 100, or 1000 mg/kg) (Figure 2.5B). Our results demonstrate that NAcTCVC is a major conjugative metabolite (~98% of combined amount of TCVG, TCVC, and NAcTCVC) excreted in urine. This is not surprising because the renal transport systems favor reabsorption of amino acids, but excretion of mercapturates. Our method is able to profile urinary levels of NAcTCVC in mice treated with as little as 10 mg/kg PCE (46.8±9.1 pmol/mLurine, approximately 100 pmoles total) using only 50 µL of sample volume. In a previous study, rats and humans exposed to 10 ppm PCE by inhalation for 6 h excreted (24 hr urine collection) ~500 pmol and 40 nmol of NAcTCVC, respectively (Volkel *et al.*, 1998). Therefore, our method should be sufficiently sensitive for detection of urinary NAcTCVC in PCE-exposed animals and humans.

The sensitivity of our method also allowed us to demonstrate the linear dose-dependent increase of NAcTCVC, which suggests that the conjugative metabolism of PCE remains unsaturated at doses up to 1000 mg/kg. Lack of saturation of the GSH conjugation

metabolism pathway of PCE is noteworthy because the oxidative metabolism is saturated above 100 mg/kg (Philip, *et al.*, 2007) and may reflect the small overall flux of PCE through conjugation in mice.

2.5 Conclusions

Metabolism of PCE is qualitatively similar in humans and rodents, although quantitative differences do exist (Cichocki, *et al.*, 2016). These quantitative differences in metabolism may be important for extrapolation of data derived from rodents to human health assessments for PCE.

It is now assumed that flux of PCE through conjugative pathways is minimal as compared to oxidative pathways; these assumptions are largely based on the data for trichloroethylene and quantification of urinary NAcTCVC and oxidative PCE metabolites in PCE-exposed humans and laboratory rodents (Bartels, 1994; Birner, *et al.*, 1996; Volkel, *et al.*, 1999). However, urinary NAcTCVC may represent only a fraction of the overall flux of PCE through GSH conjugation (IARC, 2014).

Little is known about PCE conjugative metabolism *in vivo* due to the lack of a sensitive analytical assays; to our knowledge, no previously published method for analysis of multiple PCE conjugative metabolites exists. To address these critical gaps in our knowledge of PCE toxicity, we developed a rapid, sensitive, and robust UPLC-ESI^+-MS/MS method. For the first time, we provide quantitative data for levels of TCVG, TCVC, and NAcTCVC in multiple mouse tissues after exposure to PCE. We demonstrated that this method has a limit of quantitation of 1-2.5, 1-10, 1-2.5, and 2.5-5 pmol/mL in

liver, kidney, serum, and urine, respectively, while maintaining selectivity of the method and a short duration of analysis.

We also demonstrated that successful quantitation of PCE GSH metabolites can be achieved in all tissues tested despite small amounts of starting material. TCVC and TCVG can be detected and quantified in animals that were dosed with 100 mg/kg or more of PCE, while NAcTCVC is quantifiable in the urine of animals that were dosed with as little as 10 mg/kg of PCE. The range of doses used in this study is well within the range of doses used in PCE rodent cancer bioassays and other animal studies. Thus, our method and data provide important information for interpreting the findings from cancer bioassays in rodents. In addition, it is important to note that this method may have utility for the internal dosimetry of conjugative metabolites in studies of occupational and even environmental exposures in humans because PBPK modeling shows that the PCE fraction conjugated via GSH pathway may be 100 to 1000 fold higher in humans than in mice (Chiu and Ginsberg, 2011).

One important limitation of this method, however, is its focus on proximal metabolites of the GSH conjugation pathway and not on some of the more reactive and toxic downstream metabolites such as TCVC sulfoxide (Elfarra and Krause, 2007). Still, the method reported herein will be applicable to further toxicokinetic studies of PCE and inform human health assessments of this ubiquitous environmental toxicant.

CHAPTER III

CHARACTERIZATION OF INTER-TISSUE AND INTER-STRAIN VARIABILITY OF TCE GLUTATHIONE CONJUGATION METABOLITES DCVG, DCVC, AND NACDCVC IN THE MOUSE[2]

3.1 Overview

Trichloroethylene (TCE) is a ubiquitous environmental toxicant that is a liver and kidney carcinogen. Conjugation of TCE with glutathione leads to formation of nepthrotoxic and mutagenic metabolites thought to be critical for kidney cancer; however, relatively little is known about their tissue levels because previous analytical methods for their detection lacked sensitivity. Here, an LC-MS/MS-based method for simultaneous detection of S-(1,2-dichlorovinyl)-glutathione (DCVG), S-(1,2-dichlorovinyl)-L-cysteine (DCVC), and N-acetyl-S-(1,2-dichlorovinyl)-L-cysteine (NAcDCVC) in multiple mouse tissues was developed. This analytical method is rapid, sensitive (limits of detection 3-30 fmol across metabolites and tissues), and robust to quantify all three metabolites in liver, kidney and serum. The method was used to characterize the inter-tissue and inter-strain variability in formation of conjugative metabolites of TCE. Single oral dose of TCE (24, 240 or 800 mg/kg) was administered to male mice from 20 inbred strains of Collaborative

[2] The text of this chapter is an Author's Original Manuscript of an article published by Taylor & Francis Group in the Journal of Toxicology and Environmental Health, Part A on 30 November 2017, available online: https://doi.org/10.1080/15287394.2017.1408512

Cross. Inter-strain variability in the levels of DCVG, DCVC, and NAcDCVC (GSD=1.6-2.9) was observed. Whereas NAcDCVC was distributed equally among analyzed tissues, the highest levels of DCVG were detected in liver and DCVC in kidney. It is concluded that inter-strain variability in conjugative metabolite formation of TCE can affect the susceptibility to adverse health effects and that this method can aid in filling the data gaps in the human health assessment of TCE.

3.2 Introduction

Trichloroethylene (TCE), a ubiquitous environmental toxicant, causes liver cancer in mice and kidney cancer in rats and humans (IARC, 2014; U.S. EPA, 2011c). It remains a top ten priority chemical of concern to human health (U.S. EPA, 2017). Upon absorption, TCE is metabolized through cytochrome P450 oxidation and glutathione conjugation pathways in both rodents and humans (Lash *et al.*, 2000). Glutathione conjugation of TCE occurs primarily via glutathione-*S*-transferases (GSTs) in liver to form DCVG. DCVG can be metabolized via liver or kidney gamma-glutamyl transferase and di-peptidase to generate DCVC, which is then further transformed into NAcDCVC via *N*-acetyl transferase. In addition, NAcDCVC can be deacetylated by acylase to regenerate DCVC. Aside from the *N*-acetylation, DCVC can be further metabolized by cysteine conjugate β-lyase to form reactive thioketenes, or undergo sulfoxidation by flavin-containing monooxygenase to form a reactive DCVC-sulfoxide (Lash, *et al.*, 2001b; Sausen and Elfarra, 1990).

Metabolites that are generated through both oxidation and glutathione conjugation pathways are thought to be involved in organ-specific toxicity of TCE (Cichocki, *et al.*,

2016; Lash *et al.*, 2014). While the effects of the oxidative metabolites of TCE have been widely studied (Corton *et al.*, 2014; Rusyn *et al.*, 2014), the metabolites from glutathione conjugation pathway receive less attention because of their low abundance and lack of sensitive analytical methods (Chiu *et al.*, 2009). However, these metabolites are thought to be the cause of kidney cancer in rats and humans (Chiu *et al.*, 2013; Guha *et al.*, 2012). Glutathione conjugation metabolites of TCE are cytotoxic *in vitro* and nephrotoxic *in vivo*; they are also mutagenic in bacterial and mammalian model systems (Chiu, *et al.*, 2013; Dekant, 2003; Guha, *et al.*, 2012; Irving and Elfarra, 2013; Lash, *et al.*, 2014; Lash *et al.*, 2001a; Lash, *et al.*, 2007; Lash, *et al.*, 2001b). Still, the relationship between tissue levels of glutathione conjugation metabolites of TCE and cancer remains unclear (Green *et al.*, 1997; Yoo, *et al.*, 2015b).

Previous studies examined the flux of TCE through glutathione conjugation pathway in tissues of TCE-exposed animals and humans (Bloemen *et al.*, 2001; Kim, *et al.*, 2009a; Lash *et al.*, 1999; Lash *et al.*, 2006; Yoo, *et al.*, 2015a; Yoo, *et al.*, 2015b). The analytical techniques ranged from LC-UV, to GC-MS and LC-MS/MS, and detection limits varied from 25 to 50,000 fmoles for DCVG and DCVC. One study reported a method for NAcDCVC with a detection limit of 80 fmoles (Bloemen, *et al.*, 2001). Most sensitive was the LC-MS/MS-based method for analysis of DCVG and DCVC in mouse tissues (Kim, *et al.*, 2009a; Yoo, *et al.*, 2015a; Yoo, *et al.*, 2015b); however, extraction protocols inconsistency confounds cross-tissue comparisons.

Because of the complexity of metabolism-related effects of TCE, inter-individual variability in pharmacokinetics can play a major role in the susceptibility to toxicity and tissue specificity (Chiu *et al.*, 2006a). Our previous study in mice showed considerable

inter-strain variability in DCVG and DCVC in the liver (Bradford, *et al.*, 2011); there was a greater than 10-fold inter-strain variability in flux of TCE metabolism through glutathione conjugation (Chiu *et al.*, 2014). This study aimed to further characterize inter-individual variability in TCE metabolism through glutathione conjugation, and to extend the quantitative estimates to other tissues. To achieve this, a sensitive analytical method for simultaneous detection of DCVG, DCVC, and NAcDCVC in various tissues was developed using ultra-high performance liquid chromatography coupled with triple quadruple tandem mass spectrometry (LC-MS/MS). Furthermore, the inter-strain variability in levels of TCE conjugation metabolites in various tissues was characterized using 20 inbred strains of Collaborative Cross mice.

3.3 Materials and Methods

3.3.1 Chemicals

S-(1,2-dichlorovinyl)-glutathione (DCVG, purity: 98.9%), 2-amino-5-[(2-([(¹³C)carboxy(¹³C)methyl](¹⁵N)amino)-1-([1,2-dichloroethenyl]sulfanyl)-2-oxoethyl)amino]-5-oxopentanoic acid (DCVG*, purity: 94.4%, isotopic enrichment: 99.0%), S-(1,2-dichlorovinyl)-L-cysteine (DCVC, purity: 98.4%), and 2-(¹⁵N)amino-3-([1,2-dichloroethenyl]sulfanyl)(¹³C_3)propanoic acid (DCVC*, purity: 96.9%, isotopic enrichment: 99.0%) were obtained from TLC pharmaceutical standards (Vaughan, Canada). N-acetyl-S-(1,2-dichlorovinyl)-L-cysteine (NAcDCVC, purity: 99.8%) and 3-([1,2-dichloroethenyl]sulfanyl)-2-[(1-¹³C, d_3)ethanoylamino]propanoic acid (NAcDCVC*, purity: 97.6%, isotopic enrichment: 99.0%) were purchased from Toronto Research Chemicals (Toronto, Canada). Acetic acid (>99.7%), TCE (>99.5%), and

chloroform (>99.9%) were obtained from Sigma-Aldrich (St. Louis, MO). Methanol (>99.9%) was purchased from Fischer Chemicals (Fair Lawn, NJ). De-ionized water was generated by Arium®Pro Ultrapure Water System (Goettingen, Germany).

3.3.2 Animals and treatments

Two animal studies were conducted, both used male mice because TCE is more efficiently metabolized in male, as compared to female, mice (National Toxicology Program, 1990). First was to demonstrate the application of the validated LC-MS/MS method in an *in vivo* study. Second was to characterize inter-individual variability of tissue levels of DCVG, DCVC, and NAcDCVC using a panel of mouse strains. All animal treatments and procedures were approved by the Institutional Animal Care and Use Committee at Texas A&M University and the University of North Carolina at Chapel Hill.

First study was conducted in male B6C3F1/J mice (6-8 wks old) obtained from the Jackson Laboratory (Bar Harbor, ME). Mice were housed in standard polycarbonate shoebox mouse cages with air filtration system on a 12:12 hr light/dark cycle with free access to food (standard laboratory mouse chow) and filtered tap water. After a week-long acclimation, mice (n=3/group) were dosed with 0, 24, 240, 800 mg/kg of TCE (5 mL/kg in 5% alkamus-EL620 in saline) via oral gavage. The aqueous emulsion vehicle was used to aid oral absorption of TCE (Lee *et al.*, 1996; Lee *et al.*, 2000). Dose range was selected based on previous acute and sub-chronic mouse studies showing that these amounts are well-tolerated; doses also corresponded to the range used in both 90-day and 2-year mouse studies (Buben and O'Flaherty, 1985; National Toxicology Program, 1990; Yoo, *et al.*, 2015b). It is also noted that mice form ~100 fold less GSH conjugation pathway

metabolites of TCE as compared to humans (Chiu, *et al.*, 2009) which necessitated the use of doses that are higher than those expected in human exposures.

Second study was conducted in male mice (8-12 weeks old) from 20 Collaborative Cross strains. The Collaborative Cross (CC) is a panel of inbred mouse strains that were recently developed through a community effort (Threadgill and Churchill, 2012). The CC addresses many shortcoming of other available mouse populations such as limited genetic diversity and a non-ideal population structure. The CC strains were derived from an eight way cross using a set of founders that include three wild-derived strains (A/J, C57BL/6J, 129S1/SvImJ, NOD/LtJ, NZO/HlLtJ, CAST/EiJ, PWK/PhJ, and WSB/EiJ) to capture nearly 90% of the known variation present in laboratory mice. The goal of this study was to test inter-strain variability; therefore, the number of CC strains used is comparable to previous studies of inbred mouse panels (Bradford et al., 2011). Mice were acquired from the University of North Carolina Systems Genetics Core (Chapel Hill, NC). Housing and treatment conditions were identical to those detailed above. Mice were orally administered a single dose of TCE (800 mg/kg) prepared in 5% Alkamuls EL-620. In both studies, mice were euthanized with pentobarbital (50 mg/kg, *i.p.*) 2 hrs after dosing and tissues immediately dissected for collection of liver, kidney, and blood. Tissues were snap-frozen in liquid nitrogen and stored at -80^{o}C until analyses. The time point for tissue collection was based on a toxicokinetic study of TCE metabolism that showed peak levels of glutathione conjugates several hours after dosing (Kim, *et al.*, 2009b).

The potential for *ex vivo* formation of conjugation metabolites of TCE was tested using serum (50 μl) and liver (50 mg) samples from untreated mice (male, B6C3F1/J). TCE (5 μM) was reacted with glutathione (5 mM) in saline, serum, or liver homogenates

for 1 hr at 37ºC. Some reactions were carried out with or without protein inactivation (by heating for 10 min at 90ºC), or glutathione depletion through addition of 2,4-dinitrochlorobenzene (0.2 mM). Upon completion of these incubations, samples were extracted and analyzed as detailed below.

3.3.3 Sample preparation

Serum (50 µL) samples were spiked with 10 µL of internal standard mixture (5 µM for each analyte), mixed with 100 µL of methanol to precipitate protein, and then vortexed and centrifuged (10,000 g, 10 min, room temperature). Thereafter, the supernatant was diluted with 850 µL of distilled deionized water for solid phase extraction (SPE). Liver or kidney (50 mg) samples were spiked with 10 µL of internal standard mixture (5 µM for each analyte), and then homogenized in 200 µL of methanol and 200 µL of chloroform using stainless steel beads in a Bead Ruptor 24 (Omni Inc, Kennesaw, GA) for 30 s at 4 m/s. Homogenates were centrifuged (10,000g, 5 min, room temperature), the supernatant was diluted with 1 mL of distilled deionized water, and the diluent was used for SPE. Strata-X-AW 96-well SPE plate (cat no. 8E-SO38-TGB, sorbent lot no. S308-0066; Phenomenex, Torrance, CA) was used. The SPE procedure was slightly modified from our previously published method (Luo *et al.*, 2017). In the final step, the dried residue was reconstituted in 30 µL of water:methanol (9:1, v/v) containing 0.1% acetic acid. Samples were then transferred to an autosampler vial with a 200 µL insert, and stored at -20ºC prior to analysis.

3.3.4 LC-MS/MS Method

Samples (10 μL) were automatically injected and chromatographed on a ZORBAX SSHD Eclipse Plus C18 column (3.0 x 50 mm, 1.8 μm, cat no. 959757-302; Agilent, Santa Clara, CA) with a guard column (2.1x5 mm, 1.8 μm, cat no.821725-901; Agilent) via a Waters Acquity H-class LC system (Waters, Milford, MA). Column temperature was maintained at 25ºC. Initial chromatographic condition was maintained at 90% solvent A (water with 0.1% acetic acid, v/v) and 10% solvent B (methanol with 0.1% acetic acid, v/v) for 1 mins, then increased to 90% solvent B by 3 mins, then to 98% solvent B by 4 mins, and then returned to initial condition until 7 mins for sufficient equilibration prior to next run. Flow rate was set at 0.4 mL/min. All analyses were performed using Agilent 6740 triple-quadrupole mass spectrometer. The optimal MS/MS parameters were obtained via direct infusion of standards and isotopically-labeled internal standards in mobile phase at the flow rate of 0.5 mL/min (1:1 methanol:water, v/v, containing 0.1% formic acid). An Agilent Optimizer Tool (MassHunter, ver B.08.00) was used to finalize the optimal parameters of the fragmentor, collision energy, cell accelerator voltage and mass transition for each analyte (Table 3.1). Along with the real chromatographic condition, capillary voltage was optimal at 3500V, sheath gas pressure and sheath gas temperature were optimal at 35 psi and 350ºC, and the gas temperature was optimal at 300ºC.

Table 3.1 Quantifiers and qualifiers for analysis of DCVG, DCVC, and NAcDCVC in multiple tissue.

Analytes	Ion transition (*m/z*)	Collision energy (V)	Fragmentor
DCVG	402.0→272.9	13	110
	402.0→169.9†	25	110
	402.0→133.9	37	110
DCVG*	409.0→173.9†	25	110
	405.0→169.9	25	110
DCVC	216.0→198.9†	8	70
	216.0→126.9	25	70
	216.0→82.9	45	70
DCVC*	222.0→128.9†	25	80
	220.0→201.9	10	80
NAcDCVC	258.0→215.9	9	90
	258.0→198.8†	17	90
	258.0→179.9	5	90
NAcDCVC*	262.0→216.9	9	90
	262.0→198.8†	17	90

† Selected quantifier for analysis. ‾ Alternative quantifier of DCVC* in serum. Dwell time and cell accelerator voltage were set at 25 ms and 2 V

3.3.5 Method validation

Selectivity of the method was determined by using pooled tissues and/or serum of untreated male animals of the same strain. Sensitivity was defined by both the limit of detection (LOD, the concentration with signal to noise ratio of 3) and the limit of quantification (LOQ, the concentration with signal to noise ratio of 10). Inter-channel cross talk and sample-to-sample carry over effects were evaluated by using the highest concentration in the calibration curve. Calibration curves of DCVG, DCVC, and NAcDCVC were prepared in liver, kidney, or serum samples obtained from untreated mice. Blank liver, kidney, or serum (50 mg or μL) was spiked with standard mixture at 0, 0.25, 0.5, 1.25, 2.5, 6.25, 18.75, and 31.25 pmoles for each analyte. All standard solutions were also spiked with 50 pmole of each internal standard. Peak area ratio of standard and internal standard was used for quantitation of DCVG, DCVC, and NAcDCVC.

Intra-day precision and accuracy (six replicates per matrix) were assessed in liver, kidney, and serum of untreated mice and in artificial urine (Surine^{TM} negative urine control, Cerilliant, Round Rock, TX) after spiking in 2.5 pmole for each analyte. Inter-day precision and accuracy were evaluated over six consecutive days. Extraction performance was evaluated by recovery, matrix effect, and process efficiency as described elsewhere (Matuszewski, *et al.*, 2003). Freeze and thaw stability (three freeze-thaw cycles on dry ice), short-term stability (storing samples at room temperature for 4 hrs), long-term stability (storing samples at -20^{o}C for 30 days), and on-tray stability (storing samples at 4^{o}C for 8 hrs) of DCVG, DCVC, and NAcDCVC were evaluated by comparing extracted

samples before and after each test condition. Stability of the stock solutions was evaluated after they were stored at room temperature for 6 hrs.

3.3.6 Statistical analyses

One-way ANOVA and post-hoc tests were conducted by using GraphPad Prism (ver. 5, GraphPad Software, La Jolla, CA). A p-value of less than 0.05 was considered significant in all analyses.

3.3.7 Calculation of uncertainty factors for toxicokinetic variability

To avoid underestimation of toxicokinetic variability, concentrations for peaks between LOD and LOQ were estimated via extrapolation from the calibration curves. Values below LOD were replaced by ½ of the LOD, as recommended by US EPA (USEPA, 2000). For kidney DCVC, values below the background concentration were replaced by the background concentration derived from matrix-matched calibration curve.

The uncertainty factor for human toxicokinetic variability ($UF_{H,TK}$) can be expressed as the ratio between the internal dose in a "sensitive" individual (e.g., 95^{th} or 99^{th} percentile) to that in a "typical" individual (e.g., median) (WHO/IPCS, 2005). For a number of chemicals, including TCE, population PBPK modeling has been used to estimate this ratio (U.S. EPA, 2011a; U.S. EPA, 2011c). For TCE, Chiu et al. (2014) showed that mouse inter-strain variability is in agreement with human inter-individual variability. Whereas previously, $UF_{H,TK}$ was estimated only for the overall flux of GSH conjugation, here we can extend this to tissue- and metabolite-specific dose metrics.

Therefore, for each tissue and metabolite, given an inter-strain variance σ^2, the $UF_{H,TK}$ was estimated for the 95th and 99th percentile as $UF_{H,TK,95} = \exp(z_{95}\ \sigma)$ and $UF_{H,TK,99} = \exp(z_{99}\ \sigma)$, respectively, where z_{95} and z_{99} are the z-scores for the corresponding percentiles.

The inter-strain variability of glutathione conjugation metabolites of TCE was estimated by decomposing the total observed variance across CC strains into two components: intrinsic inter-strain heterogeneity and intra-strain variability (e.g., due to environmental factors and measurement error). Only one sample from each CC strain was available, so the intra-strain variability was estimated by the observed variation across B6C3F1 mice, as follows: $\sigma^2_{inter\text{-}strain} = \sigma^2_{total} - \sigma^2_{intra\text{-}strain}$; σ^2_{total}= variance of log-transformed data across 20 CC mice; $\sigma^2_{intra\text{-}strain}$= variance of log-transformed data across B6C3F1 mice.

The uncertainty factor of the inter-strain variability in toxicokinetics (UF_{TKvar}) is calculated from $UF_{TKvar} = e^{z*\sigma}$, where z= Z statistics and σ represents the square root of variance. The UF_{TKvar} of glutathione conjugation metabolites are derived at 95% and 99%, respectively.

3.3.8 Population PBPK modeling

For comparison, mouse population PBPK modeling was used to estimate of serum concentrations of DCVG and DCVC was generated from 100 different populations (500 individuals/population) as detailed in (Chiu, *et al.*, 2014).

3.4 Results

3.4.1 LC-MS/MS method for detection of DCVG, DCVC, and NAcDCVC

Figure 3.1 shows the LC-MS/MS chromatogram of DCVG, DCVC, and NAcDCVC in blank kidney tissue spiked with 0.25 pmoles of standards and 50 pmoles of isotopically labeled internal standards. Representative retention time was 2.5 min for DCVC and DCVC*, 3.35 min for DCVG and DCVG*, and 3.79 min for NAcDCVC and NAcDCVC*.

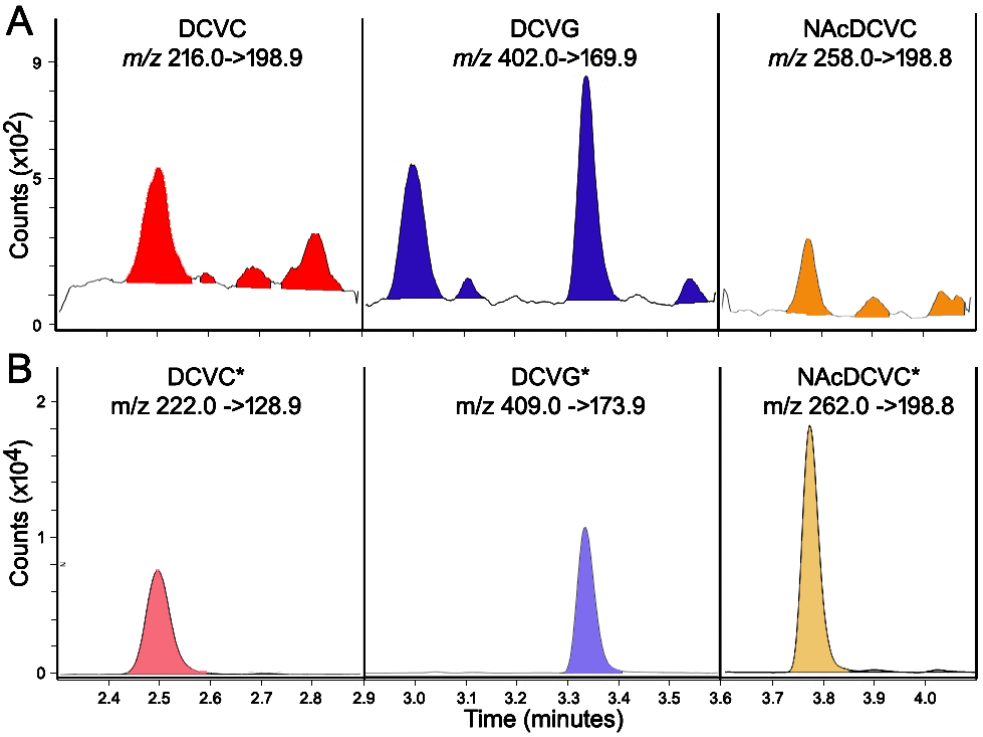

Figure 3.1 Representative LC-MS/MS chromatograms and mass transitions for parent compounds (A) and isotopically labeled standards (B) of DCVG, DCVC, and NAcDCVC in kidney. The spiked amount on-column was 0.25 pmoles for standards and 50 pmoles for internal standards.

Selectivity test showed that a peak at 2.75 min in the mass transition of *m/z* 220.0→201.9 and a peak at 2.55 min in the mass transition of *m/z* 216.0→82.9 commonly appeared in liver, kidney, and serum. A peak at 4.05 min in the mass transition of m/z 258.0→179.9 and m/z 262.0→216.9 specifically appeared in serum. Even though the peaks of the target analytes were chromatographically separated from the aforementioned peaks, these mass transitions as quantifiers were not used to minimize the potential influences on our quantitative results. Calibration curves across different tissue matrices showed excellent linearity (r^2>0.998), and the relative standard deviations of the slopes were less than 3% (1.1% for DCVG, 2.5% for DCVC, and 0.8% for NAcDCVC; Figure 3.2). No inter-channel cross talk between standards and isotopically labeled standards occurred during the analysis. The sample-to-sample carry over effect at the highest concentration of calibration curve was less than 0.08% for DCVG, 0.03% for DCVC, and 1.4% for NAcDCVC. Interestingly, a positive intercept was observed in the calibration curve of DCVC in kidney and serum, this background signal disappeared in the absence of isotopically labeled internal standards (Figure A-3). However, no background was observed in DCVC signal in liver, even in presence of isotopically labeled internal standards. It is likely that a small amount of the unlabeled portion of the internal standards (-dichloroethyl group) is released from the parent compound, and then reacts with the endogenous unbound S-cysteine, which is abundant in kidney and plasma, to generate a minute amount of DCVC as background signal. Therefore, a matrix-matched calibration curve is highly recommended to subtract the background signals specifically in kidney or

serum, even though the calibration curve in water showed excellent consistency with matrix-matched calibration curves. To test whether these metabolites can form *ex vivo*, TCE (5 μM) was reacted with glutathione (5 mM) in saline, as well as serum and liver homogenates. These reactions were carried out with or without protein inactivation or glutathione depletion. No *ex vivo* formation of DCVG, DCVC or NAcDCVC was observed at levels exceeding the limits of detection (data not shown).

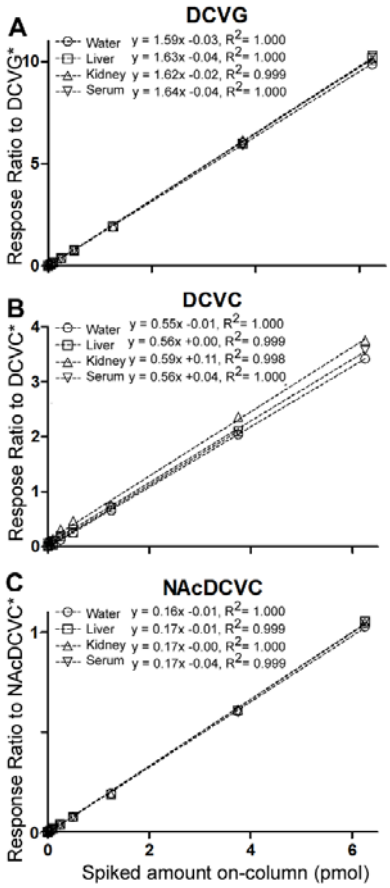

Figure 3.2 Matrix-matched calibration curves of DCVG, DCVC, and NAcDCVC in mouse tissues. The influence of matrix effects on quantitative analysis has been minimized by using isotopically labeled internal standards, with a relative standard deviation of slopes less than 3%.

Table 3.2 shows the method performance of DCVG, DCVC, and NAcDCVC in multiple mouse tissues. In serum, recovery of DCVG (43-73%) and DCVC (10-53%) was about 3-fold higher than previously reported (Kim, *et al.*, 2009a). The low recovery of DCVC in liver and kidney likely results from sample loss during liquid-liquid extraction; however, to the best of our knowledge, the liquid-liquid extraction is required to minimize the matrix interference especially in liver and kidney. The ion suppression of DCVG, DCVC, and NAcDCVC was most pronounced (40-50%) in liver, it was more variable in serum [22% DCVG, 10% DCVC, and 40% NAcDCVC], and minimal in kidney (10-15%). The matrix effects on DCVG and DCVC reported herein were less pronounced as compared to those reported in (Kim, *et al.*, 2009a) (up to 45% for DCVG and up to 78% for DCVC). Even though ion suppression effect occurs during the analysis, this method is accurate (bias <15%) and reliable (precision<15%) in liver, kidney, and serum by using isotopically-labeled internal standards (Table 3.2). The stability of DCVG, DCVC, and NAcDCVC was assessed with stock solutions and extracted samples under various storage conditions. Stock solutions were stable at room temperature for up to 8 hours (DCVG: 98.3%, DCVC: 102.5%, NAcDCVC: 94.8%). Analytes in extracted samples were stable in liver, kidney, and serum when subjected to on-tray, short-term, long-term, and freeze-thaw storage conditions (Table 3.2).

Table 3.2 Comparative analysis of method performance of DCVG, DCVC, and NAcDCVC in multiple tissues

		Liver			Kidney			Serum		
		DCVG	DCVC	NAcDCVC	DCVG	DCVC	NAcDCVC	DCVG	DCVC	NAcDCVC
	RE(%)[†]	73	15	58	43	10	57	69	53	83
	ME(%)	60	62	50	85	85	90	78	90	60
	PE(%)	44	9	29	37	8	52	54	48	50
Intra-day[Ŧ]	Accuracy(%)	-3.4	+5.8	-0.3	-4.2	+13.6	-5.4	-3.3	-3.5	-5.4
	Precision(%)	1.4	7.9	3.0	1.5	7.5	3.0	2.0	6.3	1.6
Inter-day	Accuracy(%)	-1.9	-2.4	-4.7	-4.2	+8.0	-4.5	-2.8	-9.9	-5.7
	Precision(%)	2.5	7.5	3.5	0.5	10.0	3.8	2.0	5.2	2.1
On-tray stability (%)[*]		99.6±16.5	116.8±5.4	94.3±4.9	107.5±2.7	101.2±5.4	102.0±1.9	97.1±0.6	99.8±1.4	101.3±2.2
Short-term stability (%)		98.5±1.3	100.6±13.8	101.9±1.5	97.4±1.9	106.3±4.2	107.1±3.4	99.9±2.1	93.6±6.5	104.1±2.7
Long-term stability (%)		102.3±1.7	109.1±13.3	101.8±1.6	99.7±1.0	89.0±2.8	100.2±5.1	99.3±0.7	94.1±6.8	99.7±1.4
Freeze-thaw stability (%)		100.4±0.9	101.0±0.3	100.9±5.0	98.7±0.9	96.8±3.1	97.7±1.8	97.3±2.8	113.0±3.0	100.3±5.6

[†] Method validation for analysis of DCVG, DCVC, and NAcDCVC was compared at level of 50 pmole/g tissue or mL serum across different tissues. Recovery (RE), matrix effect (ME), and process efficiency (PE) were determined from n=5.

[Ŧ] Inter-day (n=6) and intra-day (n=6) accuracy (%) are expressed as bias deviated from the nominal concentration. Precision (%) is expressed as relative standard deviation.

* Results of stabilities are expressed in average±standard deviation (n=3).

3.4.2 Toxicokinetic profiling of TCE glutathione conjugates across tissues and strains

The levels of DCVG, DCVC, and NAcDCVC were quantified in multiple tissues of B6C3F1 mice treated with single dose of TCE (24, 240, or 800 mg/kg) 2 hrs after oral gavage (Figure 3.3, Table B-10). DCVG and NAcDCVC were most abundant in liver, while DCVC was most abundant in kidney. Significant dose-response in formation of the conjugates was observed for all tissues and metabolites where levels were detectable in at least two dose groups, except for DCVC in kidney where non-linear kinetics was observed.

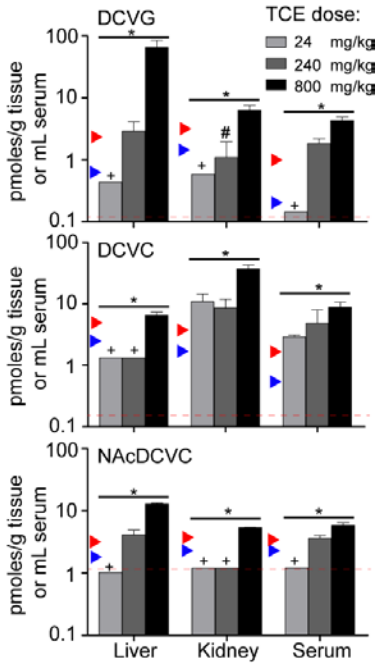

Figure 3.3 Dose-dependent increases of (A) DCVG, (B) DCVC, and (C) NAcDCVC in liver, kidney, and serum of B6C3F1 mice treated with TCE (n=3 /group). The red dashed line indicates the instrumental LODs; the blue and red triangles locate the matrix-matched LODs (S/N=3) and LOQs (S/N=10), respectively. One-way ANOVA and post hoc test for a linear trend was used to test the dose–response relationships in each tissue (*p<0.05). [+]The bar is shown as ½ LOD if an analyte was below the LOD. [#]Measurements between LOD and LOQ are expressed as estimated values.

The levels of DCVG, DCVC, and NAcDCVC were also successfully quantified in multiple tissues of CC mice treated with TCE (single dose, 800 mg/kg, Table B-11). Figure 3.4 shows that in liver, DCVG showed the highest detection rate (>LODs, 100%) as compared to DCVC (65%) and NAcDCVC (85%). Similarly, the detection rate of DCVG (89%) in serum was higher than that of DCVC (42%) and NAcDCVC (63%). NAcDCVC was most detectable in kidney (74%), followed by DCVG (68%) and DCVC (63%). Levels of glutathione conjugation metabolites in B6C3F1 mice were among the highest as compared to those in 20 CC strains.

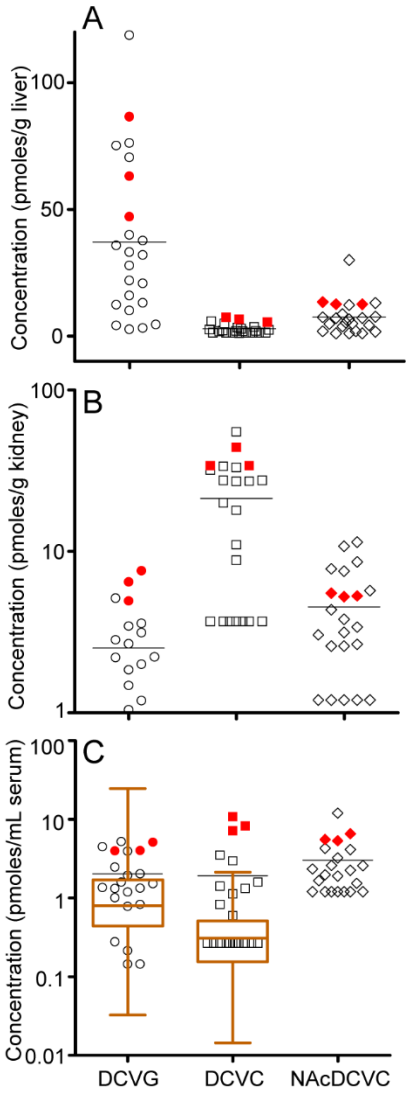

Figure 3.4 Inter-individual variability of conjugative metabolites of TCE in (A) liver, (B) kidney, and (C) serum of mice at 2 hour after dosing with TCE (800 mg/kg, oral gavage). Each data point represents the value reported in a CC mouse strain. The data point is shown as ½ LOD if an analyte was below the LOD. Data points with red color refer to the metabolite levels reported in male B6C3F1 mice. Middle line indicates the mean concentration among 20 CC strains. The box and whiskers plots (Min to Max) show the PBPK modeling estimates for serum levels of DCVG and DCVC based on Chiu et al 2014. The estimates were generated from the median distribution out of 100 different populations, with 500 individuals in each population. Different letters indicate different statistical groups, as determined by ANOVA with Turkey's post hoc test ($p<0.05$).

Pairwise correlation analysis was conducted for all metabolites and tissues using data from 20 CC strains (Figure 3.5 and Figure A-4). Strong positive correlations were observed between liver DCVG and NAcDCVC (r=0.89), serum DCVG and liver DCVG (r=0.68), and liver NAcDCVC and kidney NAcDCVC (r=0.64). Medium positive correlations were observed between kidney DCVG and serum DCVC (r=0.57), liver DCVG and kidney DCVG (r=0.49), liver DCVG and serum DCVG (r=0.54), kidney DCVG and DCVC (r=0.50), kidney DCVG and NAcDCVC (r=0.53). Interestingly, the correlation between liver DCVG and kidney DCVC was statistically insignificant.

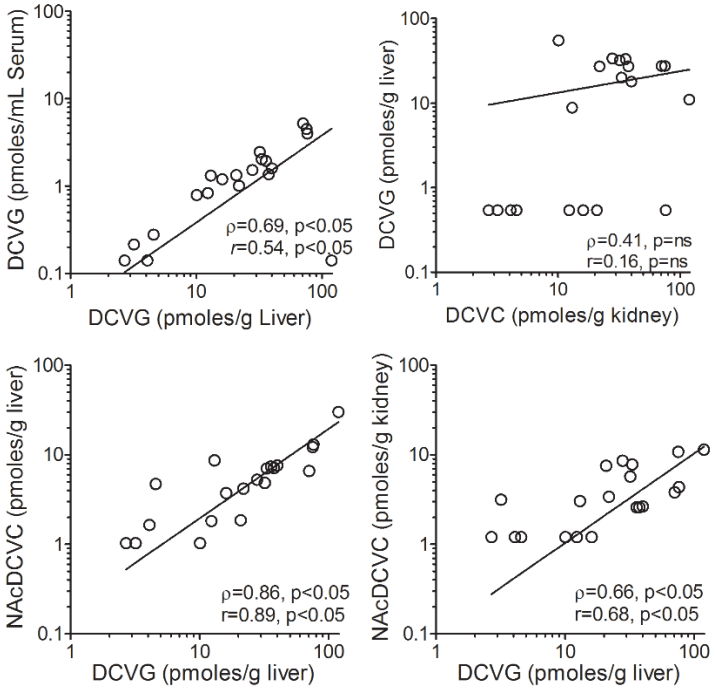

Figure 3.5 Pairwise correlation analysis of DCVG, DCVC, and NAcDCVC across tissues. The correlation results are expressed in Spearman coefficient (ρ) and Pearson coefficient (r). A p-value less than 0.05 was considered significant across all analyses. ns, not significant.

As was hypothesized by Chiu et al (2014), inter-strain variability was used as a surrogate for human inter-individual variability to estimate uncertainty factors human toxicokinetic variability ($UF_{H\text{-}TK}$) for DCVG, DCVC, and NAcDCVC in liver, kidney and serum (Table 3.3). As described in Methods, the variance obtained from B6C3F1 mice was used to estimate the intra-strain variability in a single CC strain, which was then subtracted from the overall observed variance across CC strains. The values of $UF_{H\text{-}TK}$ for the 95th percentile were 3.3-5.8 for DCVG, 2.1-6.7 for DCVC, and 2.7-4.6 for NAcDCVC. Values for the 99th percentile were correspondingly higher. DCVG and NAcDCVC showed the highest $UF_{H\text{-}TK}$ in liver, while DCVC showed the highest $UF_{H\text{-}TK}$ in kidney.

The extent of variability in the levels of DCVG in serum was less than the population variability estimates from a PBPK model (Chiu, *et al.*, 2014) (Figure 3.4). Specifically, using the Chiu et al (2014) PBPK model, $UF_{H\text{-}TK,95}$ for DCVG and DCVC in serum had 95% confidence intervals of (16-110) and (5-26), respectively, whereas the values estimated here were 5.8 and 4.5 (Table 3.3). Additionally, model-derived estimates for DCVC in serum were lower than the measured values (Figure 3.4). These discrepancies may result from the relatively low detection rate of DCVC in serum (42%). About half of the model estimates are below the detection limit, which is also consistent with the percentage of undetectable samples.

Table 3.3 Derivation of uncertainty factors for inter-strain variability in toxicokinetics of DCVG, DCVC, and NAcDCVC in multiple mouse tissues.

	DCVG			DCVC			NAcDCVC		
	Liver	Kidney	Serum	Liver	Kidney	Serum	Liver	Kidney	Serum
GM	20.3	1.5	1.1	2.0	10.5	0.5	4.4	3.3	2.1
GSD	2.9	2.1	2.9	1.6	3.3	2.5	2.5	2.2	1.8
σ^2_{total} *	1.22	0.57	1.15	0.23	1.06	0.86	0.86	0.61	0.37
$\sigma^2_{intra\text{-}strain}$	0.09	0.05	0.02	0.02	0.02	0.04	0.001	0.0007	0.012
$\sigma^2_{inter\text{-}strain}$	1.12	0.52	1.13	0.20	1.04	0.82	0.86	0.61	0.36
$UF_{H\text{-}TK,95}$	5.72	3.27	5.75	2.10	5.4	4.45	4.61	3.60	2.66
$UF_{H\text{-}TK,99}$	11.84	5.35	11.93	2.87	10.9	8.28	8.71	6.15	4.01

* GM= geometric mean, pmole/g tissue or mL serum; GSD= geometric standard deviation; Var_{total}= Variance of log-transformed data of 20 CC study; $Var_{intra\text{-}strain}$= Variance of log-transformed data of B6C3F1 study; $Var_{inter\text{-}strain} = Var_{total} - Var_{intra\text{-}strain}$; UF_{TKvar}, Uncertainty factors for inter-strain variability in toxicokinetics of DCVG, DCVC, and NAcDCVC.

3.5 Discussion

Characterization of tissue levels of nephrotoxic glutathione metabolites of TCE is an important challenge in regulatory toxicology, compounded by lack of sensitive analytical methods. Several analytical methods are available for analysis of DCVG, DCVC, and NAcDCVC (Table 3.4). In general, LC-MS/MS-based methods (Kim, *et al.*, 2009a; Yoo, *et al.*, 2015a; Yoo, *et al.*, 2015b) have superior sensitivity for DCVG and DCVC. The LC-MS/MS based method for simultaneous detection of DCVG and DCVC was developed for mouse serum (Kim, *et al.*, 2009a); however, the applicability of this method to parenchymal tissues (e.g. liver and kidney), especially at lower doses of TCE, was questionable. Yoo et al. tailored extraction methods to quantify DCVG and DCVC in liver (Yoo, *et al.*, 2015a) and kidney (Yoo, *et al.*, 2015b); still, difference in extraction methods may result in a systematic bias (Luo, *et al.*, 2017). In this study, tissue extraction protocols were optimized, the sensitivity of detection for DCVG and DCVC across tissues further enhanced, and the method extended to quantification of NAcDCVC.

The method was used to characterize tissue-specific variation in formation of glutathione conjugation metabolites of TCE. Consistent with our knowledge of the metabolic pathways for glutathione metabolism of halogenated solvents, the most abundant metabolites of TCE were the glutathione conjugate in liver and the cysteine conjugate in kidney (Krzysik and Adibi, 1977; Moron, *et al.*, 1979; Whitfield, 2001). Importantly, our study allows addressing several additional important gaps in our knowledge with respect to glutathione conjugation metabolism of TCE.

Table 3.4 Comparative analysis of sensitivities for DCVG, DCVC, and NAcDCVC between tissues and studies.

Reference	Matrix	Extraction method*	Detect Method	DCVG† (fmole)	DCVC (fmole)	NAcDCVC (fmole)
This study	Liver	LL-SPE	LC-MS/MS	8.7	26.3	20.6
	Kidney			11.7	10.8	24
	Serum	PP-SPE		2.9	5.3	24.1
	Instrumental LOD∓			0.8	1.2	11
Kim et al., 2009	Serum	LL-SPE	LC-MS/MS	37.5	37.5	N/R
Lash et al., 1999	Blood/urine	PP-derivatization with iodoaceatate and 1-fluoro-2,4-dinitrobenzene	LC-UV	50,000	5,000	N/R
Yoo et al., 2015	Kidney	LL-SPE	LC-MS/MS	25⊥	250	N/R
Yoo et al., 2015	Liver	SPE	LC-MS/MS	100‡	1,000	N/R
Lash et al., 2006	Blood/urine	Derivatization with iodoaceatate and 1-fluoro-2,4-dinitrobenzene	LC-UV	110⊤	110	N/R
	Liver			1,100	1,100	N/R
	Kidney			2,200	2,200	N/R
Bloemen et al., 2001	Urine	Derivatization with HCl and diethyl ether	GC-MS	N/R	N/R	80⌜

† Limit of detection (LOD) is defined as the tested concentration with the signal-to-noise ratio equals to 3, and expressed with the on-column amount of analyte. N/R: Not reported. ∓ Instrumental LOD was tested in de-ionized water. *LL-SPE: liquid-liquid extraction coupled with SPE; PP-SPE: protein precipitation coupled with SPE. ⊥Estimated on-column amount from LLOQ of 1 pmole/g kidney with starting tissue materials of 50 mg tissue. ‡Estimated on-column amount from LLOQ of 2 pmole/g liver with starting tissue materials of 100 mg tissue. ⊤Estimated on-column amount from LODs of urine/blood (1.1 pmol/ml), liver (11 pmol/g tissue), and kidney (22 pmol/g tissue) with starting tissue materials of 0.5 ml/500 mg tissue. ⌜Estimated on-line amount from LOD of 0.04 μmol/L.

First, it is interesting that NAcDCVC was most abundant in liver. Formation of mercapturic acids from glutathione conjugates involves both liver and kidney (Hinchman and Ballatori, 1994; Inoue *et al.*, 1984; Inoue *et al.*, 1987; Lash, *et al.*, 1998). DCVG synthesized within hepatocytes can be secreted across the canalicular membrane into bile, broken down to form DCVC, reabsorbed and n-acetylated to form NAcDCVC in liver. No *ex vivo* formation of glutathione conjugates from TCE was observed. When quantified across tissues and individual strains, high correlations were found for liver DCVG and serum DCVG, and for liver DCVG and NAcDCVC which suggests that DCVG can be directly transported from liver into blood. Fast conversion from DCVG to NAcDCVC is also plausible in liver. Interestingly, liver DCVG and NAcDCVC were not correlated with kidney DCVC, but they were correlated with kidney NAcDCVC. These findings suggest that i) formation and elimination of DCVC in kidney may be a critical source of inter-individual variability among strains, and ii) liver may be the primary site for generation of NAcDCVC.

Second, this study enabled quantitative comparisons of conjugative metabolism pathways between TCE and tetrachloroethylene (PCE). Levels of glutathione conjugation metabolites in all tissues examined were lower upon exposure to TCE at the equivalent molar dose (6 mmole/kg) and time point as compared to PCE (Luo, *et al.*, 2017). Specifically, concentrations of DCVG were lower by 3.9-fold in liver, 2.4-fold in kidney, and 3.3-fold in serum as compared to *S*-(1,2,2-trichlorovinyl) glutathione (TCVG). Concentrations of DCVC were 2.6-fold lower in kidney and 5.3-fold in serum, while were 1.2-fold higher in liver, as compared to S-(1,2,2-trichlorovinyl)-L-cysteine (TCVC).

These findings are consistent with reports that in the absence of hepatic metabolism of glutathione conjugates, PCE is more cytotoxic than TCE to isolated kidney cells (Lash, *et al.*, 2007), and that DCVC is less nephrotoxic than TCVC *in vivo* (Birner, *et al.*, 1997). However, kidney cancer hazard evidence in humans is stronger for TCE than PCE (Guha, *et al.*, 2012), indicating that bioactivation to downstream reactive sulfoxides, DCVCSO and NAcDCVCSO, may be most critical part of cancer etiology in the kidney (Irving *et al.*, 2013; Lash *et al.*, 1994). It is also plausible that lower levels of DCVC and NAcDCVC, as compared to those of TCVC and NAcTCVC, are the product of a higher conversion rate to their corresponding sulfoxides, a process that is mediated by hepatic cytochrome P450 3A enzymes (Werner *et al.*, 1996).

Third, this study characterized inter-strain variability in toxicokinetics of TCE glutathione conjugates (Table B-12). Inter-strain variability in toxicokinetics of DCVG was greatest in liver (GSD=2.9, 44-fold differences). Corresponding values for serum and kidney were 2.5 (6-fold) and 2.1 (5-fold). These differences may result from the inter-strain variability in enzyme activities, or in other PK modifiers such as absorption and elimination efficiency of TCE, cellular transporters, and plasma protein levels. The inter-individual variability in human enzyme activities related to formation of DCVG, DCVC, and NAcDCVC has been reported for GSTs (4-92 fold differences), gamma-glutamyl transferase (3-fold), n-acetyltransferase (70-fold), and acylase (7.4-fold), as well as flavin monooxygenase 3 (10-fold), beta-lyase (4-fold), and CYP3A (40-fold) (Gul Altuntas and Kharasch, 2002; Helander *et al.*, 1998; Lamba *et al.*, 2002; Mccarthy *et al.*, 1994; Slone *et al.*, 1995; Stormer *et al.*, 2000). The importance of both toxicokinetic and

toxicodynamic variability is further supported by observations that allelic variations in human enzymes involved in both toxicokinetics and toxicodynamics, such as GSTθ and renal β lyase, have been associated with TCE renal cancer risk (Moore *et al.*, 2010; Spearow *et al.*, 2017).

Quantitative estimates of variability among strains and tissues have important implications for risk assessment because in the absence of chemical-specific data a default "uncertainty factor" of $10^{0.5}$ (3.16) is used for inter-individual variability in toxicokinetics. Although intended to be "conservative," it is common for variability to exceed this value. In the most recent analysis by WHO/IPCS (Chiu and Slob, 2015), the GSD for toxicokinetic variability has a 90% confidence interval of 1.2 to 2.6, which corresponds to $UF_{H\text{-}TK,99}$ protecting 99% of the population of 1.4 to 8.9, with a median of 3.6. Thus, the "default" value is actually closer to a central estimate of toxicokinetic variability, suggesting that chemical-specific data are needed. Indeed, consistent with previous analyses by Chiu et al. (2009, 2014), the data for GSH conjugation metabolites of TCE suggest that for most tissues and metabolites, a factor of 3.16 is not sufficient to cover 99% of the population variability in toxicokinetics (Table 3.3).

There are several key limitations to this study. First, the analyte recovery of DCVC is inadequate (10~15%) as compared to those of DCVG and NAcDCVC. Improvements in sample preparation techniques are needed to further enhance the sensitivity of DCVC detection. Second, because only a single sample from each CC strain was available, inter-strain variability was estimated by subtracting total observed variability from intra-strain variability in B6C3F1 mice. Future studies may benefit from the characterization of intra-

strain variability in CC strains. Third, the data in CC mice was only at a single dose and time point. Future studies need to include time-course data at multiple dose levels to improve the estimates of tissue-specific GSH conjugation dosimetry, particularly if incorporated into a population PBPK model. To date, the PBPK modeling of inter-strain variability in oxidative metabolism of TCE has been well characterized, but the PBPK compartments in conjugative metabolism of TCE, especially at target organs, are yet to be fully established (Chiu, *et al.*, 2014).

3.6 Conclusions

Herein, a LC-MS/MS method that simultaneously detects DCVG, DCVC, and NAcDCVC in multiple mouse tissues has been successfully developed, and applied in animal studies. With this method, for the first time, the inter-individual variability in conjugative metabolism of TCE has been characterized in multiple tissues of a panel of genetically diverse CC mice. Despite some study limitations, our data suggest that for TCE, the default uncertainty factor of 3.16 for toxicokinetic variability would be inadequate to protect 99% of the population for organ-specific toxicity mediated by DCVG, DCVC, and NAcDCVC.

CHAPTER IV

MODULATION OF TETRACHLOROETHYLENE-ASSOCIATED KIDNEY EFFECTS BY NONALCOHOLIC FATTY LIVER OR STEATOHEPATITIS IN MALE C57BL/6J MICE

4.1 Overview

Accounting for genetic and other (e.g., underlying disease states) factors that may lead to inter-individual variability in susceptibility to xenobiotic-induced injury is a challenge in human health assessments. A previous study demonstrated that nonalcoholic fatty liver disease (NAFLD), one of the common underlying disease states, enhances tetrachloroethylene (PCE)-associated hepatotoxicity in mice. Interestingly, NAFLD resulted in a decrease in metabolism of PCE to nephrotoxic glutathione conjugates; we therefore hypothesized that NAFLD would protect against PCE-associated nephrotoxicity. Male C57BL/6J mice were fed a low-fat (LFD), high-fat (31% fat, HFD), or high-fat methionine/choline/folate-deficient (31% fat, MCD) diets. After 8 weeks mice were administered either a single dose of PCE (300 mg/kg *i.g.*) and euthanized at 1-36 hours post dose, or five daily doses of PCE (300 mg/kg/d; 4 hrs post-dose). Relative to LFD-fed mice, HFD- or MCD-fed mice exhibited decreased PCE concentrations and increased trichloroacetate (TCA) in kidneys. S-(1,2,2-trichlorovinyl)glutathione (TCVG), S-(1,2,2-trichlorovinyl)-L-cysteine (TCVC), and N-acetyl-S-(1,2,2,-trichlorovinyl)-L-cysteine (NAcTCVC) were also significantly lower in kidney and urine of HFD- or MCD-fed mice

compared to LFD-fed mice. Despite differences in levels of nephrotoxic PCE metabolites in kidney, LFD- and MCD-fed mice demonstrated similar degree of nephrotoxicity. However, HFD-fed mice were less sensitive to PCE-induced nephrotoxicity. Thus, while both MCD- and HFD-induced fatty liver reduced the delivered dose of nephrotoxic PCE metabolites to the kidney, only HFD was protective against PCE-induced nephrotoxicity, possibly due to greater toxicodynamic sensitivity induced by methyl and choline deficiency. These results therefore demonstrate that preexisting disease conditions can lead to a complex interplay of toxicokinetic and toxicodynamic changes that modulate susceptibility to the toxicity of xenobiotics.

4.2 Introduction

Human health risk assessors face a considerable challenge when it comes to addressing inter-individual variability of adverse health effects associated with environmental exposures (Zeise, *et al.*, 2013). In addition to genetics, sex and diet, pre-existing disease states may also affect inter-individual variability. Nonalcoholic fatty liver disease (NAFLD) is a good example of a prevalent chronic disease in the developed countries such as the United States, Germany, and Israel (Browning *et al.*, 2004; Kuhn *et al.*, 2017; Zelber-Sagi *et al.*, 2006). The global prevalence of NAFLD is estimated to be ~25% (Younossi *et al.*, 2016b), and associated economic burden on health care is substantial (Younossi *et al.*, 2016a). NAFLD is a spectrum of health conditions that initially presents as nonalcoholic fatty liver (NAFL) and that can progress to nonalcoholic steatohepatitis (NASH), a liver disease state characterized by accumulation of fat,

inflammation, and cell injury (ballooning) (Chalasani, *et al.*, 2012). Even though NAFL is considered a benign form of the disease, subjects with NAFL may be more susceptible to further liver damage by other exposures. Exacerbated liver injury has been demonstrated in rodents with experimental NAFLD that were exposed to vinyl chloride (Lang *et al.*, 2018), methotrexate (Hardwick, *et al.*, 2014), or a ubiquitous environmental contaminant tetrachloroethylene (PCE) (Cichocki, *et al.*, 2017b).

PCE is a chemical that was extensively used in metal degreasing, as a feedstock in chemical syntheses, or in dry-cleaning (IARC, 2014; U.S. EPA, 2011b). PCE is one of the most commonly found contaminants at hazardous waste sites (National Research Council, 2010). In the United States, 90% of the population had detectable levels of PCE in their blood (Jia, *et al.*, 2012). PCE exposure has been associated with cancer and non-cancer toxicity, including nephrotoxicity in humans and rodents (Cichocki, *et al.*, 2016; U.S. EPA, 2011b). Toxicity of PCE in the kidney has been attributed to its tissue-specific metabolism (Cichocki, *et al.*, 2016).

Metabolism of PCE is mediated by both cytochrome P450s (CYPs) and glutathione-S transferases (GSTs) in the liver (Lash and Parker, 2001). The oxidative pathway yields trichloroacetate (TCA), a rodent hepatocarcinogen (Bull *et al.*, 1990; Herren-Freund *et al.*, 1987). The glutathione conjugation pathway in the liver forms 1,2,2-trichlorovinyl-L-glutathione (TCVG) which can be transported via circulation to the kidney where it is further metabolized to 1,2,2-trichlorovinyl-L-cysteine (TCVC) (Lash and Parker, 2001). The fate of TCVC is either metabolic activation to reactive species, including cytotoxic TCVC-sulfoxide (Elfarra and Krause, 2007), or detoxification via N-

acetyltransferase-mediated formation of N-acetyl-1,2,2,-trichlorovinyl-L-cysteine (NAcTCVC), a mercapturate that is excreted in the urine in humans and rodents (Lash and Parker, 2001). NAcTCVC can also be converted to NAcTCVC-sulfoxide, which is another nephrotoxic metabolite both *in vivo* and *in vitro* (Cristofori *et al.*, 2015).

A previous study characterized the toxicokinetics of PCE, as well as its oxidative (TCA) and glutathione conjugation metabolites (TCVG, TCVC, and NAcTCVC) in the liver, serum, and urine of mice with various degrees of NAFLD that were exposed to a single dose of PCE (Cichocki, *et al.*, 2017a). Interestingly, mice with NAFLD generated higher levels of liver TCA, which in turn resulted in more pronounced liver injury (Cichocki, *et al.*, 2017b). While much is known about the oxidative metabolites of PCE, little information is available on the toxicokinetics of glutathione conjugates of PCE *in vivo*. NAFLD resulted in a significant reduction in levels of TCVG, TCVC, and NAcTCVC in liver, serum, and urine (Cichocki, *et al.*, 2017a); however, the kinetics of PCE glutathione conjugates has not been explored in kidney, a target organ for PCE toxicity. Therefore, we tested the hypothesis that, compared to healthy mice, mice with diet-induced NAFLD would have lower kidney concentrations of TCVG, TCVC, and NAcTCVC following exposure to PCE, and this reduction in metabolite concentration would be associated with decreased sensitivity to PCE-associated nephrotoxicity.

4.3 Material and Methods

4.3.1 Chemicals

PCE (CAS 127-18-4) was obtained from Sigma Aldrich (Cat No. 270393, Batch No. SHLFD9374V, purity 99.93%; St. Louis, MO). S-(1,2,2-trichlorovinyl) glutathione (TCVG), $^{13}C_{2,}{}^{15}N$-TCVG, S-(1,2,2-trichlorovinyl)-L-cysteine (TCVC), $^{13}C_{5,}{}^{15}N$-TCVC, N-acetyl-S-(1,2,2-trichlorovinyl)-L-cysteine (NAcTCVC), and $^{13}C_{3,}{}^{15}N$-NAcTCVC were graciously provided by Dr. Avram Gold at the University of North Carolina, Chapel Hill. The purity of all standards was determined to be >95% by NMR and HPLC-UV. All other chemicals were of the highest purity available and were acquired from Sigma Aldrich.

4.3.2 Animals

The in-life portion of this study has been previously described in (Cichocki, *et al.*, 2017a). Briefly, five-week-old male C57BL/6J mice (n=150) were obtained from the Jackson Laboratory (Bar Harbor, ME) and acclimatized for one week on a standard rodent chow containing 4% calories from fat (low-fat diet; LFD; Teklad Rodent Diet #8604; Harlan, Madison, WI). Mice were randomly assigned (five mice per cage) into groups fed a control LFD, a diet containing 31% calories from fat (high fat diet, HFD; Diet #519567; Dyets Inc., Bethlehem, PA), or a diet depleted in methionine and devoid of choline and folate (methyl and choline-deficient diet, MCD; Diet #519541; Dyets, Bethlehem, PA). The overall study design is shown in Figure 4.1 and the study aimed to model conditions of (i) healthy liver and (ii) mild, or (iii) severe NAFLD phenotypes.

4.3.3 Toxicokinetic Study Design

Following eight weeks of feeding with the aforementioned diets, mice were exposed to a single dose of PCE (300 mg/kg in 5% Alkamuls-EL620 in saline; 5 mL/kg). All exposures took place between 07:00 and 10:00 hours. Mice (n=5/diet/time-point) were euthanized at 1, 2, 4, 12, or 24 hours after gavage (total n=75). An additional four mice per diet group were individually housed in stainless steel metabolic cages with wire mesh bottoms (Techniplast, Chester, PA) for 36 hours for urine collection (total n=12). Five mice per diet were treated with vehicle and euthanized at 24 hours post gavage to perform additional biochemical analyses (total n=15). Serum was prepared from blood drawn at exsanguination via centrifugation (Z gel tubes; Sarstedt, Nümbrecht, Germany). Kidneys were excised, rinsed in saline, blotted dry, weighed, snap-frozen in liquid nitrogen, and stored at -80^{o}C until analyzed.

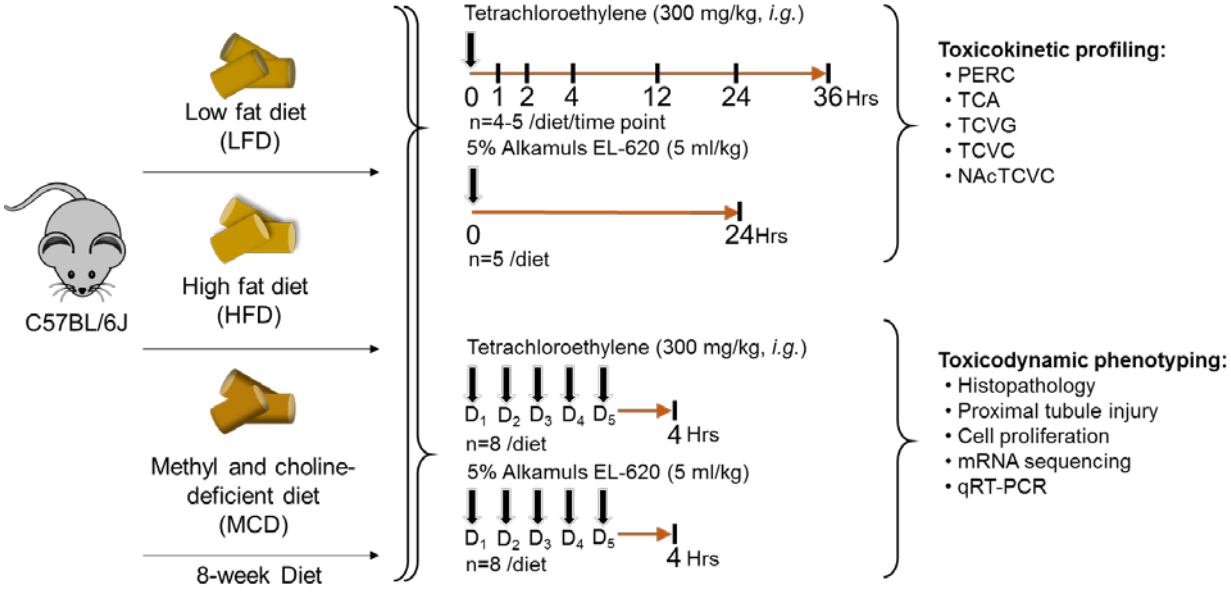

Figure 4.1 Schematic representation of study designs. Adult male C57BL/6J mice were used in these studies. Mice were fed with low fat diet (LFD), high fat diet (HFD), or methionine and choline-deficient diet (MCD) for 8 weeks, and then intragastrically dosed with tetrachloroethylene (PCE). The first study investigated the toxicokinetics of PCE metabolites up to 36 hrs after a single dose of PCE (300 mg/kg). The second study examined the toxicodynamic phenotypes of mice administered with repeated doses for 5 consecutive days (300 mg/kg/d); samples were collected 4 hrs after the last dose. Vertical lines indicate the time points of sample collections. Down arrows represent chemical treatments. Collected endpoints in each study are shown as a bulleted list.

4.3.4 Toxicodynamic Study Design

After eight weeks of feeding with the diets above, mice were intragastrically administered a single dose of PCE (300 mg/kg/d in 5% Alkamuls-EL620 in saline, 5 mL/kg) or vehicle for five consecutive days (n=8/diet/treatment). This dose was selected as the toxicokinetics of PCE and TCA in male mice after exposure to 150-1000 mg/kg PCE has been characterized in liver and blood and was shown to be well-tolerated in acute (Philip, *et al.*, 2007) and sub-chronic studies (National Toxicology Program, 1977). All

exposures took place between 07:00 and 10:00 hours. Three days prior to necropsy, animals were administered 5-bromo-2'-deoxyuridine in drinking water (0.02%, w/v). At four hours following the last dose of PCE, animals were deeply anesthetized with pentobarbital (50 mg/kg, *i.p.*) and sacrificed via exsanguination through the vena cava. This time point was selected based on our previously published toxicokinetic data where we showed that PCE and its oxidative and conjugative metabolites were detectable in mouse liver and serum four hours following a single dose of PCE (Cichocki, *et al.*, 2017a; Luo, 2018). Mice were euthanized, and serum and kidneys were harvested as described above. A small section of one kidney was fixed in formalin for histological examination.

4.3.5 Analysis of PCE and TCA via Gas Chromatography/Mass Spectrometry

PCE and TCA were measured in kidney tissue as previously described . Briefly, methanolic kidney homogenates were analyzed for PCE via purge-and-trap (dynamic) headspace gas chromatography/mass spectrometry (GC/MS). TCA was analyzed via a modified US EPA Method (EPA 815-B-03-002). Briefly, aqueous kidney homogenates were incubated with 10 % (v:v) sulfuric acid in methanol (50 ^{o}C, 2 hr) to generate TCA methyl ester. After liquid-liquid extraction, the derivatives were analyzed via GC/MS.

4.3.6 Liquid Chromatography/Mass-Spectroscopy (LC/MS) Analysis of TCVG, TCVC, and NAcTCVC

The method of Luo et al. (Luo, *et al.*, 2017) was used for detection of TCVG, TCVC, and NAcTCVC in kidney tissue. Briefly, kidney homogenates were subjected to

liquid-liquid extraction, and solid-phase extraction prior to chromatographic separation and detection via LC/MS-MS.

4.3.7 Serum clinical chemistry

Blood urea nitrogen (BUN) and serum creatinine levels were measured in serum samples using a VetScan 2 (Abaxis, Union City, CA) and a Comprehensive Diagnostic Profile rotor according to the manufacturer's instructions.

4.3.8 Histopathology

Kidney samples were embedded in paraffin, sectioned at 5 µm, and stained with hematoxylin and eosin (H&E). A veterinary pathologist who was blinded to the experimental design and sample identification numbers evaluated the slides.

4.3.9 Immunohistochemical staining of Kidney injury molecule-1 (KIM-1)

Tissues were sectioned at 5 µm onto poly-l-lysine-coated slides. Deparaffinized and rehydrated slides were hydrolyzed with warm (37^{o}C) 2N HCl for 20 minutes in an oven. Slides were rinsed with water (1 minute) and then placed in pre-warmed water in a 37^{o}C oven for 20 minutes. Samples were then incubated in pre-warmed pepsin solution (2g/500 mL of 0.2N HCl; Dako, Santa Clara, CA) for 15 min at 37^{o}C. Slides were rinsed with water twice (1 minute each), and then with phosphate-buffered saline with 0.1% Tween-20 (PBS-T) twice (3 minutes each). Endogenous peroxidase activity was blocked using a Peroxidase Blocking Reagent (Dako) for 5 minutes. After washing with PBS-T,

slides were incubated for 10 minutes at room temperature with a goat anti KIM-1 antibody (1 µg/mL; AF1817, Lot KCA0415031; R&D systems, Minneapolis, MN) prepared in an Antibody Diluent (Dako). After washing with PBS-T, slides were incubated with rabbit anti-goat HRP-conjugated secondary antibody (1:200 dilution; 10 minutes at room temperature), washed with PBS-T again, and then incubated with 3,3'-diaminobenzidine reagent (Dako) for 8 minutes at room temperature. After ample washing in deionized water, slides were placed in Mayer's Hematoxylin (1 minute), and then thoroughly washed under running tap water. Slides were dehydrated, mounted using Permount (Thermo Fisher Scientific), and examined using light microscopy. Approximately 250 tubules from 5 random fields (100X) were evaluated for each animal. The ratio of positively-stained tubules to the total number of tubules was recorded. Results were verified by an individual who was blinded to study design and animal identification numbers.

4.3.10 Enzyme-linked immunosorbent assay (ELISA) detection of KIM-1 protein

Kidney levels of KIM-1 protein were determined by using a Mouse TIM-1/KIM-1/HAVCR Quantikine ELISA Kit (R & D systems, Minneapolis, MN). Briefly, kidney tissue (10 mg) was homogenized in 1 mL of calibrator diluent RD5-26 buffer using Bead Ruptor 24 Elite (Omni International, Kennesaw, GA). The homogenate was centrifuged at 10,000 rpm for 5 mins, and the supernatant was subject to ELISA detection of KIM-1 according to the manufacturer's instructions.

4.3.11 Immunohistochemical Detection of BrdU

BrdU-positive cells were counted on paraffin-embedded sections using a commercially available kit (Invitrogen, Carlsbad, CA). Each slide contained a section of duodenum for positive control of BrdU incorporation. Five random fields (200X), or at least 500 tubular nuclei, were counted for each animal. The ratio of positively stained nuclei to total nuclei was determined for each animal. Results were verified by an individual who was blinded to study design and animal identification numbers.

4.3.12 Quantitative Reverse Transcriptase real-time polymerase chain reaction (qRT-PCR)

qRT-PCR was carried out using 40 ng of kidney cDNA as previously described for liver tissue (Cichocki *et al.*, 2017c). TaqMan probes (*Havcr1*: Mm00506686_m1; *Fabp1*: Mm00444340_m1; *Lcn2*: Mm01324470_m1; *Tbp*: Mm01277042_m1; Thermo Fisher Scientific) were used as per the manufacturer's instructions. Expression of *Tbp* was used as a reference.

4.3.13 mRNA sequencing

The protocol for mRNA sequencing has been previously described . Briefly, cDNA libraries were generated from high-quality (RNA integrity number >8.0) RNA samples from RNA extracted from pulverized kidney tissue using an Illumina TruSeq mRNA stranded HT kit (Illumina, San Diego, CA). An Illumina HT-2500 was used for sequencing; all samples were run on the same flow cell. After filtering and mapping to the

GRcm38/mm10 assembly, a list of 20,032 genes was obtained. Differential gene expression was determined via the R (v 3.3.1) package DESeq2 (v 1.12.3) (Love *et al.*, 2014), following recommended guidelines by the authors. To be deemed differentially-expressed, $\log_2$ fold-changes and false discovery rate (FDR)-adjusted p-values were cut off at 0.58 and 0.1, respectively. A cut-off for $\log_2$ of 0.58 represents an approximate 1.5-fold change in expression level compared to the reference (LFD) group. Default settings in DESeq2 were used for FDR adjustment.

4.3.14 Statistical Analyses

GraphPad Prism (v 5.0), was used for statistical analysis for biochemical analyses. One-way ANOVA followed by Newman-Keuls post-hoc test was used for comparisons between different disease states, where a p-value <0.05 was deemed statistically significant. For analysis of correlations between metabolizing enzyme transcript abundance and toxicokinetic phenotype, Pearson correlation coefficients were determined and associated p-values were corrected for multiple comparisons .

4.3.15 Data Availability

RNA sequencing data are publically-available through Gene Expression Omnibus (GEO; accession ID: GSE115641; http://www.ncbi.nlm.nih.gov/geo/query/acc.cgi?acc=GSE115641) and individual animal phenotype data are supplied as Supplementary Files. In addition to GEO, complete lists of

differentially-expressed genes and enriched pathways are provided as Supplementary Files.

4.4 Results

4.4.1 NAFLD affects the toxicokinetics of PCE and its oxidative and conjugative metabolites.

We first determined whether experimental NAFLD affects the kidney toxicokinetics of parent compound (PCE), oxidative (TCA), and GSH conjugative metabolites (TCVG, TCVC, and NAcTCVC) up to 36 hours after a single oral dose of PCE (300 mg/kg). The kidney kinetics of PCE were qualitatively similar among LFD-, HFD-, and MCD-fed mice (Figure 4.2, left panel). However, HFD- or MCD-fed mice had lower concentrations of PCE in the kidney, where the area under the concentration-time curve (AUC) of PCE was 1.3-fold or 2.1-fold lower in HFD- or MCD-fed mice, respectively, compared to LFD-fed mice (Figure 4.2, right panel). HFD- or MCD-fed mice showed a delayed or inhibited clearance of TCA from kidney tissue compared to LFD-fed mice, which led to an apparent accumulation of TCA in the kidneys. Correspondingly, the AUC of TCA in the kidney was approximately 1.6- to 1.7-fold higher in HFD- and MCD-fed mice compared to LFD-fed mice. While the results for PCE and TCA were interesting, perhaps the more toxicologically-relevant finding was that mice with NAFLD had considerably lower AUCs of TCVG, TCVC, and NAcTCVC in kidney tissue. Of particular note was the finding that the AUC of TCVC, which may be metabolically-activated to electrophilic, cytotoxic, genotoxic, and/or mutagenic intermediates, was

approximately 30-40% lower in the kidneys of mice with NAFLD compared to LFD-fed mice.

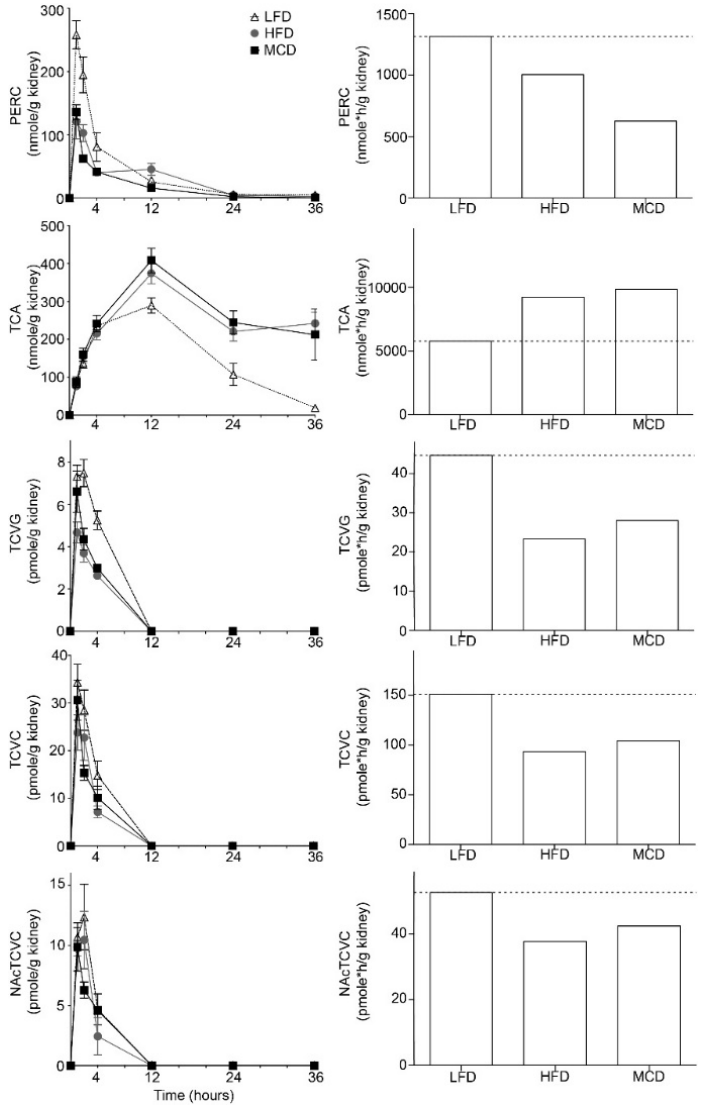

Figure 4.2 Kidney toxicokinetics of parent compound (PCE), oxidative metabolite (TCA), and glutathione conjugation metabolites of PCE (single dose, 300 mg/kg, i.g.) in male C57BL/6J mice fed with low fat diet (LFD), high fat diet (HFD), or methyl and choline deficient diet (MCD). Left panel shows the kinetic profiles, where the diet groups are identified by symbols (triangle, LFD; circle, HFD; square, MCD) and the line graph are shown as mean ± SD (n=4-5/time point/group). Right panel indicates the area under the concentration-time curves (AUCs) that are derived from the group mean kinetic profiles of PCE metabolites up to 36 hrs after dosing. The dotted-line represents values for LFD-fed mice.

4.4.2 Biochemical and histopathological evaluation of kidney injury.

Absolute kidney weight, but not kidney-to-bodyweight ratio, has been shown to correlate strongly with sub-chronic and chronic renal injury in rats (Craig *et al.*, 2015). Absolute kidney weight was unaffected by diet or PCE exposure (Table 4.1); however, kidney-to-body weight ratio was decreased in HFD-fed mice compared to LFD-fed control, and was significantly increased by PCE exposure in all three diet groups. This effect was likely due to PCE causing about a 10% decrease in body weight (Cichocki, *et al.*, 2017b). There was no effect of diet or PCE exposure on BUN or serum creatinine levels. Histopathological assessment of PCE effects on the kidneys showed no pathological changes in either group (data not shown).

Table 4.1 Absolute kidney weight and kidney to bodyweight ratio in this study

	LFD		HFD		MCD	
	Vehicle	PCE	Vehicle	PCE	Vehicle	PCE
Absolute kidney weight	0.28±0.03	0.30±0.02	0.31±0.02	0.31±0.02	0.29±0.01	0.30±0.02
Kidney: BW ratio	1.07±0.09[a]	1.19±0.08[b]	0.90±0.06[c]	1.00±0.03[a]	1.01±0.05 [a]	1.09±0.07 [a]

*Different superscripts indicate different statistical groups (ANOVA with Tukey's post-hoc test; $p<0.05$)

4.4.3 HFD-induced NAFLD manifests protective effects on kidney proximal tubule injury caused by PCE.

KIM-1 is a sensitive marker of acute renal injury and is especially useful for diagnosing xenobiotic-induced proximal tubular injury (Vaidya *et al.*, 2008). We observed very few KIM-1-stained proximal tubules in vehicle-treated mice (Figure 4.3A). In PCE-exposed LFD- and MCD-fed mice, approximately 40-50% of the proximal tubules were

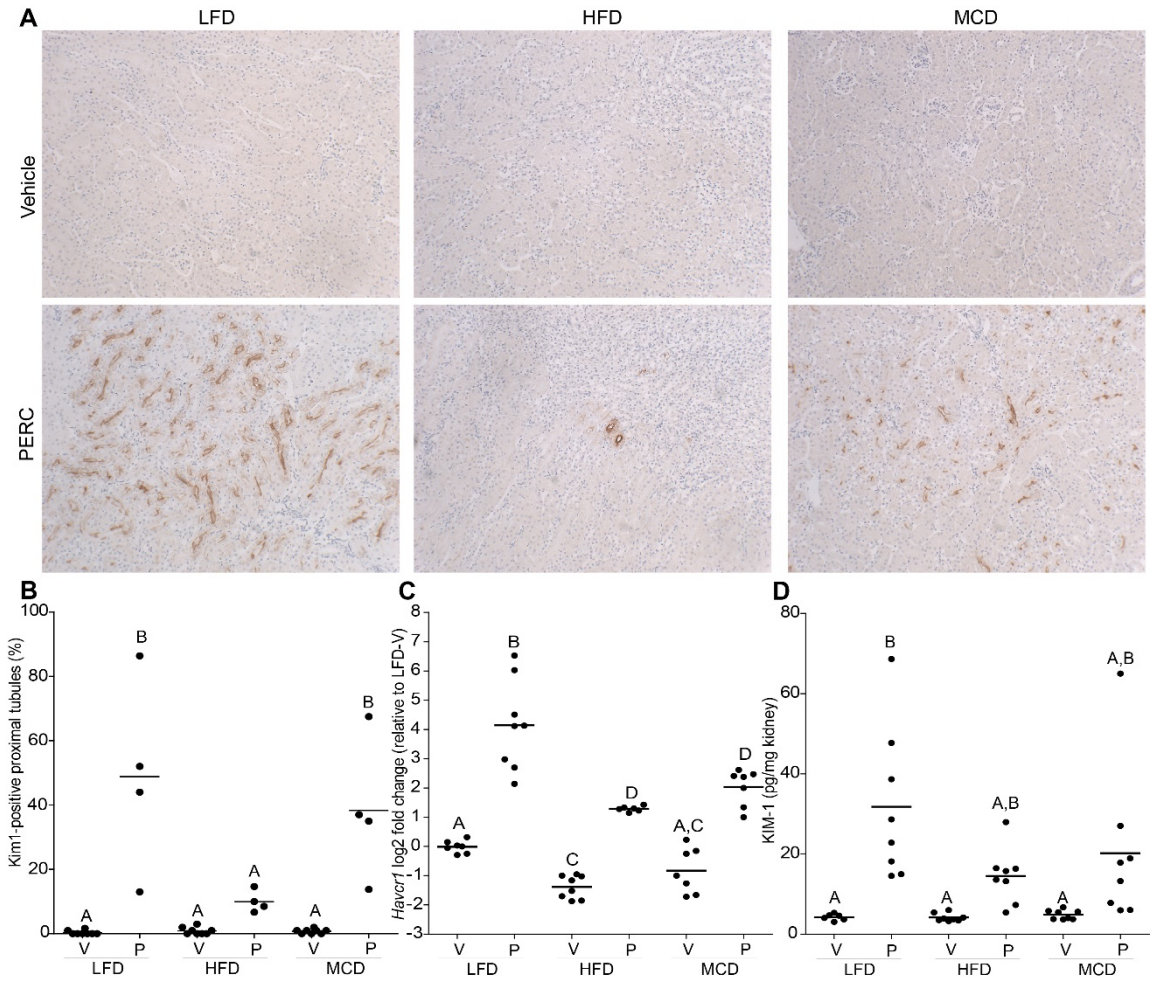

Figure 4.3 PCE-induced proximal tubular injury in mice after 8 weeks of low fat diet (LFD), high fat diet (HFD), or methyl and choline deficient diet (MCD). The PCE-induced proximal tubular injury is visualized by staining kidney injury molecule-1 (A). The percentage of positively-stained proximal tubules (B), gene expressions (C) and protein levels (D) of KIM-1 are shown in scatter plots. Groups with different letters are significantly different (One-way ANOVA with Newman-Keuls post hoc test, $p<0.05$).

positively-stained for KIM-1, indicating kidney injury, whereas only about 10% of the proximal tubules expressed detectable levels of KIM-1 in HFD-fed mice (Figure 4.3B). Data from immunohistochemical detection of KIM-1 were in concordance with gene expression of Havcr1 (Figure 4.3C) and KIM-1 protein levels in kidney homogenates (Figure 4.3D).

4.4.4 Effect of NAFLD on kidney transcriptome.

To characterize the molecular effects of PCE exposure on the kidneys in mice with or without NAFLD we used RNA sequencing. First, we sought to understand the effect of HFD and MCD diets on kidney gene expression in absence of PCE. Principal component analysis revealed that LFD-fed mice were completely separated from HFD- and MCD-fed mice, but the two NAFLD groups clustered together (Figure 4.4A). In HFD- or MCD-fed mice, a total of 223 and 165 genes, respectively, were differentially expressed compared to LFD-fed mice, with the majority of genes overlapping between these two groups (Figure 4.4B). There was a strong positive correlation between the gene expression data in HFD- and MCD-fed mice (Pearson's r=0.80), indicating that the directionality of change in expression (*i.e.* up-regulated or down-regulated) was similar between these two groups (Figure 4.4C). Molecular pathway analysis of the 125 genes that were differentially expressed in both HFD- and MCD-fed mice revealed altered retinol and drug metabolism and glycolysis/gluconeogenesis in the kidneys of mice with NAFLD (Table 4.2). With respect to genes involved in xenobiotic metabolism that were differentially-expressed in HFD- of MCD-fed vehicle-treated mice (Figure 4.4D), we found that *Ces1g*, *Cyp2d12*, *Cyp2c68*, *Cyp2c69*, and *Slc22a29* were down-regulated in HFD- or MCD-fed mice. At

the same time, *Slco1a1*, *Nat8f5*, *Ugt2b5*, and *Ugt2b37* were up-regulated compared to vehicle-treated LFD-fed mice. Generally, the effect of NAFLD on the expression of genes involved in xenobiotic metabolism was more pronounced in HFD- compared to MCD-fed mice.

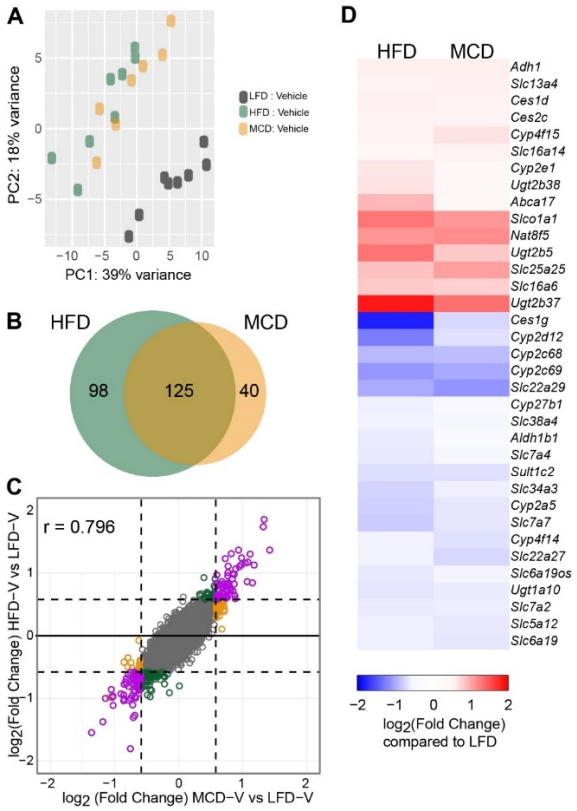

Figure 4.4 Effect of diets on kidney transcriptome. All analyses were conducted on vehicle-treated mice (24 hr time point) after 8 weeks of low fat diet (LFD), high fat diet (HFD), or methyl and choline deficient diet (MCD). (A) Principle component analysis of diet-mediated effects on kidney transcriptome. (B) Venn diagram showing the differentially-expressed genes of HFD or MCD group as compared to LFD group. Transcript with an absolute value of log2 fold change > 0.58 and an adjusted q-value < 0.1 is deemed to be differentially-expressed. (C) Plot of fold changes (log2, compared with LFD) of individual transcripts in HFD- and MCD-fed mice. Transcripts changed by diets are colored in green (HFD), orange (MCD), or purple (both). (D) Heatmap of diet effects on xenobiotic metabolism-associated genes. Transcripts changed by diet are colored by red (up-regulation) or blue (down-regulation).

Table 4.2 Molecular pathways perturbed by HFD or MCD in mouse kidney

KEGG_PATHWAY	No. of genes	Fold Enrichment	Benjamini corrected q-value
HFD: 223			
mmu01100:Metabolic pathways	33	2.2	8.56E-04
mmu00140:Steroid hormone biosynthesis	9	8.7	1.10E-03
mmu00830:Retinol metabolism	8	7.5	3.88E-03
mmu00983:Drug metabolism - other enzymes	6	9.9	9.20E-03
mmu00053:Ascorbate and aldarate metabolism	5	15.5	9.49E-03
mmu00980:Metabolism of xenobiotics by cytochrome P450	6	7.9	1.47E-02
mmu00982:Drug metabolism - cytochrome P450	6	7.6	1.52E-02
mmu00010:Glycolysis / Gluconeogenesis	6	7.6	1.52E-02
mmu01130:Biosynthesis of antibiotics	10	3.9	1.64E-02
mmu00040:Pentose and glucuronate interconversions	5	11.7	1.67E-02
mmu05204:Chemical carcinogenesis	7	6.4	1.76E-02
mmu04610:Complement and coagulation cascades	6	6.6	2.59E-02
mmu00340:Histidine metabolism	4	14.0	3.26E-02
mmu04512:ECM-receptor interaction	6	5.7	4.13E-02
MCD: 165			
mmu04610:Complement and coagulation cascades	9	12.9	4.63E-05
mmu00830:Retinol metabolism	7	8.6	9.44E-03
mmu00140:Steroid hormone biosynthesis	6	7.5	4.74E-02
mmu01100:Metabolic pathways	23	2.0	4.84E-02
Common genes 125			
mmu00830:Retinol metabolism	7	10.5	5.46E-03
mmu00140:Steroid hormone biosynthesis	6	9.2	2.58E-02
mmu01100:Metabolic pathways	21	2.2	2.06E-02
mmu00010:Glycolysis / Gluconeogenesis	5	10.1	4.09E-02

4.4.5 NAFLD-dependent perturbation of kidney lipid metabolism in mice following PCE exposure.

PCE exposure was associated with differential expression of 378, 315, and 222 genes in kidneys of LFD-, HFD-, and MCD-fed mice, respectively. Of these genes, 109

overlapped among all three groups (Figure 4.5A). Gene set enrichment analysis revealed a number of molecular pathways in the kidneys were perturbed by PCE exposure, including fatty acid synthesis and metabolism, PPARα signaling, and xenobiotic metabolism (Figure 4.5B), among which biosynthesis of unsaturated fatty acids and fatty acid metabolism were the most enriched pathways in MCD-fed mice. While many pathways were enriched in all diet groups, a few PCE-dependent pathways were modulated in a diet-specific fashion. Xenobiotic metabolism and transport were enriched only in PCE-exposed LFD-fed mice, while butanoate metabolism and amino acid degradation were enriched only in PCE-exposed MCD-fed mice.

Next, we extracted unique genes from the top five enriched pathways ("biosynthesis of unsaturated fatty acids", "fatty acid metabolism", PPAR signaling pathways", "drug metabolism", and "metabolism of xenobiotics by cytochrome P450") and performed unsupervised hierarchical clustering of the individual genes (Figure 4.5C). Two anion transporter genes (*Slc7a13* and *Slc22a7*) were down-regulated in all PCE-treated animals. Metabolism–associated genes (*Ugt1a10, Ugt1a2, Aldh1b1, and Pck2*), amino acid transporter gene (*Slc43a1*), and Kim-1 gene (*Havcr1*) are up-regulated in PCE-treated animals; the effects were more pronounced in LFD-fed mice. The rest of xenobiotic metabolism-associated genes were also induced by PCE, but were more pronounced in HFD-fed mice. As a PPARα responsive gene, *Cyp4a10* expression was induced by PCE in all three diet groups, with the greatest induction being observed in MCD- and HFD-fed mice compared to LFD-fed mice. The extent of *Cyp4a10* induction is concordant with the kidney levels of TCA, which is a known PPARα activator. To confirm these diet-

dependent effects of PCE on kidney gene expression that were discovered by RNA-sequencing, we measured the expression of *Lcn2*, *Havcr1*, and *Fabp1* via qRT-PCR. The results were largely similar between qRT-PCR (Figure A-5A-C) and RNA-sequencing (Figure A-5D-F).

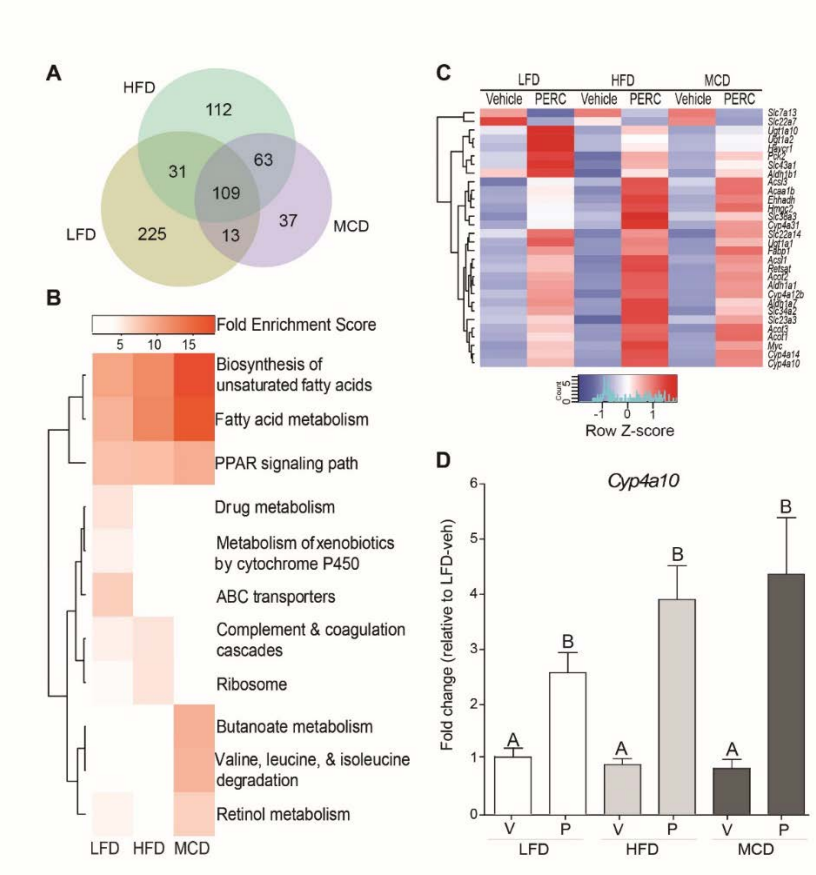

Figure 4.5 Diet-specific effects of PCE exposure on kidney transcriptomes. (A) Venn diagram showing the differentially-expressed genes in PCE-exposed group as compared to diet-matched, vehicle-treated group. Transcript with an absolute value of log2 fold change > 0.58 and an adjusted q-value < 0.1 is deemed to be differentially-expressed. (B) Perturbed biological pathways due to PCE exposure in mice fed with LFD, HFD, or MCD for 8 weeks. The fold enrichment scores are colored, and scaled from 0 (white) to 20 (orange). (C) Heatmap of diet-and PCE-induced effects on xenobiotic metabolism-associated genes. Transcripts are colored by row Z-score, and scaled from -2 (blue) to 2 (red). (D) Quantitative RT-PCR results for *Cyp4a10* expression in mouse kidney.

4.5 Discussion

NAFLD is known to alter the expression of transporter and metabolism genes in the liver (Cichocki, *et al.*, 2017b; Clarke *et al.*, 2014; Hardwick, *et al.*, 2014; Uno, *et al.*, 2018), which in turn can affect the delivered dose of xenobiotics to this organ (Cichocki, *et al.*, 2017a). The differences in a delivered dose depending on the liver disease state contributes to altered chemical-induced effects in the liver, as shown for benzo[a]pyrene (Uno, *et al.*, 2018), vinyl chloride (Lang, *et al.*, 2018), carbon tetrachloride (Donthamsetty *et al.*, 2007) and PCE (Cichocki, *et al.*, 2017b). However, even though NAFLD has also been shown to change the expression of renal xenobiotic transporters (Canet *et al.*, 2015), few studies examined the effects of NAFLD on xenobiotic-induced renal injury. In this study, by using PCE as a model compound, we reveal several important findings for the effects of NAFLD on kidney metabolism and toxicity in mice.

First, NAFLD can modulate the metabolism and disposition of xenobiotics in the kidney. In this study, mice fed either a HFD or MCD had 0.5- to 0.8-fold lower levels of PCE in kidney tissue compared to LFD-fed mice. It was previously demonstrated in liver tissue from these same mice that HFD- or MCD-fed mice had higher 1.5- to 2-fold higher PCE levels compared to LFD-fed mice, an effect which was attributed to an increased affinity of PCE for the lipid-laden liver tissue of mice with NAFLD (Cichocki, *et al.*, 2017a). Indeed, the liver:air partition coefficients were reported to be 2.4- to 4.9-fold higher in HFD- or MCD-fed mice compared to LFD-fed mice (Cichocki, *et al.*, 2017a). As PCE also induces liver fat accumulation (Cichocki, *et al.*, 2017b; Cichocki, *et al.*,

2017c), it is not surprising that the majority of PCE, a lipophilic compound, is retained in fatty liver tissue, thereby decreasing its transport to the kidney for subsequent metabolism.

Interestingly, HFD- or MCD-fed mice had greater TCA levels in kidney tissue compared to those in liver tissue (Cichocki, *et al.*, 2017a). The elimination of TCA from kidney also appeared to be considerably delayed in HFD- or MCD-fed mice, as supported by observations of increased retention of TCA in the liver and decreased urinary elimination of TCA (Cichocki et al 2017b). Even though the expression of hepatic genes associated with PCE oxidation (*Cyp2c29*, *Cyp3a11*, and *Cyp2b10*) are downregulated in HFD- or MCD-fed mice (Cichocki, *et al.*, 2017b), we observed higher levels of TCA in liver and kidney tissue from HFD- or MCD-fed mice compared to LFD-fed mice, an effect which may have been due to xenobiotic transporter activity or physiochemical properties.

We also found that levels of the PCE glutathione conjugation metabolites TCVG, TCVC, and NAcTCVC were lower in the kidney of HFD- or MCD-fed mice compared to LFD-fed mice, which is concordant with the levels of these metabolites previously measured in liver and urine (Cichocki, *et al.*, 2017a). The lower levels of glutathione conjugation metabolites are consistent with the repressed expression of GSTs in the liver of HFD- or MCD-fed mice compared to LFD-fed mice (Cichocki, *et al.*, 2017a). Notably, the tissue disposition of glutathione conjugation metabolites is qualitatively similar among LFD-, HFD-, and MCD-fed mice, where the most abundant metabolite is TCVG in liver but TCVC in kidney. The tissue-specific disposition of TCVG and TCVC is consistent with the results from previous studies (Luo, *et al.*, 2017). Collectively, these data suggest that the effect of liver disease state on the toxicokinetic properties of a xenobiotic is

complex and involves hepatic and extrahepatic tissue (*e.g.* kidney), chemical-physiological factors (*e.g.* liver:blood partition coefficient), metabolism (*e.g. Cyp* expression), and elimination (*e.g.* urinary clearance).

Second, we show that NAFLD can also modulate chemical-induced kidney toxicity. Sub-chronic or chronic exposure to PCE via inhalation was associated with karyomegaly of the renal tubular epithelial cells, renal casts, and nephrosis in mice, and tubular cell karyomegaly and hyperplasia in rats (Japanese Industrial Safety Association, 1993; National Toxicology Program, 1986). Traditional measures of kidney dysfunction, such as blood urea nitrogen levels and histopathological assessment fail to detect kidney injury by PCE as shown in this study and by others (Philip, *et al.*, 2007). However, renal proximal tubular injury by PCE has been reported with more sensitive markers of kidney injury, such as KIM-1 (Luo *et al.*, 2018b). Indeed, in our study we also observed kidney damage in LFD-fed mice. What is most intriguing, this effect was almost fully abrogated in HFD-fed mice, but not in MCD-fed mice. Severe methyl and choline deficiency during weaning is known to result in acute kidney failure(Roberti *et al.*, 1988), but more tempered dietary deficiency that is used to model NAFLD in rodents, even when administered for up to 10 months, has no pathologic effects(Porta *et al.*, 1985). Thus, it is possible that MCD diet in conjunction with PCE exhibited a potentiation effect on kidney injury through increased toxicodynamic sensitivity, counter-balancing the decreased toxicokinetic sensitivity exhibited by reduced glutathione conjugation metabolite levels. In support of this hypothesis, it was previously shown that rats with MCD-induced NAFLD were more sensitive to the nephrotoxic effects of methotrexate, including tubular

generation, necrosis, and the inability to regenerate damaged tubules, compared to control diet-fed rats (Hardwick, *et al.*, 2014).

Gene expression profiling served as another sensitive measure of diet- and PCE-induced effects on the kidney. Methyl-donor deficient diet induces profound changes in gene expression in mouse liver (Cichocki, *et al.*, 2017a; Tryndyak *et al.*, 2012a); however, the effects of this diet on gene expression in the mouse kidney is negligible (Glen *et al.*, 2015). We also found that the effect of either HFD or MCD on the kidney transcriptome was mild and similar between the two diets. MCD diet results in major epigenetic effects in the liver, but produces no changes in DNA methylation level or activity of DNA methyltransferase in the rat kidney, even when treated for up to 36 weeks (Pogribny *et al.*, 2004). These studies show that overall, MCD diet has little effect on the molecular changes in the kidney, as opposed to the liver. However, the modifications of the PCE-induced effects on the kidney transcriptome by HFD- or MCD-feeding were noteworthy. For example, mice fed the HFD and, especially, MCD exhibited more pronounced PCE-induced changes in lipid metabolism, but less pronounced PCE-induced changes in xenobiotic metabolism and ABC transporters. Interestingly, transcripts related to amino acid transporters (e.g. *Slc38a3*, *Slc34a2*, *Slc22a3*, and *Slc22a14*) are more profoundly upregulated in kidney of HFD- or MCD-fed mice. Increased transcription of these amino acid transporters may contribute to the lower levels of TCVG, TCVC, and NAcTCVC in kidney; however, whether these compounds are substrates for renal xenobiotic transporters remain to be determined.

Overall, relative insensitivity of HFD-fed mice to PCE-induced kidney injury, as compared to MCD-fed mice, is a noteworthy finding. One possible explanation is the degree of NAFLD in these mouse models (Machado *et al.*, 2015) and its role in kidney disease (Musso *et al.*, 2015). Indeed, in the animals examined herein, MCD diet resulted in NASH, whereas HFD diet produced only NAFL (Cichocki, *et al.*, 2017b). Our finding of greater PCE-induced kidney injury in MCD-fed mice are in a good agreement with previous reports that NASH is associated with a higher prevalence of chronic kidney disease in humans (Musso *et al.*, 2014). Mechanistically, the development of kidney injury in MCD-fed mice may be attributed, at least in part, to (*i*) inflammation induced by pro-inflammatory cytokines released from NASH-inflamed liver; (*ii*) dysregulated lipid metabolism and toxic lipid accumulation in kidney; and (*iii*) deregulation of lipoprotein metabolism (Musso, *et al.*, 2015; Rivkin *et al.*, 2016).

Third, the internal dosimetry of PCE and its metabolites agree with what is known and/or hypothesized about the target organ toxicity of PCE. For instance, the greater tissue levels of TCA in HFD- or MCD-fed mice concur with the more pronounced PPARα activation in the liver and kidney of these mice compared to LFD-fed controls. Likewise, the lower glutathione metabolite levels in kidney is concordant with the milder proximal tubule injury found in mice with NAFLD, particularly in HFD-fed mice, and with the lower number of differentially-expressed genes observed in kidney tissue. These observations are in accord with the results from a study using cytochrome P450 2E1 (CYP2E1) knockout and humanized transgenic mice to investigate the metabolism and toxicity of PCE (Luo, *et al.*, 2018b), in which CYP2E1 knockout mice exhibited lower

TCVG, TCVC, and NAcTCVC levels in kidney, which was associated with a milder PCE-induced proximal tubular injury as compared to wild-type mice. Collectively, these data support the long-lasting hypothesis that glutathione-derived metabolites are the major determinants of PCE-induced nephrotoxicity *in vivo*.

There are a number of limitations to this study. For example, animals were administered a relatively high dose of PCE (300 mg/kg, *i.g.*), which is unlikely to occur in humans. PCE oxidation is saturable at doses over 200 mg/kg (Buben and O'Flaherty, 1985), which may limit our interpretation for the kinetics observed in this study to those that occur at environmentally-relevant exposures. However, the glutathione conjugation pathway is approximately 100-fold less efficient in mice compared to humans for the related compound trichloroethylene (Chiu, *et al.*, 2009), therefore suggesting that the internal dose of glutathione metabolites in mouse kidney could still be relevant to PCE exposures to humans, albeit human data are not available and a PBPK model showed 1000-fold uncertainty in PCE glutathione conjugation (Chiu and Ginsberg, 2011). The other limitation of this study is the applicability of animal NAFLD/NASH models to human NAFLD, a contentious issue in the field (Maher, 2011; Teufel *et al.*, 2016). Even though HFD-fed animals can mimic the histopathological phenotype of human NAFLD, the degree of injury depends on a number of factors including rodent strains (Lau *et al.*, 2017). In addition, the metabolic profile of methionine/choline/folate-deficient (e.g. MCD-fed) mice is different from human NASH (Rinella and Green, 2004) and is also dependent on rodent strain (Tryndyak *et al.*, 2012b). Despite these limitations, in this study

we were able to characterize the effects of pre-existing liver disease on kidney metabolism and toxicity of PCE.

In summary, we confirmed that NAFLD can alter the internal dosimetry of PCE and its metabolites in kidney, which in turn affects PCE-induced nephrotoxicity *in vivo*. While experimental NAFLD sensitized mice to PCE-induced liver toxicity (Cichocki, *et al.*, 2017b), we show here that NAFLD may be a protective factor for PCE-associated kidney effects due to reduced production and delivery of nephrotoxic glutathione conjugation-derived metabolites, as shown in male C57BL/6J fed HFD. However, this protective effect was abrogated in MCD-fed mice, which showed similarly decreased toxicokinetic sensitivity in the form of reduced nephrotoxic metabolite concentrations, but increased toxicodynamic sensitivity. These data, along with our previous study of how NAFLD affects liver toxicity (Cichocki, *et al.*, 2017b), demonstrate not only that underlying disease state could be an important factor to consider in future human health assessments of environmental toxicants, but also that the relationship between common diseases such as NAFLD and xenobiotic-induced toxicity may involve a complex, organ-specific interplay of toxicokinetic and toxicodynamic effects.

Table 4.3 Molecular pathways perturbed by PCE in mouse kidney

KEGG_PATHWAY	No. of genes	Enrichment	Benjamini q-value
LFD: 378			
mmu00980:Metabolism of xenobiotics by cytochrome P450	14	10.3	1.05E-07
mmu00982:Drug metabolism - cytochrome P450	14	10.0	7.88E-08
mmu01100:Metabolic pathways	58	2.1	4.04E-07
mmu03320:PPAR signaling pathway	14	8.2	4.70E-07
mmu00830:Retinol metabolism	14	7.4	1.42E-06
mmu00071:Fatty acid degradation	11	10.6	1.78E-06
mmu05204:Chemical carcinogenesis	14	7.2	1.53E-06
mmu01040:Biosynthesis of unsaturated fatty acids	6	10.5	5.40E-03
mmu00053:Ascorbate and aldarate metabolism	6	10.5	5.40E-03
mmu04146:Peroxisome	9	5.1	7.50E-03
mmu00140:Steroid hormone biosynthesis	9	4.9	9.30E-03
HFD: 315			
mmu00071:Fatty acid degradation	15	14.2	1.85E-10
mmu00830:Retinol metabolism	14	7.3	4.52E-06
mmu00980:Metabolism of xenobiotics by cytochrome P450	12	8.7	6.10E-06
mmu03320:PPAR signaling pathway	13	7.5	5.63E-06
mmu01100:Metabolic pathways	54	2.0	2.48E-05
mmu00040:Pentose and glucuronate interconversions	9	11.6	2.36E-05
mmu01212:Fatty acid metabolism	10	9.1	3.20E-05
mmu00053:Ascorbate and aldarate metabolism	8	13.7	2.92E-05
mmu00982:Drug metabolism - cytochrome P450	10	7.0	2.30E-04
mmu00983:Drug metabolism - other enzymes	9	8.2	2.26E-04
mmu01040:Biosynthesis of unsaturated fatty acids	7	12.0	3.37E-04
mmu00860:Porphyrin and chlorophyll metabolism	8	9.0	3.83E-04
mmu05204:Chemical carcinogenesis	11	5.5	3.95E-04
mmu04610:Complement and coagulation cascades	10	6.1	4.73E-04
mmu00140:Steroid hormone biosynthesis	10	5.3	1.30E-03
mmu00062:Fatty acid elongation	6	10.7	2.49E-03
MCD: 222			
mmu00071:Fatty acid degradation	14	20.2	1.10E-11
mmu01100:Metabolic pathways	43	2.4	1.63E-06
mmu03320:PPAR signaling pathway	11	9.7	7.77E-06
mmu00062:Fatty acid elongation	7	19.1	5.08E-05
mmu01040:Biosynthesis of unsaturated fatty acids	7	18.4	5.17E-05
mmu00830:Retinol metabolism	10	8.0	1.04E-04
mmu01212:Fatty acid metabolism	8	11.1	1.46E-04
mmu01130:Biosynthesis of antibiotics	13	4.3	8.60E-04
mmu04146:Peroxisome	8	6.8	2.82E-03

CHAPTER V

METABOLISM AND TOXICITY OF TRICHLOROETHYLENE AND TETRACHLOROETHYLENE IN CYTOCHROME P450 2E1 KNOCKOUT AND HUMANIZED TRANSGENIC MICE[3]

5.1 Overview

Trichloroethylene (TCE) and tetrachloroethylene (PCE) are structurally similar olefins that can cause liver and kidney toxicity. Adverse effects of these chemicals are associated with metabolism to oxidative and glutathione conjugation moieties. It is thought that CYP2E1 is crucial to the oxidative metabolism of TCE and PCE, and may also play a role in formation of nephrotoxic metabolites; however, inter-species and inter-individual differences in contribution of CYP2E1 to metabolism and toxicity are not well understood. Therefore, the role of CYP2E1 in metabolism and toxic effects of TCE and PCE was investigated using male and female wild-type [129S1/SvlmJ], *Cyp2e1(-/-),* and humanized *Cyp2e1* [*hCYP2E1*] mice. To fill in existing gaps in our knowledge, we conducted a toxicokinetic study of TCE (600 mg/kg, single dose, *i.g.*) and a sub-acute study of PCE (500 mg/kg/d, 5 days, *i.g.*) in three strains. Liver and kidney tissues were

[3] This is a pre-copyedited, author-produced version of an article accepted for publication in Toxicological Sciences following peer review. The version of record is available online at https://doi.org/10.1093/toxsci/kfy099

subject to profiling of oxidative and glutathione conjugation metabolites of TCE and PCE, as well as toxicity endpoints. The amounts of TCA formed in the liver was *hCYP2E1*≈ 129S1/SvlmJ>*Cyp2e1*(-/-) for both TCE and PCE; levels in males were about 2-fold higher than in females. Interestingly, 2-3-fold higher levels of conjugation metabolites were observed in TCE-treated *Cyp2e1*(-/-) mice. PCE induced lipid accumulation only in liver of 129S1/SvlmJ mice. In the kidney, PCE exposure resulted in acute proximal tubule injury in both sexes in all strains (*hCYP2E1*≈129S1/SvlmJ>*Cyp2e1*(-/-)). In conclusion, our results demonstrate that CYP2E1 is an important, but not exclusive actor in the oxidative metabolism and toxicity of TCE and PCE.

5.2 Introduction

Trichloroethylene (TCE) and tetrachloroethylene (PCE) are structurally-similar olefins and high-production volume chemicals that have been used in chemical synthesis, metal degreasing, dry cleaning, and other industrial applications (U.S. EPA, 2011b; U.S. EPA, 2011c). TCE and PCE are extensively present in air, soil, and surface and ground water supplies (IARC, 2014). They are also frequently found at the hazardous waste sites on the National Priorities List (ATSDR, 2014). TCE and PCE are also detectable in human blood samples collected in the National Health and Nutrition Examination Survey (Jia, *et al.*, 2012). TCE and PCE are classified as "carcinogenic to humans" and "probably carcinogenic to humans," respectively, by the International Agency for Research on Cancer (Guha, *et al.*, 2012). They also can cause non-cancer effects in liver and kidney

(Cichocki, *et al.*, 2016). TCE and PCE are among the top 10 chemicals of concerns for the risks to human health and environment under the revised Toxic Substances Control Act (U.S. EPA, 2017).

Tissue-specific toxicity of TCE and PCE results from metabolism through the oxidative and glutathione conjugation pathways. Oxidation of TCE and PCE occurs on the double bond via cytochrome P450s (CYP) to form an epoxide intermediate, which is subsequently metabolized to oxidative species, including trichloroacetic acid (TCA) and/or TCE-specific metabolite trichloroethanol (TCOH) (Cichocki, *et al.*, 2016). TCA is a ligand to mouse and human peroxisome proliferation activated receptor alpha (PPARα) (Zhou and Waxman, 1998), which may be associated with cell proliferation in liver (Laughter *et al.*, 2004). Both TCE and PCE are also metabolized by glutathione conjugation via glutathione-S-transferases (GSTs) to generate dichloro- or trichloro-glutathione conjugates (DCVG/TCVG) (Lash, *et al.*, 2000). These conjugates can be further metabolized by hepatic or renal gamma glutamyl transferase and dipeptidase to form cysteine conjugates (DCVC/TCVC), and then are subject to n-acetylation to form NAcDCVC or NAcTCVC. These can be further bio-activated by a number of enzymes, including cysteine s-conjugate beta lyase, flavin monooxygenase, and CYPs, to form nephrotoxic metabolites such as reactive thiols (Volkel and Dekant, 1998) and sulfoxides (Elfarra and Krause, 2007; Lash, *et al.*, 2001a; Lash, *et al.*, 2003; Ripp, *et al.*, 1997; Werner, *et al.*, 1996). For both TCE and PCE, various CYPs play a critical role in generating metabolites that cause toxicity in both liver and kidney.

Among the CYPs isoenzymes, cytochrome P450 2E1 (CYP2E1) is the major contributor to oxidation of chlorinated solvents (Kim and Ghanayem, 2006; Nakajima *et al.*, 1993; Ramdhan, *et al.*, 2008). CYP2E1 is highly variable in expression (12-fold) in human liver (Lin and Lu, 2001) and inter-individual differences in CYP activity are thought to be a major contributor to population variability in adverse effects of TCE and PCE (Cichocki, *et al.*, 2016). In studies with TCE, both hepatotoxicity and production of oxidative metabolites were ameliorated in CYP2E1 knockout mice (Kim and Ghanayem, 2006; Ramdhan, *et al.*, 2008), albeit little is known about the exact role of CYP2E1 in TCE toxicokinetics. In experiments with PCE, one study posited that CYP2E1 can contribute to PCE toxicity (Hanioka *et al.*, 1995), but another study concluded that CYP2E1 is not the critical enzyme in sub-chronic effects of PCE (Philip, *et al.*, 2007). No study examined metabolism or toxicity of PCE in CYP2E1 knockout or humanized mice.

Therefore, in this work, we aimed to address existing knowledge gaps on the role of mouse and human CYP2E1 in the metabolism and toxicity of TCE and PCE. Because several studies already established that CYP2E1 is playing a role in liver effects of TCE, but its precise role in the formation of TCE metabolites is largely unknown, we conducted a toxicokinetic study of TCE in male and female 129S1/SvlmJ, *Cyp2e1(-/-)*, and humanized *(hCYP2E1)* mice. For PCE, we aimed to test whether CYP2E1 plays a role in the toxicity of PCE by using the same genetic models and a sub-acute study design.

5.3 Materials and Methods

5.3.1 Chemicals

TCE (≥99.5%), PCE (≥99.9%), TCA (≥99.0%), TCOH (≥99.0%), 2-bromobutyric acid (≥ 97%), chloroform (≥99.9%), and formic acid (≥95%) were obtained from Sigma-Aldrich (St. Louis, MO). Methanol (≥99.9%) was from Fischer Scientific (Hampton, NH). S-(1,2-dichlorovinyl)-cysteine (DCVC, ≥98.0%), S-(1,2-dichlorovinyl)-cysteine-$^{13}C_3$-^{15}N (DCVC*, purity ≥95.0%, isotopic purity ≥98.0%), S-(1,2-dichlorovinyl)-glutathione (DCVG, ≥98.9%), and S-(1,2-dichlorovinyl)-glutathione-$^{13}C_2$-^{15}N (DCVG*, purity ≥90.0%, isotopic purity ≥98.0%) were obtained from TLC Pharmaceutical Standards (Aurora, Canada). N-acetyl-S-(1,2-dichlorovinyl)-cysteine (NAcDCVC, 99.8%) and N-acetyl-S-(1, 2-dichlorovinyl)-cysteine-^{13}C, d_3 (NAcDCVC*, purity: 97.6%, isotopic purity: 99.0%), and NAcTCVC (purity: 99.7%) were purchased from Toronto Research Chemicals (Toronto, Canada). S-(1,2,2-trichlorovinyl)-glutathione-$^{13}C_2$-^{15}N (TCVG*, purity: 90.4%), S-(1,2,2-trichlorovinyl)-cysteine-$^{13}C_3$-^{15}N (TCVC*, purity: 97.5%), and N-acetyl-S-(1,2-dichlorovinyl)-cysteine-$^{13}C_3$-^{15}N (NAcTCVC*, purity: 99.0%) were used as internal standards for TCVG, TCVC, and NAcTCVC, respectively. TCVG (purity: 98.9%), TCVC (purity: 98.4%), and all stable isotopically-labeled internal standards were synthesized by Dr. Avram Gold at the University of North Carolina at Chapel Hill.

5.3.2 Animals and treatments

Male and female wild type, *Cyp2e1(-/-)*, and *hCYP2E1* mice on 129S1/SvlmJ (Sv129, The Jackson Laboratory, Bar Harbor, ME) were used in this study. Transgenic

mice were bred and genotyped by PCR before being used in this study. The primer sequences are detailed in Table B-13. Mice were housed in polycarbonate cages on Sani-Chips irradiated hardwood bedding (P.J. Murphy Forest Products, Montville, NJ), and supplied with NTP-2000 (Zeigler Brothers, Gardners, PA) wafer diet and water *ad libitum* on a 12 h light-dark cycle. After a week-long acclimatization, mice were intragastrically administered with TCE or PCE as detailed below (Figure 5.1). All treatments and procedures were approved by the Institutional Animal Care and Use Committee at the University of North Carolina at Chapel Hill.

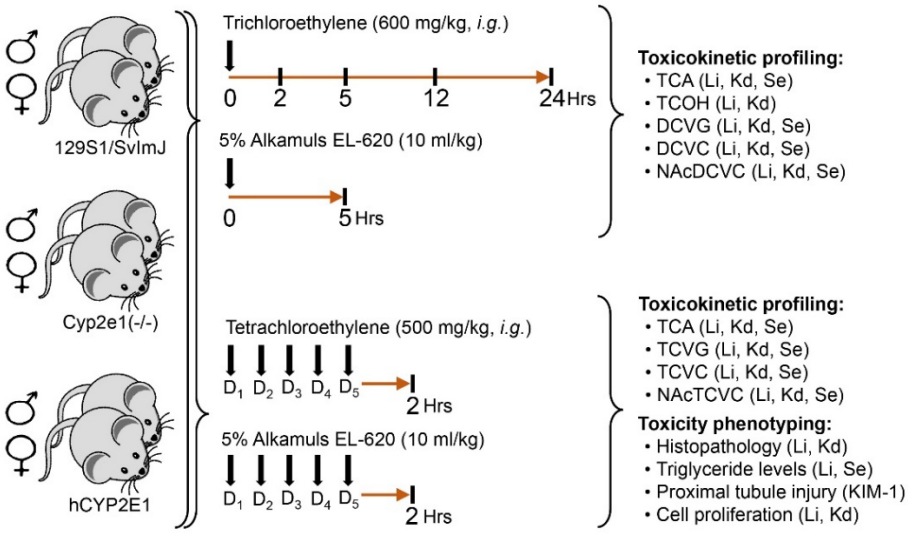

Figure 5.1 Schematic representation of study designs. Male and female mice from three strains (129S1/SvlmJ wild type, *Cyp2e1(-/-)* and *hCYP2E1*) were used in these studies. One study examined toxicokinetics of trichloroethylene in a single dose (600 mg/kg, gavage) study where samples were collected for up to 24 hrs. Second study examined metabolism and toxicity of tetrachloroethylene that was administered for 5 consecutive days (500 mg/kg, gavage); samples were collected 2 hrs after the last dose. Alkamuls EL-620 (5%, 10 ml/kg) was used as an aqueous emulsion vehicle for administration of both chemicals. Vertical lines indicate time points of sample collection. Down-arrows indicate chemical treatments. Endpoints collected in each study are shown as a bulleted list.

In a study of TCE toxicokinetics, mice were administered a single dose of 600 mg/kg TCE or vehicle (5% Alkamuls EL-620 in saline). The dose was selected based upon previous mouse studies showing that this amount was well tolerated in acute, 90-day, and 2-year studies (Buben and O'Flaherty, 1985; Luo *et al.*, 2018a; National Toxicology Program, 1990; Yoo, *et al.*, 2015a). In addition, mice form approximately 100-fold less glutathione conjugation metabolites (Chiu, *et al.*, 2009), which justifies the use of a dose that is higher than the environmental exposure to TCE. After dosing, mice were anesthetized (pentobarbital, 50 mg/kg i.p.) and sacrificed by exsanguination through the *vena cava* at 2, 5, 12, and 24 h (n=2-4 per group per time point, as detailed in Table B-14). Mice dosed with vehicle were sacrificed at 5 h after gavage. Livers and kidneys were collected, blotted dry, and snap-frozen in liquid nitrogen. Serum was prepared by using Z-gel tubes (Sarstedt, Darmstadt, Germany). All tissues and serum were stored at -80^{o}C until analyzed.

In a study of PCE metabolism and toxicity, mice were treated for 5 days with single daily dose (9 am) of 500 mg/kg/d PCE or vehicle (5% Alkamuls EL-620 in saline). The dose was selected based upon previous studies showing no saturation of PCE oxidation at similar doses (Buben and O'Flaherty, 1985; Philip, *et al.*, 2007), and that this amount was well tolerated in acute, 90-day, and 2-year studies (Buben and O'Flaherty, 1985; Cichocki, *et al.*, 2017a; Luo, *et al.*, 2017; National Toxicology Program, 1977). Mice were given drinking water containing 5-bromo-2′-deoxyuridine (BrdU) 72 hr prior to sacrifice. Mice were anesthetized and sacrificed by exsanguination through *vena cava* 2 h after the last dose of PCE or vehicle (n=4-7 per group, as detailed in Table B-15). Serum was prepared

by using Z-gel tubes, and then stored at -80^{o}C until analyzed. Tissue sections from left liver lobe and kidney were fixed in 10% formalin and embedded in paraffin. The remaining tissues were snap-frozen in liquid nitrogen and stored at -80^{o}C until analyzed.

5.3.3 Protein measurement of CYP 2E1

Total proteins were extracted from 20 mg of liver and kidney samples using T-PER Tissue Protein Extraction Reagent (Thermo Scientific, Rockford, IL) with Halt Protease Inhibitor Cocktail (Thermo Scientific). Protein concentration was determined using Pierce BCA Protein Assay Kit (Thermo Scientific) and a DTX 880 Multimode detector (Beckman Coulter, Brea, CA). Protein extract (20 μg) was loaded onto a Mini-Protein TGX Precast Gel (Bio-Rad, Hercules, CA) and transferred to a polyvinylidene difluoride membrane. Membrane was blocked with Odyssey Blocking Buffer (LI-COR, Lincoln, NE), probed with CYP2E1 primary antibody (1:5000, catalogue #: 28146, abcam, Cambridge, MA) or beta-actin primary antibody (1:2500, catalogue #: ab8227, abcam, Cambridge, MA) overnight at 4^{o}C, washed with 0.1% Tween 20 in 0.01M PBS buffer, probed with goat anti rabbit IgG antibody (1:2500, catalogue #: AP132P, Millipore Corp., Billerica, MA) for 90 min at room temperature, and detected using an Odyssey Infared Imaging system (LI-COR).

5.3.4 Quantification of TCA

Tissue levels of TCA were measured using the US EPA method 815-B-03-002 (Domino *et al.*, 2003) with slight modifications. Tissues (50 mg) were spiked with 11

nmole of internal standard (2-bromobutyric acid), and homogenized in 1 mL of methanol:chloroform (1:1). After centrifugation at 14,000 g for 10 mins, supernatant was mixed with 1.5 mL of methanolic sulfuric acid (10%, v:v). The mixture was incubated in water batch at 55^{o}C for 2 h to derive respective methyl esters. The derivative was then mixed well with 2 mL of methyl tert-butyl ether and 3 mL of sodium sulfate buffer (150 g/L). The upper layer was collected and mixed well with 3 mL of saturated sodium bicarbonate. Again, the upper layer was collected, concentrated under nitrogen stream to a volume of ~20 μL, and analyzed via gas chromatography mass spectrometry. Quantitative analyses were achieved by using the peak area ratios of TCA to internal standards in an eight-point calibration curve (0, 4.1, 12.3, 37.0, 111.1, 333.3, 1000, and 3000 nmole spiked TCA).

5.3.5 Quantification of TCOH

Liver or kidney tissues (30 mg) were homogenized in 0.5 mL of sodium acetate (0.1 M, pH 4.6), spiked in 1000 units of beta-glucuronidase, and incubated in a thermomixer overnight at 37^{o}C. The incubated homogenate was spiked with 20 μl of ethyl benzene (1000 nmol/mL), and then incubated in 1.5 mL of 10% sulfuric acid in methanol at 50 ^{o}C for 1 h. Afterwards, the incubated solution was evenly mixed with 2 mL of MTBE and 3 mL of sodium sulfate (150 g/L), and centrifuged at 2,500 g for 3 min. The MTBE layer was neutralized by 3 mL of saturated sodium bicarbonate, collected, and concentrated with nitrogen gas to ~20 μL for GC-MS analysis (Song and Ho, 2003).

Quantitative analyses were achieved by using the peak area ratios of TCOH to ethyl benzene in an eight-point calibration curve (0-1200 nmole TCOH/g tissue).

5.3.6 Quantification of D/TCVG, D/TCVC, and NAcD/TCVC

Tissue levels of dichloro and trichloro conjugates of TCE and PCE (D/TCVG, D/TCVC, and NAcD/TCVC) were evaluated as reported in (Luo, *et al.*, 2017; Luo, *et al.*, 2018a). In brief, tissue homogenate underwent a liquid-liquid extraction with 400 µL of methanol:chloroform (1:1) and a solid-phase extraction using a weak anion C-18 cartridge (Strata-X-AW, Phenomenex, Torrance, CA). The eluent was dried under vacuum, and reconstituted with 50 µL of methanol:water (20:80) with 0.1 % acetic acid. Tissue levels of metabolites were quantified by using the peak area ratios of standards to isotopically-labeled internal standards in an eight-point calibration curve (0, 0.25, 0.5, 1.25, 2.5, 6.25, 18.75, and 31.25 pmole) via UPLC-MS/MS.

5.3.7 Serum Alanine Aminotransferase and Aspartate Aminotransferase

Serum alanine aminotransferase (ALT) and aspartate aminotransferase (AST) were determined by commercially available kits (Sigma Aldrich) according to the manufacturer's instructions.

5.3.8 Triglyceride Measurements

Serum and liver triglycerides were measured with a commercially available kit (Wako, Richmond, Virginia) according to the manufacturer's instructions.

5.3.9 Histopathological Evaluation

Formalin-fixed/paraffin embedded liver and kidney sections were stained with hematoxylin/eosin (H&E). Stained H&E slides were evaluated in a blind manner by a certificated veterinary pathologist.

5.3.10 KIM-1 Immunohistochemistry Staining

Kidney sections were dewaxed in xylene and rehydrated in graded ethanols, and then subjected to hydrochloric acid and pepsin antigen retrieval. Endogenous peroxidase activity was blocked with peroxidase and alkaline phosphatase blocking reagent (Dako, Carpinteria, CA) at 25 ^{o}C for 10 mins. Thereafter, kidney sections were subsequently incubated with goat anti-mouse TIM-1/KIM-1/HAVCR (R&D systems, Minneapolis, MN; 2 μm/ml, 10 min, room temperature) and secondary goat IgG HRP-conjugated antibody (R&D systems, Minneapolis, MN; 1:100, 10 min, room temperature) using Dako Antibody Dilution solution (Dako), and visualized by Dako Liquid DAB+Substrate chromogen System (Dako). Processed slides were counterstained with hematoxylin for 5 mins. Quantitative analysis was performed by using Image-Pro Premier 9.1 (Media Cybernetics, Silver Spring, MD) at 200× magnification. Five fields of kidney section were randomly selected to calculate the percentage of positive proximal tubules versus total proximal tubules.

5.3.11 BrdU Immunohistochemistry Staining

Kidney sections were subject to de-paraffinization, rehydration, antigen retrieval, and peroxidase blocking procedures as described above. Thereafter, Dako EnVision System HRP kit with a monoclonal anti-BrdU antibody (1:200 dilution, M074401-8, Dako) was used for detection of BrdU-incorporated nuclei. Quantitative analysis was performed by using Image-Pro Premier 9.1 (Media Cybernetics) at 200× magnification. Five fields of each kidney section were randomly selected for evaluation. Data are presented as a fraction of positively stained nuclei versus total proximal tubule nuclei (%).

5.4 Results

5.4.1 Protein Expression of CYP2E1

CYP2E1 status in various strains was verified by genotyping before the study. In addition, to quantify the effects of treatments on CYP2E1 protein levels, we conducted Western blotting experiments. In agreement with previous studies of *Cyp2e1(-/-)* and *hCYP2E1* transgenic mice (Lu *et al.*, 2010), CYP2E1 expression in liver was higher in *hCYP2E1* strain than in Sv129 strain, it was undetectable in *Cyp2e1(-/-)* mice (Figure 5.2). Protein levels of CYP2E1 were much greater in liver than in kidney, also concordant with previous reports of gene expression in the mouse (Yue *et al.*, 2014). Lack of expression of CYP2E1 in mouse kidneys is also consistent with low levels of CYP2E1 in human kidneys (Fagerberg, *et al.*, 2014). In addition, protein levels of CYP2E1 were slightly higher in liver of male mice as compared to female mice. This sex-dependent difference was even more pronounced in kidneys where no detectable CYP2E1 protein was found in

females. The sex difference was not found in the liver of Sv129 mice (Nakajima *et al.*, 2000) or CD-1 mice (Hoivik *et al.*, 1995); however, it was observed in kidney of CD-1 mice (Hoivik, *et al.*, 1995) where protein level of CYP2E1 was higher in male mice as compared to female mice. We found that TCE induced expression in CYP2E1 only in liver of female mice of both *hCYP2E1* and Sv129 strains, suggesting that TCE treatment and sex hormones may regulate liver expression of CYP2E1.

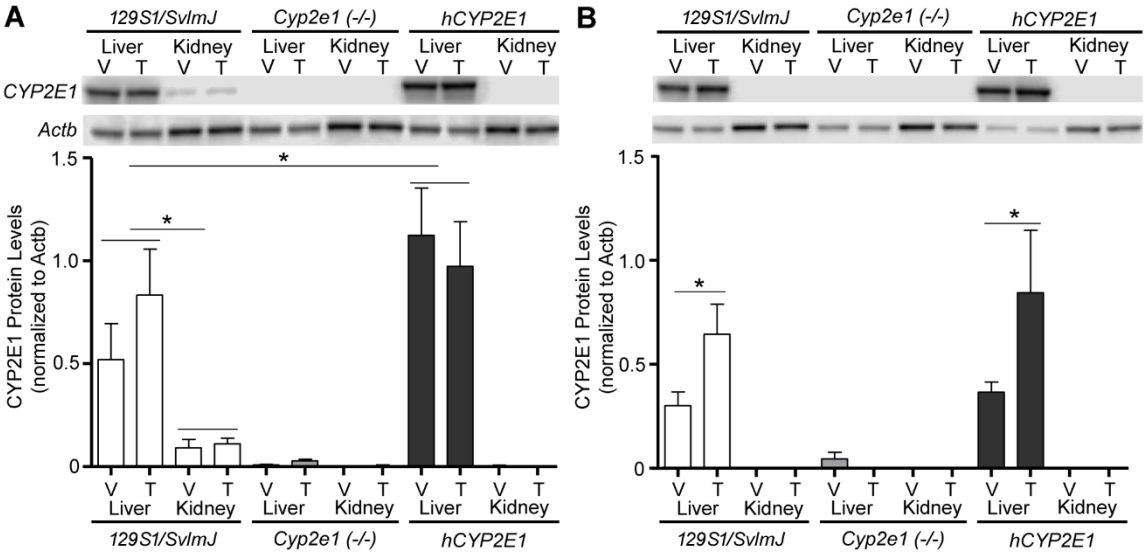

Figure 5.2 Protein expression of CYP2E1 in liver and kidney of (A) male and (B) female 129S1/SvlmJ, Cyp2e1(-/-), and hCYP2E1 mice at 4 hours after dosing with a single dose of vehicle (V, Alkamuls EL-620) or TCE (T, 600 mg/kg). Representative Western blots and quantitative analysis of CYP2E1 protein expression are shown (n=4/group). Expression of beta actin (Actb) was used to normalize for protein loading. Data are shown as mean±SD. Asterisks denote statistical significant difference between groups (one-way ANOVA with Newman-Keuls post hoc test, $p<0.05$).

5.4.2 The Role of CYP2E1 in Toxicokinetics of TCE

Next, we sought to examine TCE toxicokinetics as a factor of CYP2E1 status in each strain and sex. We examined concentration-time profiles of TCA, TCOH, DCVG and

NAcDCVC in liver (Figure 5.3). In male Sv129 mice, we found that liver toxicokinetics of TCA, TCOH, and DCVG were similar to those reported in previous studies using 129S1/SvImJ mice (Yoo, *et al.*, 2015a; Yoo, *et al.*, 2015c), B6C3F1/J mice (Luo, *et al.*, 2018a), and Collaborative Cross mice (Venkatratnam *et al.*, 2017). The area under curve (AUC) analysis of the metabolite levels revealed sex-dependent differences in liver toxicokinetics of TCE. In Sv129 mice, AUC was higher in male mice as compared to female mice for TCA and TCOH (2.2-fold for TCA and 33.9fold for TCOH), but lower for DCVG and NAcDCVC(1.9 fold for DCVG and 1.6 fold for NacDCVC). The sex-dependent differences in liver toxicokinetics for TCA and TCOH were also observed in the previous study (Yoo, *et al.*, 2015c), while the sex differences for liver toxicokinetics of DCVG and NAcDCVC has not been previously investigated.

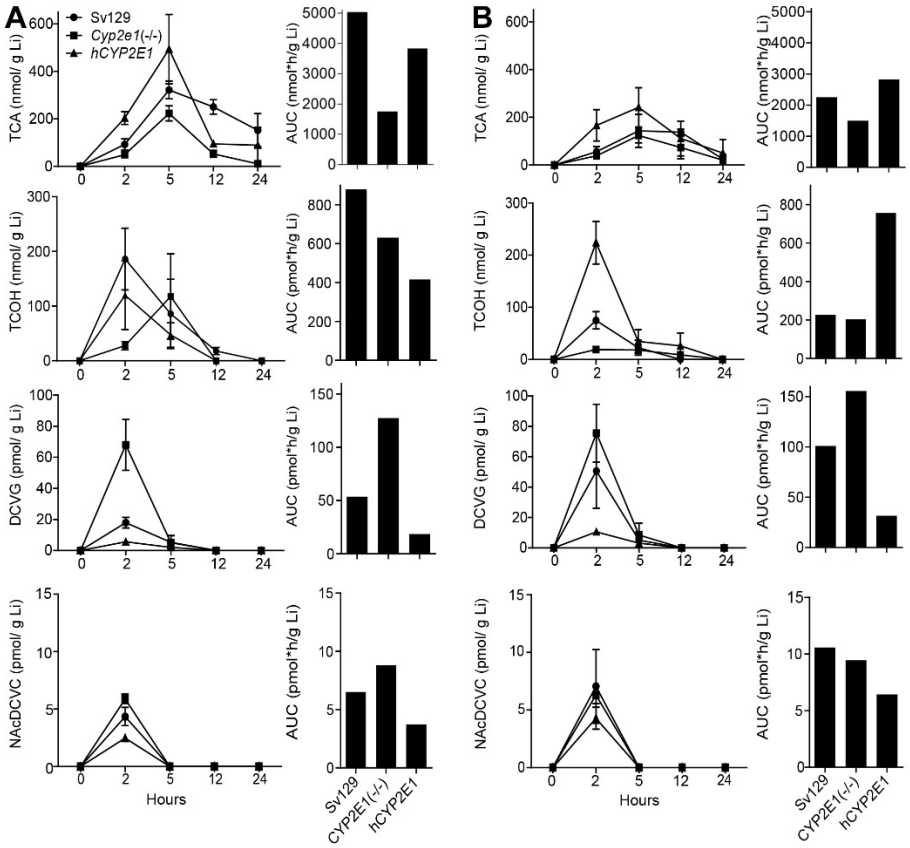

Figure 5.3 Comparative analysis of liver (Li) toxicokinetics of major oxidative (TCA and TCOH), and glutathione conjugation (DCVG) metabolites of trichloroethylene (600 mg/kg) in (A) male and (B) female 129S1/SvlmJ (SV129), Cyp2e1(-/-), and hCYP2E1 mice. Average kinetic profiles (left panels, strains are identified by symbols as shown in an inset in the top left graph) and area under the curve (AUC, right panels) are shown (n=2-4 per group per time point, as detailed in **Table** B-14)

In agreement with the lack of CYP2E1 expression, the AUCs were 2.9-fold lower for TCA, and 1.4-fold lower for TCOH in male *Cyp2e1(-/-)* mice as compared to those in male Sv129 mice. A decrease in formation of oxidative metabolites of TCE was less pronounced in female *Cyp2e1(-/-)* mice. Interestingly, elimination of TCA in the liver was slower in Sv129 mice as compared to *Cyp2e1(-/-)*and *hCYP2E1* mice. Slower formation of TCOH was most pronounced in male *Cyp2e1(-/-)* mice with a peak concentration

(Cmax) at 5 h and the differences in the timing of C_{max} for TCOH between *Cyp2e1(-/-)*and *hCYP2E1* mice may have affected the AUC values. Interestingly, the AUC of DCVG was 1.5-2.4 fold higher in *Cyp2e1(-/-)* mice of both sexes, but 2.9-3.2 fold lower in *hCYP2E1* mice as compared to Sv129 mice. For the AUCs of NAcTCVC, similar trend was observed in male mice but not in female mice.

Metabolites from GSH conjugative pathway have been postulated to cause kidney toxicities; therefore, we also examined concentration-time profiles of TCA, DCVG, DCVC, and NAcDCVC in the kidney (Figure 5.4). In male Sv129 mice, we found that kidney toxicokinetics of TCA, DCVG, and DCVC was similar to that previously reported in 129S1/SvImJ mice (Yoo, *et al.*, 2015c), B6C3F1/J mice (Luo, *et al.*, 2018a), and C57BL/6J and NOD/ShiLtJ mice (Yoo, *et al.*, 2015b). Similar to the observations in the liver, there were pronounced sex-dependent differences in kidney levels of TCA, TCOH, and NAcDCVC. In male Sv129 mice, the kidney AUC values were 2.2 fold higher for TCA, but 2.5 fold lower for NAcDCVC compared to female mice. With respect to the CYP2E1-mediated effects, the kidney AUCs were 1.6-5.1 fold lower for TCA, and 1.9-3.3 fold lower for TCOH in *Cyp2e1(-/-)* mice as compared to Sv129 mice, whereas these differences were less pronounced in female mice. Interestingly, in both male and female mice, the elimination of TCA was the slowest in the kidney of Sv129 of the strains examined herein. The AUC of DCVG was 1.4-1.9 fold higher in *Cyp2e1*(-/-) mice, but 1.2-1.4 fold lower in *hCYP2E1* mice, as compared to Sv129 mice.

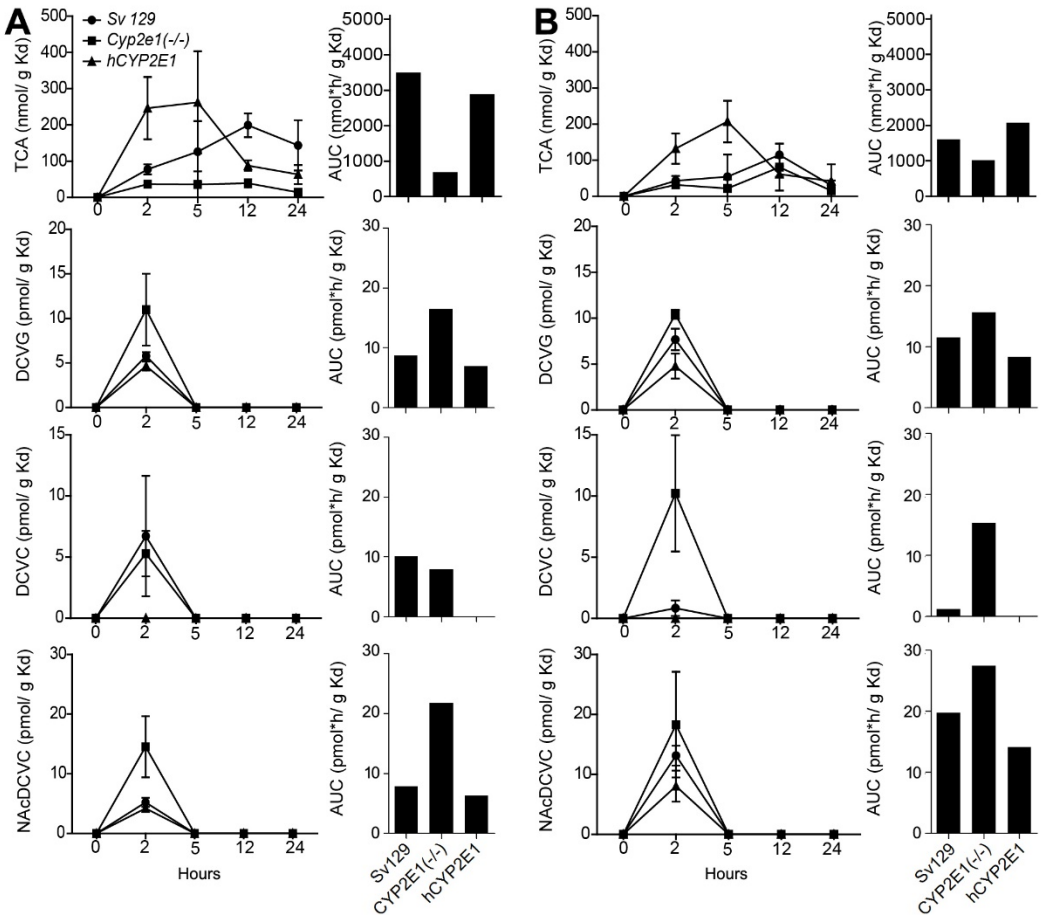

Figure 5.4 Comparative analysis of kidney (Kd) toxicokinetics of oxidative (TCA), and glutathione conjugation metabolites (DCVG, DCVC and NAcDCVC) of TCE (single dose, 600 mg/kg) in (A) male and (B) female 129S1/SvlmJ (SV129), *Cyp2e1(-/-)*, and *hCYP2E1* mice. Average kinetic profiles (left panels, strains are identified by symbols as shown in an inset in the top left graph) and area under the curve (AUC, right panels) are shown (n=2-4 per group per time point, as detailed in **Table** B-14).

5.4.3 Comparison of the Effect of CYP2E1 on Metabolisms of TCE and PCE

Much less is known about metabolism and toxicity of PCE, as compared to TCE (Cichocki, *et al.*, 2016). No study has tested the role of CYP2E1 in metabolism of PCE. Therefore, we compared the levels of key oxidative and glutathione conjugation metabolites of TCE and PCE in the liver and kidney of three strains of mice 2 hours after

the last dose (Figure 5.5). The comparison for TCA levels between TCE-treated and PCE-treated mice has limitations because TCE was administered as a single dose while PCE treatment was repeated over 5 days; still, the patterns of differences between sexes and strains are informative. In Sv129 strain, liver levels of TCA were about 2-fold higher in PCE-treated male and female mice as compared to TCE-treated mice. In our recent study in B6C3F1 mice we found that at equimolar doses, more TCA was found in both liver and kidney tissue from PCE-exposed mice compared with TCE-exposed groups (Zhou *et al.*, 2017). In male and female *Cyp2e1(-/-)* mice, TCA level in liver was about half of that in Sv129 mice. At the same time, TCA levels in liver of *hCYP2E1* mice were the same as in Sv129 mice, in both males and females.

Importantly, there are major differences in the flux of metabolism through glutathione pathway for PCE as compared to TCE, even though we consider different dosing designs between TCE and PCE. Metabolites from GSH conjugative pathway are rapidly excreted within 24 h after dosing. In addition, the relationship between T/PCE dose and GSH metabolites is linear within the dose range used in this study. Therefore, the comparison for GSH conjugates between TCE and PCE is more relevant than that for TCA levels. In the liver, the glutathione conjugate of PCE – TCVG – was found to be present at over 5-fold greater levels than DCVG. Kidney glutathione metabolites of PCE – TCVC and NAcTCVC – were found in the amounts greater than one order of magnitude than DCVC and NAcDCVC. Interestingly, levels of TCVG in the liver and TCVC in the kidney were lower in male *Cyp2e1(-/-)* mice, but unchanged in female *Cyp2e1(-/-)* mice..

NAcTCVC in the kidney was lower in male and female *Cyp2e1(-/-)* mice as compared to either Sv129 or *hCYP2E1* mice.

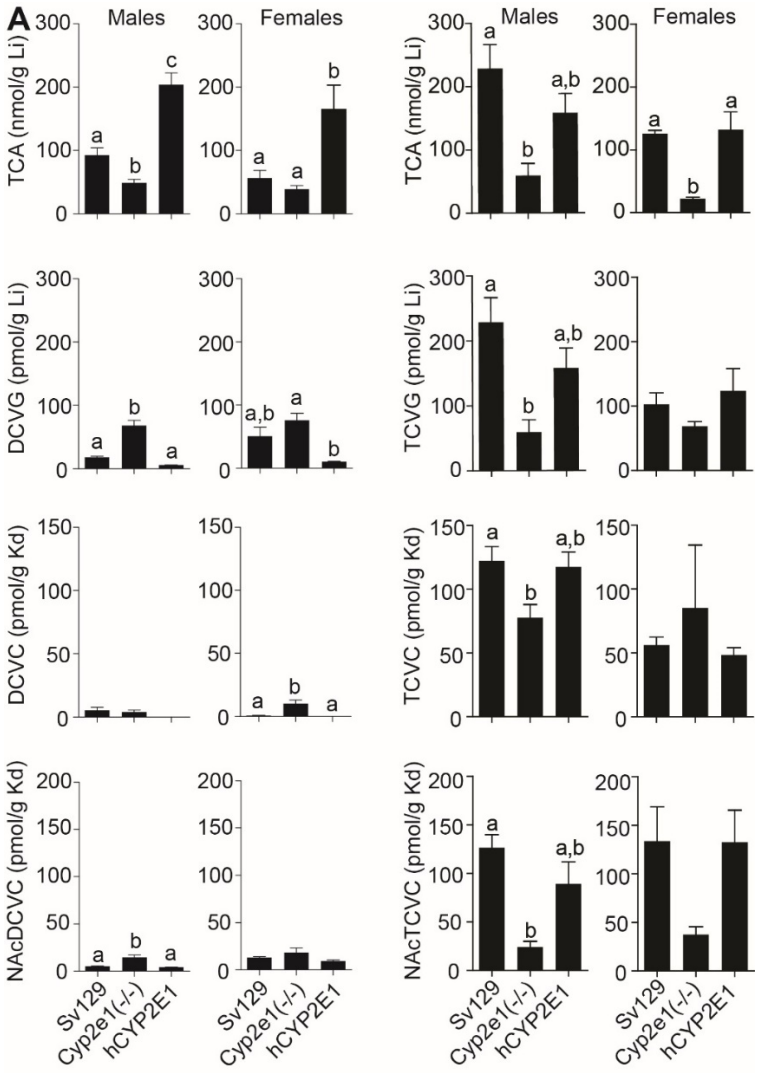

Figure 5.5 Comparative analysis of liver (Li) and kidney (Kd) levels of major oxidative (TCA), and glutathione conjugation (DCVG, DCVC and NAcDCVC for trichloroethylene; TCVG, TCVC and NAcTCVC for tetrachloroethylene) metabolites. Data for (A) trichloroethylene (600 mg/kg) and (B) tetrachloroethylene (5 daily doses, 500 mg/kg) in male and female 129S1/SvlmJ (Sv129), *Cyp2e1(-/-)*, and *hCYP2E1* mice are shown. Metabolite levels shown are for a 2 hrs time point after dosing. Data are shown as mean±SD. Bars with different letters are significantly different (one-way ANOVA with Newman-Keuls post hoc test, $p<0.05$).

5.4.4 Effect of CYP2E1 on PCE-induced Liver and Kidney Toxicity

We also examined whether strain-specific differences in PCE metabolism are associated with differences in toxicity in liver and kidney. Liver toxicity was investigated by histopathological evaluation, triglycerides measurements and assessment of cell proliferation. Treatment with PCE for 5 days induced lipid accumulation in the liver of male Sv129 mice, but had no such effect in male *Cyp2e1(-/-)* or *hCYP2E1* mice (Figure 5.6A). This histopathological finding was confirmed by measurements of liver and serum triglycerides. Liver triglycerides were about 6-fold higher and serum about 2-fold lower in PCE-treated male Sv129 mice as compared to vehicle-treated mice (Figures 5.6B-C). Similar observations were made in female mice of three strains, with PCE effect being observed only in Sv129 mice. There was no PCE-induced acute liver injury as assessed by serum ASTs and ALT, and there was no significant effect on liver cell proliferation.

Kidney effects of PCE were evaluated by measuring proximal tubule injury and cell proliferation in male (Figure 5.7) and female mice. We found that PCE treatment induced proximal tubule injury (16.4~39.3% increase in KIM-1 positive proximal tubules), an effect that was significant in male and female Sv129 mice and male *hCYP2E1* mice. No increase in cell proliferation was found in the kidney of PCE-treated male mice; in fact, cell proliferation was significantly lower in PCE-treated male Sv129 mice compared to strain-matched control group. Interestingly, we found higher basal levels of proximal tubule injury and cell proliferation in kidneys of female mice as compared to male mice.

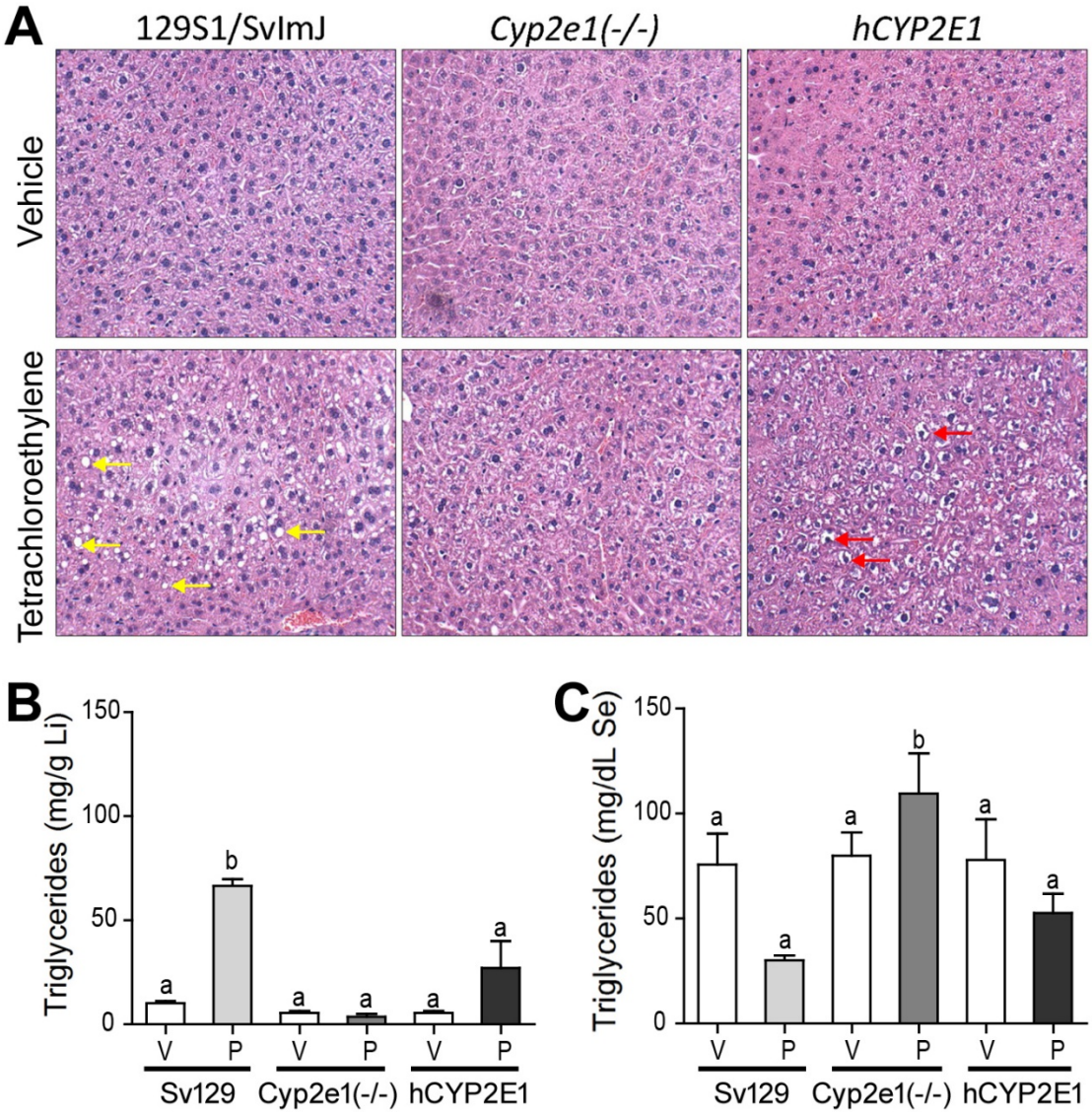

Figure 5.6 Effects of tetrachloroethylene on liver fat accumulation in male 129S1/SvlmJ (Sv129), Cyp2e1(-/-), and hCYP2E1 mice treated with five consecutive daily doses of vehicle (V, Alkamuls EL-620) or tetrachloroethylene (P, 500 mg/kg). (A) Representative images of H&E staining with 200× magnification. Yellow arrows point to fat accumulation. Red arrows point to accumulation of glycogen. Triglyceride levels in (B) liver (Li) and (C) serum (Se) are shown as mean±SD. Bars with letters are significantly different from other groups (one-way ANOVA with Newman-Keuls post hoc test, $p<0.05$).

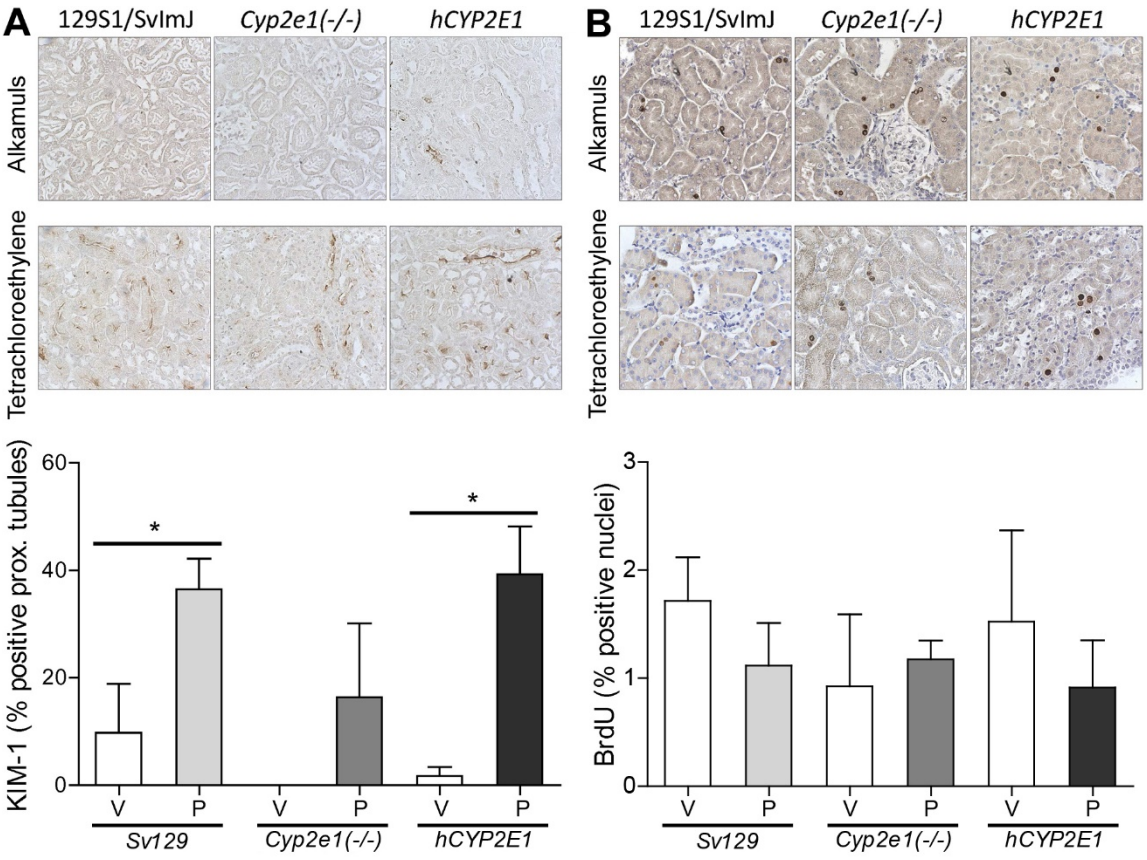

Figure 5.7 Effects of tetrachloroethylene on (A) proximal tubule injury and (B) cell proliferation in kidney of male 129S1/SvlmJ (SV129), Cyp2e1 (-/-), and hCYP2E1 mice treated with five consecutive daily doses of vehicle (V, Alkamuls EL-620) or PCE (500 mg/kg) The top figures show the representative images of KIM-1 or BrdU staining with 400× magnification. Quantitative results of proximal tubule injury and cell proliferation are expressed as % positive/total proximal tubules or nuclei, and are summarized in the lower bar charts. Asterisks denote significant difference by paired t-test ($p<0.05$).

5.5 Discussion

The role of CYP2E1 in TCE metabolism has been studied by comparing wild-type mice and CYP2E1 transgenic mice (Forkert *et al.*, 2006; Kim and Ghanayem, 2006; Ramdhan, *et al.*, 2008). Even though these studies focused on CYP2E1-mediated toxic

effects of TCE, CYP2E1-mediated effects on metabolism were also investigated by measuring the urinary excretion of TCA and TCOH. Decreased TCA and TCOH levels were found in urine of *Cyp2e1(-/-)* mice; however, the internal dosimetry of these oxidative metabolites in liver and kidney, as well as that of glutathione conjugation metabolites, was not explored in these studies. To address this significant data gap, we conducted a study of concentration-time profiles of both oxidative and glutathione conjugation metabolites of TCE in liver and kidney. Furthermore, we included both *Cyp2e1(-/-)* and *hCYP2E1* mice and both males and females to provide insights into the role that CYP2E1 plays in TCE metabolism. We also extended this study to investigate the CYP2E1-mediated metabolism and toxic effects of a related chemical of human health concern, PCE.

First, we found that CYP2E1 has a role in generation of oxidative metabolites of TCE in liver and kidney. Formation of TCA from TCE in liver was reduced by about 65 % without the expression of CYP2E1, which concurs with previous observations in urine of *Cyp2e1(-/-)* mice (Ramdhan, *et al.*, 2008). However, *Cyp2e1(-/-)* mice still can generate TCA from TCE, suggesting that other CYPs, such as CYP2F and CYP2B1, may also participate in TCE oxidation (Forkert *et al.*, 2005). Interestingly, *Cyp2e1(-/-)* mice exhibit a retarded T_{max} for TCOH, but generate a comparable amount of TCOH in liver. In addition, *hCYP2E1* mice, which had the highest level of CYP2E1 expression in liver, formed the lowest amount of TCOH. Collectively, these results suggest that CYP2E1 plays a major, but not exclusive, role in converting TCOH to TCA. Importantly, in absence of CYP2E1 expression, an increase in generation of glutathione conjugates was observed.

This result supports the notion that even though glutathione conjugation is a minor pathway of TCE metabolism in the mouse, CYP-mediated oxidation does compete with glutathione conjugation.

Second, we found quantitative differences in the extent of metabolism between TCE and PCE and that CYP2E1 also has a role in formation of TCA in PCE-treated mice. It has been assumed that PCE metabolism and toxicity are similar to TCE due to their structural similarity (Cichocki, *et al.*, 2016). Even though qualitative and quantitative differences in oxidative metabolisms between TCE and PCE are known (IARC, 2014; U.S. EPA, 2011b; U.S. EPA, 2011c), data on glutathione conjugation metabolism are still limited. Overall, the flux to both oxidative and glutathione conjugation metabolites is higher in PCE-treated mice compared to TCE-treated mice. Taking into account the dose differences, we found that PCE-produced metabolite levels were approximately 3-fold greater for TCA, 4-fold greater for the glutathione conjugate, and 25-fold greater for cysteine and n-acetyl cysteine conjugates. These quantitative differences are in agreement with those reported recently (Luo, *et al.*, 2017; Luo, *et al.*, 2018a; Zhou, *et al.*, 2017).

In addition, our results show that CYP2E1 status could modify glutathione conjugative metabolism differently between TCE and PCE. Knocking out the expression of CYP2E1 led to increases in DCVG, DCVC, and NAcDCVC, but decreases levels of TCVG, TCVC, and NAcTCVC in livers and kidneys. In PCE-treated mice, CYP2E1-mediated oxidation was not competing with the glutathione conjugation. This suggests that other CYPs could be important in PCE oxidation. An *in vitro* study also showed that PCE oxidation is primarily catalyzed by the CYP2B family, rather than CYP2E1 (White

and De Matteis, 2001). The role for CYP2E1 in the conversion from TCOH to TCA may also account for, at least in part, the competition between oxidation and glutathione conjugation pathways in TCE-treated mice. TCOH is a TCE-specific metabolite (Chiu, *et al.*, 2007; Zhou, *et al.*, 2017) and the conversion from TCOH to TCA is thought to be catalyzed by CYPs (Lash, *et al.*, 2014). Lack of CYP2E1 was likely the cause of TCOH accumulation, which in turn impedes the initial oxidation of TCE. Correspondingly, the total flux through glutathione conjugation would increase in CYP-deficient individuals.

Third, we found that presence of mouse CYP2E1 results in PCE-induced liver steatosis, while kidney effects of PCE are largely unaffected by CYP2E1 status. Liver fat accumulation has been reported in PCE-treated mice but not in TCE-treated mice (Buben and O'Flaherty, 1985; Cichocki, *et al.*, 2017c). However, liver steatosis was observed in TCE-treated, *Pparα(-/-)* and *hPPARα* transgenic mice (Ramdhan *et al.*, 2010). PPARα activation results in an increase in fatty acid catabolism in liver (Rakhshandehroo *et al.*, 2010; Ramdhan, *et al.*, 2010), and the suppression of PPARα activation causes hepatosteatosis. Interestingly, hepatic level of TCA, a PPARα activator, was the highest in liver of wild type mice compared to *Pparα(-/-)* and *hPPARα* transgenic mice (Yoo, *et al.*, 2015c), supporting the aforementioned hypothesis. In our study, the amount of TCA generated in PCE-treated mice was even greater than that in TCE-treated mice; however, we found fat accumulation in the liver of Sv129 mice. Surprisingly, there was no liver steatosis in PCE-treated *Cyp2e1(-/-)* and *hCYP2E1* mice. These observations suggest that, aside from PPARα activation, CYP2E1 status also may affect lipid metabolism in liver.

Additional studies are required to uncover the underlying molecular mechanisms behind the CYP2E1-mediated effects of PCE in mouse liver.

Similar to no effect of CYP2E1 status on glutathione conjugation metabolite formation from PCE, we found no effect of CYP2E1 status on kidney injury. We did observe an increase in KIM-1 staining in PCE-treated mice, showing that kidney is a target tissue in the mouse. It has been postulated that the bio-activation of TCVC and NAcTCVC, catalyzed by renal β lyase or other enzymes such as flavin monooxygenase and CYP3A, is a critical step for nephrotoxicity of PCE (Irving, *et al.*, 2013; Lash, *et al.*, 1994). It is likely that CYP2E1 may also play a role in sulfoxidation of cysteine and n-acetyl cysteine conjugates of PCE, as it was shown that CYP2E1 is involved in sulfoxidation of S-methyl N,N-diethylthiolcarbamate (Madan *et al.*, 1995) and diethyldithiocarbamate methyl ester (Madan *et al.*, 1998).

Fourth, our data provide important clues into sex differences in metabolism and toxicity of chlorinated solvents. Protein levels of CYP2E1, as well as the oxidative metabolites of TCE and PCE, were higher in liver and kidney of male mice as compared to female mice. The sex-dependent difference in metabolism of TCE was previously reported (Yoo, *et al.*, 2015c). Indeed, studies showed that steroid sex hormones can regulate constitutive expression of CYP2E1 in mice (Konstandi *et al.*, 2013; Penaloza *et al.*, 2014), which can further modulate chemical-induced toxicity (Hu *et al.*, 1993).

We also note that this study is not without limitations. First, the experimental designs were not identical between TCE and PCE arms of the study. Still, we are able to indirectly compare TCE and PCE metabolites, and we report that there are potential

differences in glutathione conjugative metabolism between TCE and PCE. However, direct comparison between toxicokinetics of TCE and PCE will further advance our knowledge in the relationship between metabolism and toxicity. Second, due to difficulties in breeding transgenic mice, the number of *Cyp2e1(-/-)* mice were limited. Future studies may benefit from increasing the sample size and breeding scale, if technically and economically possible.

In summary, this study provides a comprehensive analysis of the role of CYP2E1 in the metabolism and toxicity of TCE and PCE. CYP2E1 status affects levels of both oxidative and glutathione conjugation metabolites in mouse liver and kidney. We conclude that CYP2E1 is an important, but not exclusive actor in the oxidative metabolism and toxicity of TCE and PCE. CYP2E1 status also affects liver fat accumulation in PCE-treated mice.

CHAPTER VI

COMPARATIVE ANALYSIS OF METABOLISM OF TRICHLOROETHYLENE AND TETRACHLOROETHYLENE AMONG TISSUES AND MOUSE STRAINS

6.1 Overview

Trichloroethylene (TCE) and tetrachloroethylene (PCE) are structurally similar chemicals that are metabolized through oxidation and glutathione conjugation pathways. Both chemicals have been shown to elicit liver and kidney toxicity in rodents and humans; however, TCE has been studied much more extensively in terms of both metabolism and toxicity. Despite their qualitative similarities, quantitative comparison of tissue- and strain-specific metabolism of TCE and PCE has not been performed. To fill this gap, we conducted a comparative toxicokinetic study where equimolar single oral doses of TCE (800 mg/kg) or PCE (1000 mg/kg) were administered to male mice of C57BL/6J, B6C3F1/J, and NZW/LacJ strains. Samples of liver, kidney, serum, brain, and lung were obtained for up to 36 hours after dosing. For each tissue, concentrations of parent compounds, as well as their oxidative and glutathione conjugation metabolites were measured and concentration-time profiles constructed. A multi-compartment toxicokinetic model was developed to quantitatively compare TCE and PCE metabolism. As expected, the flux through oxidation metabolism pathway predominated over that through conjugation across all mouse strains examined, it is 1,200-3,800 fold higher for

TCE and 26-34 fold higher for PCE. However, the flux through glutathione conjugation, albeit a minor metabolic pathway, was 21-fold higher for PCE as compared to TCE. The degree of inter-strain variability was greatest for oxidative metabolites in TCE-treated and for glutathione conjugation metabolites in PCE-treated mice. This study provides critical data for quantitative comparisons of TCE and PCE metabolism, and may explain the differences in organ-specific toxicity between these structurally similar chemicals.

6.2 Introduction

Trichloroethylene (TCE) and tetrachloroethylene (PCE) are structurally similar chlorinated olefins that are used in chemical manufacture, metal degreasing, and other industrial applications (U.S. EPA, 2011b; U.S. EPA, 2011c). TCE and PCE are high production volume chemicals and are ubiquitous in air, soil, and surface and ground water (IARC, 2014). Humans can be exposed to these chemicals via inhalation and ingestion (ATSDR, 1997; Wu and Schaum, 2000). For TCE, assuming an ambient TCE concentration range of 100-500 ppt and an adult breathing rate of 20 m^3/day, the average daily intake of TCE through inhalation for the general population is estimated as 11-33 µg/day. The average daily intake of TCE through ingestion is 2-20 µg/day, assuming a concentration range of 2-7 ppb and total water consumption of 2 liters/day. For PCE, the total daily intake was estimated in the range of 1.22 to 2.67 µg/body weight (bw) for the general population in Canada, where drinking water ingestion only accounts for a small amount of the total exposure, estimated to be 0.002 to 0.06 µg/kg bw per day (CEPA, 1993). In a National Health and Nutrition Examination Survey (2013-2014), the rate of

detection for TCE and PCE in blood was 0.6% for TCE and 7.4% for PCE (CDC, 2017), which had dramatically declined compared to those reported in 2000 (Jia, *et al.*, 2012). These data demonstrate that the exposure of TCE and PCE to the general population has declined; however, TCE and PCE are still prioritized for evaluation of the risks to human health and environment (U.S. EPA, 2017).

There are differences in toxic effects of TCE and PCE in liver, kidney and other tissues (Cichocki, *et al.*, 2016). TCE is classified as "carcinogenic to humans" by US EPA (U.S. EPA, 2011c) and IARC (Guha, *et al.*, 2012); while PCE is classified as "likely to be a human carcinogen" by US EPA (U.S. EPA, 2011b) and as "probably carcinogenic to humans" by IARC (Guha, *et al.*, 2012). A comparative study of toxicodynamics of TCE and PCE in mice showed differences in the effects on liver and kidney, PCE perturbed more molecular pathways in mouse liver and kidney as compared to TCE (Zhou, *et al.*, 2017). However, no study performed comparative analysis of toxicokinetics of TCE and PCE.

Upon absorption, TCE and PCE are metabolized through oxidative and glutathione conjugation pathways. Initial oxidation occurs on the double bond by cytochrome P450s (CYPs) to generate an epoxide, which can be further metabolized. Trichloroacetic acid (TCA) is the major oxidative metabolite of both TCE and PCE, and is a common urinary biomarker of exposure (Forkert *et al.*, 2003; Volkel, *et al.*, 1998). The other oxidative metabolite, trichloroethanol (TCOH), is a TCE-specific oxidative metabolite that is formed through oxidation of TCE to chloral hydrate (CH), while PCE oxidation occurs through trichloroacetyl chloride (Chiu, *et al.*, 2007). Both TCE and PCE can enzymatically

conjugate with glutathione to form dichloro- or trichloro-glutathione conjugates (DCVG or TCVG) (Lash, *et al.*, 2000). These conjugates can be further metabolized via hepatic or renal gamma-glutamyl transferase and di-peptidase to form corresponding cysteine conjugates, DCVC or TCVC, which are then n-acetylated via N-acetyltransferase to generate NAcDCVC or NAcTCVC, respectively. In addition, both NAcDCVC or NAcTCVC can be deacetylated via acylase to yield DCVC or TCVC. Apart from N-acetylation, DCVC and TCVC can be further bio-activated via cysteine conjugate β lyase to generate reactive thioketenes, or flavin-containing monooxygenase to form sulfoxides DCVCSO or TCVCSO (Lash, *et al.*, 2014). These and other reactive species derived from glutathione conjugation are thought to be significant contributors to the nephrotoxicity of TCE and PCE (Lash, *et al.*, 2001a; Lash, *et al.*, 2003).

Quantitative estimation of inter-individual variability in metabolism is also a critical challenge in human health assessments of TCE and PCE (Cichocki, *et al.*, 2017c; Cichocki, *et al.*, 2016; Venkatratnam, *et al.*, 2017). The inter-strain variability in TCE metabolism has been characterized by using a multi-strain panel of inbred mice (Bradford, *et al.*, 2011) and the Collaborative Cross mouse population (Luo, *et al.*, 2018a; Venkatratnam, *et al.*, 2017; Venkatratnam *et al.*, 2018). Likewise, the inter-individual variability in PCE metabolism has also been studied in the Collaborative Cross mouse population (Cichocki, *et al.*, 2017c), and a nonalcoholic steatohepatitis mouse model (Cichocki, *et al.*, 2017a). However, these studies of inter-strain variability in metabolism and toxicity were conducted separately for TCE or PCE and using doses that were not equivalent. Because of the close structural similarity of these chemicals and paucity of the

available toxicokinetic data, a comparative study of equimolar doses was conducted concurrently using three inbred strains, selected based on variability observed across strains with respect to oxidative and glutathione conjugation metabolism for TCE (Bradford, *et al.*, 2011). The data from this study fill critical gaps in our understanding of the quantitative differences in TCE and PCE toxicokinetics.

6.3 Methods

6.3.1 Chemicals

TCE (PN: 24254, ≥ 99.0%), PCE (PN: 270393, ≥ 99.9%), TCA (PN: T6399, ≥ 99.0%), TCOH (PN: T54801, ≥ 99%), 2-bromobutyric acid (PN: 147877, 97%), ethylbenzene (PN: E12508, 99%), methyl tert-butyl ether (PN: 443808, ≥ 99.0%), chloroform (PN: 650498, ≥ 99.9%), sulfuric acid (PN: 339741, ≥ 99.999%), sodium sulfate (PN: 239313, ≥ 99.0%), β-glucuronidase (PN: G0751, ≥300,000 units/ g solid), and sodium bicarbonate (PN: S6014, ≥ 99.7%) were obtained from Sigma Aldrich (St Louis, MO). Methanol (HPLC grade) was from Fischer Chemicals (Fair Lawn, NJ). S-(1,2-dichlorovinyl)-cysteine (DCVC, ≥98.0%), 2-(^{15}N)amino-3-([1,2-dichloroethenyl]sulfanyl)($^{13}C_3$)propanoic acid (DCVC*, purity ≥95.0%, isotopic purity ≥98.0%), S-(1,2-dichlorovinyl)-glutathione (DCVG, ≥98.9%), and 2-amino-5-[(2-([(^{13}C)carboxy(^{13}C)methyl] (^{15}N)amino)-1-([1,2 dichloroethenyl]sulfanyl)-2-oxoethyl)amino]-5-oxopentanoic acid (DCVG*, purity ≥90.0%, isotopic purity ≥98.0%) were purchased from TLC Pharmaceutical Standards (Aurora, Canada). N-acetyl-S-(1,2-dichlorovinyl)-cysteine (NAcDCVC, 99.8%) and 3-([1,2-dichloroethenyl]sulfanyl)-2-[(1-

^{13}C, d_3)ethanoylamino]propanoic acid (NAcDCVC*, purity: 97.6%, isotopic purity: 99.0%), and NAcTCVC (purity: 99.7%) were obtained from Toronto Research Chemicals (Toronto, Canada). TCVG (purity: 98.9%), TCVC (purity: 98.4%), 2-Amino-5-[(1-{[(^{13}C)carboxy(^{13}C)methyl](^{15}N) amino}-1-oxo-3-[(trichloroethenyl)sulfanyl]propan-2-yl)amino]-5-oxopentanoic acid (TCVG*, purity: 90.4%), 2-(^{15}N)amino-3-[(trichloroethenyl)sulfanyl]($^{13}C_3$)propanoic acid (TCVC*, purity: 97.5%), and 2-[acetyl(^{15}N)amino]-3-[(trichloroethenyl)sulfanyl] ($^{13}C_3$)propanoic acid (NAcTCVC*, purity: 99.0%) were synthesized by Dr. Avram Gold at the University of North Carolina at Chapel Hill. De-ionized water was generated via Arium®Pro Ultrapure Water System (Gottingen, Germany).

6.3.2 Animals and treatments

Adult male C57BL/6J, B6C3F1/J, and NZW/LacJ mice (6-7 weeks of age) were obtained from the Jackson laboratory (Bar Harbor, ME). Animals were housed in polycarbonate cages on Sani-Chips irradiated hardwood bedding (P.J. Murphy Forest Products, Montville, NJ), and fed with NTP-2000 (Zeigler Brothers, Gardners, PA) wafer diet and water *ad libitum* on a 12 h light-dark cycle. Animals were acclimated for one week, and then gavaged (Figure 6.1) with a molar-equivalent single dose (6 mmole/kg) of TCE or PCE in vehicle (5% Alkamuls El-620 in saline, 5 mL/kg). Mice were sacrificed with overdose anesthesia (pentobarbital, 50 mg/kg i.p.) at 1, 2, 6, 12, 24, 36 h after dosing. The dose was selected based on our previous study comparing transcriptomic effects of TCE and PCE (Zhou, *et al.*, 2017), and other studies showing that this dose is well-

tolerated in acute, sub-chronic, 90-day, and 2-year studies in mice (Buben and O'Flaherty, 1985; Cichocki, *et al.*, 2017a; Cichocki, *et al.*, 2017c; National Toxicology Program, 1977; National Toxicology Program, 1990; Philip, *et al.*, 2007; Yoo, *et al.*, 2015c). Time points (1, 2, 6, 12, 24, 36 h) were selected to maximize the metabolic information from both oxidative and glutathione conjugation pathways (Kim, *et al.*, 2009b). Organs (liver, kidney, brain, and lung) were rinsed in phosphate-buffered saline, blotted dry, weighed, and snap-frozen in liquid nitrogen. Serum was prepared using Z-gel tubes (Sarstedt, Germany) by centrifugation of blood collected from *vena cava*. All studies were conducted and approved by the Institutional Animal Care & Use Committee at the University of North Carolina-Chapel Hill. Raw data at the individual mouse level are available at the Mouse Phenome Database (https://phenome.jax.org/projects/Rusyn10 and https://phenome.jax.org/projects/Rusyn11).

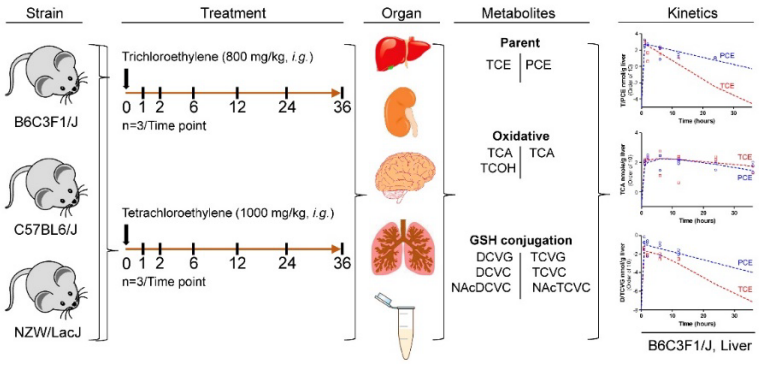

Figure 6.1 Schematic representation of study design. Male mice from one hybrid strain and two inbred strain (B6C3F1/J, C57BL/6J, and NZW/LacJ) were used in this study. Mice were intragastrically administered with a single dose of trichloroethylene or tetrachloroethylene (6 mmole/kg in 5% Alkamuls EL-620 (5 ml/kg)). Unchanged (T/PCE), oxidative (TCA and TCOH), and GSH conjugation metabolites (D/TCVG, D/TCVC, and NAcD/TCVC) were quantified in liver, kidney, brain, lung, and serum at various time points up to 36 hours (n=3/ time point/strain).

6.3.3 Quantification of TCE and PCE

Tissue levels of TCE and PCE were quantified via a dynamic headspace gas chromatography-mass spectrometry as reported in (Cichocki, *et al.*, 2017c). Briefly, tissues (20 mg) were homogenized with 0.5 mL of ethylbenzene solution (0.5 µM in methanol). Homogenate was transferred to a 40 mL amber glass headspace vial containing 4 mL of deionized water, and analyzed via a dynamic headspace purge & trap GC-MS with single ion monitoring mode. The peak area ratio of TCE or PCE to ethylbenzene was used to construct an eight-point calibration curve (0, 0.015, 0.045, 0.137, 0.41, 1.23, 3.70, and 11.11 nmole spiked TCE or PCE) for quantitation of TCE or PCE.

6.3.4 Quantification of TCA

Tissue levels of TCA were measured according to the US EPA method 815-B-03-002 (Domino, *et al.*, 2003) with slight modifications. Tissue samples (liver: 50 mg; kidney, brain, and lung: 30 mg; serum: 30 µL) were spiked with 11 nmole of 2-bromobutyric acid, homogenized in 1 mL of methanol:chloroform (1:1), and centrifuged at 14,000 g for 10 mins. The supernatant was mixed well with 1.5 mL of methanolic sulfuric acid (10%, v:v), and incubated in water batch at 55^{o}C for 2 h to derive respective methyl esters. Thereafter, the derivative was mixed with 2 mL of methyl tert-butyl ether and 3 mL of sodium sulfate buffer (150 g/L). The collected upper layer was mixed well with 3 mL of saturated sodium bicarbonate. Again, the upper layer was collected, concentrated under nitrogen stream to a volume of ~20 µL, and analyzed via GC-MS. The peak area ratio of TCA to internal

standards was used to construct an eight-point calibration curve (0, 4.1, 12.3, 37.0, 111.1, 333.3, 1000, and 3000 nmole spiked TCA) for quantitation of TCA.

6.3.5 Quantification of TCOH

Tissue levels of TCOH were determined as described elsewhere(Luo, *et al.*, 2018b). Briefly, liver (50 mg), kidney (30 mg), brain (30mg), serum (30 µL), and lung (20 mg) tissues were homogenized with sodium acetate (0.1 M, pH 4.6), and mixed well with beta-glucuronidase (2000 units/ ml) in a thermomixer. After overnight incubation at 37 ^{o}C, the incubated homogenate was spiked with ethyl benzene (20 nmole), and then further incubated in 10% sulfuric acid in methanol (1.5 ml) at 50 ^{o}C for 1 h. Afterwards, the reaction mixture was evenly mixed with MTBE (2 mL) and sodium sulfate (3 mL, 150 g/L), and then centrifuged at 2,500 g for 3 min. The extracted MTBE layer was neutralized by saturated sodium bicarbonate (3 mL), transferred to a new vial, and concentrated with nitrogen gas to ~20 µL for GC-MS analysis (Song and Ho 2003). Peak area ratio of TCOH to ethyl benzene was used to establish an eight-point calibration curve (0, 0.37, 1.11, 3.33, 10, 20, 30, and 60 nmole spiked TCOH) for quantification of total TCOH (free TCOH +TCOH-glucuronide (TCOG)).

6.3.6 Quantification of DCVG/TCVG, DCVC/TCVC, and NAcDCVC/NAcTCVC

Tissue levels of DCVG/TCVG, DCVC/TCVC, and NAcDCVC/NAcTCVC were measured as detailed in (Luo, *et al.*, 2017; Luo, *et al.*, 2018a). In brief, tissue homogenates were subject to a liquid-liquid extraction with 400 µL of methanol:chloroform (1:1) and a

solid-phase extraction (SPE) using a weak anion C-18 cartridge (Strata-X-AW, PN: 8E-S038-TGB, Phenomenex, Torrance, CA). Serum samples were mixed with methanol, centrifuged and the supernatant was collected. The supernatant was diluted with water and further processed by solid-phase extraction. The SPE eluent was dried under vacuum, and reconstituted with 50 µL of methanol: water (20:80) with 0.1 % acetic acid. Tissue levels of metabolites were determined by an eight-point calibration curve (0, 0.25, 0.5, 1.25, 2.5, 6.25, 18.75, and 31.25 pmole) using the peak area ratios of standards to isotopically-labeled internal standards via UPLC-MS/MS.

6.3.7 Toxicokinetic model

A multi-compartment model to describe the toxicokinetics of TCE and PCE was developed based on the model reported in Kim *et al*. (2009). A compendium of differential equations with first-order kinetics was used to describe the metabolism, and elimination of TCE or PCE and their metabolites from oxidative and glutathione conjugation pathways (Figure 6.2). The model also includes formation of reactive species from cysteine conjugates. Additionally, we assumed that the ingested dose of TCE or PCE was rapidly absorbed into the blood and distributed to other tissues. Unlike physiologically-based pharmacokinetic (PBPK) models that use the partition coefficient to describe the ratio of concentration in blood and tissues, this model utilized a “lumped” compartment to represent the total quantity of each compound in the body. To describe the quantity of TCE or PCE and its metabolites in tissues, we created fraction parameters that individually distribute the cumulative dose in the lumped compartment, which can be represented as,

$Q_T = Q_T(f_{Srm} + f_{Liv} + f_{Kid} + f_{Brn} + f_{Lng} + f_{Oth})$, where Q_T is the quantity of parent compounds (or its metabolites). The fraction parameters include serum (f_{Srm}), liver (f_{Liv}), kidney (f_{Kid}), brain (f_{Kid}), lung (f_{Lng}), and all other tissues (f_{Oth}), respectively. The quantity of a chemical can be calculated by multiplying the total quantity and distributed fraction such as, $Q_{Liv} = Q_T \cdot f_{Liv}$. Then, we can estimate the concentration by using tissue weights measured in this study and the reference blood volume. To investigate the disposition of TCE and PCE metabolites, we estimated the final cumulative dose in the compartments of all elimination (TCE/PCE, TCA, TCOH, and GSH conjugation) and bio-activation routes (the dotted boxes shown in Figure 6.2). The estimations followed the mass-balance rule, where the final cumulative dose from elimination and bio-activation routes was equal to the initial oral dose of TCE/PCE. The percentage of excreted T/PCE, TCA, TCOH, and GSH conjugation was obtained by dividing the excreted amount of individual compound with the given oral dose. We estimated metabolism, excretion, and fraction parameters using a Bayesian approach, assuming non-informative priors for each parameter, and estimating posterior distributions using Markov chain Monte Carlo simulations.

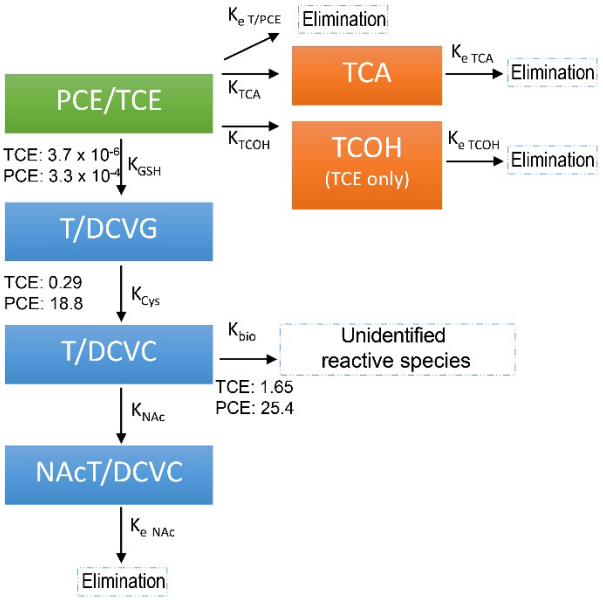

Figure 6.2 Toxicokinetics analyses of TCE and PCE metabolites. The model is composed of one parent compartment (TCE or PCE), up to two oxidative compartments (TCA and TCOH), three GSH conjugation compartments (D/TCVG, D/TCVC, and NAcD/TCVC), and one bio-activation compartment ("Reactive species"). The first order kinetics of formation of TCA, TCOH, D/TCVG, D/TCVC, NAcD/TCVC, and reactive species was described by rate constants K_{TCA}, K_{TCOH}, K_{GSH}, K_{Cys}, K_{NAc}, and K_{bio} accordingly. The first order elimination kinetics of T/PCE, TCA, TCOH, and NAcD/TCVC was described by $K_{eT/PCE}$, K_{eTCA}, K_{eTCOH}, and K_{eNAc}. Median estimates of selected rate constants are shown. All rate constants are listed in Table 1.

6.3.8 Statistical analysis

The fitness of toxicokinetic models developed in this study was examined by using Spearman (ρ) and Pearson (*r*) correlation. The correlation was deemed to be statistically significant if $p<0.05$. The area under curve within the study period (AUC_{0-36}) was calculated based on a trapezoidal rule by using the R software (v 3.3.3).

6.4 Results

Levels of parent compounds (TCE and PCE), as well as their oxidative (TCA and TCOH) and glutathione conjugation metabolites (DCVG, DCVC, NAcDCVC, TCVG, TCVC, and NAcTCVC) [see comparative schematics of metabolism for TCE and PCE in (Cichocki, *et al.*, 2016; Luo, *et al.*, 2018b)] were quantified in liver, kidney, brain, lung and serum of male mice of three strains across a range of time points. These data were used to develop toxicokinetic models for TCE and PCE metabolism.

6.4.1 Model evaluation

The model (Figure 6.2) fits well to oxidative (r=0.69-0.81; ρ=0.69-0.73) and glutathione conjugation (r=0.52-0.64; ρ=0.55-0.79) metabolites of TCE or PCE in multiple tissues of male C57BL/6J, B6C3F1/J, and NZW/LacJ mice (Figure 6.3). With respect to each parent chemical and their oxidative metabolites, the model demonstrated higher performance in TCE-treated mice (r= 0.81; ρ=0.73) as compared to PCE-treated mice (r=0.69; ρ=0.69). For glutathione conjugation metabolites, the model fits better in PCE-treated mice (r=0.64; ρ=0.79) than in TCE-treated mice (r=0.52; ρ=0.55).

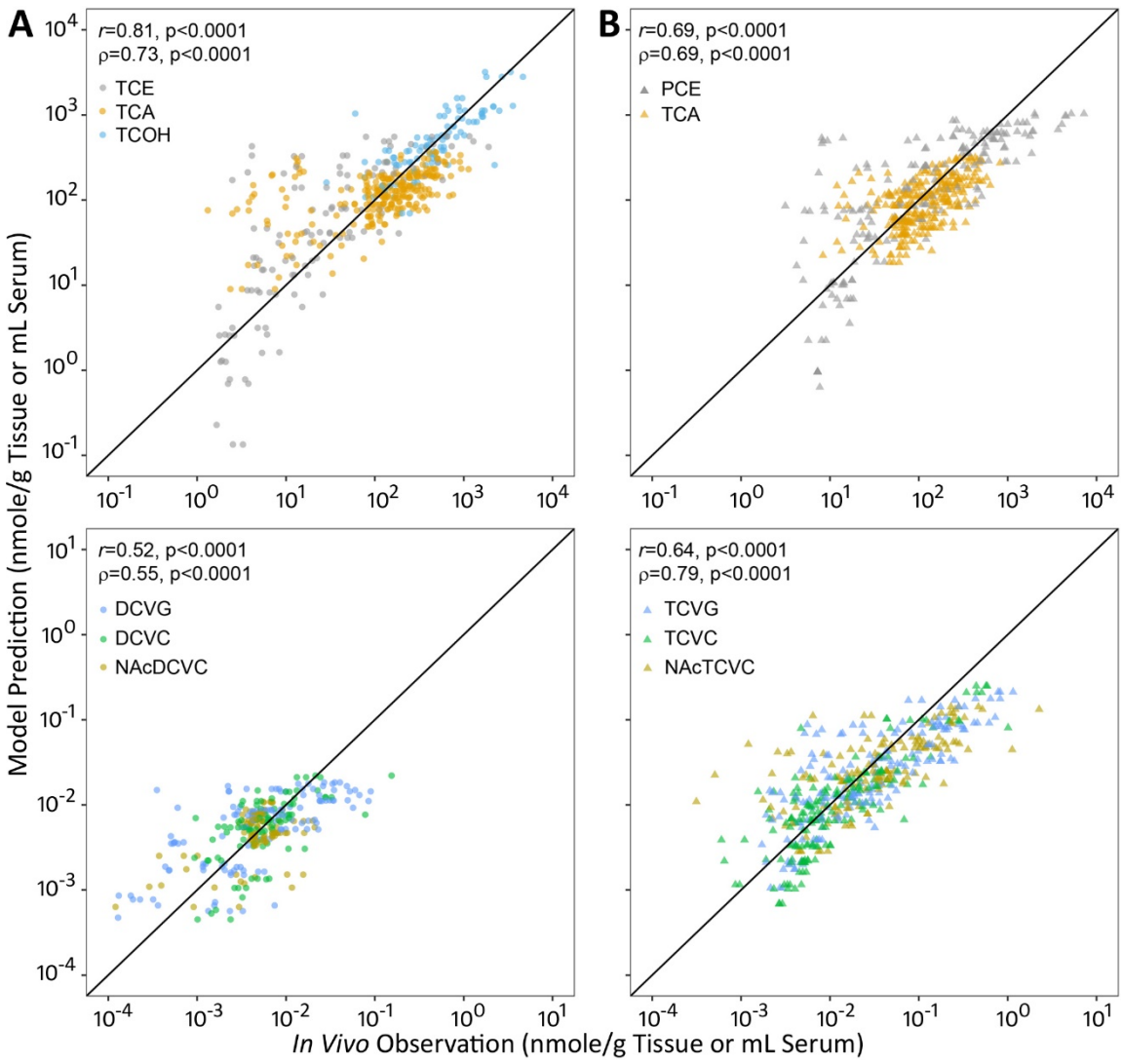

Figure 6.3 Global evaluation of toxicokinetic model fit for TCE (A), PCE (B), and their respective metabolites. Pearson (r) and spearman (ρ) correlation were used to evaluate the model fit. The correlation was considered statistically significant if p-value was lower than 0.05.

6.4.2 Toxicokinetics of TCE and PCE metabolites in multiple mouse tissues

Based on the model outputs, we compared the toxicokinetics of TCE and PCE metabolites in multiple tissues of male B6C3F1/J, C57BL/6J, and NZW/LacJ mice. Tissue

levels of TCE were lower than those of PCE; this was most pronounced in kidney. The $AUC_{0\text{-}36}$ of TCE was 2.3-3.4 fold lower in serum, liver, brain, and lung, and 49-fold lower in kidney as compared to the $AUC_{0\text{-}36}$ of PCE in B6C3F1/J mice (Figure 6.4, Table B-16). TCE elimination rate constant was 2.8-fold higher than that for PCE (Table 6.1, Figure A-6). These data are concordant with the results from previous studies (Cichocki, *et al.*, 2017a; Yoo, *et al.*, 2015c), suggesting that TCE may be metabolized and eliminated more rapidly than PCE in male mice. In addition, saturation of the metabolism of PCE at dose of 1000 mg/kg (Buben and O'Flaherty 1985) may also contribute to the higher $AUC_{0\text{-}36}$ of PCE and lower $K_{e,\,pce}$ compared to those of TCE.

Upon absorption, TCE and PCE are metabolized primarily via oxidation to TCA and/or TCOH (TCOH is a TCE-specific metabolite). Tissue levels of TCA were largely comparable between TCE- and PCE-treated mice. Except the C57BL/6J mice, the $AUC_{0\text{-}36}$ of TCA in TCE-treated mice was 1.2-1.7 fold higher in serum, liver, brain, and lung, but similar in kidney as compared to PCE-treated mice. The formation rate constant of TCA (K_{TCA}) in TCE-treated mice was 2.4 fold higher than that in PCE-treated mice. The elimination rate constant (K_e) of TCA in TCE-treated mice was 1.6-fold lower than that in PCE- treated mice (Table 1). The more rapid formation of TCA concurs with the faster elimination of TCE, as compared to PCE-treated mice. With regard to the TCE-specific metabolite TCOH, it was generally most abundant in kidney. Interestingly, the $AUC_{0\text{-}36}$ of TCOH was 2-2.5 fold lower in serum, brain, and lung, but 2.7-3.2fold higher in kidney than those of TCA. These findings showed that generation of TCOH and TCOG is more

efficient in kidney, which is concordant with the higher expression of UDP-glucuronosyltransferases and alcohol dehydrogenase in mouse kidney (Yue, *et al.*, 2014).

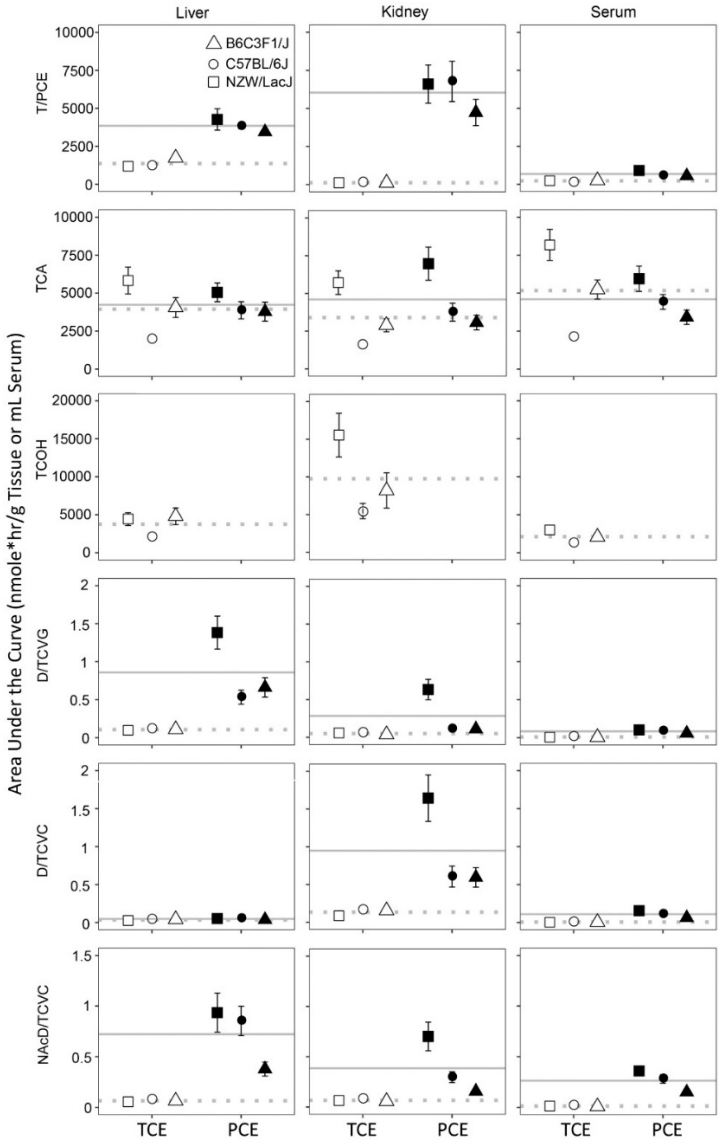

Figure 6.4 The AUCs of parent compound (TCE or PCE), oxidative metabolites (TCA and TCOH), and GSH conjugation metabolites (D/TCVG, D/TCVC, and NAcD/TCVC) in liver, kidney, and serum of male B6C3F1/J (Δ), C57BL/6J (○), and NZW/LacJ (□) mice. Data points are shown as mean ± standard deviation. Open symbols represent TCE, and closed symbols PCE. The grey lines represent the population means of TCE-treated (dashed line) and PCE-treated (solid line) groups.

Table 6.1 Toxicokinetic parameter estimates (mean ± sd) for TCE and PCE metabolism.

		TCE	PCE
Oxidation	T/PCE→TCA	0.034±0.010	0.014±0.003
	T/PCE→TCOH	0.13±0.04	—
GSH conjugation	T/PCE→D/TCVG	$(3.5\pm1.1)*10^{-6}$	$(460\pm230)*10^{-6}$
	D/TCVG→D/TCVC	0.30±0.07	31.9±20.6
	D/TCVC→NAcD/TCVC	73.4±17.4	43.2±28.7
	D/TCVC→Reactive species	1.69±0.45	37.4±19.2
Excretion	T/PCE→	0.49±0.12	0.17±0.04
	TCA→	0.05±0.02	0.08±0.02
	TCOH→	0.49±0.13	—
	NAcT/DCVC→	23.8±10.5	16.4±10.1

On the other hand, GSH conjugation pathway was approximately 30-3000 fold less efficient than oxidative pathway for TCE and PCE, where the flux through glutathione conjugation pathway was even smaller in TCE-treated mice compared to PCE-treated mice. In TCE-treated mice, the $AUC_{0\text{-}36}$ values for GSH conjugates were 4.9-12.8 fold lower in liver, with a net difference of 0.43-1.12 nmole*hr/g liver, and the $AUC_{0\text{-}36}$ values for cysteine conjugates were 2.4-13.3 fold lower in kidney, with a net difference of 0.33-1.47 nmole*hr/g kidney compared with PCE. The formation rate constant was 131.4-fold lower for GSH conjugates, 106-fold lower for cysteine conjugates, and 1.7-fold higher for

n-acetylcysteine conjugates in TCE-treated mice as compared to PCE-treated mice. On the other hand, the K_e was 1.5-fold higher for n-acetylcysteine conjugates in TCE-treated mice as compared to PCE-treated mice. Tissue-specific variation of these GSH conjugation metabolites was similar between TCE-treated and PCE-treated mice, with the highest level of the GSH conjugates found in liver and the highest level of the cysteine conjugates found in kidney, in accord with recent studies (Luo, *et al.*, 2017; Luo, *et al.*, 2018a; Yoo, *et al.*, 2015a; Yoo, *et al.*, 2015b).

We also examined the inter-strain variability in formation of TCE and PCE metabolites based on the model-derived AUCs (Table B-17). The AUC values across strains were similar for parent compounds (geometric standard deviation, GSD=1.10-1.46 for TCE, and =1.02-1.30 for PCE). For oxidative metabolites (TCA and TCOH), the inter-strain variability was larger in TCE treated mice (GSD=1.24-2.04) as compared to PCE-treated mice (GSD=1.06-1.52). However, for glutathione conjugation metabolites, the inter-strain variability was more prominent in PCE treated mice (GSD=1.12-2.77) as compared to TCE treated mice (GSD=1.04-1.92).

6.4.3 Disposition of TCE and PCE in male B6C3F1/J, C57BL/6J, and NZW/Lac mice

The fractions of administered TCE or PCE that were metabolized to oxidative or glutathione conjugation metabolites in each strain at steady state were also estimated (Figure 6.5). Most of the parent compounds remained unmetabolized until excretion, the fraction of the total administered dose ranged from 61.7% to 84.3% for TCE, and from

90.3% to 93.5% for PCE. The unmetabolized fractions of TCE and PCE are likely cleared via exhalation, as shown in mice orally dosed with 500 mg/kg ^{14}C-labelled PCE where exhalation fraction of PCE was 82.6 % (Schumann *et al.*, 1980). Excreted TCA accounted for 3.5%-7.1% of the total dose for TCE, and 6.4-9.4% for PCE. With respect to the TCE-specific oxidative metabolite TCOH, it accounted for 12.2-31.2% of the total dose for TCE.

With respect to the glutathione conjugation metabolism, the overall flux to conjugation was less than 0.3% of the administered dose for both chemicals. However, it was 20-fold higher in PCE-treated mice (0.19%-0.30%) as compared to TCE-treated mice (0.010%-0.013%). Importantly, the estimated fraction of the reactive species formation from cysteine conjugates ranged from 2.1% to 2.4% for TCE, but from 46.7% to 52.6% for PCE.

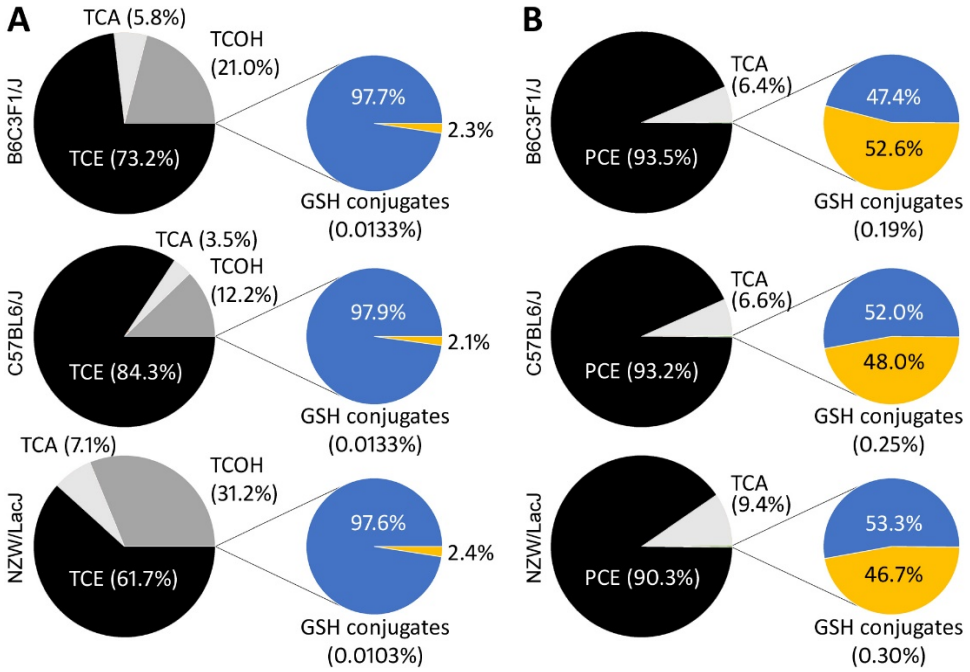

Figure 6.5 Predicted disposition of TCE (A), PCE (B), and their respective metabolites in male B6C3F1/J, C57BL/6J, and NZW/LacJ mice. Pie charts are used to provide a relative comparison among various metabolites as predicted by the model in each strain. Parent compounds (black) or their oxidative metabolites (TCOH, dark gray; TCE, light gray) are shown on the left with the GSH conjugation fraction magnified to the right of the main pie chart. For GSH conjugate pie charts, the fraction of reactive species formed is represented by a yellow slice.

6.5 Discussion

The most notable finding of this comparative study of toxicokinetics of TCE and PCE in mice is the observation of considerable differences in metabolism between these structurally-similar compounds. A larger portion of the parent compound undergoes metabolism in TCE-treated mice (15.7%-38.3%) as compared to PCE-treated mice (6.6%-9.7%), a finding that provides empirical data in strong support of the estimates from PBPK models (Chiu, *et al.*, 2014; Chiu and Ginsberg, 2011). The more efficient oxidative

metabolism of TCE as compared to PCE is also concordant with previous animal studies (Cichocki, *et al.*, 2017a; Green and Prout, 1985; Larson and Bull, 1992) and PBPK modeling estimates (Chiu, *et al.*, 2014; Chiu and Ginsberg, 2011; Chiu, *et al.*, 2009).

Previous PBPK models were developed using only limited data for glutathione conjugation pathway and suggested that the overall flux through the glutathione conjugation pathway was comparable between TCE and PCE (Tables 6.2 and 6.3). However, the model estimates presented herein for activation of cysteine conjugates to reactive metabolites showed that this process is more efficient in PCE-treated mice as compared to TCE-treated mice. In this study, we show that even though the glutathione conjugation pathway only accounts for less than 0.3% of the total dose of TCE and PCE, the metabolic flux through glutathione conjugation is approximately 21-fold higher for PCE compared to TCE. Higher levels of glutathione conjugation metabolites were previously reported for PCE as compared to TCE in previous studies in mice (Cichocki, *et al.*, 2017a; Luo, *et al.*, 2017; Luo, *et al.*, 2018a; Luo, *et al.*, 2018b); however, the dissimilarities in dose and times of metabolite detection made direct comparisons difficult. Therefore, our findings are significant with respect to providing direct evidence for considerable differences in toxicokinetics between TCE and PCE and are consistent with the observations that PCE is more extensively metabolized via glutathione conjugation that TCE (U.S. EPA, 2011b).

Table 6.2 Comparative analysis of toxicokinetics of TCE metabolites in mice, rat, and humans.

Study	Dose†	Route	Species	Strains	Sex	TCA (%)‡	TCOH (%)	GSH conjugation (%)	Oxidation to GSH
This study	800	oral	mice	B6C3F1/J	M	5.8	21	0.0131	2045.8
				C57BL/6J		3.5	12	0.0129	1201.6
				NZW/LacJ		7.1	31	0.0104	3663.5
Chiu et al 2014‖	2100	oral	mice	B6C3F1/J	M	4.4	—	0.065	290
Chiu et al 2009‖	1000	oral	mice	—	—	90		0.2	450
Larson and Bull 1992	600	oral	mice	B6C3F1/J	M	3.9	31	—	—
Fisher et al. 1991‖	368	inhalation	mice	B6C3F1/J	M	7	—	—	—
Green and Prout 1985	500	oral	mice	B6C3F1/J	M	7.2*	91.1*	—	—
Dekant et al. 1984	200	stomach tube	mice	NMRI	F	0.1*	94.3*	—	—
Chiu et al 2009‖	100	inhalation	rat	—	—	40		0.06	666.7
Bernauer et al 1996	160	inhalation	rat	Wistar	M&F	—	—	—	2562¶
Larson and Bull 1992	600	oral	rat	Sprague-Dawley	M	4.1	23.2	—	—
Fisher et al. 1991‖	505	inhalation	rat	F344	M	6	—	—	—
Commandeur 1990	400	*i.p.*	rat	Wistar	M	—	—	0.0026¶	—
Green and Prout 1985	500	oral	rat	Osborne-Mendal	M	6.3*	90.1*	—	—
Dekant et al. 1984	200	stomach tube	rat	Wistar	F	15.3*	73.6*	—	—
Chiu et al 2009‖	1	inhalation	human	—	—	38		5	7.6
Chiu et al 2006	1	inhalation	human	—	M	1-2	16-28	—	—
Bernauer et al 1996	160	inhalation	human	—	M	—	—	—	7163¶
Monster 1979	70	inhalation	human	—	M	21	43	—	—
Monster 1976	70	inhalation	human	—	M	18	39	—	—

† Dose units: ppm for inhalation route; mg/kg for other routes. ‡ Percentage of administered TCE excreted in urine. ‖ Estimates derived from PBPK model. * Percentage of total urinary metabolite calculated based on radioactivity. ¶ Use excreted n-acetyl cysteine conjugates to represent GSH conjugation of TCE.

Table 6.3 Comparative analysis of toxicokinetics of PCE metabolites in mice, rat, and humans.

Study	Dose[†]	Route	Species	Strains	Sex	TCA (%)[‡]	GSH conjugation (%)	Oxidation to GSH
This study	800	oral	mice	B6C3F1/J	M	6.4	0.187	34.2
				C57BL/6J	M	6.6	0.253	26.1
				NZW/LacJ	M	9.4	0.298	31.5
Cichocki et al 2017	300	oral	mice	C57BL/6J	M	5.9	0.79	7.5
Chiu et al 2011[I]	10	inhalation	mice	—	—	12	0.02	600
	100	oral	mice	—	—	35	0.07	500
	10	inhalation	rat	—	—	3.9	0.2	19.5
	100	oral	rat	—	—	8.9	0.6	14.8
Volkel et al 1998	40	inhalation	rat	Wistar	M&F	—	—	316.4
	20					—	—	540.6
	10					—	—	623.6
Chiu et al 2011[I]	10	inhalation	human	—	—	0.98	9.4	0.1
	100	oral	human	—	—	1.8	18	0.1
Chiu et al 2006	1	inhalation	human	—	M	0.2-0.8	—	—
Volkel et al 1998	40	inhalation	human	—	M&F	—	—	96.3
	20			—		—	—	89.1
	10			—		—	—	107.7
Monster 1979	72	inhalation	human	—	M	2	—	—

[†] Dose units: ppm for inhalation route; mg/kg for other routes. [‡] Percentage of administered TCE excreted in urine. [I]Estimates derived from PBPK models

The toxicokinetic profiles for TCE and PCE metabolites are modified by doses, species, and administration routes (Tables 6.2 and 6.3) (Bernauer *et al.*, 1996; Chiu, *et al.*, 2014; Chiu and Ginsberg, 2011; Chiu, *et al.*, 2007; Chiu, *et al.*, 2009; Cichocki, *et al.*, 2017a; Commandeur and Vermeulen, 1990; Dekant *et al.*, 1984; Fisher *et al.*, 1991; Green and Prout, 1985; Larson and Bull, 1992; Monster *et al.*, 1976; Monster and Houtkooper, 1979; Volkel, *et al.*, 1998). Inter-species differences in toxicokinetics of TCE and PCE metabolites has also been reported. In general, mice are thought to be more efficient in oxidative metabolism, but less efficient in glutathione conjugation as compared to rats and humans, whether in TCE-treated or PCE-treated mice (Chiu and Ginsberg, 2011; Chiu, *et al.*, 2009). However, our results show that the quantitative differences in metabolism between rats and mice may not be as large as the previously modeled estimates. The ratio of oxidative metabolites to glutathione conjugation metabolites is closer to that predicted in rats (Chiu and Ginsberg, 2011). The measurement of glutathione conjugates in rats and humans would be of great interests to address the inter-species differences in GSH conjugative metabolism of TCE and PCE.

It has been postulated that the reactive species generated from cysteine conjugates of chlorinated solvents are the critical nephrotoxic metabolites in animals and humans (Lash, *et al.*, 2001a; Lash, *et al.*, 2007; Lash, *et al.*, 2001b; Lash, *et al.*, 2002). Thus, the difference in flux through glutathione metabolites of TCE and PCE reported herein needs to be reconciled with the evidence for kidney toxicity and carcinogenicity of TCE and PCE (Cichocki, *et al.*, 2016). For the parent compounds, the strength of evidence for human kidney cancer is greater for TCE as compared to PCE (IARC, 2014). Similarly, non-cancer effects were found at lower doses of TCE as compared to PCE (U.S. EPA,

2011b; U.S. EPA, 2011c). Studies that used more sensitive markers of kidney toxicity, such as Kim-1 (Luo, *et al.*, 2018b; Yoo, *et al.*, 2015b) and gene expression (Zhou, *et al.*, 2017), also confirmed that TCE is more toxic to the kidney as compared to PCE when dose is taken into account.

A different picture emerges from studies in rats and mice that examined kidney toxicity of directly administered cysteine conjugates of TCE and PCE in a variety of acute, sub-acute and sub-chronic exposure scenarios (Birner, *et al.*, 1997; Shirai *et al.*, 2012; Vaidya *et al.*, 2003). Nephrotoxicity of DCVC and TCVC is firmly established and most studies reported effects at doses above 10 mg/kg, with some adverse effects observable as doses as low as 1 mg/kg (Shirai, *et al.*, 2012). It should be noted that all of these studies did not use sensitive markers of kidney injury and relied on histopathology and relatively insensitive serum markers of kidney injury. Furthermore, not many studies conducted a comparative analysis of the effects of DCVC and TCVC, one study showed that TCVC is more nephrotoxic than DCVC when equimolar doses were compared (Birner, *et al.*, 1997). Thus, our toxicokinetic study is highly informative with respect to this apparent disconnect because we show that the total amount of reactive glutathione conjugates that can be formed from a high dose of either TCE or PCE is at least an order of magnitude lower than that which has been shown to elicit nephrotoxicity in rodents and suggests that other mechanisms of kidney injury may exist.

One such additional mechanism is through TCOH, a metabolite that is specific to TCE (Chiu, *et al.*, 2007). We found that upon administration of TCE, TCOH levels were the highest in kidney among the tissues examined, suggesting that this can be another mechanism for kidney toxicity of TCE. The enzymes associated with generation of TCOH

(i.e., ADHs) and its conversion to TCOG (i.e., UGTs) have high activity in kidney, which may account for the high total TCOH level observed in kidney. To date, there is no consensus on TCOH-induced kidney toxicity, but it is likely resulting through perturbation of formate metabolism. The oxidative metabolites of TCE, TCA and TCOH, are known to mediate formic aciduria in rats (Yaqoob, *et al.*, 2013) and mice (Lock, *et al.*, 2017). It was also reported that TCE, but not TCOH, can induce elevated renal injury markers in rats after 12 weeks of exposure (Yaqoob, *et al.*, 2014), even though both chemicals can cause formic aciduria in rats and mice. However, with chronic exposure up to 52 weeks, TCOH has been shown to stimulate formic acid excretion, cell replication, protein accumulation, and increased incidence of basophilic tubules in the cortex of rat kidney (Green, *et al.*, 2003). Although TCOH alone does not sufficiently explain the full range of renal effects after TCE exposure (U.S. EPA, 2011c), the high level of TCOH found in the kidney is consistent with the hypothesis that TCE-induced formic aciduria may contribute to chronic renal injury observed in rats and mice, a mechanism that is absent in PCE-treated mice.

The inter-strain variability in metabolism has been demonstrated in mice for TCE (Bradford, *et al.*, 2011; Luo, *et al.*, 2018a; Venkatratnam, *et al.*, 2017; Yoo, *et al.*, 2015a; Yoo, *et al.*, 2015b) and PCE (Cichocki, *et al.*, 2017a; Cichocki, *et al.*, 2017c). Even though TCE and PCE differ only by one chlorine atom in structure, we found substantial differences in metabolism between TCE and PCE *in vivo*, especially in the products of glutathione conjugation pathway. We selected three strains, B6C3F1/J, C57BL/6J, and NZW/LacJ, based on their differences in formation of TCA and glutathione conjugates in a multi-strain study of TCE (Bradford, *et al.*, 2011). We posited that these strains would

be informative of the range of inter-strain variability in metabolism of TCE and PCE. Results from our study lead to several important findings for the metabolism of TCE and PCE. The inter-strain variability was larger for TCA, but smaller for glutathione conjugates in TCE-treated mice as compared to PCE-treated mice (Table B-17). These findings show that chemical-specific data are needed for even structurally similar chemicals. The inter-strain variability of TCA levels in liver was recently examined by using the Collaborative Cross mouse population with a single oral dose of TCE or PCE, where the GSD was 2.24 for TCE-treated mice (Venkatratnam, *et al.*, 2017) and 1.64 for PCE-treated mice (Cichocki, *et al.*, 2017c). Our study confirms this difference, we also observed a larger variability of TCA level in TCE-treated mice (GSD=1.81) as compared to PCE-treated mice (GSD=1.19). The larger inter-strain variability seen in TCE treated mice may result from the generation of TCE-specific metabolite TCOH, which was highly variable across strains in this study (Figure 6.5). The production and subsequent metabolism of TCOH involves a number of metabolic enzymes such as alcohol dehydrogenase, CYPs, and UDP-glucuronosyltransferases, and could be the source of the observed inter-strain variability. In addition, the enterohepatic recirculation of TCE specific metabolites CH, TCOH, and TCOG would also be a significant source of TCA, and may introduce the observed inter-strain variability (Stenner, *et al.*, 1997). With regard to the glutathione conjugation metabolites, the inter-strain variability is larger in PCE-treated mice as compared to TCE-treated mice (Table B-17). This observation can be attributed to the higher metabolic flux through glutathione conjugation in PCE-treated mice as compared to TCE-treated mice. Interestingly, for both TCE and PCE, the highest metabolite levels were found in NZW/LacJ mice. This finding is concordant with

previously reports that NZW/LacJ mice produced the highest levels of TCA when treated with TCE (Bradford, *et al.*, 2011; Yoo, *et al.*, 2015b).

We note that this study is not without limitations. First, the doses used in this study (6 mmoles/kg) are orders of magnitude higher than those expected in the general human population; still, the doses used herein are in the range of doses used in other animal studies, including sub-chronic and chronic animal bioassays with both TCE and PCE (National Toxicology Program, 1990). Second, the oxidative metabolism of PCE is likely saturated at these high oral doses (Buben and O'Flaherty, 1985). Saturation of oxidation leads to greater relative formation of glutathione conjugates, which may have greater human relevance given evidence that at low doses rodents form approximately 100-fold less glutathione conjugation pathway metabolites of TCE as compared to humans (Chiu, *et al.*, 2009). Still, some caution is warranted in interpreting our comparative analysis due to non-linearities at high doses, so understanding of toxicokinetics at lower doses is an area of future research focus that would benefit from more sensitive methods for measuring oxidative and glutathione conjugation metabolites, as well as use of PBPK modeling to address non-linearities due to metabolic saturation. Our recent analytical methods (Luo, *et al.*, 2017; Luo, *et al.*, 2018a) can be applied in the dose range of 10-100 mg/kg, but additional improvements to the sensitivity are needed. Third, the use of one hybrid and two inbred mouse strains may not be representative for the inter-strain variability of T/PCE metabolites. The selection of these three strains was based on the crude estimate of the inter-strain variability (Bradford, *et al.*, 2011). A population-based mouse model, such as the Collaborative Cross mouse population, would advance our knowledge of inter-strain variability in metabolism and toxicity of T/PCE. Finally, the

presumed bio-activation of cysteine conjugates necessitates an additional compartment in the current model. However, further experimental data (e.g., measurement of dichloroacetic acid [DCA] or unidentified reactive metabolites) would be useful to confirm our predictions. DCA in particular is of interest because it is a multispecies hepatocarcinogen and can be formed via multiple pathways from TCE and PCE, but there have been long-standing concerns about its measurement due to the potential for *ex vivo* formation (Chiu *et al.*, 2006b). Still, this study is the first to systematically compare oxidative and GSH conjugative metabolism between TCE and PCE. Our next step will be updating the PBPK models for TCE and PCE, which is of importance for the health risk assessments of TCE and PCE.

CHAPTER VII

SUMMARY AND CONCLUSIONS

7.1 Summary

The goal of these studies was to advance our knowledge in organ-specific metabolism and toxicity of chlorinated olefins, and to a broader context, in inter-individual variability in metabolism and toxicity of environmental toxicants. In summary, we showed that the xenobiotic metabolism drove the organ-specific toxicity of chlorinated olefins and that the extrinsic (e.g., diet-triggered disease states) and intrinsic factor (e.g., genetics) could alter xenobiotic metabolism, and thus may affect the individual's susceptibility to chemical exposures.

Little is known regarding GSH conjugation pathway of TCE and PCE *in vivo* due to the lack of sensitive analytical assays. Herein, we validated two LC-MS/MS methods for simultaneous detection of GSH conjugates in multiple mouse tissues for PCE (**Specific Aim 1**) and TCE (**Specific Aim 2**).

The advancement in the analytical methods for detection of GSH metabolites of TCE and PCE has opened up a new horizon for studies on metabolism and toxicity of TCE and PCE. By applying the newly developed LC-MS/MS method in a study of 20 strains of Collaborative Cross mice, we demonstrated that the default uncertainty factor for TKs variability (3.16) would be inadequate to protect 99% of the general population for organ-

specific toxicity of TCE mediated by GSH conjugation metabolites DCVG, DCVC, and NAcDCVC (**Specific Aim 2**).

We also found that liver disease states (i.e., NAFLD) and the status of a major oxidative enzyme (i.e., CYP2E1) could affect metabolism and toxicity of TCE and PCE. Specifically, tissue levels of oxidative metabolite TCA were higher in NAFLD mice but lower in Cyp2e1(-/-) mice, as compared to the respective wild-type mice. On the other hand, tissue levels of GSH conjugation metabolites were lower in NAFLD mice and Cyp2e1(-/-) mice for PCE, but higher in Cyp2e1(-/-) mice for TCE. The difference in tissue levels of TCA aligned well with the extent of PPARα activation, and that the tissue levels of GSH conjugation metabolites concurred with the extent of the PCE-induced proximal tubular injury, as indicated in NAFLD mice **(Specific Aim 3)** and Cyp2e1(-/-) mice **(Specific Aim 4)**.

The differences in TK of GSH conjugation between TCE and PCE in Cyp2e1(-/-) mice are intriguing; therefore, we directly compared the TK of TCE and PCE, and their respective metabolites, in multiple organs of male B6C3F1/J, C57BL/6J, and NZW/LacJ mice. We found that one chlorine atom replacement in structure led to considerable differences in TKs *in vivo* (**Specific Aim 5**). In the case of TCE and PCE, significant differences were observed in the GSH conjugation pathways, where PCE generated approximately 20-fold higher metabolic flux through GSH conjugation compared to TCE. In addition, TCOH in which is a TCE-specific metabolite was found in the highest levels in the kidney.

Collectively, in this dissertation, two LC-MS/MS methods for the simultaneous detection of GSH conjugation metabolites at multiple tissues have been developed and

validated. With these advancements in the analytical assays, we demonstrated that chemical-specific uncertainty factor for TK variability is necessary to protect the 99% of the population, especially for the xenobiotics with complex metabolism. Using TCE and PCE as model compounds, we concluded that the intrinsic (e.g., genetics) and extrinsic (e.g., diet-triggered disease states) factors could introduce inter-individual variability in TKs of xenobiotics, which in turn determine the individual susceptibility toward chemical exposures. Additionally, one atom replacement in structure could substantially alter the metabolism and toxicity of xenobiotics.

7.2 The significance of this study

The National Research Council has identified improving the technical analysis as one of the future directions for advancing risk assessments (National Research Council, 2009). Specifically, critical data gaps lie in the uncertainty and variability analyses. Uncertainty and variability are inherent properties that are critical to the quality of the risk assessment process. Both uncertainty and variability can be better characterized but not fully eliminated. Uncertainty results from lack of data; while variability stems from the inherent characteristics of a population, from exposure to the adverse effects of exposures (National Research Council, 2009).

Herein, we provide a generalized scheme that improves characterization of the variability in metabolism and toxicity of xenobiotics, by using CC mice, a transgenic mouse model, and two mouse models for fatty liver disease. The CC is derived from eight founder strains, which captures over 90% of the known genetic variability in laboratory mice (Churchill, 2007). In addition, this genetic variability is randomly assigned to

individual CC lines (Aylor *et al.*, 2011). Combined with the known genetic background, CC mice are an ideal animal model to probe the hereditary variability in TKs and TDs of xenobiotics in general. In Specific Aim 2, we demonstrated that CC mouse population is a useful population-based model to derive the tissue-specific uncertainty factors for TK variability.

Narrowing down to the context of a specific enzyme, transgenic mice can provide mechanistic insights into the mode of action of xenobiotics, by knocking in or knocking down the gene of interest. Transgenic mouse models have been widely used to study the role of specific enzyme in diseases (Agrawal *et al.*, 2015; Epstein *et al.*, 1987; Kostic *et al.*, 1997; Langley *et al.*, 2017; Leissring *et al.*, 2003; Liu *et al.*, 2001; Ripps *et al.*, 1995) and in developing toxicities of xenobiotics (Boverhof *et al.*, 2011; Gonzalez, 2002; Gonzalez and Kimura, 2003; Reno *et al.*, 2015). If *a priori* knowledge of the toxicant's mode of action exists, the transgenic mouse model is the most straightforward way to investigate how the protein of interest contributes to xenobiotic's toxicity *in vivo*. For example, with this information, we could determine whether a fast or slow metabolizer would increase susceptibility to chemical exposures. Indeed, we found that the PCE-induced kidney toxicity has been ameliorated in Cyp2e1(-/-) mice, suggesting that individuals with higher activity of CYP2E1 may be more susceptible to PCE induced kidney toxicity.

Likewise, the use of mouse models for disease states can also help identifying the susceptible individuals toward chemical exposures. Aside from the effects of NAFLD on xenobiotic toxicity examined here, the xenobiotic-disease state associations can also be evaluated in other disease models, such as diabetes (Kachapati *et al.*, 2012; Lovati *et al.*,

2013; Mallipattu *et al.*, 2014) and cardiovascular disease (Doggrell and Brown, 1998; Hasenfuss, 1998). The data acquired from these disease models would be helpful for addressing specific risk-management questions, e.g., the chemical health risk assessment for the individual with the hereditary disease.

The National Academy of Sciences consultation panel has highlighted several key scientific issues regarding the MOAs for TCE toxicity, including (i) the toxicological importance of TCA and DCA in rodents and humans for liver cancer, (ii) the toxicological importance of GSH conjugation metabolites for kidney cancer, and (iii) strength of evidence for hypothesized MOAs for liver cancer (e.g., peroxisome proliferation, cell replication, selection, and/or apoptosis) and kidney cancer (e.g., genotoxicity, α2μ-globulin accumulation, peroxisome proliferation, and nephrotoxicity/cytotoxicity) (Chiu, *et al.*, 2006a). Our results indicate that the treatment of TCE and PCE could upregulate the PPARα responsive genes (i.e., *Acox 1* and *Cyp4a10*). However, the activation of PPARα responsive genes did not translate into the cell proliferation in liver and kidney, as evidenced by the cell proliferation in liver and kidney of PCE treated mice.

The work presented in Aim 1&2 has opened up a new horizon for studies regarding GSH conjugation and toxicity of TCE and PCE. With these sensitive analytical methods, we can study the associations between GSH conjugation metabolites and kidney toxicity of TCE and PCE *in vivo*, especially at a more biologically-relevant tissue level. Our findings showed that despite a relatively small flux through GSH pathway, the tissue levels of GSH conjugation metabolites aligned well with the extent of proximal tubular injury of PCE, as evidenced in CYP2E1 transgenic mice and NAFLD mice. Additionally, the higher flux through GSH conjugation pathway also aligned well with the more pronounced

transcriptional effects in mouse kidney for PCE, as compared to TCE (Zhou, *et al.*, 2017) . These results support the long-lasting hypothesis that metabolites from GSH conjugation pathway can contribute to the nephrotoxicity *in vivo*. However, for chronic kidney toxicity, the strength of evidence is stronger for TCE than PCE. Alternative MOAs may participate in developing kidney tumors in animals and humans.

Indeed, we found an unusually high level of TCOH in the kidney as compared to the other tissues. TCOH is a TCE-specific metabolite, which is stemming from CH. Subject to chronic exposure of TCOH, rodents can develop formic aciduria and manifest an elevated level of kidney injury biomarker (Green, *et al.*, 2003). It is known that formic acid can lead to histological changes in rabbit kidney (Liesivuori *et al.*, 1987). As this MOA is largely uncharacterized for PCE, multiple MOAs, including the contributions of GSH conjugation metabolites and TCOH, are plausible for developing kidney tumors for TCE.

In addition, the interconversion of TCOH and TCOG could be a potential source of inter-individual variability in TKs of TCE metabolites. We found a higher TK variability for TCE metabolites across B6C3F1/J, C57BL/6J, and NZW/LacJ mice, as compared to PCE (Specific Aim 5). This finding also concurred with the results in CC mice, where the TKs of TCE metabolites are more variable than those of PCE metabolites (Cichocki, *et al.*, 2017c). TCOH and TCOG can be subject to enterohepatic recirculation and would be a significant source of TCA (Stenner, *et al.*, 1997). Therefore, UGTs may be a critical enzyme to study the inter-individual variability in metabolism and responses to TCE exposure.

Aside from the metabolism of TCE and PCE, the chemical and physical properties of xenobiotic could also be a crucial determinant of the interaction with different disease states. For instance, PCE is a lipophilic chemical, which manifests a higher affinity to adipose tissues (Cichocki, *et al.*, 2017a). Liver steatosis is anticipated to retain PCE in the liver and reduce the delivered dose of PCE in other organs. Indeed, our results showed that PCE levels were higher in the liver (Cichocki, *et al.*, 2017b), but lower in the kidney and feces of NAFLD mice compared to LFD mice. The higher internal dose of PCE increased the production of TCA in the liver of NAFLD mice, which caused more severe PCE-induced liver effects (Cichocki, *et al.*, 2017b). This result reveals that chemical and physical properties of xenobiotics could be critical factors to identifying susceptible individuals, considering the nature of disease states.

Collectively, this dissertation fills in several data gaps from a broader context of risk assessment, to a specific case-scenario of TCE and PCE. With the animal models demonstrated in this dissertation, we can better characterize the variability in TKs and TDs of xenobiotics and improve the quality of human health risk assessment.

7.3 Limitations

Even though the studies from this dissertation have enlightened us on inter-individual variability in metabolism and toxicity of TCE and PCE, and advanced our knowledge in metabolism and toxicity of TCE and PCE, there are several limitations in these studies.

First, the monitoring metabolites in these studies were confined to the parent compounds TCE and PCE, major oxidative metabolites TCA and TCOH, and GSH conjugation metabolites D/TCVG, D/TCVC, and NAcD/TCVC. Other minor metabolites from oxidative (i.e., CTAC, DCA, and DCVT) and GSH conjugation pathways (i.e., DCVCSO and TCVCSO) may also be of interest because of their potential toxicities. However, there is little or no analytical capability to detect these minor, but reactive metabolites in target organs, partly because these metabolites are too unstable to develop analytical methods for targeted analysis. The alternative approach would be using untargeted approaches (e.g., NMR, IM-MS, etc.) to compare the differences between chemical-exposed and control groups.

Second, species differences do exist in the metabolism and toxicity of xenobiotics. For instance, mice manifest a higher metabolic rate for the oxidative metabolism (e.g., via CYPs), but a lower efficiency in GSH conjugative metabolism as compared to rats and humans (Chiu, *et al.*, 2009). Other physiological parameters also vary among species. Therefore, humanized CYP2E1 mice used in this dissertation would reflect the traits that may or may not be found in humans. Besides, the relevance of the animal NAFLD/NASH models to human NAFLD remains to be a contentious issue in the field (Maher, 2011; Teufel, *et al.*, 2016). Even though HFD- and MCD-fed animals can mimic the histopathological phenotypes of human NAFLD and NASH, the degree of injury depends on several factors including rodent strains (Lau, *et al.*, 2017; Tryndyak, *et al.*, 2012a; Tryndyak, *et al.*, 2012b). Also, the metabolic profile of MCD-fed mice is different from human NASH (Rinella and Green, 2004).

Third, we note that the administered dose of TCE and PCE used in these studies is relatively high, which may not be correspondent to the exposures to humans. As the oxidation of TCE and PCE is even more efficient in mice, tissue levels of oxidative metabolites would be several orders of magnitude higher in mice compared to humans. However, the GSH conjugation pathway is approximately 100-fold less efficient in mice compared to humans, therefore suggesting that tissue levels of GSH conjugates may be still close to human exposure of TCE and PCE. In addition, the relationship between TCE and PCE dose and GSH metabolites is linear within the dose range used in this study. An appropriate PBPK model can help extrapolate the mouse data to humans and provide valuable information for the human health risk assessment.

The limitations described above direct us for the future studies regarding the mechanistic toxicology and human health risk assessment of environmental toxicants. In the next section, we will discuss the potential directions that would move forward in the fields of basic mechanistic toxicology, exposure sciences, to regulatory science and human health risk assessment.

7.4 Future directions

The advancement in analytical chemistry would improve the characterization from exposure to toxicity of xenobiotics in humans

Unlike the traditional studies using a targeted, hypothesis-driven approach to explore the associations between a specific xenobiotic and biological endpoints, exposome is a bottom-up approach that represents a life course of environmental exposures (Cui *et al.*, 2016). This approach allows for the consideration of multiple chemicals, rather than a

single chemical, on the progression of specific biological response (Wild, 2005). Accordingly, an untargeted approach is proposed and would be useful to characterize the complex exposures that are relevant to the real-life scenario. Recent advances in development of analytical chemistry have enable the practice of environment-wide association study (EWAS), by using nuclear magnetic resonance (NMR) spectroscopy (Beckonert *et al.*, 2007; Gil *et al.*, 2018; Maitre *et al.*, 2017), LC/GC coupled with Fourier-transformed mass spectrometry (Go *et al.*, 2015; Johnson *et al.*, 2010; Soltow *et al.*, 2013), hybrid ion-trap-orbitrap MS (Jamin *et al.*, 2014), quadrupole-time-of-flight mass spectrometry (Andra *et al.*, 2015; Diaz *et al.*, 2012; Fan *et al.*, 2014), or triple-quadrupole tandem mass spectrometry (Cui *et al.*, 2018; Hoeke *et al.*, 2015).

Another technology for characterization of exposome is ion-mobility spectroscopy (IMS) coupled with MS-based detectors (Metz *et al.*, 2017). IMS introduces several advantages for the untargeted analysis. First, IMS provides additional resolution for isobaric ions, because it allows the conformational separation of ions based on the electronic field and the drag force from ion-gas collisions (Kyle *et al.*, 2016; Poyer *et al.*, 2017; Williams *et al.*, 2009; Zheng *et al.*, 2017a). Second, IMS increases the dynamic range of existing LC-MS based methods (Metz, *et al.*, 2017). Finally, IMS separations are ultra-high throughput, with a single separation occurring in 10-100 ms, as compared to LC (~minutes) or GC (~hours) techniques. These advantages make IMS-MS a promising tool in EWAS research; however, several analytical and data processing challenges need to be resolved for the implementation of IMS in exposome workflow. For instance, adducts/dimers annotation need to be distinguished from the principle monoisotopic ion as determined by IMS. In addition, as an emerging analytical technique, the database for

unknown-known analysis is limited, which requires in-house derivation of experimental (i.e., via infusion of known standards) or theoretical (i.e., derived *in silico*) collision cross section (CCS) values.

Metabolomics can be considered as a subset of exposomics (Athersuch and Keun, 2015); however, it also shows the perturbed metabolic pathways that potentially associated with toxic effects of xenobiotics. The analytical tools discussed above have also been widely used for metabolomics (Cajka and Fiehn, 2016; Ghaste *et al.*, 2016; Khamis *et al.*, 2017). After decades of study, MS-based (Wishart *et al.*, 2009) and NMR-based databases (i.e., Biological Magnetic Resonance Data) have been well established for human metabolomics. On the other hand, the application of IMS-MS in human metabolomics is still at an infant stage. The public-available database generated by Pacific Northeast National Laboratory reports the CCS values for approximately 500 primary metabolites, secondary metabolites, and xenobiotics (Zheng *et al.*, 2017b). Nevertheless, these advanced technologies would be potential tools to characterize the xenobiotic-associated perturbation in metabolism and toxicity, in an untargeted, high-throughput manner.

Toxicity assessment of metabolite mixtures of TCE and PCE: Insights into the observed inter-species variability

Exposure to a chemical with complicated metabolism creates an exposure scenario of mixtures. In the case of chlorinated olefins, the interactions among the parent compound, oxidative metabolites, and GSH conjugation metabolites remain unclear. Effects of chemical co-exposure have been investigated for TCE and PCE in simple mixtures. For instance, TCE has shown a potentiation effect with carbon tetrachloride on

hepatotoxicity (Pessayre *et al.*, 1982), and a synergistic effect with di(2-ethylhexyl)phthalate on developmental toxicity (Narotsky *et al.*, 1995) in rats. Additionally, TCE manifested synergistic interactions with methylmercury and benzene on liver and kidney transcriptomes in rats, after 14-day exposures at the lowest-observed-adverse-effect-level (LOAEL) (Hendriksen *et al.*, 2007). The pharmacokinetic interactions among TCE, PCE, and 1,1,1-trichloroethane were also examined by using a PBPK model (Dobrev *et al.*, 2001).

However, traditional simple-mixture studies require a considerable amount of time and efforts but maybe still too simplified for the real-life conditions. From this dissertation, we found that the inter-species and inter-individual differences in toxicity of TCE and PCE result from the quantitative differences in their metabolism. The different combination of the parent compound, oxidative metabolites, and GSH conjugation metabolites creates a different chemical mixture, which in turn may affect the toxicity of TCE and PCE.

Because of the complex nature of chemical mixtures, the simple, *in vitro* cell-based assays would be a good starting point for toxicity assessment of mixtures. Based on the results from experimental and PBPK studies, we can create a list of mixtures representing the metabolism in mice, rats, and humans. By testing these mixtures and individual components in the *in vitro* assays targeting specific bioactivity, we can understand the inter-species difference from a comprehensive view and explore the interactions, if any, among the parent compound and its downstream metabolites.

Incorporate the tissue-specific data regarding GSH conjugation pathway into PBPK models to refine the health risk assessment of TCE and PCE

PBPK models have been widely used to bridge the animal and human, low and high doses for the health risk assessments of xenobiotics. In the case of TCE and PCE, several PBPK modeling papers have been published (Abbas and Fisher, 1997; Allen and Fisher, 1993; Chiu, *et al.*, 2014; Chiu and Ginsberg, 2011; Chiu, *et al.*, 2009; Clewell *et al.*, 2000; Cronin *et al.*, 1995; Dobrev, *et al.*, 2001; Evans *et al.*, 2009; Fisher, 2000; Fisher, *et al.*, 1991; Fisher *et al.*, 1998; Gearhart *et al.*, 1993; Greenberg *et al.*, 1999; Hissink *et al.*, 2002; Loizou, 2001; Reitz *et al.*, 1996; Stenner *et al.*, 1998). Only a few papers included the compartment regarding GSH conjugative pathway of TCE or PCE. Because of lack of tissue-specific data, these papers may either use urinary n-acetyl cysteine conjugates or serum levels of GSH conjugation metabolites to represent the flux through GSH conjugation pathway. However, the tissue levels of GSH conjugation metabolites are critical because these GSH metabolites have been postulated as the precursors of the nephrotoxic metabolites of TCE and PCE.

One of the essential findings from this dissertation is that we report the tissue-specific data regarding GSH conjugates, cysteine conjugates, and n-acetyl cysteine conjugates of TCE and PCE in multiple mouse tissues. The incorporation of these animal data into an updated PBPK model will be useful to give insights into the role of GSH conjugation metabolites in developing kidney toxicity, especially with a more relevant scenario to humans.

REFERENCES

Abbas, R., and Fisher, J. W. (1997). A physiologically based pharmacokinetic model for trichloroethylene and its metabolites, chloral hydrate, trichloroacetate, dichloroacetate, trichloroethanol, and trichloroethanol glucuronide in B6C3F1 mice. *Toxicol Appl Pharmacol* **147**(1), 15-30.

AboulFotouh, K., Allam, A. A., El-Badry, M., and El-Sayed, A. M. (2018). Role of self-emulsifying drug delivery systems in optimizing the oral delivery of hydrophilic macromolecules and reducing interindividual variability. *Colloids Surf B Biointerfaces* **167**, 82-92.

Agrawal, A. S., Garron, T., Tao, X., Peng, B. H., Wakamiya, M., Chan, T. S., Couch, R. B., and Tseng, C. T. (2015). Generation of a transgenic mouse model of Middle East respiratory syndrome coronavirus infection and disease. *J Virol* **89**(7), 3659-70.

Allen, B. C., and Fisher, J. W. (1993). Pharmacokinetic modeling of trichloroethylene and trichloroacetic acid in humans. *Risk Anal* **13**(1), 71-86.

Andra, S. S., Austin, C., Wright, R. O., and Arora, M. (2015). Reconstructing pre-natal and early childhood exposure to multi-class organic chemicals using teeth: Towards a retrospective temporal exposome. *Environ Int* **83**, 137-145.

Athersuch, T. J., and Keun, H. C. (2015). Metabolic profiling in human exposome studies. *Mutagenesis* **30**(6), 755-62.

ATSDR (2014). Draft Toxicological Profile for Tetrachloroethylene.

ATSDR (1997). Toxicological profile for trichloroethylene (TCE).

Aylor, D. L., Valdar, W., Foulds-Mathes, W., Buus, R. J., Verdugo, R. A., Baric, R. S., Ferris, M. T., Frelinger, J. A., Heise, M., Frieman, M. B., *et al.* (2011). Genetic analysis of complex traits in the emerging Collaborative Cross. *Genome Res* **21**(8), 1213-22.

Bartels, M. J. (1994). Quantitation of the tetrachloroethylene metabolite N-acetyl-S-(trichlorovinyl)cysteine in rat urine via negative ion chemical ionization gas chromatography/tandem mass spectrometry. *Biol Mass Spectrom* **23**(11), 689-94.

Beckonert, O., Keun, H. C., Ebbels, T. M., Bundy, J., Holmes, E., Lindon, J. C., and Nicholson, J. K. (2007). Metabolic profiling, metabolomic and metabonomic procedures for NMR spectroscopy of urine, plasma, serum and tissue extracts. *Nat Protoc* **2**(11), 2692-703.

Bernauer, U., Birner, G., Dekant, W., and Henschler, D. (1996). Biotransformation of trichloroethene: dose-dependent excretion of 2,2,2-trichloro-metabolites and mercapturic acids in rats and humans after inhalation. *Arch Toxicol* **70**(6), 338-346.

Birner, G., Bernauer, U., Werner, M., and Dekant, W. (1997). Biotransformation, excretion and nephrotoxicity of haloalkene-derived cysteine S-conjugates. *Arch Toxicol* **72**(1), 1-8.

Birner, G., Rutkowska, A., and Dekant, W. (1996). N-acetyl-S-(1,2,2-trichlorovinyl)-L-cysteine and 2,2,2-trichloroethanol: two novel metabolites of tetrachloroethene in humans after occupational exposure. *Drug Metab Dispos* **24**(1), 41-8.

Bloemen, L. J., Monster, A. C., Kezic, S., Commandeur, J. N., Veulemans, H., Vermeulen, N. P., and Wilmer, J. W. (2001). Study on the cytochrome P-450- and glutathione-dependent biotransformation of trichloroethylene in humans. *Int Arch Occup Environ Health* **74**(2), 102-8.

Boverhof, D. R., Chamberlain, M. P., Elcombe, C. R., Gonzalez, F. J., Heflich, R. H., Hernandez, L. G., Jacobs, A. C., Jacobson-Kram, D., Luijten, M., Maggi, A., *et al.* (2011). Transgenic Animal Models in Toxicology: Historical Perspectives and Future Outlook. *Toxicol Sci* **121**(2), 207-233.

Bradford, B. U., Lock, E. F., Kosyk, O., Kim, S., Uehara, T., Harbourt, D., DeSimone, M., Threadgill, D. W., Tryndyak, V., Pogribny, I. P., *et al.* (2011). Interstrain differences in the liver effects of trichloroethylene in a multistrain panel of inbred mice. *Toxicol Sci* **120**(1), 206-17.

Browning, J. D., Szczepaniak, L. S., Dobbins, R., Nuremberg, P., Horton, J. D., Cohen, J. C., Grundy, S. M., and Hobbs, H. H. (2004). Prevalence of hepatic steatosis in an urban population in the United States: impact of ethnicity. *Hepatology* **40** (6), 1387-1395.

Buben, J. A., and O'Flaherty, E. J. (1985). Delineation of the role of metabolism in the hepatotoxicity of trichloroethylene and perchloroethylene: a dose-effect study. *Toxicol Appl Pharmacol* **78**(1), 105-22.

Bull, R. J., Sanchez, I. M., Nelson, M. A., Larson, J. L., and Lansing, A. J. (1990). Liver tumor induction in B6C3F1 mice by dichloroacetate and trichloroacetate. *Toxicology* **63**(3), 341-359.

Cajka, T., and Fiehn, O. (2016). Toward Merging Untargeted and Targeted Methods in Mass Spectrometry-Based Metabolomics and Lipidomics. *Anal Chem* **88**(1), 524-45.

Canet, M. J., Hardwick, R. N., Lake, A. D., Dzierlenga, A. L., Clarke, J. D., Goedken, M. J., and Cherrington, N. J. (2015). Renal Xenobiotic Transporter Expression is Altered in Multiple Experimental Models of Nonalcoholic Steatohepatitis. *Drug Metab Dispos* **43**(2), 266-272.

Cattaneo, D., Baldelli, S., Minisci, D., Meraviglia, P., Clementi, E., Galli, M., and Gervasoni, C. (2016). When food can make the difference: The case of elvitegravir-based co-formulation. *Int J Pharmaceut* **512**(1), 301-304.

CDC (2017). National Health and Nutrition Examination Survey 2013-2014.

CEPA (1993). Canadian Environmental Protection Act. Priority substances list assessment report: Tetrachloroethylene.

Chalasani, N., Younossi, Z., Lavine, J. E., Diehl, A. M., Brunt, E. M., Cusi, K., Charlton, M., and Sanyal, A. J. (2012). The diagnosis and management of non-alcoholic fatty liver disease: practice Guideline by the American Association for the Study of Liver Diseases, American College of Gastroenterology, and the American Gastroenterological Association. *Hepatology* **55**(6), 2005-23.

Chiu, W. A., Caldwell, J. C., Keshava, N., and Scott, C. S. (2006a). Key scientific issues in the health risk assessment of trichloroethylene. *Environ Health Perspect.* **114**(9), 1445-1449.

Chiu, W. A., Campbell, J. L., Clewell, H. J., Zhou, Y. H., Wright, F. A., Guyton, K. Z., and Rusyn, I. (2014). Physiologically-Based Pharmacokinetic (PBPK) Modeling of Inter-strain Variability in Trichloroethylene Metabolism in the Mouse. *Environ Health Perspect* **122**(5), 456-463.

Chiu, W. A., and Ginsberg, G. L. (2011). Development and evaluation of a harmonized physiologically based pharmacokinetic (PBPK) model for perchloroethylene toxicokinetics in mice, rats, and humans. *Toxicol Appl Pharmacol* **253**(3), 203-34.

Chiu, W. A., Jinot, J., Scott, C. S., Makris, S. L., Cooper, G. S., Dzubow, R. C., Bale, A. S., Evans, M. V., Guyton, K. Z., Keshava, N., *et al.* (2013). Human health effects of trichloroethylene: key findings and scientific issues. *Environ Health Perspect* **121**(3), 303-11.

Chiu, W. A., Micallef, S., Monster, A. C., and Bois, F. Y. (2007). Toxicokinetics of inhaled trichloroethylene and tetrachloroethylene in humans at 1 ppm: empirical results and comparisons with previous studies. *Toxicol Sci* **95**(1), 23-36.

Chiu, W. A., Okino, M. S., and Evans, M. V. (2009). Characterizing uncertainty and population variability in the toxicokinetics of trichloroethylene and metabolites in mice, rats, and humans using an updated database, physiologically based pharmacokinetic (PBPK) model, and Bayesian approach. *Toxicol Appl Pharmacol* **241**(1), 36-60.

Chiu, W. A., Okino, M. S., Lipscomb, J. C., and Evans, M. V. (2006b). Issues in the pharmacokinetics of trichloroethylene and its metabolites. *Environ Health Perspect.* **114**(9), 1450-1456.

Chiu, W. A., and Slob, W. (2015). A Unified Probabilistic Framework for Dose-Response Assessment of Human Health Effects. *Environ Health Perspect* **123**(12), 1241-54.

Churchill, G. A. (2007). Recombinant inbred strain panels: a tool for systems genetics. *Physiol Genomics* **31**(2), 174-5.

Cichocki, J. A., Furuya, S., Konganti, K., Luo, Y. S., McDonald, T. J., Iwata, Y., Chiu, W. A., Threadgill, D. W., Pogribny, I. P., and Rusyn, I. (2017a). Impact of Nonalcoholic Fatty Liver Disease on Toxicokinetics of Tetrachloroethylene in Mice. *J Pharmacol Exp Ther* **361**(1), 17-28.

Cichocki, J. A., Furuya, S., Luo, Y. S., Iwata, Y., Konganti, K., Chiu, W. A., Threadgill, D. W., Pogribny, I. P., and Rusyn, I. (2017b). Nonalcoholic Fatty Liver Disease Is a Susceptibility Factor for Perchloroethylene-Induced Liver Effects in Mice. *Toxicol Sci* **159**(1), 102-113.

Cichocki, J. A., Furuya, S., Venkatratnam, A., McDonald, T. J., Knap, A. H., Wade, T., Sweet, S., Chiu, W. A., Threadgill, D. W., and Rusyn, I. (2017c). Characterization of Variability in Toxicokinetics and Toxicodynamics of Tetrachloroethylene Using the Collaborative Cross Mouse Population. *Environ Health Perspect* **125**(5), 057006.

Cichocki, J. A., Guyton, K. Z., Guha, N., Chiu, W. A., Rusyn, I., and Lash, L. H. (2016). Target Organ Metabolism, Toxicity, and Mechanisms of Trichloroethylene and Perchloroethylene: Key Similarities, Differences, and Data Gaps. *J Pharmacol Exp Ther* **359**(1), 110-23.

Clarke, J. D., Hardwick, R. N., Lake, A. D., Lickteig, A. J., Goedken, M. J., Klaassen, C. D., and Cherrington, N. J. (2014). Synergistic interaction between genetics and disease on pravastatin disposition. *J Hepatol* **61**(1), 139-147.

Clewell, H. J., Gentry, P. R., Covington, T. R., and Gearhart, J. M. (2000). Development of a physiologically based pharmacokinetic model of trichloroethylene and its metabolites for use in risk assessment. *Environ Health Persp* **108**, 283-305.

Commandeur, J. N., and Vermeulen, N. P. (1990). Identification of N-acetyl(2,2-dichlorovinyl)- and N-acetyl(1,2-dichlorovinyl)-L-cysteine as two regioisomeric mercapturic acids of trichloroethylene in the rat. *Chemical Res Toxicol* **3**(3), 212-218.

Corton, J. C. (2008). Evaluation of the role of peroxisome proliferator-activated receptor alpha (PPARalpha) in mouse liver tumor induction by trichloroethylene and metabolites. *Crit Rev Toxicol* **38**(10), 857-875.

Corton, J. C., Cunningham, M. L., Hummer, B. T., Lau, C., Meek, B., Peters, J. M., Popp, J. A., Rhomberg, L., Seed, J., and Klaunig, J. E. (2014). Mode of action framework analysis for receptor-mediated toxicity: The peroxisome proliferator-activated receptor alpha (PPARalpha) as a case study. *Crit Rev Toxicol* **44**(1), 1-49.

Craig, E. A., Yan, Z., and Zhao, Q. J. (2015). The relationship between chemical-induced kidney weight increases and kidney histopathology in rats. *J Appl Toxicol* **35**(7), 729-36.

Cristofori, P., Sauer, A. V., and Trevisan, A. (2015). Three common pathways of nephrotoxicity induced by halogenated alkenes. *Cell Biol Toxicol* **31**(1), 1-13.

Cronin, W. J., Oswald, E. J., Shelley, M. L., Fisher, J. W., and Flemming, C. D. (1995). A Trichloroethylene Risk Assessment Using a Monte-Carlo Analysis of Parameter Uncertainty in Conjunction with Physiologically-Based Pharmacokinetic Modeling. *Risk Anal* **15**(5), 555-565.

Cui, L., Lu, H., and Lee, Y. H. (2018). Challenges and emergent solutions for LC-MS/MS based untargeted metabolomics in diseases. *Mass Spectrom Rev* doi: 10.1002/mas.21562.

Cui, Y., Balshaw, D. M., Kwok, R. K., Thompson, C. L., Collman, G. W., and Birnbaum, L. S. (2016). The Exposome: Embracing the Complexity for Discovery in Environmental Health. *Environ Health Perspect* **124**(8), A137-40.

Dekant, W. (1993). Bioactivation of nephrotoxins and renal carcinogens by glutathione S-conjugate formation. *Toxicol Lett* **67**(1-3), 151-60.

Dekant, W. (2003). Biosynthesis of toxic glutathione conjugates from halogenated alkenes. *Toxicol Lett* **144**(1), 49-54.

Dekant, W., Metzler, M., and Henschler, D. (1984). Novel metabolites of trichloroethylene through dechlorination reactions in rats, mice and humans. *Biochem Pharmacol* **33**(13), 2021-7.

Dekant, W., Vamvakas, S., Berthold, K., Schmidt, S., Wild, D., and Henschler, D. (1986). Bacterial beta-lyase mediated cleavage and mutagenicity of cysteine conjugates derived from the nephrocarcinogenic alkenes trichloroethylene, tetrachloroethylene and hexachlorobutadiene. *Chem Biol Interact* **60**(1), 31-45.

Diaz, R., Ibanez, M., Sancho, J. V., and Hernandez, F. (2012). Target and non-target screening strategies for organic contaminants, residues and illicit substances in food, environmental and human biological samples by UHPLC-QTOF-MS. *Anal Methods-Uk* **4**(1), 196-209.

Dobrev, I. D., Andersen, M. E., and Yang, R. S. H. (2001). Assessing interaction thresholds for trichloroethylene in combination with tetrachloroethylene and 1,1,1-trichloroethane using gas uptake studies and PBPK modeling. *Arch Toxicol* **75**(3), 134-144.

Doggrell, S. A., and Brown, L. (1998). Rat models of hypertension, cardiac hypertrophy and failure. *Cardiovasc Res* **39**(1), 89-105.

Domino, M. M., Pepich, B. V., Munch, D. J., Fair, P. S., and Xie, Y. (2003). Method 552.3: Determination of haloacetic acids and dalapon in drinking water by liquid-liquid microextraction, derivatization, and gas chromatography with electron capture detection.

Donthamsetty, S., Bhave, V. S., Mitra, M. S., Latendresse, J. R., and Mehendale, H. M. (2007). Nonalcoholic fatty liver sensitizes rats to carbon tetrachloride hepatotoxicity. *Hepatology* **45**(2), 391-403.

Elfarra, A. A., and Krause, R. J. (2007). S-(1,2,2-trichlorovinyl)-L-cysteine sulfoxide, a reactive metabolite of S-(1,2,2-Trichlorovinyl)-L-cysteine formed in rat liver and kidney microsomes, is a potent nephrotoxicant. *J Pharmacol Exp Ther* **321**(3), 1095-101.

EPA, C. (2017). Dry Cleaning Program.

Epstein, C. J., Avraham, K. B., Lovett, M., Smith, S., Elroy-Stein, O., Rotman, G., Bry, C., and Groner, Y. (1987). Transgenic mice with increased Cu/Zn-superoxide dismutase activity: animal model of dosage effects in Down syndrome. *Proc Natl Acad Sci U S A* **84**(22), 8044-8.

Evans, M. V., Chiu, W. A., Okino, M. S., and Caldwell, J. C. (2009). Development of an updated PBPK model for trichloroethylene and metabolites in mice, and its application to discern the role of oxidative metabolism in TCE-induced hepatomegaly. *Toxicol Appl Pharmacol* **236**(3), 329-340.

Fagerberg, L., Hallstrom, B. M., Oksvold, P., Kampf, C., Djureinovic, D., Odeberg, J., Habuka, M., Tahmasebpoor, S., Danielsson, A., Edlund, K., *et al.* (2014). Analysis of the human tissue-specific expression by genome-wide integration of transcriptomics and antibody-based proteomics. *Mol Cell Proteomics* **13**(2), 397-406.

Fan, R. J., Zhang, F., Wang, H. Y., Zhang, L., Zhang, J., Zhang, Y., Yu, C. T., and Guo, Y. L. (2014). Reliable screening of pesticide residues in maternal and umbilical cord sera by gas chromatography-quadrupole time of flight mass spectrometry. *Sci China Chem* **57**(5), 669-677.

Fay, R. M., and Mumtaz, M. M. (1996). Development of a priority list of chemical mixtures occurring at 1188 hazardous waste sites, using the HazDat database. *Food Chem Toxicol* **34**(11-12), 1163-5.

Fisher, J. W. (2000). Physiologically based pharmacokinetic models for trichloroethylene and its oxidative metabolites. *Environ Health Perspect.* **108 Suppl 2**, 265-273.

Fisher, J. W., Gargas, M. L., Allen, B. C., and Andersen, M. E. (1991). Physiologically based pharmacokinetic modeling with trichloroethylene and its metabolite, trichloroacetic acid, in the rat and mouse. *Toxicol Appl Pharmacol* **109**(2), 183-95.

Fisher, J. W., Mahle, D., and Abbas, R. (1998). A human physiologically based pharmacokinetic model for trichloroethylene and its metabolites, trichloroacetic acid and free trichloroethanol. *Toxicol Appl Pharmacol* **152**(2), 339-59.

Forkert, P. G., Baldwin, R. M., Millen, B., Lash, L. H., Putt, D. A., Shultz, M. A., and Collins, K. S. (2005). Pulmonary bioactivation of trichloroethylene to chloral hydrate: relative contributions of CYP2E1, CYP2F, and CYP2B1. *Drug Metab Dispos* **33**(10), 1429-37.

Forkert, P. G., Lash, L., Tardif, R., Tanphaichitr, N., Vandevoort, C., and Moussa, M. (2003). Identification of trichloroethylene and its metabolites in human seminal fluid of workers exposed to trichloroethylene. *Drug Metab Dispos* **31**(3), 306-11.

Forkert, P. G., Millen, B., Lash, L. H., Putt, D. A., and Ghanayem, B. I. (2006). Pulmonary bronchiolar cytotoxicity and formation of dichloroacetyl lysine protein adducts in mice treated with trichloroethylene. *J Pharmacol Exp Ther* **316**(2), 520-9.

Gearhart, J. M., Mahle, D. A., Greene, R. J., Seckel, C. S., Flemming, C. D., Fisher, J. W., and Clewell, H. J. (1993). Variability of Physiologically-Based Pharmacokinetic (Pbpk) Model Parameters and Their Effects on Pbpk Model Predictions in a Risk Assessment for Perchloroethylene (Pce). *Toxicol Lett* **68**(1-2), 131-144.

Ghaste, M., Mistrik, R., and Shulaev, V. (2016). Applications of Fourier Transform Ion Cyclotron Resonance (FT-ICR) and Orbitrap Based High Resolution Mass Spectrometry in Metabolomics and Lipidomics. *Int J Mol Sci* **17**(6).

Gil, A. M., Duarte, D., Pinto, J., and Barros, A. S. (2018). Assessing Exposome Effects on Pregnancy through Urine Metabolomics of a Portuguese (Estarreja) Cohort. *J Proteome Res* **17**(3), 1278-1289.

Glen, C. D., McVeigh, L. E., Voutounou, M., and Dubrova, Y. E. (2015). The effects of methyl-donor deficiency on the pattern of gene expression in mice. *Mol Nutr Food Res* **59**(3), 501-6.

Go, Y. M., Walker, D. I., Liang, Y., Uppal, K., Soltow, Q. A., Tran, V., Strobel, F., Quyyumi, A. A., Ziegler, T. R., Pennell, K. D., *et al.* (2015). Reference Standardization for Mass Spectrometry and High-resolution Metabolomics Applications to Exposome Research. *Toxicol Sci* **148**(2), 531-43.

Goggin, M., Swenberg, J. A., Walker, V. E., and Tretyakova, N. (2009). Molecular dosimetry of 1,2,3,4-diepoxybutane-induced DNA-DNA cross-links in B6C3F1 mice and F344 rats exposed to 1,3-butadiene by inhalation. *Cancer Res* **69**(6), 2479-86.

Gonzalez, F. J. (2002). Transgenic animal models in toxicology studies. *Chem Res Toxicol* **15**(12), 1657-1657.

Gonzalez, F. J., and Kimura, S. (2003). Study of P450 function using gene knockout and transgenic mice. *Arch Biochem Biophys* **409**(1), 153-158.

Green, T., Dow, J., Ellis, M. K., Foster, J. R., and Odum, J. (1997). The role of glutathione conjugation in the development of kidney tumours in rats exposed to trichloroethylene. *Chem Biol Interact* **105**(2), 99-117.

Green, T., Dow, J., and Foster, J. (2003). Increased formic acid excretion and the development of kidney toxicity in rats following chronic dosing with trichloroethanol, a major metabolite of trichloroethylene. *Toxicology* **191**(2-3), 109-19.

Green, T., and Prout, M. S. (1985). Species differences in response to trichloroethylene. II. Biotransformation in rats and mice. *Toxicol Appl Pharmacol* **79**(3), 401-11.

Greenberg, M. S., Burton, G. A., and Fisher, J. W. (1999). Physiologically based pharmacokinetic modeling of inhaled trichloroethylene and its oxidative metabolites in B6C3F1 mice. *Toxicol Appl Pharmacol* **154**(3), 264-78.

Griffith, O. W., and Meister, A. (1979). Glutathione: interorgan translocation, turnover, and metabolism. *Proc Natl Acad Sci U S A* **76**(11), 5606-10.

Guengerich, F. P. (2001). Common and uncommon cytochrome P450 reactions related to metabolism and chemical toxicity. *Chem Res Toxicol* **14**(6), 611-50.

Guha, N., Loomis, D., Grosse, Y., Lauby-Secretan, B., El Ghissassi, F., Bouvard, V., Benbrahim-Tallaa, L., Baan, R., Mattock, H., Straif, K., *et al.* (2012). Carcinogenicity of trichloroethylene, tetrachloroethylene, some other chlorinated solvents, and their metabolites. *Lancet Oncol* **13**(12), 1192-3.

Gul Altuntas, T., and Kharasch, E. D. (2002). Biotransformation of L-cysteine S-conjugates and N-acetyl-L-cysteine S-conjugates of the sevoflurane degradation product fluoromethyl-2,2-difluoro-1-(trifluoromethyl)vinyl ether (compound A) in human kidney in vitro: interindividual variability in N-acetylation, N-deacetylation, and beta-lyase-catalyzed metabolism. *Drug Metab Dispos* **30**(2), 148-54.

Guyton, K. Z., Hogan, K. A., Scott, C. S., Cooper, G. S., Bale, A. S., Kopylev, L., Barone, S., Makris, S. L., Glenn, B., Subramaniam, R. P., *et al.* (2014). Human health effects of tetrachloroethylene: key findings and scientific issues. *Environ Health Perspect* **122**(4), 325-34.

Hanioka, N., Jinno, H., Takahashi, A., Nakano, K., Yoda, R., Nishimura, T., and Ando, M. (1995). Interaction of tetrachloroethylene with rat hepatic microsomal P450-dependent monooxygenases. *Xenobiotica* **25**(2), 151-165.

Hardwick, R. N., Clarke, J. D., Lake, A. D., Canet, M. J., Anumol, T., Street, S. M., Merrell, M. D., Goedken, M. J., Snyder, S. A., and Cherrington, N. J. (2014). Increased

susceptibility to methotrexate-induced toxicity in nonalcoholic steatohepatitis. *Toxicol Sci* **142**(1), 45-55.

Harrill, A. H., Watkins, P. B., Su, S., Ross, P. K., Harbourt, D. E., Stylianou, I. M., Boorman, G. A., Russo, M. W., Sackler, R. S., Harris, S. C., *et al.* (2009). Mouse population-guided resequencing reveals that variants in CD44 contribute to acetaminophen-induced liver injury in humans. *Genome Res* **19**(9), 1507-15.

Hasenfuss, G. (1998). Animal models of human cardiovascular disease, heart failure and hypertrophy. *Cardiovasc Res* **39**(1), 60-76.

Helander, A., Vabo, E., Levin, K., and Borg, S. (1998). Intra- and interindividual variability of carbohydrate-deficient transferrin, gamma-glutamyltransferase, and mean corpuscular volume in teetotalers. *Clin Chem* **44**(10), 2120-5.

Hendriksen, P. J. M., Freidig, A. P., Jonker, D., Thissen, U., Bogaards, J. J. P., Mumtaz, M. M., Groten, J. P., and Stlerurn, R. H. (2007). Transcriptomics analysis of interactive effects of benzene, trichloroethylene and methyl mercury within binary and ternary mixtures on the liver and kidney following subchronic exposure in the rat. *Toxicol Appl Pharmacol* **225**(2), 171-188.

Herren-Freund, S. L., Pereira, M. A., Khoury, M. D., and Olson, G. (1987). The carcinogenicity of trichloroethylene and its metabolites, trichloroacetic acid and dichloroacetic acid, in mouse liver. *Toxicol Appl Pharmacol* **90**(2), 183-189.

Heuner, A., Dekant, W., Schwegler, J. S., and Silbernagl, S. (1991). Localization and capacity of the last step of mercapturic acid biosynthesis and the reabsorption and acetylation of cysteine S-conjugates in the rat kidney. *Pflugers Arch* **417**(5), 523-7.

Hinchman, C. A., and Ballatori, N. (1994). Glutathione Conjugation and Conversion to Mercapturic Acids Can Occur as an Intrahepatic Process. *J Toxicol Env Health* **41**(4), 387-409.

Hinchman, C. A., Matsumoto, H., Simmons, T. W., and Ballatori, N. (1991). Intrahepatic conversion of a glutathione conjugate to its mercapturic acid. Metabolism of 1-chloro-2,4-dinitrobenzene in isolated perfused rat and guinea pig livers. *J Biol Chem* **266**(33), 22179-85.

Hissink, E. M., Bogaards, J. J., Freidig, A. P., Commandeur, J. N., Vermeulen, N. P., and van Bladeren, P. J. (2002). The use of in vitro metabolic parameters and physiologically based pharmacokinetic (PBPK) modeling to explore the risk assessment of trichloroethylene. *Environ Toxicol Pharmacol* **11**(3-4), 259-71.

Hoeke, H., Roeder, S., Bertsche, T., Lehmann, I., Borte, M., von Bergen, M., and Wissenbach, D. K. (2015). Monitoring of drug intake during pregnancy by questionnaires

and LC-MS/MS drug urine screening: evaluation of both monitoring methods. *Drug Test Anal* **7**(8), 695-702.

Hoivik, D. J., Manautou, J. E., Tveit, A., Hart, S. G., Khairallah, E. A., and Cohen, S. D. (1995). Gender-related differences in susceptibility to acetaminophen-induced protein arylation and nephrotoxicity in the CD-1 mouse. *Toxicol Appl Pharmacol* **130**(2), 257-71.

Hu, J. J., Lee, M. J., Vapiwala, M., Reuhl, K., Thomas, P. E., and Yang, C. S. (1993). Sex-related differences in mouse renal metabolism and toxicity of acetaminophen. *Toxicol Appl Pharmacol* **122**(1), 16-26.

IARC (2014). IARC Monographs on the Evaluation of Carcinogenic Risks to Humans (Vol. 106): Trichloroethylene, Tetrachloroethylene and Some Other Chlorinated Agents **106**.

Inoue, M., Okajima, K., and Morino, Y. (1984). Hepato-renal cooperation in biotransformation, membrane transport, and elimination of cysteine S-conjugates of xenobiotics. *J Biochem* **95**(1), 247-54.

Inoue, M., Okajima, K., Nagase, S., and Morino, Y. (1987). Inter-organ metabolism and transport of a cysteine-S-conjugate of xenobiotics in normal and mutant analbuminemic rats. *Biochem Pharmacol* **36**(13), 2145-50.

Irving, R. M., and Elfarra, A. A. (2013). Mutagenicity of the cysteine S-conjugate sulfoxides of trichloroethylene and tetrachloroethylene in the Ames test. *Toxicology* **306C**, 157-161.

Irving, R. M., Pinkerton, M. E., and Elfarra, A. A. (2013). Characterization of the chemical reactivity and nephrotoxicity of N-acetyl-S-(1,2-dichlorovinyl)-L-cysteine sulfoxide, a potential reactive metabolite of trichloroethylene. *Toxicol Appl Pharmacol* **267**(1), 1-10.

Jamin, E. L., Bonvallot, N., Tremblay-Franco, M., Cravedi, J. P., Chevrier, C., Cordier, S., and Debrauwer, L. (2014). Untargeted profiling of pesticide metabolites by LC-HRMS: an exposomics tool for human exposure evaluation. *Anal Bioanal Chem* **406**(4), 1149-61.

Japanese Industrial Safety Association (1993). Carcinogenicity study of tetrachloroethylene by inhalation in rats and mice.

Jia, C., Yu, X., and Masiak, W. (2012). Blood/air distribution of volatile organic compounds (VOCs) in a nationally representative sample. *Sci Total Environ* **419**, 225-32.

Johnson, J. M., Yu, T., Strobel, F. H., and Jones, D. P. (2010). A practical approach to detect unique metabolic patterns for personalized medicine. *Analyst* **135**(11), 2864-70.

Kachapati, K., Adams, D., Bednar, K., and Ridgway, W. M. (2012). The non-obese diabetic (NOD) mouse as a model of human type 1 diabetes. *Methods Mol Biol* **933**, 3-16.

Khamis, M. M., Adamko, D. J., and El-Aneed, A. (2017). Mass spectrometric based approaches in urine metabolomics and biomarker discovery. *Mass Spectrom Rev* **36**(2), 115-134.

Kim, D., and Ghanayem, B. I. (2006). Comparative metabolism and disposition of trichloroethylene in Cyp2e1-/-and wild-type mice. *Drug Metab Dispos* **34**(12), 2020-7.

Kim, S., Collins, L. B., Boysen, G., Swenberg, J. A., Gold, A., Ball, L. M., Bradford, B. U., and Rusyn, I. (2009a). Liquid chromatography electrospray ionization tandem mass spectrometry analysis method for simultaneous detection of trichloroacetic acid, dichloroacetic acid, S-(1,2-dichlorovinyl)glutathione and S-(1,2-dichlorovinyl)-L-cysteine. *Toxicology* **262**(3), 230-8.

Kim, S., Kim, D., Pollack, G. M., Collins, L. B., and Rusyn, I. (2009b). Pharmacokinetic analysis of trichloroethylene metabolism in male B6C3F1 mice: Formation and disposition of trichloroacetic acid, dichloroacetic acid, S-(1,2-dichlorovinyl)glutathione and S-(1,2-dichlorovinyl)-L-cysteine. *Toxicol Appl Pharmacol* **238**(1), 90-9.

Kivisto, K. T., Neuvonen, P. J., and Klotz, U. (1994). Inhibition of terfenadine metabolism. Pharmacokinetic and pharmacodynamic consequences. *Clin Pharmacokinet* **27**(1), 1-5.

Konstandi, M., Cheng, J., and Gonzalez, F. J. (2013). Sex steroid hormones regulate constitutive expression of Cyp2e1 in female mouse liver. *Am J Physiol Endocrinol Metab* **304**(10), E1118-28.

Kostic, V., Jackson-Lewis, V., de Bilbao, F., Dubois-Dauphin, M., and Przedborski, S. (1997). Bcl-2: prolonging life in a transgenic mouse model of familial amyotrophic lateral sclerosis. *Science* **277**(5325), 559-62.

Krzysik, B. A., and Adibi, S. A. (1977). Cytoplasmic dipeptidase activities of kidney, ileum, jejunum, liver, muscle, and blood. *Am J Physiol* **233**(6), E450-6.

Kuhn, J. P., Meffert, P., Heske, C., Kromrey, M. L., Schmidt, C. O., Mensel, B., Volzke, H., Lerch, M. M., Hernando, D., Mayerle, J., *et al.* (2017). Prevalence of Fatty Liver Disease and Hepatic Iron Overload in a Northeastern German Population by Using Quantitative MR Imaging. *Radiology* **284**(3), 706-716.

Kyle, J. E., Zhang, X., Weitz, K. K., Monroe, M. E., Ibrahim, Y. M., Moore, R. J., Cha, J., Sun, X., Lovelace, E. S., Wagoner, J., *et al.* (2016). Uncovering biologically significant lipid isomers with liquid chromatography, ion mobility spectrometry and mass spectrometry. *Analyst* **141**(5), 1649-59.

Lamba, J. K., Lin, Y. S., Schuetz, E. G., and Thummel, K. E. (2002). Genetic contribution to variable human CYP3A-mediated metabolism. *Adv Drug Deliv Rev* **54**(10), 1271-94.

Lang, A. L., Chen, L., Poff, G. D., Ding, W. X., Barnett, R. A., Arteel, G. E., and Beier, J. I. (2018). Vinyl chloride dysregulates metabolic homeostasis and enhances diet-induced liver injury in mice. *Hepatol Commun* **2**(3), 270-284.

Langley, M., Ghosh, A., Charli, A., Sarkar, S., Ay, M., Luo, J., Zielonka, J., Brenza, T., Bennett, B., Jin, H., *et al.* (2017). Mito-Apocynin Prevents Mitochondrial Dysfunction, Microglial Activation, Oxidative Damage, and Progressive Neurodegeneration in MitoPark Transgenic Mice. *Antioxi Redox Sign* **27**(14), 1048-1066.

Larson, J. L., and Bull, R. J. (1992). Species differences in the metabolism of trichloroethylene to the carcinogenic metabolites trichloroacetate and dichloroacetate. *Toxicol Appl Pharmacol* **115**(2), 278-285.

Lash, L. H., Chiu, W. A., Guyton, K. Z., and Rusyn, I. (2014). Trichloroethylene biotransformation and its role in mutagenicity, carcinogenicity and target organ toxicity. *Mutat Res Rev Mutat Res* **762**, 22-36.

Lash, L. H., Fisher, J. W., Lipscomb, J. C., and Parker, J. C. (2000). Metabolism of trichloroethylene. *Environ Health Perspect* **108 Suppl 2**, 177-200.

Lash, L. H., Hueni, S. E., and Putt, D. A. (2001a). Apoptosis, necrosis, and cell proliferation induced by S-(1,2-dichlorovinyl)-L-cysteine in primary cultures of human proximal tubular cells. *Toxicol Appl Pharmacol* **177**(1), 1-16.

Lash, L. H., and Parker, J. C. (2001). Hepatic and renal toxicities associated with perchloroethylene. *Pharmacol Rev* **53**(2), 177-208.

Lash, L. H., Putt, D. A., Brashear, W. T., Abbas, R., Parker, J. C., and Fisher, J. W. (1999). Identification of S-(1,2-dichlorovinyl)glutathione in the blood of human volunteers exposed to trichloroethylene. *J Toxicol Environ Health A* **56**(1), 1-21.

Lash, L. H., Putt, D. A., Huang, P., Hueni, S. E., and Parker, J. C. (2007). Modulation of hepatic and renal metabolism and toxicity of trichloroethylene and perchloroethylene by alterations in status of cytochrome P450 and glutathione. *Toxicology* **235**(1-2), 11-26.

Lash, L. H., Putt, D. A., Hueni, S. E., Krause, R. J., and Elfarra, A. A. (2003). Roles of necrosis, Apoptosis, and mitochondrial dysfunction in S-(1,2-dichlorovinyl)-L-cysteine sulfoxide-induced cytotoxicity in primary cultures of human renal proximal tubular cells. *J Pharmacol Exp Ther* **305**(3), 1163-72.

Lash, L. H., Putt, D. A., and Parker, J. C. (2006). Metabolism and tissue distribution of orally administered trichloroethylene in male and female rats: identification of glutathione- and cytochrome P-450-derived metabolites in liver, kidney, blood, and urine. *J Toxicol Environ Health A* **69**(13), 1285-1309.

Lash, L. H., Qian, W., Putt, D. A., Desai, K., Elfarra, A. A., Sicuri, A. R., and Parker, J. C. (1998). Glutathione conjugation of perchloroethylene in rats and mice in vitro: sex-, species-, and tissue-dependent differences. *Toxicol Appl Pharmacol* **150**(1), 49-57.

Lash, L. H., Qian, W., Putt, D. A., Hueni, S. E., Elfarra, A. A., Krause, R. J., and Parker, J. C. (2001b). Renal and hepatic toxicity of trichloroethylene and its glutathione-derived metabolites in rats and mice: sex-, species-, and tissue-dependent differences. *J Pharmacol Exp Ther* **297**(1), 155-164.

Lash, L. H., Qian, W., Putt, D. A., Hueni, S. E., Elfarra, A. A., Sicuri, A. R., and Parker, J. C. (2002). Renal toxicity of perchloroethylene and S-(1,2,2-trichlorovinyl)glutathione in rats and mice: sex- and species-dependent differences. *Toxicol Appl Pharmacol* **179**(3), 163-71.

Lash, L. H., Sausen, P. J., Duescher, R. J., Cooley, A. J., and Elfarra, A. A. (1994). Roles of cysteine conjugate beta-lyase and S-oxidase in nephrotoxicity: studies with S-(1,2-dichlorovinyl)-L-cysteine and S-(1,2-dichlorovinyl)-L-cysteine sulfoxide. *J Pharmacol Exp Ther* **269**(1), 374-83.

Lau, J. K., Zhang, X., and Yu, J. (2017). Animal models of non-alcoholic fatty liver disease: current perspectives and recent advances. *J Pathol* **241**(1), 36-44.

Laughter, A. R., Dunn, C. S., Swanson, C. L., Howroyd, P., Cattley, R. C., and Corton, J. C. (2004). Role of the peroxisome proliferator-activated receptor alpha (PPARalpha) in responses to trichloroethylene and metabolites, trichloroacetate and dichloroacetate in mouse liver. *Toxicology* **203**(1-3), 83-98.

Lee, K. M., Bruckner, J. V., Muralidhara, S., and Gallo, J. M. (1996). Characterization of presystemic elimination of trichloroethylene and its nonlinear kinetics in rats. *Toxicol Appl Pharmacol* **139**(2), 262-71.

Lee, K. M., Muralidhara, S., White, C. A., and Bruckner, J. V. (2000). Mechanisms of the dose-dependent kinetics of trichloroethylene: oral bolus dosing of rats. *Toxicol Appl Pharmacol* **164**(1), 55-64.

Leissring, M. A., Farris, W., Chang, A. Y., Walsh, D. M., Wu, X., Sun, X., Frosch, M. P., and Selkoe, D. J. (2003). Enhanced proteolysis of beta-amyloid in APP transgenic mice prevents plaque formation, secondary pathology, and premature death. *Neuron* **40**(6), 1087-93.

Liesivuori, J., Kosma, V. M., Naukkarinen, A., and Savolainen, H. (1987). Kinetics and toxic effects of repeated intravenous dosage of formic acid in rabbits. *Br J Exp Pathol* **68**(6), 853-61.

Lin, J. H., and Lu, A. Y. (2001). Interindividual variability in inhibition and induction of cytochrome P450 enzymes. *Annu Rev Pharmacol Toxicol* **41**, 535-67.

Liu, C. H., Chang, S. H., Narko, K., Trifan, O. C., Wu, M. T., Smith, E., Haudenschild, C., Lane, T. F., and Hla, T. (2001). Overexpression of cyclooxygenase-2 is sufficient to induce tumorigenesis in transgenic mice. *J Biol Chem* **276**(21), 18563-18569.

Lock, E. A., Keane, P., Rowe, P. H., Foster, J. R., Antoine, D., and Morris, C. M. (2017). Trichloroethylene-induced formic aciduria in the male C57 Bl/6 mouse. *Toxicology* **378**, 76-85.

Loizou, G. D. (2001). The application of physiologically based pharmacokinetic modelling in the analysis of occupational exposure to perchloroethylene. *Toxicology letters* **124**(1-3), 59-69.

Lovati, A. B., Drago, L., Monti, L., De Vecchi, E., Previdi, S., Banfi, G., and Romano, C. L. (2013). Diabetic mouse model of orthopaedic implant-related Staphylococcus aureus infection. *PloS one* **8**(6), e67628.

Love, M. I., Huber, W., and Anders, S. (2014). Moderated estimation of fold change and dispersion for RNA-seq data with DESeq2. *Genome Biol* **15**(12), 550.

Lu, Y., Wu, D., Wang, X., Ward, S. C., and Cederbaum, A. I. (2010). Chronic alcohol-induced liver injury and oxidant stress are decreased in cytochrome P4502E1 knockout mice and restored in humanized cytochrome P4502E1 knock-in mice. *Free radical biology & medicine* **49**(9), 1406-16.

Luo, Y. S., Cichocki, J. A., McDonald, T. J., and Rusyn, I. (2017). Simultaneous detection of the tetrachloroethylene metabolites S-(1,2,2-trichlorovinyl) glutathione, S-(1,2,2-trichlorovinyl)-L-cysteine, and N-acetyl-S-(1,2,2-trichlorovinyl)-L-cysteine in multiple mouse tissues via ultra-high performance liquid chromatography electrospray ionization tandem mass spectrometry. *J Toxicol Environ Health A* **80**(9), 513-524.

Luo, Y. S., Furuya, S., Chiu, W., and Rusyn, I. (2018a). Characterization of inter-tissue and inter-strain variability of TCE glutathione conjugation metabolites DCVG, DCVC, and NAcDCVC in the mouse. *J Toxicol Environ Health A* **81**(1-3), 37-52.

Luo, Y. S., Furuya, S., Soldatov, V. Y., Kosyk, O., Yoo, H. S., Fukushima, H., Lewis, L., Iwata, Y., and Rusyn, I. (2018b). Metabolism and Toxicity of Trichloroethylene and Tetrachloroethylene in Cytochrome P450 2E1 Knockout and Humanized Transgenic Mice. *Toxicol Sci* **in press**.

Luo, Y. S., Hsieh, N. H., Soldatow, V. Y., Chiu, W. A., and Rusyn, I. (2018). Comparative analysis of metabolism of trichloroethylene and tetrachloroethylene among tissues and mouse strains. *Toxicology* **In review**

Machado, M. V., Michelotti, G. A., Xie, G., Almeida Pereira, T., Boursier, J., Bohnic, B., Guy, C. D., and Diehl, A. M. (2015). Mouse models of diet-induced nonalcoholic

steatohepatitis reproduce the heterogeneity of the human disease. *PloS one* **10**(5), e0127991.

Madan, A., Parkinson, A., and Faiman, M. D. (1995). Identification of the human and rat P450 enzymes responsible for the sulfoxidation of S-methyl N,N-diethylthiolcarbamate (DETC-ME). The terminal step in the bioactivation of disulfiram. *Drug Metab Dispos* **23**(10), 1153-62.

Madan, A., Parkinson, A., and Faiman, M. D. (1998). Identification of the human P-450 enzymes responsible for the sulfoxidation and thiono-oxidation of diethyldithiocarbamate methyl ester: role of P-450 enzymes in disulfiram bioactivation. *Alcohol Clin Exp Res* **22**(6), 1212-9.

Maher, J. J. (2011). New insights from rodent models of fatty liver disease. *Antioxid Redox Sign* **15**(2), 535-50.

Maitre, L., Lau, C. H. E., Vizcaino, E., Robinson, O., Casas, M., Siskos, A. P., Want, E. J., Athersuch, T., Slama, R., Vrijheid, M., *et al.* (2017). Assessment of metabolic phenotypic variability in children's urine using H-1 NMR spectroscopy. *Sci Rep-Uk* **7**.

Mallipattu, S. K., Gallagher, E. J., LeRoith, D., Liu, R., Mehrotra, A., Horne, S. J., Chuang, P. Y., Yang, V. W., and He, J. C. (2014). Diabetic nephropathy in a nonobese mouse model of type 2 diabetes mellitus. *Am J Physiol-Renal* **306**(9), F1008-17.

Maloney, E. K., and Waxman, D. J. (1999). Trans-activation of PPARalpha and PPARgamma by structurally diverse environmental chemicals. *Toxicol Appl Pharmacol* **161**(2), 209-218.

Matuszewski, B. K., Constanzer, M. L., and Chavez-Eng, C. M. (2003). Strategies for the assessment of matrix effect in quantitative bioanalytical methods based on HPLC-MS/MS. *Anal Chem* **75**(13), 3019-30.

Mccarthy, R. I., Lock, E. A., and Hawksworth, G. M. (1994). Cytosolic C-S Lyase Activity in Human Kidney Samples - Relevance for the Nephrotoxicity of Halogenated Alkenes in Man. *Toxicol Ind Health* **10**(1-2), 103-112.

Metz, T. O., Baker, E. S., Schymanski, E. L., Renslow, R. S., Thomas, D. G., Causon, T. J., Webb, I. K., Hann, S., Smith, R. D., and Teeguarden, J. G. (2017). Integrating ion mobility spectrometry into mass spectrometry-based exposome measurements: what can it add and how far can it go? *Bioanalysis* **9**(1), 81-98.

Monster, A. C., Boersma, G., and Duba, W. C. (1976). Pharmacokinetics of trichloroethylene in volunteers, influence of workload and exposure concentration. *Int Arch Occup Environ Health* **38**(2), 87-102.

Monster, A. C., and Houtkooper, J. M. (1979). Estimation of individual uptake of trichloroethylene, 1,1,1-trichloroethane and tetrachloroethylene from biological parameters. *Int Arch Occup Environ Health* **42**(3-4), 319-23.

Moore, L. E., Boffetta, P., Karami, S., Brennan, P., Stewart, P. S., Hung, R., Zaridze, D., Matveev, V., Janout, V., Kollarova, H., *et al.* (2010). Occupational trichloroethylene exposure and renal carcinoma risk: evidence of genetic susceptibility by reductive metabolism gene variants. *Cancer Res* **70**(16), 6527-36.

Moron, M. S., Depierre, J. W., and Mannervik, B. (1979). Levels of glutathione, glutathione reductase and glutathione S-transferase activities in rat lung and liver. *Biochim Biophys Acta* **582**(1), 67-78.

Musso, G., Cassader, M., Cohney, S., Pinach, S., Saba, F., and Gambino, R. (2015). Emerging Liver-Kidney Interactions in Nonalcoholic Fatty Liver Disease. *Trends Mol Med* **21**(10), 645-662.

Musso, G., Gambino, R., Tabibian, J. H., Ekstedt, M., Kechagias, S., Hamaguchi, M., Hultcrantz, R., Hagstrom, H., Yoon, S. K., Charatcharoenwitthaya, P., *et al.* (2014). Association of non-alcoholic fatty liver disease with chronic kidney disease: a systematic review and meta-analysis. *PLoS Med* **11**(7), e1001680.

Nakajima, T., Kamijo, Y., Usuda, N., Liang, Y., Fukushima, Y., Kametani, K., Gonzalez, F. J., and Aoyama, T. (2000). Sex-dependent regulation of hepatic peroxisome proliferation in mice by trichloroethylene via peroxisome proliferator-activated receptor alpha (PPARalpha). *Carcinogenesis* **21**(4), 677-82.

Nakajima, T., Wang, R. S., Elovaara, E., Park, S. S., Gelboin, H. V., and Vainio, H. (1993). Cytochrome P450-related differences between rats and mice in the metabolism of benzene, toluene and trichloroethylene in liver microsomes. *Biochem Pharmacol* **45**(5), 1079-85.

Narotsky, M. G., Weller, E. A., Chinchilli, V. M., and Kavlock, R. J. (1995). Nonadditive developmental toxicity in mixtures of trichloroethylene, Di(2-ethylhexyl) phthalate, and heptachlor in a 5 x 5 x 5 design. *Fundam Appl Toxicol* **27**(2), 203-16.

National Research Council (2010). *Review of the Environmental Protection Agency's Draft IRIS Assessment of Tetrachloroethylene*. The National Academies Press, Washington, DC.

National Research Council (2009). *Science and Decisions: Advancing Risk Assessment*. National Academies Press, Washington, DC.

National Toxicology Program (1977). Bioassay of tetrachloroethylene for possible carcinogenicity. *Natl Cancer Inst Carcinog Tech Rep Ser* **13**, 1-83.

National Toxicology Program (1990). Carcinogenesis Studies of Trichloroethylene (Without Epichlorohydrin) (CAS No. 79-01-6) in F344/N Rats and B6C3F1 Mice (Gavage Studies). *Natl Toxicol Program Tech Rep Ser* **243**, 1-174.

National Toxicology Program (1986). NTP Toxicology and Carcinogenesis Studies of Tetrachloroethylene (Perchloroethylene) (CAS No. 127-18-4) in F344/N Rats and B6C3F1 Mice (Inhalation Studies). *Natl Toxicol Program Tech Rep Ser* **311**, 1-197.

NTP (2015). Report on Carcinogens: Monograph on Trichloroethylene In (P. H. S. US Department of Health and Human Services, Ed.), Research Triangle Park, NC.

Penaloza, C. G., Estevez, B., Han, D. M., Norouzi, M., Lockshin, R. A., and Zakeri, Z. (2014). Sex-dependent regulation of cytochrome P450 family members Cyp1a1, Cyp2e1, and Cyp7b1 by methylation of DNA. *FASEB J* **28**(2), 966-77.

Pessayre, D., Cobert, B., Descatoire, V., Degott, C., Babany, G., Funck-Brentano, C., Delaforge, M., and Larrey, D. (1982). Hepatotoxicity of trichloroethylene-carbon tetrachloride mixtures in rats. A possible consequence of the potentiation by trichloroethylene of carbon tetrachloride-induced lipid peroxidation and liver lesions. *Gastroenterology* **83**(4), 761-72.

Philip, B. K., Mumtaz, M. M., Latendresse, J. R., and Mehendale, H. M. (2007). Impact of repeated exposure on toxicity of perchloroethylene in Swiss Webster mice. *Toxicology* **232**(1-2), 1-14.

Pogribny, I. P., James, S. J., Jernigan, S., and Pogribna, M. (2004). Genomic hypomethylation is specific for preneoplastic liver in folate/methyl deficient rats and does not occur in non-target tissues. *Mutat Res* **548**(1-2), 53-9.

Porta, E. A., Markell, N., and Dorado, R. D. (1985). Chronic alcoholism enhances hepatocarcinogenicity of diethylnitrosamine in rats fed a marginally methyl-deficient diet. *Hepatology* **5**(6), 1120-5.

Poyer, S., Lopin-Bon, C., Jacquinet, J. C., Salpin, J. Y., and Daniel, R. (2017). Isomer separation and effect of the degree of polymerization on the gas-phase structure of chondroitin sulfate oligosaccharides analyzed by ion mobility and tandem mass spectrometry. *Rapid Commun Mass Spectrom* **31**(23), 2003-2010.

Rakhshandehroo, M., Knoch, B., Muller, M., and Kersten, S. (2010). Peroxisome proliferator-activated receptor alpha target genes. *PPAR Res* **2010**.

Ramdhan, D. H., Kamijima, M., Yamada, N., Ito, Y., Yanagiba, Y., Nakamura, D., Okamura, A., Ichihara, G., Aoyama, T., Gonzalez, F. J., *et al.* (2008). Molecular mechanism of trichloroethylene-induced hepatotoxicity mediated by CYP2E1. *Toxicol Appl Pharmacol* **231**(3), 300-307.

Ramdhan, D. H., Komijima, M., Wang, D., Ito, Y., Naito, H., Yanagiba, Y., Hayashi, Y., Tanaka, N., Aoyama, T., Gonzalez, F. J., *et al.* (2010). Differential response to trichloroethylene-induced hepatosteatosis in wild-type and PPARa-humanized Mice. *Environ Health Perspect.* **118**(11), 1557-1563.

Reitz, R. H., Gargas, M. L., Mendrala, A. L., and Schumann, A. M. (1996). In vivo and in vitro studies of perchloroethylene metabolism for physiologically based pharmacokinetic modeling in rats, mice, and humans. *Toxicol Appl Pharmacol* **136**(2), 289-306.

Reno, F. E., Normand, P., McInally, K., Silo, S., Stotland, P., Triest, M., Carballo, D., and Piche, C. (2015). A novel nasal powder formulation of glucagon: toxicology studies in animal models. *Bmc Pharmacol Toxico* **16**.

Rinella, M. E., and Green, R. M. (2004). The methionine-choline deficient dietary model of steatohepatitis does not exhibit insulin resistance. *J Hepatol* **40**(1), 47-51.

Ripp, S. L., Overby, L. H., Philpot, R. M., and Elfarra, A. A. (1997). Oxidation of cysteine S-conjugates by rabbit liver microsomes and cDNA-expressed flavin-containing mono-oxygenases: studies with S-(1,2-dichlorovinyl)-L-cysteine, S-(1,2,2-trichlorovinyl)-L-cysteine, S-allyl-L-cysteine, and S-benzyl-L-cysteine. *Mol Pharmacol* **51**(3), 507-15.

Ripps, M. E., Huntley, G. W., Hof, P. R., Morrison, J. H., and Gordon, J. W. (1995). Transgenic mice expressing an altered murine superoxide dismutase gene provide an animal model of amyotrophic lateral sclerosis. *Proc Natl Acad Sci U S A* **92**(3), 689-93.

Rivkin, M., Simerzin, A., Zorde-Khvalevsky, E., Chai, C., Yuval, J. B., Rosenberg, N., Harari-Steinfeld, R., Schneider, R., Amir, G., Condiotti, R., *et al.* (2016). Inflammation-Induced Expression and Secretion of MicroRNA 122 Leads to Reduced Blood Levels of Kidney-Derived Erythropoietin and Anemia. *Gastroenterology* **151**(5), 999-1010 e3.

Roberti, M. F., Perazzo, J. C., and Monserrat, A. J. (1988). Effects of unilateral ureteric occlusion on renal necrosis occurring in rats fed a methyl-deficient diet. *Br J Exp Pathol* **69**(4), 449-56.

Rusyn, I., Chiu, W. A., Lash, L. H., Kromhout, H., Hansen, J., and Guyton, K. Z. (2014). Trichloroethylene: Mechanistic, epidemiologic and other supporting evidence of carcinogenic hazard. *Pharmacol Therapeut* **141**(1), 55-68.

Sausen, P. J., and Elfarra, A. A. (1990). Cysteine conjugate S-oxidase. Characterization of a novel enzymatic activity in rat hepatic and renal microsomes. *J Biol Chem* **265**(11), 6139-45.

Sbrana, I., Di Sibio, A., Lomi, A., and Scarcelli, V. (1993). C-mitosis and numerical chromosome aberration analyses in human lymphocytes: 10 known or suspected spindle poisons. *Mutat Res* **287**(1), 57-70.

Schaeffer, V. H., and Stevens, J. L. (1987). The transport of S-cysteine conjugates in LLC-PK1 cells and its role in toxicity. *Mol Pharmacol* **31**(5), 506-12.

Schumann, A. M., Quast, J. F., and Watanabe, P. G. (1980). The pharmacokinetics and macromolecular interactions of perchloroethylene in mice and rats as related to oncogenicity. *Toxicol Appl Pharmacol* **55**(2), 207-19.

Shirai, N., Ohtsuji, M., Hagiwara, K., Tomisawa, H., Ohtsuji, N., Hirose, S., and Hagiwara, H. (2012). Nephrotoxic effect of subchronic exposure to S-(1,2-dichlorovinyl)-L-cysteine in mice. *J Toxicol Sci* **37**(5), 871-8.

Shirasaka, Y., Chaudhry, A. S., McDonald, M., Prasad, B., Wong, T., Calamia, J. C., Fohner, A., Thornton, T. A., Isoherranen, N., Unadkat, J. D., *et al.* (2016). Interindividual variability of CYP2C19-catalyzed drug metabolism due to differences in gene diplotypes and cytochrome P450 oxidoreductase content. *Pharmacogenomics J* **16**(4), 375-387.

Slone, D. H., Gallagher, E. P., Ramsdell, H. S., Rettie, A. E., Stapleton, P. L., Berlad, L. G., and Eaton, D. L. (1995). Human variability in hepatic glutathione S-transferase-mediated conjugation of aflatoxin B1-epoxide and other substrates. *Pharmacogenetics* **5**(4), 224-33.

Soltow, Q. A., Strobel, F. H., Mansfield, K. G., Wachtman, L., Park, Y., and Jones, D. P. (2013). High-performance metabolic profiling with dual chromatography-Fourier-transform mass spectrometry (DC-FTMS) for study of the exposome. *Metabolomics : Official journal of the Metabolomic Society* **9**(1 Suppl), S132-S143.

Song, J. Z., and Ho, J. W. (2003). Simultaneous detection of trichloroethylene alcohol and acetate in rat urine by gas chromatography-mass spectrometry. *J Chromatogr B Analyt Technol Biomed Life Sci* **789**(2), 303-9.

Spearow, J. L., Gettmann, K., and Wade, M. (2017). Review: Risk assessment implications of variation in susceptibility to perchloroethylene due to genetic diversity, ethnicity, age, gender, diet and pharmaceuticals. *Hum Ecol Risk Assess* **23**(6), 1466-1492.

Stclair, M. B. G., Amarnath, V., Moody, M. A., Anthony, D. C., Anderson, C. W., and Graham, D. G. (1988). Pyrrole Oxidation and Protein Cross-Linking as Necessary Steps in the Development of Gamma-Diketone Neuropathy. *Chem Res Toxicol* **1**(3), 179-185.

Stenner, R. D., Merdink, J. L., Fisher, J. W., and Bull, R. J. (1998). Physiologically-based pharmacokinetic model for trichloroethylene considering enterohepatic recirculation of major metabolites. *Risk Anal* **18**(3), 261-9.

Stenner, R. D., Merdink, J. L., Stevens, D. K., Springer, D. L., and Bull, R. J. (1997). Enterohepatic recirculation of trichloroethanol glucuronide as a significant source of trichloroacetic acid - Metabolites of trichloroethylene. *Drug Metab Dispos* **25**(5), 529-535.

Stormer, E., Roots, I., and Brockmoller, J. (2000). Benzydamine N-oxidation as an index reaction reflecting FMO activity in human liver microsomes and impact of FMO3 polymorphisms on enzyme activity. *Br J Clin Pharmacol* **50**(6), 553-561.

Teufel, A., Itzel, T., Erhart, W., Brosch, M., Wang, X. Y., Kim, Y. O., von Schonfels, W., Herrmann, A., Bruckner, S., Stickel, F., *et al.* (2016). Comparison of Gene Expression Patterns Between Mouse Models of Nonalcoholic Fatty Liver Disease and Liver Tissues From Patients. *Gastroenterology* **151**(3), 513-525 e0.

Threadgill, D. W., and Churchill, G. A. (2012). Ten years of the Collaborative Cross. *Genetics* **190**(2), 291-4.

Thummel, K. E., and Lin, Y. S. (2014). Sources of interindividual variability. *Methods Mol Biol* **1113**, 363-415.

Tracy, T. S., Chaudhry, A. S., Prasad, B., Thummel, K. E., Schuetz, E. G., Zhong, X. B., Tien, Y. C., Jeong, H., Pan, X., Shireman, L. M., *et al.* (2016). Interindividual Variability in Cytochrome P450-Mediated Drug Metabolism. *Drug Metab Dispos* **44**(3), 343-51.

Tryndyak, V., de Conti, A., Kobets, T., Kutanzi, K., Koturbash, I., Han, T., Fuscoe, J. C., Latendresse, J. R., Melnyk, S., Shymonyak, S., *et al.* (2012a). Interstrain differences in the severity of liver injury induced by a choline- and folate-deficient diet in mice are associated with dysregulation of genes involved in lipid metabolism. *FASEB J* **26**(11), 4592-602.

Tryndyak, V. P., Latendresse, J. R., Montgomery, B., Ross, S. A., Beland, F. A., Rusyn, I., and Pogribny, I. P. (2012b). Plasma microRNAs are sensitive indicators of inter-strain differences in the severity of liver injury induced in mice by a choline- and folate-deficient diet. *Toxicol Appl Pharmacol* **262**(1), 52-9.

U.S. EPA (2017). *EPA Names First Chemicals for Review Under New TSCA Legislation.* Available at: https://www.epa.gov/newsreleases/epa-names-first-chemicals-review-under-new-tsca-legislation. Accessed May 19, 2017.

U.S. EPA (2011a). Toxicological Review of Dichloromethane (Methylene Chloride) (CAS No. 75-09-2): In Support of Summary Information on the Integrated Risk Information System (IRIS).

U.S. EPA (2011b). Toxicological Review of Tetrachloroethylene (CAS No. 127-18-4): In Support of Summary Information on the Integrated Risk Information System (IRIS). In (U.S. Environmental Protection Agency, Washington, DC.

U.S. EPA (2011c). Toxicological Review of Trichloroethylene (CAS No. 79-01-6): In Support of Summary Information on the Integrated Risk Information System (IRIS).

Uno, S., Nebert, D. W., and Makishima, M. (2018). Cytochrome P450 1A1 (CYP1A1) protects against nonalcoholic fatty liver disease caused by Western diet containing benzo[a]pyrene in mice. *Food Chem Toxicol* **113**, 73-82.

USEPA (2000). Guidance for data quality assessment: Practical methods for data analysis .Washington, DC.

USEPA (2018). TRI Explorer (2016 Dataset (released March 2018)) [Internet database]. U.S. Environmental Protection Agency.

Uttamsingh, V., Keller, D. A., and Anders, M. W. (1998). Acylase I-catalyzed deacetylation of N-acetyl-L-cysteine and S-alkyl-N-acetyl-L-cysteines. *Chemical research in toxicology* **11**(7), 800-9.

Vaidya, V. S., Ferguson, M. A., and Bonventre, J. V. (2008). Biomarkers of acute kidney injury. *Annu Rev Pharmacol Toxicol* **48**, 463-93.

Vaidya, V. S., Shankar, K., Lock, E. A., Bucci, T. J., and Mehendale, H. M. (2003). Renal injury and repair following S-1, 2 dichlorovinyl-L-cysteine administration to mice. *Toxicol Appl Pharmacol* **188**(2), 110-21.

Vamvakas, S., Dekant, W., and Henschler, D. (1989a). Assessment of unscheduled DNA synthesis in a cultured line of renal epithelial cells exposed to cysteine S-conjugates of haloalkenes and haloalkanes. *Mutat Res* **222**(4), 329-35.

Vamvakas, S., Elfarra, A. A., Dekant, W., Henschler, D., and Anders, M. W. (1988). Mutagenicity of amino acid and glutathione S-conjugates in the Ames test. *Mutat Res* **206**(1), 83-90.

Vamvakas, S., Herkenhoff, M., Dekant, W., and Henschler, D. (1989b). Mutagenicity of tetrachloroethene in the Ames test--metabolic activation by conjugation with glutathione. *J Biochem Toxicol* **4**(1), 21-7.

Venkatratnam, A., Furuya, S., Kosyk, O., Gold, A., Bodnar, W., Konganti, K., Threadgill, D. W., Gillespie, K. M., Aylor, D. L., Wright, F. A., *et al.* (2017). Collaborative Cross Mouse Population Enables Refinements to Characterization of the Variability in Toxicokinetics of Trichloroethylene and Provides Genetic Evidence for the Role of PPAR Pathway in Its Oxidative Metabolism. *Toxicol Sci* **158**(1), 48-62.

Venkatratnam, A., House, J. S., Konganti, K., McKenney, C., Threadgill, D. W., Chiu, W. A., Aylor, D. L., Wright, F. A., and Rusyn, I. (2018). Population-based dose-response analysis of liver transcriptional response to trichloroethylene in mouse. *Mamm Genome* **29**(1-2), 168-181.

Volkel, W., and Dekant, W. (1998). Chlorothioketene, the ultimate reactive intermediate formed by cysteine conjugate beta-lyase-mediated cleavage of the trichloroethene

metabolite S-(1,2-Dichlorovinyl)-L-cysteine, forms cytosine adducts in organic solvents, but not in aqueous solution. *Chem Res Toxicol* **11**(9), 1082-8.

Volkel, W., Friedewald, M., Lederer, E., Pahler, A., Parker, J., and Dekant, W. (1998). Biotransformation of perchloroethene: dose-dependent excretion of trichloroacetic acid, dichloroacetic acid, and N-acetyl-S-(trichlorovinyl)-L-cysteine in rats and humans after inhalation. *Toxicol Appl Pharmacol* **153**(1), 20-7.

Volkel, W., Pahler, A., and Dekant, W. (1999). Gas chromatography-negative ion chemical ionization mass spectrometry as a powerful tool for the detection of mercapturic acids and DNA and protein adducts as biomarkers of exposure to halogenated olefins. *J Chromatogr A* **847**(1-2), 35-46.

Werner, M., Birner, G., and Dekant, W. (1996). Sulfoxidation of mercapturic acids derived from tri- and tetrachloroethene by cytochromes P450 3A: A bioactivation reaction in addition to deacetylation and cysteine conjugate beta-lyase mediated cleavage. *Chem Res Toxicol* **9**(1), 41-49.

White, I. N., and De Matteis, F. (2001). The role of CYP forms in the metabolism and metabolic activation of HCFCs and other halocarbons. *Toxicol Lett* **124**(1-3), 121-8.

Whitfield, J. B. (2001). Gamma glutamyl transferase. *Crit Rev Clin Lab Sci* **38**(4), 263-355.

WHO/IPCS (2005). Chemical-specific adjustment factors for interspecies differences in human variability: Guidance document for use of data in dose/concentration-response assessment.

Wijma, R. A., Koch, B. C. P., van Gelder, T., and Mouton, J. W. (2018). High interindividual variability in urinary fosfomycin concentrations in healthy female volunteers. *Clin Microbiol Infect* **24**(5), 528-532.

Wild, C. P. (2005). Complementing the genome with an "exposome": the outstanding challenge of environmental exposure measurement in molecular epidemiology. *Cancer Epidem Biomar* **14**(8), 1847-50.

Williams, J. P., Bugarcic, T., Habtemariam, A., Giles, K., Campuzano, I., Rodger, P. M., and Sadler, P. J. (2009). Isomer separation and gas-phase configurations of organoruthenium anticancer complexes: ion mobility mass spectrometry and modeling. *J Am Soc Mass Spectrom* **20**(6), 1119-22.

Wishart, D. S., Knox, C., Guo, A. C., Eisner, R., Young, N., Gautam, B., Hau, D. D., Psychogios, N., Dong, E., Bouatra, S., *et al.* (2009). HMDB: a knowledgebase for the human metabolome. *Nucleic Acids Res* **37**(Database issue), D603-10.

Wu, C., and Schaum, J. (2000). Exposure assessment of trichloroethylene. *Environ Health Perspect.* **108 Suppl 2**, 359-363.

Yaqoob, N., Evans, A., Foster, J. R., and Lock, E. A. (2014). Trichloroethylene and trichloroethanol-induced formic aciduria and renal injury in male F-344 rats following 12 weeks exposure. *Toxicology* **323**, 70-7.

Yaqoob, N., Evans, A. R., and Lock, E. A. (2013). Trichloroethylene-induced formic aciduria: effect of dose, sex and strain of rat. *Toxicology* **304**, 49-56.

Yoo, H. S., Bradford, B. U., Kosyk, O., Shymonyak, S., Uehara, T., Collins, L. B., Bodnar, W. M., Ball, L. M., Gold, A., and Rusyn, I. (2015a). Comparative analysis of the relationship between trichloroethylene metabolism and tissue-specific toxicity among inbred mouse strains: liver effects. *J Toxicol Environ Health A* **78**(1), 15-31.

Yoo, H. S., Bradford, B. U., Kosyk, O., Uehara, T., Shymonyak, S., Collins, L. B., Bodnar, W. M., Ball, L. M., Gold, A., and Rusyn, I. (2015b). Comparative analysis of the relationship between trichloroethylene metabolism and tissue-specific toxicity among inbred mouse strains: kidney effects. *J Toxicol Environ Health A* **78**(1), 32-49.

Yoo, H. S., Cichocki, J. A., Kim, S., Venkatratnam, A., Iwata, Y., Kosyk, O., Bodnar, W., Sweet, S., Knap, A., Wade, T., *et al.* (2015c). The Contribution of Peroxisome Proliferator-Activated Receptor Alpha to the Relationship Between Toxicokinetics and Toxicodynamics of Trichloroethylene. *Toxicol Sci* **147**(2), 339-49.

Younossi, Z. M., Blissett, D., Blissett, R., Henry, L., Stepanova, M., Younossi, Y., Racila, A., Hunt, S., and Beckerman, R. (2016a). The economic and clinical burden of nonalcoholic fatty liver disease in the United States and Europe. *Hepatology* **64**(5), 1577-1586.

Younossi, Z. M., Koenig, A. B., Abdelatif, D., Fazel, Y., Henry, L., and Wymer, M. (2016b). Global epidemiology of nonalcoholic fatty liver disease-Meta-analytic assessment of prevalence, incidence, and outcomes. *Hepatology* **64**(1), 73-84.

Yue, F., Cheng, Y., Breschi, A., Vierstra, J., Wu, W., Ryba, T., Sandstrom, R., Ma, Z., Davis, C., Pope, B. D., *et al.* (2014). A comparative encyclopedia of DNA elements in the mouse genome. *Nature* **515**(7527), 355-64.

Zeise, L., Bois, F. Y., Chiu, W. A., Hattis, D., Rusyn, I., and Guyton, K. Z. (2013). Addressing human variability in next-generation human health risk assessments of environmental chemicals. *Environ Health Perspect* **121**(1), 23-31.

Zelber-Sagi, S., Nitzan-Kaluski, D., Halpern, Z., and Oren, R. (2006). Prevalence of primary non-alcoholic fatty liver disease in a population-based study and its association with biochemical and anthropometric measures. *Liver Int* **26**(7), 856-63.

Zheng, X., Zhang, X., Schocker, N. S., Renslow, R. S., Orton, D. J., Khamsi, J., Ashmus, R. A., Almeida, I. C., Tang, K., Costello, C. E., *et al.* (2017a). Enhancing glycan isomer

separations with metal ions and positive and negative polarity ion mobility spectrometry-mass spectrometry analyses. *Anal Bioanal Chem* **409**(2), 467-476.

Zheng, X. Y., Aly, N. A., Zhou, Y. X., Dupuis, K. T., Bilbao, A., Paurus, V. L., Orton, D. J., Wilson, R., Payne, S. H., Smith, R. D., *et al.* (2017b). A structural examination and collision cross section database for over 500 metabolites and xenobiotics using drift tube ion mobility spectrometry. *Chem Sci* **8**(11), 7724-7736.

Zhou, Y. C., and Waxman, D. J. (1998). Activation of peroxisome proliferator-activated receptors by chlorinated hydrocarbons and endogenous steroids. *Environ Health Perspect.* **106 Suppl 4**, 983-988.

Zhou, Y. H., Cichocki, J. A., Soldatow, V. Y., Scholl, E. H., Gallins, P. J., Jima, D., Yoo, H. S., Chiu, W. A., Wright, F. A., and Rusyn, I. (2017). Comparative Dose-Response Analysis of Liver and Kidney Transcriptomic Effects of Trichloroethylene and Tetrachloroethylene in B6C3F1 Mouse. *Toxicol Sci* **160**(1), 95-110.

APPENDIX A

FIGURES

Figure A-1 Purity of the standards used in this study. Purity of TCVC (A), TCVC* (B), TCVG (C), TCVG* (D), and NAcTCVC* (E) was determined using HPLC-UV/Vis detection in a full scan mode for the wavelength range from 190 to 600 nm (left image in each panel) followed by a detection at the wavelength set at 254 nm (right image in each panel).

A: TCVC

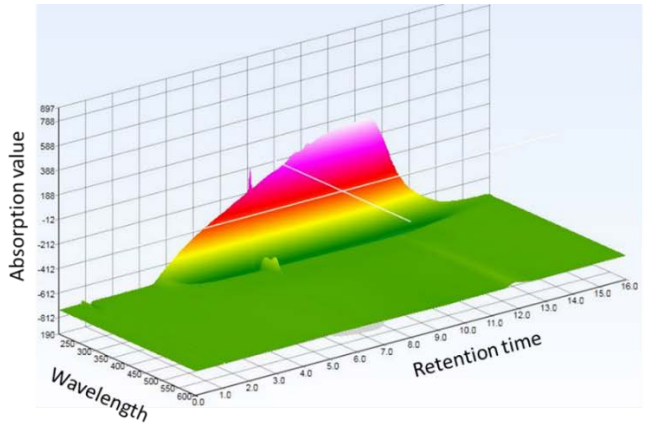

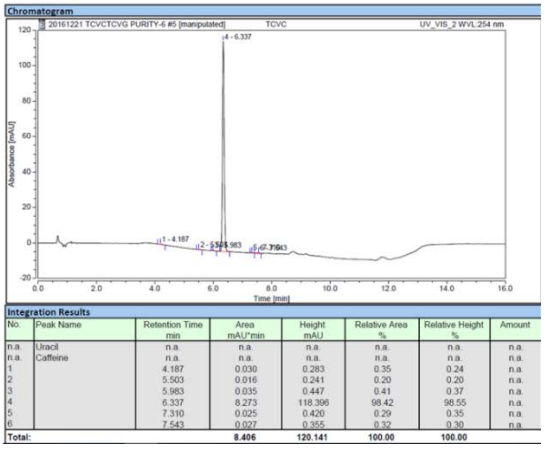

Integration Results

No.	Peak Name	Retention Time min	Area mAU*min	Height mAU	Relative Area %	Relative Height %	Amount
n.a.	Uracil	n.a.	n.a.	n.a.	n.a.	n.a.	n.a.
n.a.	Caffeine	n.a.	n.a.	n.a.	n.a.	n.a.	n.a.
1		4.187	0.030	0.283	0.35	0.24	n.a.
2		5.503	0.016	0.241	0.20	0.20	n.a.
3		5.983	0.035	0.447	0.41	0.37	n.a.
4		6.337	8.273	118.396	98.42	98.55	n.a.
5		7.310	0.025	0.420	0.29	0.35	n.a.
6		7.543	0.027	0.355	0.32	0.30	n.a.
Total:			8.406	120.141	100.00	100.00	

B: TCVC*

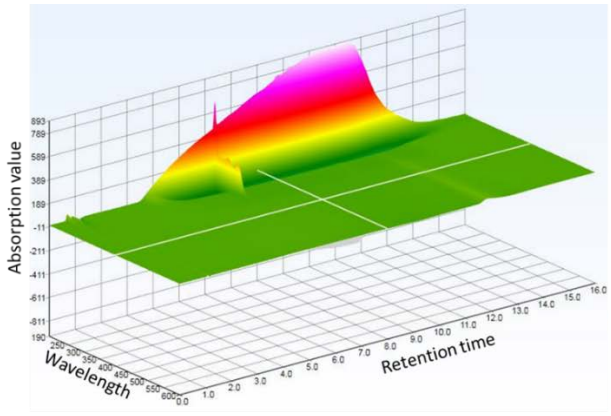

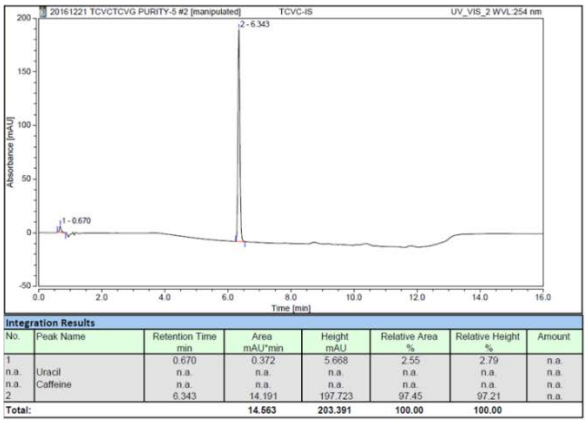

Integration Results

No.	Peak Name	Retention Time min	Area mAU*min	Height mAU	Relative Area %	Relative Height %	Amount
1		0.670	0.372	5.668	2.55	2.79	n.a.
n.a.	Uracil	n.a.	n.a.	n.a.	n.a.	n.a.	n.a.
n.a.	Caffeine	n.a.	n.a.	n.a.	n.a.	n.a.	n.a.
2		6.343	14.191	197.723	97.45	97.21	n.a.
Total:			14.563	203.391	100.00	100.00	

C: TCVG

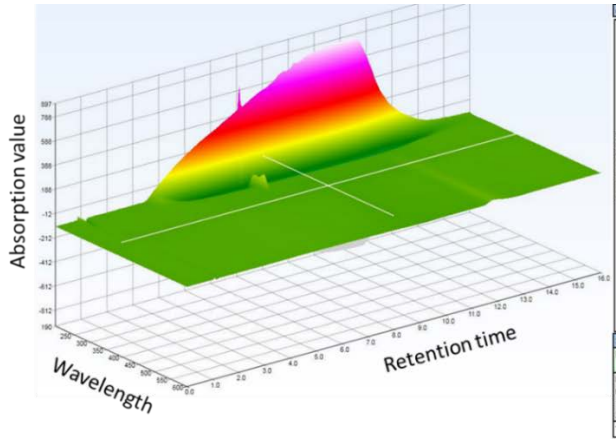

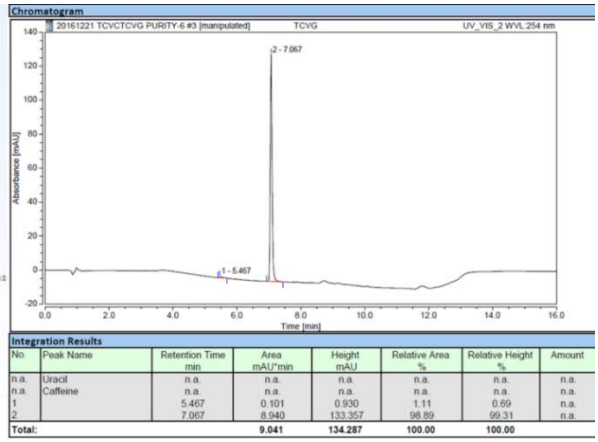

Integration Results

No.	Peak Name	Retention Time min	Area mAU*min	Height mAU	Relative Area %	Relative Height %	Amount
n.a.	Uracil	n.a.	n.a.	n.a.	n.a.	n.a.	n.a.
n.a.	Caffeine	n.a.	n.a.	n.a.	n.a.	n.a.	n.a.
1		5.467	0.101	0.930	1.11	0.69	n.a.
2		7.067	8.940	133.357	98.89	99.31	n.a.
Total:			9.041	134.287	100.00	100.00	

D: TCVG*

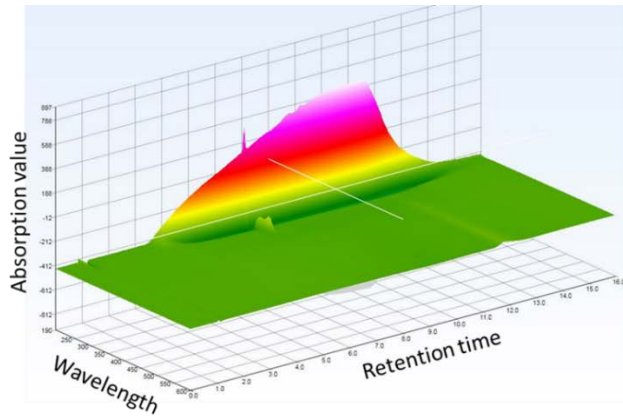

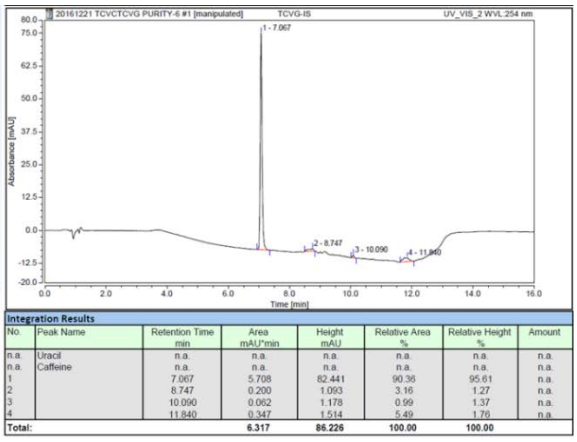

Integration Results

No.	Peak Name	Retention Time min	Area mAU*min	Height mAU	Relative Area %	Relative Height %	Amount
n.a.	Uracil	n.a.	n.a.	n.a.	n.a.	n.a.	n.a.
n.a.	Caffeine	n.a.	n.a.	n.a.	n.a.	n.a.	n.a.
1		7.067	5.708	82.441	90.36	95.61	n.a.
2		8.747	0.200	1.093	3.16	1.27	n.a.
3		10.090	0.062	1.178	0.99	1.37	n.a.
4		11.840	0.347	1.514	5.49	1.76	n.a.
Total:			6.317	86.226	100.00	100.00	

E: NAcTCVC*

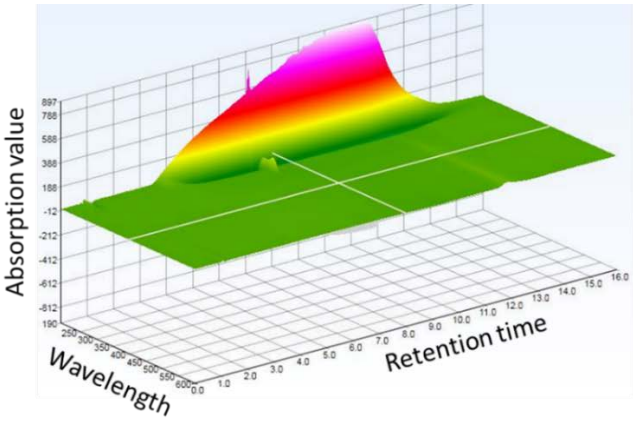

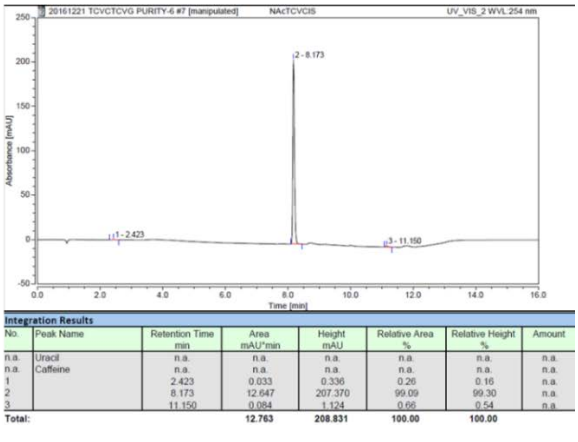

Integration Results

No.	Peak Name	Retention Time min	Area mAU*min	Height mAU	Relative Area %	Relative Height %	Amount
n.a.	Uracil	n.a.	n.a.	n.a.	n.a.	n.a.	n.a.
n.a.	Caffeine	n.a.	n.a.	n.a.	n.a.	n.a.	n.a.
1		2.423	0.033	0.336	0.26	0.16	n.a.
2		8.173	12.647	207.370	99.09	99.30	n.a.
3		11.150	0.084	1.124	0.66	0.54	n.a.
Total:			12.763	208.831	100.00	100.00	

Figure A-2 Analysis of the effect of extraction procedures and solvents on recovery of TCVG, TCVC, and NAcTCVC in liver and kidney tissue in mice. (A) LC-MS/MS chromatogram peak intensity of the neat standards (25 µL of 0.1 µM STD) spiked into PBS, methanol/chloroform (M/C) or distilled deionized water. (B) LC-MS/MS chromatogram peak intensity of the standards (25 µL of 0.1 µM STD) extracted in mouse liver tissue homogenized in PBS, methanol/chloroform (M/C), or in tissue that was first homogenized in PBS and then boiled for 10 min at 90^{o}C prior to addition of the analytes. (C) Same as B, except mouse kidney tissue was used. Experiments were repeated three times and group means with standard deviations are shown. Statistical significance (*, $p<0.05$), as compared to PBS groups for each analyte, was determined by one-way ANOVA with Tukey's post-hoc test.

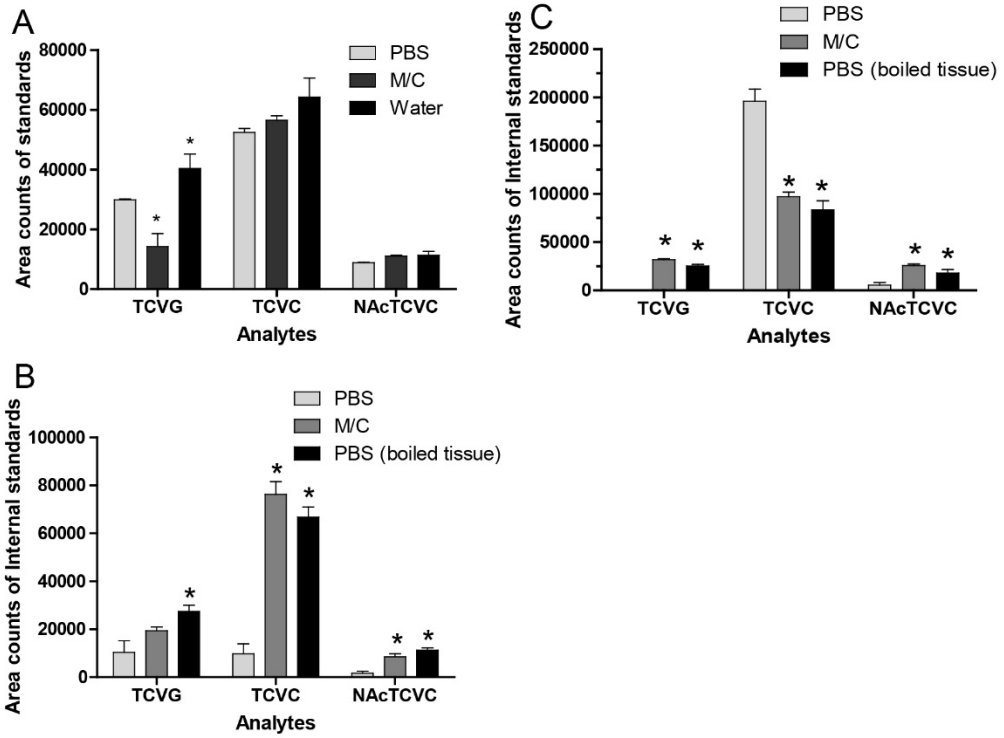

Figure A-3 The LC-MS/MS chromatogram of DCVC in tissue blank and IS blank samples of (A) serum, (B) liver, and (C) kidney.

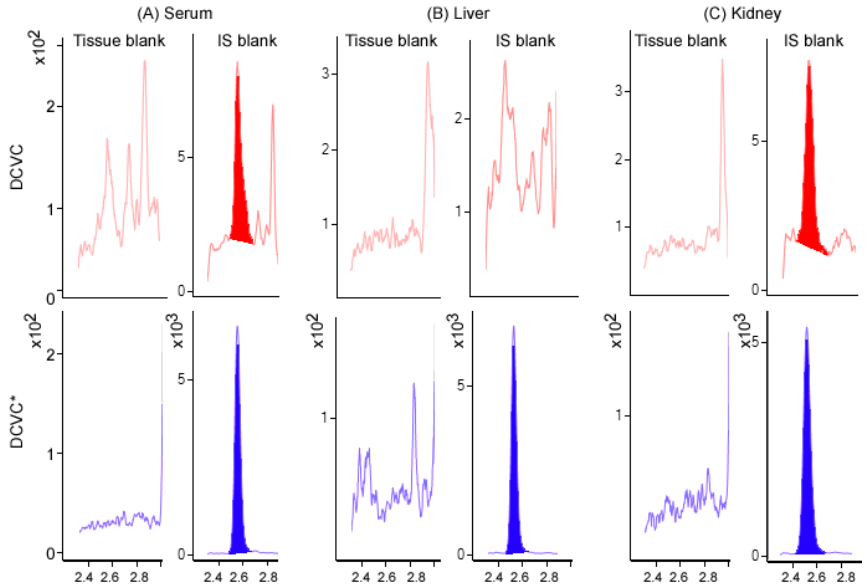

Figure A-4 Pearson correlation analysis of DCVG, DCVC, and NAcDCVC across tissues. Labels indicate statistical significance: * p<0.05, ** p< 0.01, *** p< 0.001.

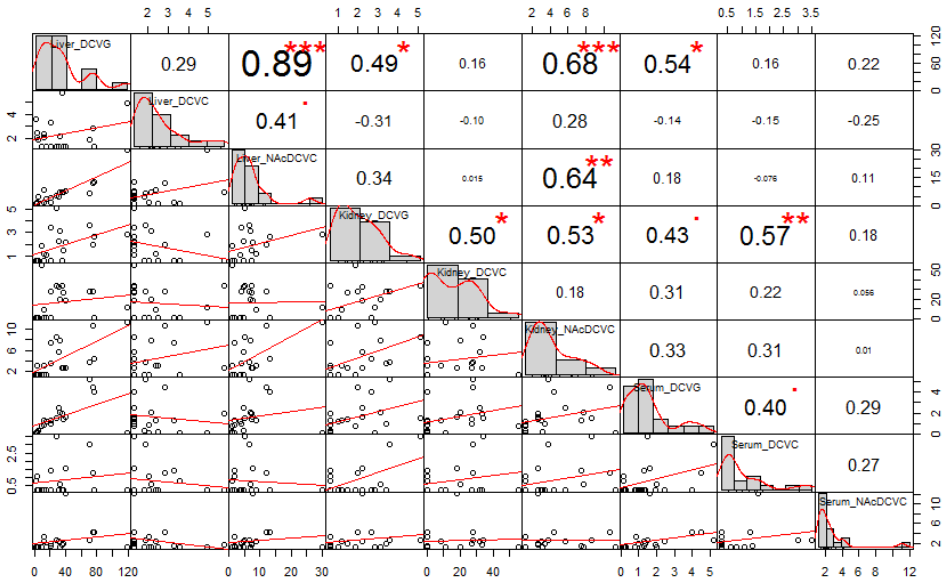

Figure A-5 Gene expression results of *Havcr1*, *Fabp1*, and *Lcn2* align well between qRT-PCR and mRNA sequencing

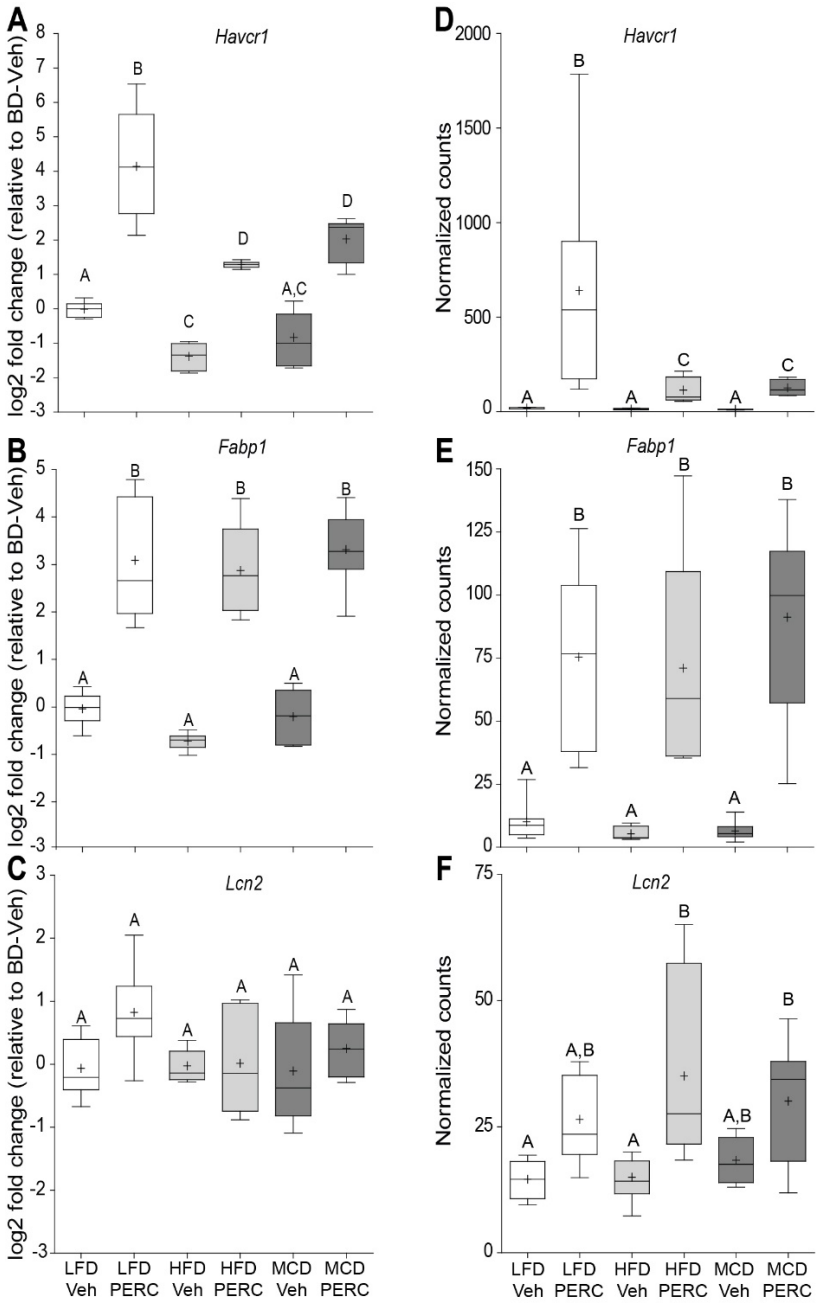

Figure A-6 Comparative analysis of toxicokinetic parameters of TCE (blue) and PCE (red) metabolites in male B6C3F1/J (●), C57BL/6J (▲), and NZW/LacJ (■) mice. The units of first order rate constants are expressed as h^{-1}.

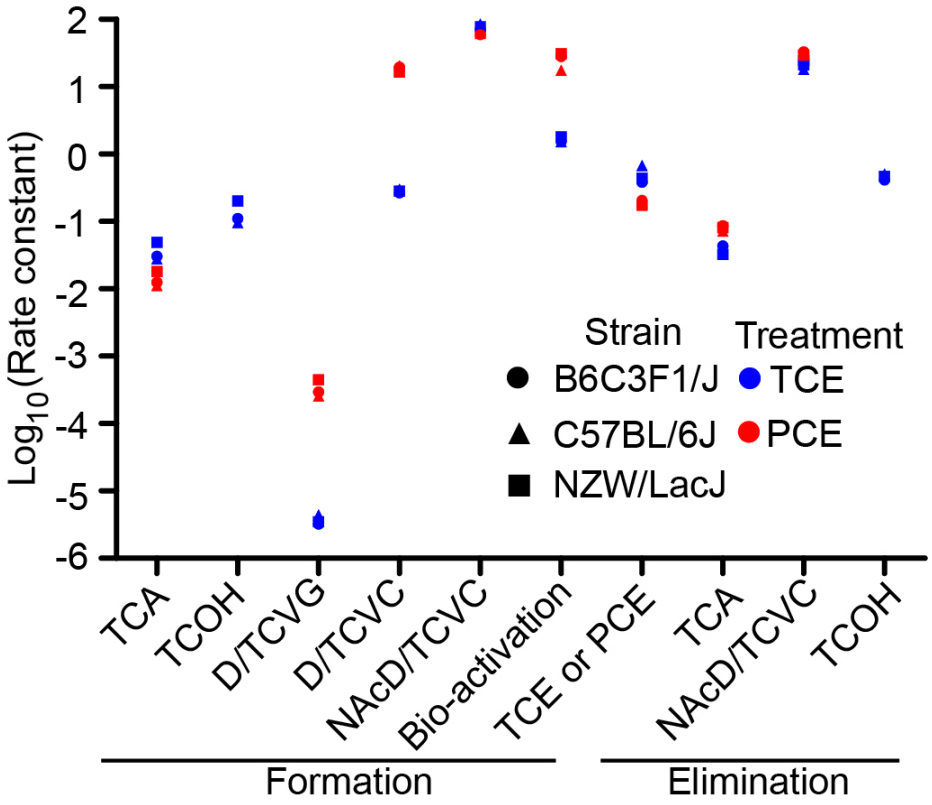

Figure A-7 Toxicokinetic profile of parent compounds (TCE or PCE; red), oxidative metabolites (TCA and TCOH; dark and light green), and glutathione conjugation metabolites (D/TCVG, D/TCVC, and NAcD/TCVC; blue, brown, and pink) in multiple tissues of male B6C3F1/J mice. Each data point represents a single mouse. The color matched dash line shows the modeling estimate for individual toxicokinetic profile.

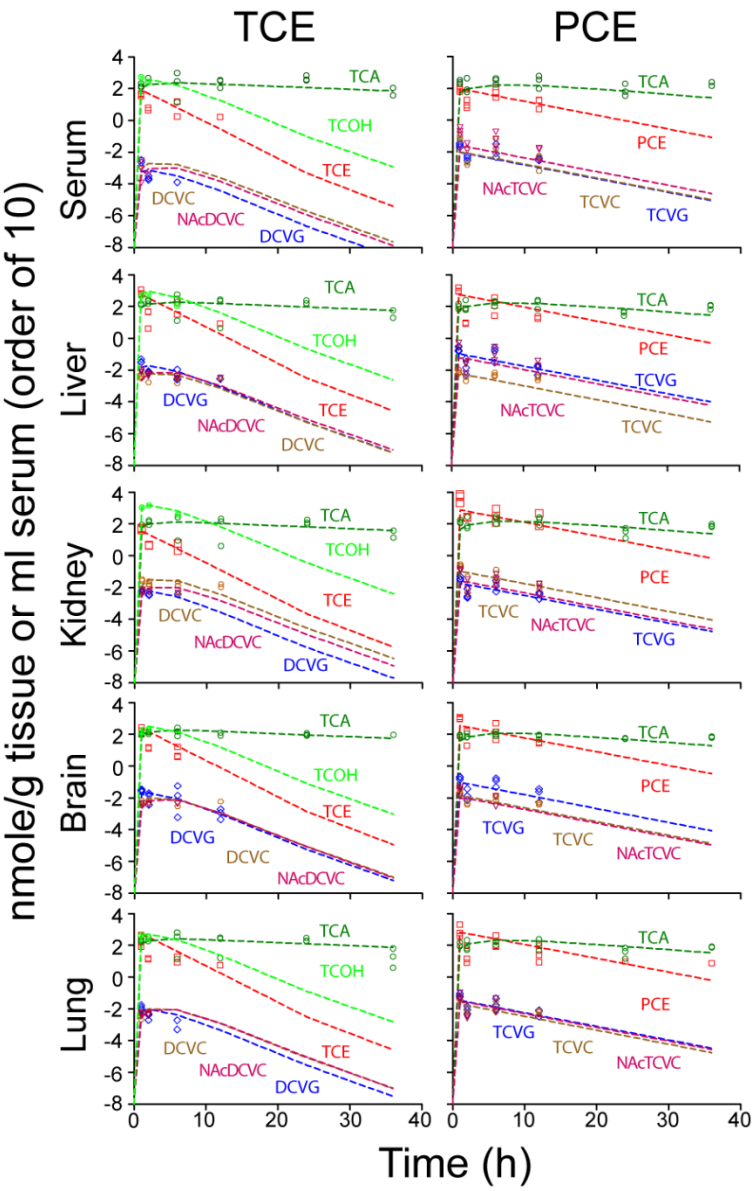

APPENDIX B

TABLES

Table B-1 Quantifiers and qualifiers for analysis of TCVG, TCVG, and NAcTCVC in multiple tissue.

Analytes	Ion transition (*m/z*)	Collision energy (V)	Fragmentor (V)
TCVG	436.0→306.8	13	118
	436.0→203.9	25	118
	438.0→308.8†	13	118
TCVG*	443.0→313.8†	17	118
	439.0→309.8	13	118
TCVC	251.9→234.8†	9	90
	249.9→160.8	21	90
	249.9→232.8	9	90
TCVC*	255.9→237.8†	9	90
	255.9→162.9‡	21	90
NAcTCVC	291.9→249.8†	9	90
	291.9→232.8	17	90
	293.9→251.8	9	90
NAcTCVC*	295.9→235.8†	9	90
	295.9→253.8	17	90

† Selected quantifier for analysis. ‡ Alternative quantifier of TCVC* in serum. Dwell time and cell accelerator voltage were set at 25 ms and 2 V.

Table B-2 Optimization of nebulizer gas pressure

Nebulizer gas pressure						
TCVC	1	2	3	Average	STD	CV
10	56904	58104	60691	58566	1935.4	3.3%
15	80005	79812	78432	79416	857.9	1.1%
20	91324	88898	91142	90455	1351.2	1.5%
25	101797	94471	100037	98911	3824.2	3.9%
30	108307	108587	108771	108756	233.6	0.2%
35	112670	116330	113840	114579	1869.3	1.6%
40	116430	117606	119049	117695	1311.8	1.1%
45 [a]	119356	120647	118140	119381	1253.7	1.1%
TCVG	1	2	3	Average	STD	CV
10	31674	32350	34581	32868	1521.2	4.6%
15	50793	50337	49965	50365	414.7	0.8%
20	60131	60654	61364	60716	618.9	1.0%
25	68367	63026	67917	66391	2962.3	4.5%
30	71085	72185	72970	72365	946.9	1.3%
35 [a]	74582	73943	74600	74055	374.2	0.5%
40	69163	70756	73613	71177	2254.7	3.2%
45	72455	71875	71491	71940	485.3	0.7%
NAcTCVC	1	2	3	Average	STD	CV
10	43022	44392	45915	44443	1447.2	3.3%
15	60473	60901	60725	60700	215.1	0.4%
20	69250	69417	70029	69565	410.1	0.6%
25	75049	73547	73696	74172	827.5	1.1%
30 [a]	76599	75993	77821	76929	931.1	1.2%
35	76105	76478	76472	76486	213.6	0.3%
40	69497	71811	73568	71625	2041.8	2.9%
45	71643	73028	71235	71969	939.8	1.3%

[*]The values represent the instrumental responses of injected compounds subject to various conditions of nebulizer gas pressure. [a] Indicates optimal ionization parameter.

Table B-3 Optimization of capillary voltage

Capillary voltage						
TCVC	1	2	3	Average	STD	CV
3000	103739	108606	108666	107004	2827.4	2.6%
3200	109513	111883	112484	111293	1570.8	1.4%
3400	114497	116304	117587	116129	1552.4	1.3%
3600 [a]	117669	120271	117209	118383	1651.2	1.4%
3800	111324	108803	103991	108039	3725.7	3.4%
4000	99144	98883	95269	97765	2165.8	2.2%
TCVG	1	2	3	Average	STD	CV
3000	65154	66823	67152	66376	1071.3	1.6%
3200	70336	71154	72691	71394	1195.7	1.7%
3400	75595	75221	76151	75656	468.0	0.6%
3600 [a]	77739	81310	75644	78231	2864.9	3.7%
3800	75347	72436	69269	72351	3039.9	4.2%
4000	68289	67317	63823	66476	2348.7	3.5%
NAcTCVC	1	2	3	Average	STD	CV
3000	71182	74036	75266	73495	2095.1	2.9%
3200	75596	77311	78382	77096	1405.4	1.8%
3400	80378	80049	80360	80262	185.0	0.2%
3600 [a]	80902	82951	78868	80907	2041.5	2.5%
3800	76414	75017	71316	74249	2634.3	3.5%
4000	67493	66438	64990	66307	1256.6	1.9%

[*]The values represent the instrumental responses of injected compounds subject to various conditions of nebulizer gas pressure. [a] Indicates optimal ionization parameter.

Table B-4 Optimization of sheath gas temperature

Sheath gas temperature						
TCVC	1	2	3	Average	STD	CV
150	75118	75232	72074	74141	1791.3	2.4%
200	75153	75820	74122	75032	855.5	1.1%
250	72878	69316	68149	70114	2463.5	3.5%
300	74137	73604	71748	73163	1254.1	1.7%
350[a]	76631	76293	77726	76883	749.1	1.0%
400	82172	69410	73559	75047	6509.8	8.7%
TCVG	1	2	3	Average	STD	CV
150	47227	47303	45724	46751	890.5	1.9%
200	46403	47009	46146	46519	443.1	1.0%
250	45567	43285	43154	44002	1356.9	3.1%
300	47249	47256	46068	46858	683.9	1.5%
350 [a]	49770	49912	50406	50029	333.8	0.7%
400	54779	45642	49022	49814	4619.7	9.3%
NAcTCVC	1	2	3	Average	STD	CV
150	43395	44383	42140	43306	1124.2	2.6%
200	46337	46466	45805	46203	350.4	0.8%
250	45157	42770	42706	43544	1397.0	3.2%
300	46856	47911	46427	47065	763.7	1.6%
350 [a]	50031	48920	49724	49558	573.7	1.2%
400	55759	44368	49044	49724	5725.8	11.5%

[*]The values represent the instrumental responses of injected compounds subject to various conditions of nebulizer gas pressure. [a] Indicates optimal ionization parameter.

Table B-5 Optimization of nebulizer gas temperature

Nebulizer gas temperature						
TCVC	1	2	3	Average	Std	CV
150	75744	77896	80260	77967	2258.8	2.9%
200	80482	81424	79237	80381	1097.0	1.4%
250	82780	82500	82717	82666	146.9	0.2%
300 [a]	82304	83912	81747	82654	1124.2	1.4%
350	61821	62739	60678	61746	1032.5	1.7%
TCVG	1	2	3	Average	Std	CV
150	41434	41864	43360	42219	1011.0	2.4%
200	45371	45878	45802	45684	273.4	0.6%
250	48531	46482	48478	47830	1168.0	2.4%
300 [a]	48705	51039	49445	49730	1192.8	2.4%
350	40013	40174	39326	39838	450.4	1.1%
NAcTCVC	1	2	3	Average	Std	CV
150	46060	48183	49188	47810	1597.0	3.3%
200	50005	51384	49804	50398	860.1	1.7%
250	52053	52003	52932	52329	522.5	1.0%
300 [a]	51857	54556	52430	52948	1422.0	2.7%
350	41088	40764	39145	40332	1040.9	2.6%

[*]The values represent the instrumental responses of injected compounds subject to various conditions of nebulizer gas pressure. [a] Indicates optimal ionization parameter.

Table B-6 Method validation of TCVG, TCVC, and NAcTCVC in liver

	TCVG			TCVC			NAcTCVC	
	Low[†]	Mid	High	Low	Mid	High	Mid	High
Set 1	1479.1 ± 68.2[₸]	10282.9 ± 1516.6	127516.5 ± 12981.4	2096.5 ± 106.5	23103.6 ± 2765.5	288241.1 ± 29730.2	2155.5 ± 329.9	25872.1 ± 2471.6
Set 2	1816.3 ± 651.2	11829.1 ± 2218.0	134058.1 ± 44461.4	2541.2 ± 580.5	24590.9 ± 1933.8	299887.7 ± 34666.9	1956.8 ± 418.0	22971.5 ± 9114.7
Set 3	1205.3 ± 243.1	5893.4 ± 2037.0	85114.8 ± 15836.6	1056.3 ± 116.9	7451.8 ± 2146.7	100158.7 ± 17551.9	1136.9 ± 481.9	15070.9 ± 2442.9
RE (%)	66%	50%	63%	44%	32%	37%	58%	66%
ME (%)	123%	115%	105%	113%	100%	94%	91%	89%
PE (%)	81%	57%	67%	50%	32%	35%	53%	58%

[†] Method validation in liver was conducted at different levels across the calibration range for TCVG (On-column values, 0.05, 0.5, and 5 pmole), TCVC (0.05, 0.5, and 5 pmole), and NAcTCVC (0.5 and 5 pmole). [₸] Values are expressed in area counts as average ± standard deviation. Set 1: Standards were prepared in water; Set 2: Samples were post-spiked with standards after extraction; Set 3: Samples were pre-spiked with standards before extraction. Recovery, RE (%) = Set 3/Set 2; Matrix effect, ME (%)= Set 2/ Set 1; Process efficiency, PE (%)= Set 3/ Set 1.

Table B-7 Method validation of TCVG, TCVC, and NAcTCVC in kidney

	TCVG			TCVC			NAcTCVC	
	Low	Mid	High	Low	Mid	High	Mid	High
Set 1	1831.0 ± 200.7	13170.5 ± 961.1	145267.1 ± 3332.2	2373.0 ± 274.9	25841.3 ± 1900.1	295079.7 ± 6509.9	2490.9 ± 106.8	27367.4 ± 437.6
Set 2	1687.5 ± 541.8	14126.6 ± 272.4	144654.1 ± 31050.6	2037.6 ± 692.2	26239.7 ± 1180.2	264278.9 ± 47786.1	2117.7 ± 114.6	23085.5 ± 3935.4
Set 3	1228.9 ± 513.1	7444.2 ± 2220.0	53816.9 ± 19437.2	1399.4 ± 429.1	11404.8 ± 2124.3	92113.5 ± 28440.5	1265.1 ± 224.3	10149.5 ± 3588.8
RE (%)	73%	53%	37%	69%	43%	35%	60%	44%
ME (%)	92%	107%	100%	86%	102%	90%	85%	84%
PE (%)	67%	57%	37%	59%	44%	31%	51%	37%

Table B-8 Method validation of TCVG, TCVC, and NAcTCVC in Serum

	TCVG			TCVC			NAcTCVC		
	Low	Mid	High	Low	Mid	High	Low	Mid	High
Set 1	2103.5 ± 201.4	14829.2 ± 457.4	149155.5 ± 5204.8	2111.9 ± 233.9	23068.3 ± 564.1	239062.6 ± 7017.7	281.3 ± 31.6	2726.9 ± 94.2	28217.7 ± 936.7
Set 2	2160.9 ± 239.2	13384.0 ± 200.9	138943.8 ± 1926.9	2173.9 ± 189.6	21709.6 ± 185.7	230027.5 ± 3331.6	341.1 ± 50.5	2987.2 ± 152.8	31141.5 ± 1205.8
Set 3	1827.9 ± 146.5	7543.7 ± 1756.6	80692.8 ± 19993.5	1370.5 ± 145.2	9324.8 ± 2453.4	95905.9 ± 22656.2	319.8 ± 48.3	2025.7 ± 534.7	22237.4 ± 3812.3
RE (%)	85%	56%	58%	63%	43%	42%	94%	68%	71%
ME (%)	103%	90%	93%	103%	94%	96%	121%	110%	110%
PE (%)	87%	51%	54%	65%	40%	40%	114%	74%	79%

Table B-9 Method validation of TCVG, TCVC, and NAcTCVC in urine

	TCVG			TCVC			NAcTCVC	
	Low	Mid	High	Low	Mid	High	Mid	High
Set 1	221.6 ± 20.2	1067.4 ± 267.5	11855.4 ± 2023.0	301.4 ± 52.3	2226.9 ± 533.1	25971.6 ± 4297.0	200.1 ± 57.9	2350.8 ± 342.3
Set 2	196.3 ± 42.8	1349.8 ± 391.7	14389.5 ± 936.9	197.7 ± 25.8	2016.5 ± 550.8	22703.4 ± 895.4	210.9 ± 61.3	1846.0 ± 101.8
Set 3	174.9 ± 49.4	1087.6 ± 165.5	10195.2 ± 2486.8	189.5 ± 35.2	1838.8 ± 336.0	18514.8 ± 3718.3	214.5 ± 54.0	1532.7 ± 243.6
RE (%)	89%	81%	71%	96%	91%	82%	102%	83%
ME (%)	89%	126%	121%	66%	91%	87%	105%	79%
PE (%)	79%	102%	86%	63%	83%	71%	107%	65%

Table B-10 Levels of DCVG, DCVC, and NAcDCVC in liver, kidney, and serum of B6C3F1 mice treated with TCE (n=3/group).

	Liver			Kidney			Serum		
TCE (mg/kg)	**DCVG**	**DCVC**	**NAcDCVC**	**DCVG**	**DCVC**	**NAcDCVC**	**DCVG**	**DCVC**	**NAcDCVC**
24	*0.44	*1.3	*1.0	*0.59	10.8±3.7	*1.2	*0.15	2.9±0.2	*1.2
240	3.4±1.2	*1.3	4.1±0.8	†1.8±0.6	8.5±3.3	*1.2	1.8±0.4	4.8±3.1	3.6±0.4
800	65.7±19.9	6.4±0.9	12.8±0.5	4.1±1.4	34.2±10.6	4.1±0.5	4.4±0.7	8.7±1.9	5.8±0.7

Table B-11 Levels of DCVG, DCVC, and NAcDCVC in liver, kidney, and serum of 20 CC mice treated with TCE (800 mg/kg).

Strain	Liver			Kidney			Serum		
	DCVG	DCVC	NAcDCVC	DCVG	DCVC	NAcDCVC	DCVG	DCVC	NAcDCVC
CC028/GeniUnc	35.8	5.8	7.4	*0.6	33.2	†2.6	1.9	*0.3	†1.7
CC027/GeniUnc	76.3	*1.3	13.0	†2.7	*3.7	4.4	4.0	*0.3	4.1
CC033/GeniUnc	70.6	†1.9	6.6	†3.6	27.5	†3.8	5.2	3.0	†2.6
CC030/GeniUnc	33.1	†2.1	7.0	†3.1	20.0	7.8	2.0	†0.6	*1.2
CC008/GeniUnc	10.1	*1.3	*1.0	†1.8	55.0	*1.2	†0.8	*0.3	*1.2
CC022/GeniUnc	21.9	*1.3	4.2	†3.4	27.2	†3.4	1.0	*0.3	†1.9
CC052/GeniUnc	20.8	†3.3	†1.9	*0.6	*3.7	7.5	1.3	†1.4	†1.5
CC056/GeniUnc	32.0	*1.3	4.9	†2.2	31.9	5.7	2.5	*0.3	†2.2
CC059/TauUnc	4.1	†2.0	†1.6	*0.6	*3.7	*1.2	*0.1	†1.1	*1.2
CC037/TauUnc	75.2	†2.9	12.2	†2.0	27.5	10.8	4.5	†1.3	4.3
CC055/TauUnc	†2.7	†3.6	*1.0	*0.6	*3.7	*1.2	*0.1	†0.8	*1.2
CC007/Unc	37.7	*1.3	7.1	†1.5	27.1	†2.6	1.4	*0.3	†2.0
CC039/Unc	16.0	*1.3	†3.7	*0.6	*3.7	*1.2	1.2	*0.3	*1.2
CC021/Unc	13.1	†2.4	8.6	†1.2	8.8	†3.0	1.3	*0.3	†2.3
CC057/Unc	39.9	*1.3	7.6	†2.2	18.0	†2.7	1.6	†1.6	12.0
CC036/Unc	4.6	†1.8	4.7	*0.6	*3.7	*1.2	†0.3	*0.3	*1.2
CC035/Unc	12.3	†2.0	†1.8	*0.6	*3.7	*1.2	†0.8	*0.3	†3.2
CC046/Unc	3.2	†2.5	*1.0	*0.6	*3.7	†3.2	†0.2	*0.3	*1.2
CC047/Unc	27.9	*1.3	5.3	5.1	33.6	8.6	1.5	3.5	†2.6
CC050/Unc	118.9	4.9	30.0	†2.8	11.0	11.4	missing data	missing data	missing data

* Levels are expressed as pmole/g tissue or mL serum. The data point is shown as ½ LOD if an analyte was non-detected. The background concentration of kidney DCVC (3.7 pmole/g) is used if the measurement was below the background concentration.
† The values for levels was detectable but lower than LOQ.

Table B-12 Inter-individual variability of tissue levels of DCVG, DCVC, and NAcDCVC in B6C3F1 mice and 20 CC mice (800 mg/kg TCE).

	DCVG					
	B6C3F1 study			20 CC study		
	Liver	Kidney	Serum	Liver	Kidney	Serum
Mean	65.7	6.3	4.4	32.8	1.9	1.7
Median	63.1	6.5	4	24.9	1.8	1.3
Std	19.9	1.3	0.7	30.7	1.3	1.4
CV	30%	21%	15%	94%	68%	86%
	DCVC					
	B6C3F1 study			20 CC study		
	Liver	Kidney	Serum	Liver	Kidney	Serum
Mean	6.4	37.3	8.7	2.3	17.7	0.9
Median	6.6	34	8.2	1.9	18	0.3
Std	0.9	5.8	1.9	1.3	15.4	1
CV	14%	16%	21%	55%	86%	112%
	NAcDCVC					
	B6C3F1 study			20 CC study		
	Liver	Kidney	Serum	Liver	Kidney	Serum
Mean	12.8	5.4	5.8	6.5	4.4	2.6
Median	12.6	5.3	5.5	5.1	3.2	1.9
Std	0.5	0.1	0.7	6.5	3.3	2.5
CV	4%	3%	11%	100%	75%	96%

Table B-13 PCR primers used for genotyping CYP2E1 knockout and humanized transgenic mice

	Forward sequence	Reverse sequence
129S1/SvlmJ (125bp product)	5'-AGT GTT CAC ACT GCA CCT GG-3'	5'-CCT GGA ACA CAG GAA TGT CC-3'
Cyp2e1(-/-) (280bp product)	5'-CTT GGG TGG AGA GGC TAT TC-3'	5'-AGG TGA GAT GAC AGG AGA TC-3'
hCYP2E1 (1746 bp product)	5'-AGA TTC AGC GGT TCA TCA CC-3’	5'-AGG GCT GAG GTC GAT ATC CT-3’
hCYP2E1 (400 bp product)*	5'-AGA TTC AGC GGT TCA TCA CC-3'	5'-GCC CTA ATC TTC TCA CAG GA-3'

*This revised primer was used for genotyping the mice bred in Texas A&M Institute for Genomic Medicine.

Table B-14 Number of mice used in TCE study

Sex	Male			Female		
Strain	129S1/SvImJ	Cyp2e1 (-/-)	hCYP2E1	129S1/SvImJ	Cyp2e1 (-/-)	hCYP2E1
Treatment	TCE					
2h	4	4	2	3	3	3
5h	4	4	4	4	4	4
12h	4	3	2	3	3	3
24h	3	4	3	3	4	4
Treatment	Vehicle					
5h	4	4	4	4	4	4

Table B-15 Number of mice used in PCE study

	129S1/SvImJ				Cyp2e1 (-/-)				hCYP2E1				Total
	Male		Female		Male		Female		Male		Female		
	V	P	V	P	V	P	V	P	V	P	V	P	
July, 2013	4	4	1	2	0	0	0	0	0	1	1	1	14
July, 2013	2	2	2	2	1	1	1	1	2	2	2	2	20
October, 2013	0	0	1	2	0	1	1	2	2	3	2	2	16
January, 2018	0	0	0	0	0	1	2	0	1	0	0	0	4
March, 2018	0	0	0	0	3	2	3	3	0	2	1	1	15
N_{TK}	6	6	3	4	4	4	6	4	3	5	4	4	53
Total	6	6	4	6	4	5	7	6	5	8	6	6	69

*V, vehicle group; P, PCE-treated group

Table B-16 Area under the curve (AUC) of TCE and PCE metabolites in multiple tissues of male B6C3F1/J, C57BL/6J, and NZW/LacJ mice. The AUC values were calculated from model-predicted concentrations up to 36 hours based on trapezoidal rule.

	TCE treated mice				PCE treated mice		
Serum	**C57BL/6J**	**B6C3F1/J**	**NZW/LacJ**	**Serum**	**C57BL/6J**	**B6C3F1/J**	**NZW/LacJ**
TCE	119.1	202.5	158.5	PCE	522.3	509.3	813.2
TCA	2011	5175	8106	TCA	4219	3393	5799
TCOH	1213	2101	2894				
DCVG	0.013	0.004	0.004	TCVG	0.08	0.05	0.09
DCVC	0.021	0.016	0.016	TCVC	0.11	0.06	0.15
NAcDCVC	0.014	0.009	0.010	NAcTCVC	0.50	0.14	0.33
Liver	**C57BL/6J**	**B6C3F1/J**	**NZW/LacJ**	**Liver**	**C57BL/6J**	**B6C3F1/J**	**NZW/LacJ**
TCE	718.4	1379	809.7	PCE	3478	3140	3760
TCA	1884	4195	6023	TCA	3701	3612	4951
TCOH	1880	4877	4088				
DCVG	0.109	0.105	0.096	TCVG	0.54	0.59	1.22
DCVC	0.045	0.047	0.030	TCVC	0.05	0.03	0.05
NAcDCVC	0.083	0.063	0.050	NAcTCVC	0.79	0.36	0.87
Kidney	**C57BL/6J**	**B6C3F1/J**	**NZW/LacJ**	**Kidney**	**C57BL/6J**	**B6C3F1/J**	**NZW/LacJ**
TCE	70.66	85.53	80.15	PCE	6180	4229	5993
TCA	1470	2953	5606	TCA	3741	3072	6858
TCOH	4729	8204	14922				
DCVG	0.041	0.032	0.047	TCVG	0.10	0.10	0.58
DCVC	0.215	0.245	0.116	TCVC	0.56	0.58	1.59
NAcDCVC	0.123	0.088	0.094	NAcTCVC	0.27	0.15	0.67
Brain	**C57BL/6J**	**B6C3F1/J**	**NZW/LacJ**	**Brain**	**C57BL/6J**	**B6C3F1/J**	**NZW/LacJ**
TCE	287.1	569.8	532	PCE	1592	1961	2413
TCA	3132	4101	4792	TCA	2572	2444	2743
TCOH	711.6	1738	2545				
DCVG	0.121	0.111	0.114	TCVG	0.50	0.52	1.11
DCVC	0.078	0.076	0.063	TCVC	0.10	0.08	0.10
NAcDCVC	0.085	0.067	0.067	NAcTCVC	0.11	0.06	0.14
Lung	**C57BL/6J**	**B6C3F1/J**	**NZW/LacJ**	**Lung**	**C57BL/6J**	**B6C3F1/J**	**NZW/LacJ**
TCE	776.7	1334	923.8	PCE	3788	3682	3860
TCA	2396	5631	8657	TCA	4787	4271	6545
TCOH	1647	2806	5612				
DCVG	0.065	0.052	0.062	TCVG	0.17	0.19	0.28
DCVC	0.077	0.081	0.087	TCVC	0.15	0.11	0.15
NAcDCVC	0.073	0.077	0.078	NAcTCVC	0.28	0.17	0.35

Table B-17 Inter-strain variability of TCE and PCE metabolites in multiple tissues of male B6C3F1/J, C57BL/6J, and NZW/LacJ mice. The values show the geometric standard deviations (GSD) of metabolite AUCs across strains.

TCE-treated mice		PCE-treated mice	
Serum			
TCE	1.30	PCE	1.30
TCA	2.04	TCA	1.31
TCOH	1.25		
DCVG	1.92	TCVG	1.32
DCVC	1.16	TCVC	1.63
NAcDCVC	1.26	NAcTCVC	1.91
Liver			
TCE	1.42	PCE	1.09
TCA	1.81	TCA	1.19
TCOH	1.66		
DCVG	1.07	TCVG	1.57
DCVC	1.28	TCVC	1.22
NAcDCVC	1.29	NAcTCVC	1.64
Kidney			
TCE	1.10	PCE	1.23
TCA	1.95	TCA	1.52
TCOH	1.78		
DCVG	1.21	TCVG	2.77
DCVC	1.49	TCVC	1.81
NAcDCVC	1.19	NAcTCVC	2.13
Brain			
TCE	1.46	PCE	1.23
TCA	1.24	TCA	1.06
TCOH	1.92		
DCVG	1.04	TCVG	1.56
DCVC	1.12	TCVC	1.12
NAcDCVC	1.15	NAcTCVC	1.52
Lung			
TCE	1.32	PCE	1.02
TCA	1.92	TCA	1.25
TCOH	1.85		
DCVG	1.12	TCVG	1.29
DCVC	1.06	TCVC	1.19
NAcDCVC	1.03	NAcTCVC	1.45